ROLE OF PEROXIREDOXINS IN AMYOTROPHIC LATERAL SCLEROSIS.

SANDEEP SUNDARA RAJAN

Thesis submitted for the degree of Doctor of Philosophy (Ph. D)

Sheffield Institute for Translational Neuroscience (SITraN)
Academic Neurology Unit
University of Sheffield

March 2013

Acknowledgments

Foremost, I am thankful to the Motor Neurone Disease Association (MNDA) and the University of Sheffield for funding this work. As a student from India, I had always dreamed of the privilege to be a part of world class research. It was only because of the MNDA studentship and fee waivers given by the University of Sheffield, I was able to work with no financial problems or obligations right to the end. My sincere thanks to both these organisations for putting me a step ahead in my academic career.

I am extremely grateful to my supervisor Dr. Clare Wood-Allum (SITraN) for her guidance in this project. Her unwavering support and patience, during these four years has helped me learn and appreciate the intricacies involved in research. I must also thank her for her generous efforts in guiding me from time to time at both personal and professional fronts. I can certainly say that, this journey has definitely made me a better person for pursuing a career in academia.

I am also indebted to my co-supervisor and the Director of SITraN, Prof Pamela Shaw whose support, encouragement and faith boosted my confidence at times of need. I can honestly say that without her push and the strive towards excellence, that she sets as an example; I would not have had this enriching experience. It was truly an honour to be supervised by her and be a part of world class research in neurodegenerative diseases.

Without the support of both my supervisors, it would not have been possible for me to have carried out research with confidence. I hope that with this thesis, I have justified their faith in me and I hope that both of them are proud of this work.

During my time within the Neurosciences department, I have come across some of the most helpful people. I extend my gratitude to Dr. Adrian Higginbottom for his advice of countless occasions and also for turning on the music every morning in the labs, Dr. Sian Barber and Dr. Scott Allen for their helpful hints on tissue culture, Dr. Laura Ferraiuolo and Dr. Richard Mead for their generous time and help with transgenic mice (Richard, I think we made a good dissection team), and to all those to who returned me a smile in the corridors (especially Paul Heath).

It wouldn't be possible to complete my research without the help and support of the Neurology Technical team – Anne, Kim, Ian, Dan and Kevin. I thank all the volunteers and patients of MND who have donated samples to help me with this research and likewise my thanks also extend to all the NHS staff who made sure that these precious samples were properly taken care off until needed.

My most sincere thanks to Dr. Janine Kirby, Dr Jon Wood and Dr. Andy Grierson, all three of who knew me a bit longer, for always being there for me at the times of need. I am sure they know what I mean !

It wouldn't be right if I left out my fellow Ph D students – Rohini, Lynn, Channa, and Marc who shared their experience of excitement and frustration of research with me. Lastly, my thanks to all the members of the Academic Neurology Unit for letting me have some fun during these years.

Outside the Neurology Unit, I am most thankful to Dr. Martina Daly (Dept. of Cardiovascular Science), my personal tutor, for giving me the right advice, guidance and help to make me reach my goal.

Back home, I cannot thank enough my Amma and Appa who have been ever supportive of my work. Their constant support and words of encouragement have helped me complete yet another milestone in my career path. It was rather a difficult time for me and for them in these years but I am sure that this thesis is something that they would be very proud of. My special thanks to my sister, Soumya, whose support on numerous occasions cannot be forgotten. Her jokes, visit to UK, words of support and help at times of need made all this possible. I would also like to mention the support of my family especially my grandparents, Cheenu mama, Nandini mami, Suchi and Shreyu. I always cherish the times I spent with all of them.

Words are not enough to express my gratitude to my most dear and my best friend – Suruchi, who stuck me will all these years through the good, the bad and the ugly times. Her faith, encouragement and support have always pulled me up no matter how far down I was. These four years have flown so quickly with her that looking back, I can just see my accomplishments. I cherish all her help and suggestions with my work – both in lab and at desk, her assistance with my numerous presentations, posters and proofing-reading this thesis until the very end. I am sure that it would be impossible that I would be at this place without her.

I also have the pleasure to share memories of this journey with Jyoti aunty and Uttam uncle, who have always shared a joke with me, and supported me with all their good wishes. My thanks to my bro – Subodh for the all fun times in India and in the UK and for keeping me insane whenever possible. My thanks also to all the wonderful grandparents, aunts and uncles from Mumbai – which also includes the three brave musketeers – Khushi, Rishabh and Shishir, for their words of support at all times. It was a great pleasure to include all of them in my troubles.

Special thanks to Krishna aunty and Kishan uncle – the wise guys who actually pushed me to develop my career in the UK. Right from the start, Krishna aunty was there for me, guiding and helping me adjust to the way of life away from home. It was always fun when she used to visit my home here in UK, I hope that with this work, both uncle and aunty are proud of me and my achievements. I must also thank Dr. Shasi Kalivendi (IICT, Hyderabad) for inspiring me to pursue a career in neuroscience. I look up to him as a mentor and appreciate his encouragement and support in guiding me.

My time in Sheffield, or rather in the UK, would not be complete if it was not for all the beautiful memories made by all my friends and family here especially Sid, Defne, Siddhartha, Sindhu, Bhoomika, Yammu, Niranjan and Jojo; and who says that people who live miles and miles away can't have a say – thanks you so much Ravali for being a part of my Ph D. Your long skype calls is something that I still cherish.

My most special thanks to each and every member of my most special "gang" of friends. Without their good wishes, their magical touch and their support all of this would have never come true. Last but by no means the least; I thank the almighty for giving me the strength and courage to complete what I had started 4 years ago. Looking back I can see all those blessings that the almighty has showered upon me especially when I needed them most!

A sincere "Thank you" to each and every one of you for everything.

Sandeep Sundara Rajan

ABSTRACT

Amyotrophic lateral sclerosis (ALS) is a fatal, adult-onset neurodegenerative disorder that results in the progressive death of motor neurons leading to death typically within 3-5 years from diagnosis. About 5 % of ALS is familial which includes ALS due to mutations in superoxide dismutase 1 (SOD1) and TAR DNA binding protein (TDP43). Previous work in cellular and animal models of mutant SOD1-ALS showed alterations in the levels of a family of anti-oxidant proteins the Peroxiredoxins (Prxs). Peroxiredoxins are redox-sensitive anti-oxidant enzymes that reduce hydrogen peroxide (H_2O_2) to water, becoming oxidized themselves in the process. Upon further oxidation, some Prxs lose their hydroperoxidase activity and attain higher oxidation states. Overoxidized Prxs ($PrxSO_{2/3}$) may be returned to their reduced state via the actions of the active regenerator Sulfiredoxin 1 (Srx 1). Given the evidence for involvement of oxidative stress in ALS, I hypothesized that the Prxs are likely to spend longer in a more oxidized state in disease conditions, than in health, and that this might be of pathogenetic relevance.

Using Western blotting, levels of reduced Prxs, $PrxSO_{2/3}$ and their regenerators were assessed in NSC34 motor neuronal cells that expressed various forms of mutant SOD1, in G93A SOD1 transgenic mice and in fibroblasts derived from mutant SOD1 and mutant TDP43 ALS patients. The susceptibility of the Prxs to become overoxidized and their ability to return to a reduced state was also determined by treating cells with hydrogen peroxide and monitoring their recovery.

In ALS-patient fibroblasts, a delay in the recovery of $PrxSO_{2/3}$ was observed in stress-recovery experiments conducted using H_2O_2. This delay in $PrxSO_{2/3}$ recovery was associated with a delayed and reduced induction of the $PrxSO_{2/3}$ regenerator Srx 1 and a reduced activation of AP-1, a sulfiredoxin 1 transcription factor. The delay in $PrxSO_{2/3}$ recovery was exacerbated after application of sequential exposures to lower concentrations of H_2O_2. Efforts to reiterate the findings in ALS patient fibroblasts in motor neuronal ALS models (NSC34 cell lines and G93A mice), however, were unsuccessful.

The work presented here demonstrates a potential deficit in the recovery of overoxidized Prxs within a subset of fALS patients after exposure to an oxidative stress. As hypothesized, the 2-cys Prxs present in the fibroblast model of SOD1 fALS investigated do appear to spend longer in a higher oxidation state after application of an external oxidative stress. Given that motor neurons encounter recurrent oxidative stressors over their life-span, were recovery of overoxidized Prxs in motor neurons similarly defective, this might render them more vulnerable to the cumulative effects of recurrent physiological oxidative stresses over time. My findings provide evidence of dysregulation of the peroxiredoxin anti-oxidant system in at least one model of SOD1-related fALS that may contribute to the pathophysiology of ALS. If these deficiencies could also be shown to be a feature of motor neurons in ALS, a role in the pathogenesis of the disease is certainly a possibility.

CONTENTS

LIST OF FIGURES

LIST OF TABLES

ABBREVIATIONS

6-OHDA	:	6-hydroxydopamine
Aβ	:	Amyloid beta
ABAD	:	Amyloid binding alcohol dehydrogenase
ACh	:	Acetyl choline
AD	:	Alzheimer's disease
ALS	:	Amyotrophic lateral sclerosis
AMPA	:	α-amino-3-hydroxy-5-methyl-4-isoxazole propionic acid
ANG	:	Angiogenin
APP	:	Amyloid precursor protein
APS	:	Ammonium persulphate
AP-1	:	Activator protein-1
ARE	:	Anti-oxidant response element
ASK 1	:	Apoptosis signalling kinase 1
ATP	:	Adenosine triphosphate
ATXN	:	Ataxin 2
BDNF	:	Brain-derived neurotrophic factor
C9Orf72	:	Chromosome 9 open reading frame 72
Ca^{+}	:	Calcium
C/EBPβ	:	CAAT- enhancer binding protein transcription factor
CCS	:	Copper chaperone for SOD1
cDNA	:	Complimentary DNA
Chr9	:	Chromosome 9
ChAT	:	Choline acetyltransferase
CHAPS	:	3-[(3-cholamidopropyl)dimethylammonio]-2-hydroxy-1-propanesulfonate
CHX	:	Cycloheximide
CNS	:	Central nervous system
CNTF	:	Ciliary neurotrophic factor
CO_2	:	Carbon dioxide
Con	:	Control
COX-2	:	Cyclo-oxygenase 2
Cp	:	Peroxidatic cystiene
CQNX	:	6-cyano-7-nitroquinoxaline-dione disodium
Cr	:	Resolving cysteine
CSF	:	Cerebrospinal fluid
Cu	:	Copper
CuZn	:	Cooper/Zinc

Cys	:	Cysteine
DLB	:	Dementia with Lewy body disease
DMEM	:	Dulbecco's minimum essential medium
DMSO	:	Dimethyl sulphoxide
DNA	:	Deoxyribonucleic Acid
DTT	:	Dithiothreitol
EAAT2	:	Excitatory Amino Acid Transporter 2
EDTA	:	Ethylene diamine tetra acetic acid
EGF	:	Epidermal growth factor
EGTA	:	Ethylene glycol tetra-acetic acid
fALS	:	Familial amyotrophic lateral sclerosis
FCS	:	Fetal calf serum
FTD	:	Frontotemporal dementia
FTLD	:	Frontotemporal lobar degeneration
FUS	:	Fused in sarcoma
FUS/TLS	:	Fused in sarcoma/Translated in liposarcoma
GGLG	:	Gly-Gly-Leu-Gly
GluR2	:	Glutamate receptor 2
Gly	:	Glycine
GPx	:	Glutathione peroxidase
H	:	Hydrogen
H_2O_2	:	Hydrogen Peroxide
HEK293	:	Human embryonic kindney cells 293
HEPES	:	4-(2-hydroxyethyl)-1-piperazineethanesulfonic acid
HCI	:	Hyaline conglomerate inclusions
HOCI	:	Hypochlorous acid
HPLC	:	High performance liquid chromatography
HRP	:	Horse-radish peroxidase
HSP	:	Heat shock proteins
ICC	:	Immunocytochemistry
IGF-I	:	Insulin-like growth factor I
JNK	:	c-jun N-terminal kinases
K^+	:	Potassium
KA	:	Kainate
KCL	:	Potassium chloride
kDa	:	Kilo Daltons
Keap 1	:	Kelch-like ECH associated-protein 1
KH_2PO_4	:	Pottasium phosphate
KSP	:	Lys-Ser-Pro

LBHI	:	Lewy-body like hyaline conglomerates
Leu	:	Leucine
LMN	:	Lower motor neuron
LOA	:	Legs at Odd Angles
LSB	:	Laemmli sample buffer
MALDI-MS	:	Matrix-assisted laser desorption/ionization – Mass spectrometry
MAPT	:	Microtubule associated protein tau
mM	:	Milimolar
MND	:	Motor neuron disease
MRI	:	Magnetic resonance imaging
mtDNA	:	Mitochondrial DNA
mRNA	:	Messenger RNA
M.W	:	Molecular weight
Na^+	:	Sodium
NaCl	:	Sodium Chloride
NADPH	:	Nicotinamide adenine dinucleotide phosphate
NCIs	:	Neuronal cytoplasmic inclusions
NEM	:	N-Ethylmaleimide
NF-H	:	Neurofilament heavy chain subunit
NF-L	:	Neurofilament light chain subunit
NHS	:	National health service
Na_2HPO_4	:	Sodium phosphate
NIV	:	Non-invasive ventilation
NMDA	:	*N*-methyl-D-aspartate abbreviated
NO	:	Nitric oxide
NOS	:	Nitric oxide synthase
NOX	:	NADPH oxidase
Nrf 2	:	Nuclear factor erythroid 2-related factor
NS	:	Non-stressed
NTG	:	Non transgenic cells
O_2	:	Oxygen
OH	:	Hydroxyl group
ONOO	:	Peroxynitrite
OOH	:	Peroxide
OPTN	:	Optineurin
PAGE	:	Polyacrylamide gel electrophoresis
Pat	:	Patient
PBP	:	Progressive bulbar palsy

PBS	:	Phosphate buffer saline
PBST	:	PBS-Tween-20
PCR	:	Polymerase chain reaction
PD	:	Parkinson's disease
PDGF	:	Platelet-derived growth factor
PEG	:	Percutaneous endoscopic gastrostomy
PIC	:	Protease inhibitor cocktail
PIG	:	Per-oral image-guided gastrostomy
PIP2	:	Phosphatidylinositol 4,5-bisphosphate
PIP3	:	Phosphatidylinositol 3,4,5-triphosphate
PI3K	:	Phosphatidylinositol 3-kinase
PLS	:	Progressive lateral sclerosis
PMA	:	Progressive muscular atrophy
PMSF	:	Phenylmethanesulfonyl fluoride
PRG	:	Percutaneous radiological gastrostomy
PRGN	:	Progranulin
Prx	:	Peroxiredoxin
$PrxSO_{2/3}$	:	Overoxidized peroxiredoxins
PTEN	:	Phosphatidylinositol 3,4,5-triphosphate 3-phosphatase
PTP	:	Protein tyrosine phosphatases
PVDF	:	Polyvinlylidene difluoride
Q-PCR	:	Quantitative polymerase chain reaction
RBC	:	Red blood cells
RNA	:	Ribonucleic acid
ROOH	:	Alkyl hydroperoxides
ROS	:	Reactive oxygen species
rRNA	:	Ribosomal RNA
RTK	:	Receptor tyrosine kinases
sALS	:	Sporadic Amyotrophic lateral sclerosis
Sesn 2	:	Sestrin 2
SETX	:	Senataxin
SDS	:	Sodium dodecyl sulphate
SEM	:	Standard error of the mean
SH	:	Thiol
SOD1	:	Superoxide dismutase 1
SOH	:	Cysteine-sulfenic acid
SO_2H	:	Cysteine-sulfinic acid
SO_3H	:	Cysteine-sulfonic acid
SPG11	:	Spatacsin

Srx 1	:	Sulfiredoxin 1
STR	:	Stressed
TDP43	:	TAR DNA binding protein
TEA	:	Triethanolamine
TEMED	:	N,N,N',N'-tetramethylethylenediamine
tRNA	:	Transfer RNA
Trx	:	Thioredoxin
TrxR	:	Thioredoxin reductase
Tween-20	:	Polyoxyethylene-sorbitan monolaurate
Txnip	:	Thioredoxin-interacting protein
UBQLN2	:	Ubiquilin 2
UMN	:	Upper motor neuron
VAPB	:	Vesicle associated membrane protein
VCP	:	Valosin-containing protein
WT	:	Wild-type
YF	:	Tyrosine-phenylalanine
Zn	:	Zinc

1. INTRODUCTION

Motor neuron disease (MND) is a fatal adult-onset neurodegenerative disorder that results in the loss of motor neurons resulting in death 3-5 years after disease onset. Although significant recent progress has been made in delineating the genetic defects responsible for familial MND, what underlies the much commoner sporadic form of the disease remains unknown. Even though some of the genetic deficits underlying familial disease have been known for 20 years, the mechanisms by which motor neuronal death occurs in both familial and sporadic MND remain unclear. Riluzole is the only disease-modifying drug licensed for treatment of MND in the UK, it is only available to a subset of patients and extends life by an average of 3-4 months. Until the mechanisms underlying motor neuronal death have been clarified, improved therapy for patients seems unlikely.

This dissertation presents an investigation of the potential role in MND pathogenesis of a family of anti-oxidant proteins, the peroxiredoxins. The work has been carried out in cellular and animal models of superoxide dismutase 1 (SOD1) and TAR DNA binding protein (TDP43) associated familial MND. This introduction provides an overview of the clinical features of the disease, the challenges of diagnosis and management and the pathogenic hypotheses that have been put forward in an effort to explain what happens to motor neurons in the disease. The classification, molecular mechanisms and functions of the peroxiredoxins are then discussed along with the evidence implicating this family of proteins in the pathogenesis of MND and other neurodegenerative diseases. Finally, the rationale, aims and experimental approach used are summarized to provide an overview of the work carried out.

MOTOR NEURON DISEASE

Motor neuron disease (MND) is an adult-onset, invariably fatal neurodegenerative disorder that causes progressive loss of motor neurons leading to weakness of limb, bulbar and respiratory muscles. Onset is typically in late middle-age. Thereafter disease progresses relentlessly leaving patients unable to use their hands, walk, speak or swallow. Death typically occurs 3-5 years after symptoms first began, most frequently due to respiratory failure (Rowland and Shneider, 2001; Strong and Gordon, 2005). Currently Riluzole is the only drug licensed for use as a disease-modifying therapy in MND. On average, Riluzole extends the lives of MND patients by only 3-4 months (Bensimon et al., 1994; Lacomblez et al., 1996).

1.1 Clinical features

1.1.1 Definitions

Motor neuron disease is the term used in the United Kingdom for a group of neurodegenerative diseases characterized by loss of motor neurons leading to paralysis and ultimately death. The umbrella term MND includes primary lateral sclerosis (PLS), characterized by progressive loss of predominantly upper motor neurons (UMN), progressive muscular atrophy (PMA), distinguished by loss of predominantly lower motor neurons (LMN), and amyotrophic lateral sclerosis (ALS) which involves the loss of both upper and lower motor neurons (Strong and Gordon, 2005). Progressive bulbar palsy (PBP) is a subtype of ALS characterized by degeneration of upper and lower motor neurons innervating predominantly the bulbar muscles. The terms MND and ALS are frequently used interchangeably. In clinical practice, the term MND is often used to describe the most common syndrome, ALS, which accounts for 85% of all patients with MND (Swash, 2003). Overlap exists between PLS, PMA, PBP and ALS. Over time many PLS patients will develop some LMN features whilst many PMA patients will develop some UMN features. Similarly, some patients diagnosed initially with PBP will develop symptoms and signs in the limbs as their disease progresses (Rowland, 2003; Swash, 2003).

1.1.2 Amyotrophic lateral sclerosis

The clinical features of ALS comprise mixed upper and lower motor neuron symptoms and signs. ALS most commonly begins focally in a limb or in the bulbar region. Only rarely is respiratory function affected first. Disease onset is divided more or less evenly between the upper limbs, lower limbs and bulbar region. The disease progresses relentlessly with worsening and more widespread muscle weakness. In the limbs, loss of LMN brings about muscle wasting, fasciculation, muscle cramps, reduced or absent reflexes and reduced muscle tone. Loss of UMN causes hyperreflexia, spasticity (muscle stiffness), and muscle weakness without wasting (Andersen, 2006; Strong and Gordon, 2005). Individual patients may present with predominantly UMN or LMN symptoms and signs or a combination of both in one or more segments (bulbar, cervical, thoracic, lumbar). In the bulbar region, loss of LMN causes tongue wasting, weakness and fasciculation as well as weakness of the soft palate and upper pharynx whilst loss of UMN causes tongue spasticity and a pseudobulbar palsy. Together these are responsible for the dysphagia (difficulty in swallowing) and dysarthria (difficulty in speaking) experienced by ALS patients with bulbar involvement. Patients may eventually require tube feeding and become unable to speak (anarthria). Patients with pseudobulbar palsy are frequently emotionally labile.

The majority of sporadic ALS patients do not suffer from overt cognitive dysfunction although a significant proportion (up to 35%) can be shown to have sub-clinical features in common with sufferers of frontotemporal dementia (FTD) if they undergo formal neuropsychological testing (Tsermentseli et al., 2012). In only approximately 14% of sporadic ALS cases is the neuromuscular dysfunction accompanied by frank dementia. The frequency of clinically significant cognitive dysfunction in familial ALS depends upon the causative mutation (Andersen, 2012; Tsermentseli et al., 2012).

Progressive bulbar palsy

Progressive bulbar palsy (PBP) is a subtype of ALS which presents with symptoms and signs largely confined to the bulbar region. Clinical features reflect upper and lower motor neuron involvement of bulbar motor neurons as described above for ALS. PBP in its pure form (symptoms and signs restricted to the bulbar region for the entire duration of the illness) is rare and there is little information about its incidence and natural history. More commonly, symptoms and signs eventually extend beyond the bulbar region, with the majority of cases having some UMN and/or LMN signs outside the bulbar region at the time of diagnosis. Many go on to develop widespread disease typical of classical ALS. Indeed, autopsy examination of apparently pure PBP has shown typical ALS pathology in lower motor neurons of the spinal cord along with typical pathology in the corticospinal tract (Chad, 2006; Rowland, 2003).

1.1.3 Primary lateral sclerosis

Primary lateral sclerosis is a rare progressive UMN disorder, comprising only 1-3% of MND (Gordon et al., 2006). Patients with PLS typically survive significantly longer (on average almost 3-fold longer) than do those with ALS (Tartaglia et al., 2007). As with ALS, disease usually begins above the age of 40 although a few cases of PLS have been reported in children (Panzeri et al., 2006). The clinical features are those that would be expected from UMN involvement of the limbs and bulbar region. PLS most commonly presents with lower limb symptoms, typically a spastic paraparesis along with brisk tendon reflexes, but a pseudobulbar syndrome can sometimes occur first. Patients with bulbar involvement have dysarthria which may lead to anarthria (a total inability to speak) and are often emotionally labile. Unlike ALS, there are no clinical features of LMN involvement through most of the disease course although, as mentioned above, as the disease reaches its endstage some LMN features may become evident. Progression tends to be much slower than ALS, with one documented case developing LMN features only after 20 years (Bruyn et al., 1995).

1.1.4 Progressive muscular atrophy

Progressive muscular atrophy is a pure LMN syndrome that accounts for approximately 4% of MND cases (Visser et al., 2008). The prognosis of PMA is similar to that of ALS. Patients present with the clinical features that would be expected from LMN involvement of the limbs and bulbar region, that is weakness, wasting, muscle cramps and fasciculation. As there is little or no involvement of UMN, stiffness and emotional lability are not typically seen although, as discussed above, some UMN features may develop late in the disease course. Cognitive dysfunction is observed even less often than is it in ALS patients (Raaphorst et al., 2011). Interestingly, a subgroup of sporadic PMA cases with rapid progression has been identified who presented with LMN signs, but on autopsy were found to have clinically undetected corticospinal tract degeneration and UMN ubiquitinated inclusions typical of ALS (Ince et al., 2003).

1.2 Epidemiology

The worldwide prevalence of ALS is 4-6 per 100 000 with an incidence of 1-2 per 100 000 (Soriani and Desnuelle, 2009). Almost 90-95% of ALS is sporadic, that is it occurs in individuals with no identifiable family history. The remaining 5-10% of cases occur in individuals with a family history of ALS or of ALS/FTD (see Section 1.5). The vast majority of familial ALS is inherited in an autosomal dominant manner. In recent years the number of genes known to contribute to familial ALS has markedly expanded and importantly several mutations in genes known to cause familial ALS have also been found in ALS patients with no family history i.e., in apparently sporadic disease. The significance of this will be discussed in Section 1.5.4.

ALS is largely a disease of late middle-age with onset typically between 50-60 years, although it may less commonly occur in early adulthood and into late old-age. One recent study of 682 ALS patients had a range of age-at-onset from 19 to 92 years of age (Fig 1.1) (Personal communication, Dr C. Wood-Allum). There are also rare juvenile forms of MND many of which are familial (Chance et al., 1998). MND as a whole more commonly affects men. Various sex ratios have been published but a male to female ratio of 1.6:1 is typical (Shaw, 2005). Interestingly, the sex ratio is reversed for bulbar-onset disease, which seems more often to occur in older women.

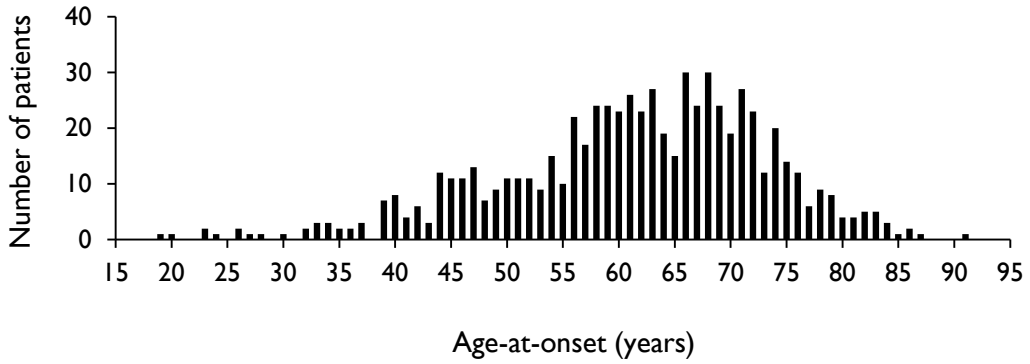

Figure 1.1 *Graph showing age-at-onset of 682 ALS patients from a recent study. Graph reproduced with the permission of Dr C. Wood-Allum.*

Although the incidence of ALS is fairly uniform worldwide where it has been measured, ALS hotspots have been identified in the islands of Guam and in the Kii peninsula of Japan (Kaji et al., 2012). Epidemiological studies conducted in the 1950s reported the incidence of ALS in the islands of Guam to be 50-100 times higher than the world-wide average. The clinical features of this disease were atypical with patients presenting with an ALS-parkinsonism-dementia complex (Plato et al., 2003). A high incidence of ALS in the Kii peninsula was first reported by Kimura and Yase in the 1960s (Kuzuhara, 2007). The clinical phenotype was similar to that of Guam in that patients presented with dementia and extrapyramidal features in addition to their neuromuscular weakness (Yase et al., 2001).

Over the years since there has been a gradual decrease in the incidence of ALS in both these regions, although it still remains higher than elsewhere (Kuzuhara, 2007).

1.2.1 Putative ALS risk factors

Advancing age, male sex and the inheritance of a genetic predisposition (as described above), are the only proven risk factors for the development of ALS. Many other risk factors have been put forward as possible candidates and numerous studies have been carried out to try and establish an association between the exposure and the subsequent development of ALS. These risk factors include dietary and lifestyle choices (Armon, 2009), occupation (Vanacore et al., 2010), environmental and occupational exposure to potentially toxic substances such as pesticides (Furby et al., 2010) and heavy metals and various forms of trauma. Although many have reported a positive association, these studies are inherently difficult to carry out and most are methodologically-flawed in one way or another (Armon, 2003). Individual cases of ALS-like disease have been reported in patients previously exposed to high doses of mercury (Adams et al., 1983; Schwarz et al., 1996), electrical shocks (Jafari et al., 2001) and physical trauma (de Carvalho and Swash, 2004; Gallagher and Sanders, 1987). Although interesting, some of these exposures have also resulted in diseases resembling other neurodegenerative diseases and there is no evidence that any of these exposures are responsible for the majority of sporadic ALS. Some associations have more support than others (smoking and physical exercise, discussed below) but it is reasonable to state that at present there are still no widely-accepted environmental risk factors associated with the development of ALS.

Smoking

In an evidence-based review of studies of exogenous ALS risk factors in 2003, Armon determined smoking as the only 'probable' risk factor and discounted trauma, physical activity and alcohol consumption (Armon, 2003). Kamel et al., showed that smokers had an increased risk (odds ratio=1.7) of developing ALS in his cohort of 109 patients and 256 controls (Kamel et al., 1999). Nelson et al., also showed an increased risk of ALS in the smokers within his study group of 161 patients and 321 controls (Nelson et al., 2000). In a 2009 follow-up review, Armon critically reviewed the literature published on the subject from 2003-2006 and suggested that smoking should now be considered a proven risk factor for ALS (Armon, 2009). A recent prospective longitudinal study of 5 large ALS cohorts containing a total of 832 patients not only suggested that smokers have a significantly higher risk (relative risk of 1.42 and 1.44 for current and former smokers respectively) of developing ALS but that the risk of developing the disease as dependent upon both the duration of smoking and number of cigarettes smoked per day (Wang et al., 2011).

Not all studies, however, came to the same conclusion. A retrospective study by Qureshi (Qureshi et al., 2006) and a meta-analysis by Alonso (Alonso et al., 2010a) demonstrated no significant association of smoking with ALS although Alonso et al. did concede that smoking might be associated with a higher risk of ALS in women (Alonso et al., 2010a; Alonso et al., 2010b). Despite this conflicting

evidence, when the results of all of the studies of smoking and ALS are considered together it seems likely that smoking may represent a contributory risk factor for the development of ALS.

Exercise and physical activity

Excess physical activity has long been suggested as an ALS risk factor. The idea that exercise beyond the norm might, at least in predisposed individuals, lead to the development of ALS is known as the exercise hypothesis. Initially this idea arose from common sense – why might not overused motor neurons "wear out" prematurely in some predisposed individuals? Anecdotally many ALS specialists notice that their MND clinics seem overpopulated with people still physically active well into middle-age.

Interest in the exercise hypothesis of ALS was renewed when a small excess of ALS cases was identified in elite Italian football players in the 1990s. Problems with confounding exposures such as pitch herbicides and performance-enhancing drugs, however, made attribution of causation difficult (Chio et al., 2005). Despite many studies, since it is still unclear whether or not the exercise hypothesis is true or not. This is due to the inherent difficulty of measuring a lifetime's exercise retrospectively in middle-aged ALS patients and controls along with problems factoring out confounding exposures. Although several studies have reported a positive association between exercise and the development of ALS, almost all have significant methodological flaws (Harwood et al., 2009). Meta-analyses of these studies suggest no convincing evidence for an association (Armon, 2009). A recent population-based case-control study by Veldink et al. which attempted to address many of these difficulties found no increase in the risk of ALS in those reporting having undertaken more physical exercise although interestingly, those individuals with ALS who reported higher amounts of leisure time physical activity in their youth had a significantly earlier disease-onset (Veldink et al., 2005).

Even if exercise were proven to predispose some individuals to ALS, exercise avoidance could not be recommended to the general population as a way of reducing ALS risk because exercise has so many other health benefits. There would, however, be implications for our understanding of disease pathogenesis. Of the current pathogenetic hypotheses of ALS the idea that excess motor neuronal firing might predispose some individuals to the disease is at least in theory relevant to two – excitotoxicity and oxidative stress. These will be discussed in more detail in Sections 1.7-1.12.

1.3 Diagnosis

The diagnosis of MND is clinical, supported by evidence obtained from electrophysiological studies. Other investigations such as neuroimaging, CSF examination and blood testing are used to help identify MND mimics in appropriate cases, but no single diagnostic test can confirm or rule out ALS. Thus the diagnosis of MND relies primarily upon careful clinical assessment by an experienced clinician with investigations used to provide supporting evidence and identify features more typical of mimics.

1.3.1 Differential diagnosis

It is difficult to make a confident clinical diagnosis of the ALS form of MND early in the disease course. In practice a working diagnosis must be made to allow the patient access to disease-modifying therapy. This approach inevitably leads to a significant number of both false positives and false negatives. For example, 8% of patients identified in a study of the Scottish ALS Registry who had received a diagnosis of clinically possible or clinically probable ALS were eventually diagnosed with another disease, ~50% of which were potentially treatable (Davenport et al., 1996). As ALS progresses and UMN and LMN signs manifest in a more widespread distribution the differential diagnosis narrows significantly (Table 1.1). The differential of PLS and even more so PMA is larger and cases presenting with a pure UMN or LMN syndrome typically require more intensive investigation before a diagnosis of MND is made.

Amyotrophic lateral sclerosis	**Progressive muscular atrophy**	**Primary lateral sclerosis**
Multi-level spinal cord & root compression	Spinal bulbar muscular atrophy	Hereditary spastic paraplegia
Thyrotoxicosis	Chronic idiopathic demyelinating polyneuropathy	Cervical myelopathy
Inclusion body myositis	Benign cramp fasciculation syndrome	Multiple sclerosis
Dual upper & lower motor neuron pathologies E.g., cervical myelopathy & a concurrent diabetic neuropathy	Multi-focal motor neuropathy with conduction block	

Table 1.1: *A non-exhaustive differential diagnosis of the three forms of MND including the most common differential diagnoses. Adapted from Wood-Allum & Shaw with permission (Wood-Allum and Shaw, 2006).*

Diagnostic criteria for ALS

To create uniformity in the diagnosis of ALS, especially for the recruitment of cases for research, the World Federation of Neurologists produced stringent diagnostic criteria for the diagnosis of ALS. These diagnostic criteria were first established in El Escorial in 1994 and were later revised at Airlie House in 1998 (Brooks et al., 2000). More recently still the incorporation of electrodiagnostic criteria has been recommended by a consensus meeting in Awaji, Japan (de Carvalho et al., 2008) in order to allow the earlier attribution of a diagnosis of ALS. These criteria are yet to be widely accepted.

In order to make a diagnosis of ALS the Airlie House criteria require the presence of symptoms and signs consistent with both UMN and LMN degeneration, with evidence of progression, in the absence of evidence of other disease processes. The criteria also make provision for the classification of diagnostic certainty. In order for ALS to be considered clinically definite there must evidence of UMN and LMN involvement in at least three of the following regions: bulbar (speech and swallowing), cervical (upper limbs), thoracic (respiratory), and lumbar (lower limbs) (Brooks et al., 2000).

Progressively less stringent criteria classify less certain cases into clinically probable, clinically probable, laboratory-supported and clinically possible ALS to allow the inclusion of less well-advanced patients in research trials. By the time patients meet the diagnostic criteria for clinically definite ALS they are by definition a considerable way into their disease course. There is an urgent need for a diagnostic test allowing a firm diagnosis to be made at a time when there are motor neurons still left to salvage.

1.4 Treatment

1.4.1 Disease-modifying therapy

Riluzole

Riluzole (2-amino-6-(trifluoromethoxy)-benzothiazole) is the only drug licensed for use as a disease-modifying agent in ALS. It is a benzothiazole, hypothesized to exert its protective effects upon motor neurons principally by blocking the presynaptic release of glutamate (Cheramy et al., 1992; Martin et al., 1993), although additional mechanisms are believed to contribute to its neuroprotective effect (Doble, 1996). The evidence for the effectiveness of Riluzole is sound (Miller et al., 2009) and was initially based on two randomized, controlled trials (Bensimon et al., 1994; Lacomblez et al., 1996). These trials indicated a modest increase in the survival of ALS patients by on average 3-4 months.

The Bensimon trial was a double-blinded, randomised trial of 100 mg Riluzole *vs* placebo (Bensimon et al., 1994). After 12 months, 58% of the placebo group was alive compared to 74% of the Riluzole-treated group and this difference was statistically significant. Of the patients in the bulbar-onset subgroup, 35% of those taking placebo were alive at 12 months compared to 73% of those taking Riluzole and this difference was again statistically significant. In the limb-onset sub-group, only a trend towards increased survival over the placebo group was observed.

The Lacomblez trial was conducted as a randomized, multi-centre, placebo-controlled, dose-ranging double-blinded study of 959 ALS patients. The trial showed that 50.4% of the placebo-treated and 56.8% of the Riluzole-treated group (100 mg/day) were alive at 18 months without intervention. In other words, there was a decrease in the risk of death or intervention (tracheostomy) of around 35% for patients receiving 100 mg riluzole. No additional benefit of higher doses was seen but there was an increased incidence of side-effects. This trial included a higher proportion of bulbar-onset patients than did the Bensimon trial and improvement in survival in riluzole-treated patients was statistically-significant in both bulbar and limb-onset patient sub-groups.

Riluzole is generally well tolerated and it is now standard practice in the UK to consider Riluzole treatment for almost all ALS patients on diagnosis. Current NICE guidelines, however, mandate the use of Riluzole for the ALS form of MND only (NICE website, accessed on 16th Sept 2012).

Other putative disease-modifying drugs

Over the last 15 years there have been many clinical trials of other potential disease-modifying agents in ALS. Many of these candidates showed promise in the transgenic mutant superoxide dismutase 1 (SOD1) mouse model of ALS. Unfortunately even the most successful agents trialled in ALS mice have had no effect in patients, leading to a reassessment of the utility of this model in the assessment of therapeutic candidates (Joyce et al., 2011; Turner and Talbot, 2008). Unsuccessful therapeutic trials in ALS patients have included various anti-oxidants (Graf et al., 2005; Louwerse et al., 1995), several neurotrophic factors (Lai et al., 1997; The BDNF Study Group, 1999), agents directed rather non-specifically at improving mitochondrial health (Shefner et al., 2004) and others directed against excitotoxicity (Cudkowicz et al., 2003; Gurney et al., 1996; Miller et al., 2001). At present, there are several other potential therapeutic agents at various stages of clinical testing. These include Dexpramipexole (Biogen Idec), Lithium carbonate, TRO19622 (Trophos Pharmaceuticals) and Memantine (MNDA website, accessed on 20th Oct 2012). Discussion of as yet unreported clinical trials, however, lies beyond the scope of this Introduction.

Future therapeutic directions

The pathogenesis of motor neuron degeneration is complex and appears to be due to multiple mechanisms (see Sections 1.7-1.12). Given this it is likely that giving patients a combination of drugs targeting different pathways will have the most impact on disease progression (McDermott and Shaw, 2008). Better targeted therapy also seems likely to be helpful, for example using viral vectors targeted to the motor neuron to deliver protective compounds (Azzouz et al., 2000; Ralph et al., 2005). This approach was shown to be effective in a transgenic SOD1 mouse model, where injecting adeno-associated virus expressing insulin-like growth factor 1 (IGF-1) directly into respiratory and limb muscles prolonged survival (Kaspar et al., 2003). Stem cell therapy aimed at the replacement of dead motor neurons by injecting neuronal stem cells into the spinal cord is another potential approach under active investigation. Stem cell therapy must overcome numerous challenges, for example the difficulty in encouraging replacement motor neurons to form effective connections and the fact that new axons would have to extend up to a metre to reach the periphery. A recent study, however, showed that stem cells might have a beneficial effect on the motor neurons of ALS patients via alternative mechanisms (Mazzini et al., 2008). Replacement of glial cells rather than motor neurons may be an alternative option as there is evidence that wild-type non-neural cells are able to slow disease progression in the SOD1 mutant mouse (Clement et al., 2003). Providing a healthy environment for affected motor neurons appeared to ameliorate the effects of the mutation.

It has been estimated that by the time patients first present with ALS they have already lost up to 50% of their motor neurons. The ability to make an earlier, confident diagnosis of ALS would allow novel disease-modifying therapies to be applied at a time when more motor neurons were still alive. The identification of novel biomarkers to aid earlier diagnosis has become a priority for this reason. At present efforts are also underway to better stratify ALS patients. Many investigators suspect that there

are likely to be sub-groups of patients more or less likely to respond to disease-modifying drugs and that the inclusion of unstratified ALS patients within clinical trials of new agents may be partially responsible for recent disappointing results. The identification of biomarkers of such subgroups is another research priority (Ganesalingam and Bowser, 2010).

1.4.2 Symptomatic therapies

With no curative treatment currently available, symptomatic therapy aimed at alleviating the symptoms that arise during the course of ALS is important for improving patients' quality of life (Talbot, 2002). There are two interventions directed chiefly towards relief of symptoms which also have the potential modestly to prolong life. The first of these is the use of non-invasive ventilation (NIV) in MND patients who have developed respiratory muscle weakness, the second the use of tube feeding in patients who have lost the ability safely to swallow. A detailed consideration of other symptomatic therapies used in ALS will not be provided here, however, a good review of this topic is provided by McDermott & Shaw (McDermott and Shaw, 2008).

Non-invasive ventilation

Hypoventilation due to diaphragmatic and intercostal muscle weakness, which initially occurs mainly during sleep, can severely diminish a patient's quality of life, causing frequent wakening, early morning headaches, daytime sleepiness and anorexia. Non-invasive ventilation (NIV) delivered via a portable ventilator using a strap-on mask efficiently alleviates these symptoms and can be used at home. A randomised controlled trial found that NIV increased survival by around seven months and improved quality of life in patients with good bulbar function (Bourke et al., 2006). Importantly, the effect of NIV on survival was much greater than that offered by Riluzole (Bourke et al., 2006). NIV is less well-tolerated in patients with significant bulbar dysfunction.

Enteral feeding

Dysphagia is a common problem in ALS. Initial management involves modification of food consistency and advice regarding safe swallowing. As the disease progresses, loss of limb strength and dexterity combined with dysphagia can cause weight loss and malnutrition which can accelerate the progression of the disease. Once a patient has lost more than 10% of their pre-morbid body weight, their body mass index decreases below 18.5, or they are having frequent choking attacks when eating, enteral feeding may be offered. Tubes may be placed endoscopically using percutaneous endoscopic gastrostomy (PEG) or in frailer patients using radiological guidance (percutaneous radiological gastrostomy - (PRG) or Per-oral image-guided gastrostomy - (PIG) (Chavada et al., 2010; Thornton et al., 2002). This allows water, nutrition and medication to be administered without danger of aspiration but does not preclude patients continuing to take some food they enjoy by mouth while it remains safe. Whilst no randomized clinical trial of enteral feeding existed at the time of the most recent Cochrane review, the reviewers tentatively concluded that enteral feeding had the potential to modestly prolong life (Chavada et al., 2010).

1.5 Familial ALS

As has been discussed above, the majority of ALS is sporadic (sALS), that is, patients have no identifiable family history. The remaining 5-10% of ALS is familial (fALS). The genes responsible for approximately 70% of fALS have now been identified (Figure 1.2 & Table 1.2), although the means by which these mutated genes cause motor neurons to die remains unclear. Most familial ALS cases are inherited in an autosomal dominant manner. Those arising from autosomal recessive, X-linked or other modes of inheritance appear to be rare (Andersen et al., 1995; Jonsson et al., 2002). There has been a spate of recent new gene discoveries in ALS. The most significant of these was the very recent report that as many as 40% of fALS cases are caused by an expansion in the number of a GGGGCC hexamer repeat found in a non-coding region of the Chromosome 9 open reading frame 72 gene (C9Orf72) (DeJesus-Hernandez et al., 2011; Renton et al., 2011). Mutations in the Cu/Zn Superoxide Dismutase gene (SOD1) account for approximately 20% of fALS (Rosen et al., 1993; Shaw, 2005). Two RNA processing proteins - TAR DNA binding protein (TDP43) and fused in sarcoma/translated in liposarcoma (FUS/TLS) each appear to account for approximately 5% of fALS. Thus, C9Orf72, SOD1, TDP43 and FUS/TLS together account for approximately 70% of familial ALS cases (C9Orf72 = 40%, SOD1 = 20%, TDP43 = 5%, FUS/TLS = 5%). Several other genes have been identified which each appear to be responsible for only a very small proportion of the remainder (see Table 1.2) leaving the genes responsible for almost 30% of inherited ALS yet to be identified. Interestingly, the strict demarcation between familial and sporadic ALS seems likely to become blurred with increasing reports of mutations known to cause familial ALS being identified in ALS patients without a family history. The significance of these mutations in apparently sporadic cases will be discussed in Section 1.5.4.

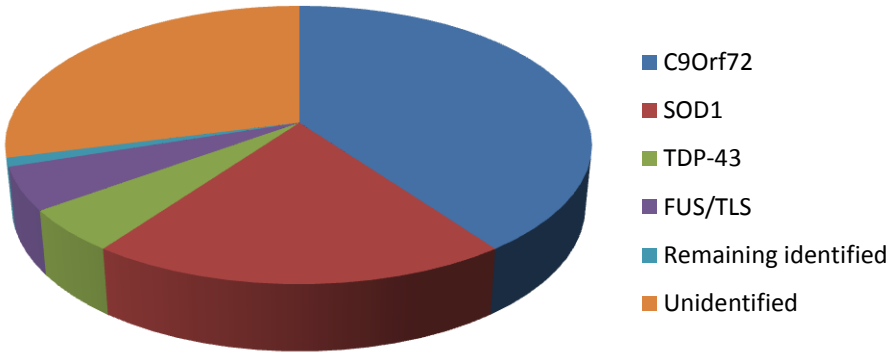

Figure 1.2: *Pie chart showing the genes responsible for familial ALS, each displayed as a percentage of all fALS.*

ALS type	Inheritance	Gene	Protein	Locus	Reference
ALS1	Dominant	*SOD1*	CuZn superoxide dismutase 1	21q22.1	(Rosen et al., 1993)
ALS2 (juvenile onset)	Recessive	*ALSIN*	Alsin	2q33	(Hadano et al., 2001; Hentati et al., 1994; Yang et al., 2001)
ALS3	Dominant			18q21	(Hand et al., 2002)
ALS4 (juvenile onset)	Dominant	*SETX*	Senataxin	9q34	(Chen et al., 2004)
ALS5	Recessive	*SPG11*	Spatacsin	15q15-q22	(Hentati et al., 1998; Orlacchio et al., 2010)
ALS6	Dominant	*FUS/TLS*	Fused in sarcoma/Translated in liposarcoma	16q12	(Kwiatkowski et al., 2009; Ruddy et al., 2003; Vance et al., 2009)
ALS7	Dominant			20ptel-p13	(Sapp et al., 2003)
ALS8	Dominant	*VAPB*	Vesicle associated membrane protein	20q13.33	(Nishimura et al., 2004)
ALS9	Dominant	*ANG*	Angiogenin	14q11.1	(Greenway et al., 2006)
ALS10	Dominant	*TARDBP*	TAR DNA binding protein	1p36.22	(Kabashi et al., 2008b; Sreedharan et al., 2008)
ALS11	Dominant	*FIG4*	Polyphosphoinositide phosphatase	6q21	(Chow et al., 2009)
ALS12	Recessive	*OPTN*	Optineurin	10p13	(Maruyama et al., 2010)
ALS13	Dominant	*ATXN2*	Ataxin 2	12q24	(Elden et al., 2010)
ALS14	Dominant	*VCP*	Valosin-containing protein	9p13-p12	(Johnson et al., 2010)
Other fALS phenotypes outwith the numbered scheme					
ALS-X	Dominant X-linked	*UBQLN2*	Ubiquilin 2	Xp11–q12	(Deng et al., 2011; Siddique et al., 1998)
ALS-D	Dominant	*MAPT*	Microtubule associated protein tau	17q21	(Hutton et al., 1998)
ALS-FTD	Dominant	*C9Orf72*	Chromosome 9 Open reading frame 72	9p21–22	(DeJesus-Hernandez et al., 2011; Hosler et al., 2000; Renton et al., 2011)

Table 1.2: *A genetic classification of ALS. Compiled with the aid of Ferraiuolo et al., (Ferraiuolo et al., 2011).*

1.5.1 CuZn Superoxide Dismutase 1 (SOD1)-related fALS

Evidence that mutations in SOD1, a ubiquitously expressed free radical scavenger, were responsible for a proportion of fALS came initially from linkage analysis (Rosen et al., 1993; Siddique et al., 1991). Since then, over 165 ALS-causing mutations spanning the entire SOD1 gene have been reported (ALSOD website, accessed on 15th Oct 2012).

Function of wild-type CuZn superoxide dismutase

CuZn superoxide dismutase is an abundant anti-oxidant enzyme. It serves to detoxify the superoxide free radical ($O_2^{\bullet-}$), preventing oxidative damage to intracellular macromolecules. The generation of reactive oxygen species (ROS) such as superoxide is an inevitable consequence of cellular metabolism. Superoxide is generated by complexes 1 and 3 of the electron transport chain during the synthesis of ATP and is released from the inner mitochondrial membrane (Han et al., 2001). As superoxide does not readily cross membranes, it needs to be dealt with at the site of generation. The presence of SOD1 in the intermembrane space of mitochondria is therefore important. Inadequate removal of superoxide will result in the generation of even more reactive species causing oxidative damage to cellular components which may even result in the initiation of apoptosis (Boveris et al., 1972; Chance et al., 1979).

Structure and mechanism of action of wild-type SOD1

CuZn superoxide dismutase (present in the cytosol and mitochondrial intermembrane space) and manganese superoxide dismutase (SOD2) (present within the mitochondria matrix) detoxify superoxide by converting it to hydrogen peroxide (H_2O_2) via a dismutase reaction. Other anti-oxidants (see Section 1.13) then deal with the resultant H_2O_2. Wild-type SOD1 functions as a homodimer. Each SOD1 monomer is 153 amino acids in length and contains a copper-binding site, a zinc-binding site and an internal disulphide bond. The active site of the enzyme is the copper-binding site where the superoxide free radical ($O_2^{\bullet-}$) is reduced to hydrogen peroxide (H_2O_2). The reaction requires the loading of copper by the copper chaperone for SOD1 (CCS) protein during catalysis (Corson et al., 1998). SOD1 then catalyzes the conversion of superoxide ($O_2^{\bullet-}$) to hydrogen peroxide via a dismutase reaction which occurs in two-steps:

1) $O_2^{\bullet-} + Cu^{2+}ZnSOD \rightarrow O_2 + Cu^{+}ZnSOD$

2) $O_2^{\bullet-} + 2H^{+} + Cu^{+}ZnSOD \rightarrow H_2O_2 + Cu^{2+}ZnSOD$

The overall reaction is therefore:

$2O_2^{\bullet-} + 2H^{+} \rightarrow H_2O_2 + O_2$

SOD1 mutations cause ALS via a toxic gain of function

The exact mechanism by which mutant SOD1 causes first the dysfunction then the death of motor neurons in fALS remains unclear. The leading hypotheses will be considered in Sections1.7-1.12. What is, however, certain is that SOD1 mutations that cause autosomal dominant ALS do so via a toxic gain of function rather than haplo-insufficiency or loss of function. Evidence for the toxic gain of function of mutant SOD1 comes from experiments in knock-out and transgenic mice as well as activity studies of mutant SOD1. Knock-out mice completely lacking SOD1 (Reaume et al., 1996) and transgenic mice engineered to overexpress wild-type (WT) human SOD1 do not develop any ALS-like motor phenotype (Dal Canto and Gurney, 1995; Jaarsma et al., 2000). Transgenic mice engineered to overexpress mutant human SOD1 species known to cause fALS in patients, however, develop a motor deficit that is strikingly similar to ALS (Gurney et al., 1994; Wong et al., 1995). Furthermore, when the dismutase activity of various species of mutant SOD1 was measured it was shown that many (the so-called wild-type group of mutations) produce a SOD1 protein with the same or even greater dismutase activity as the wild-type protein (Borchelt et al., 1994; Valentine and Hart, 2003).

RNA-silencing experiments in G93A SOD1 transgenic mice provide additional evidence. The introduction of short hairpin RNA against the mutant human SOD1 species using lentiviral vectors injected intraspinally (Raoul et al., 2005) and into muscle (Ralph et al., 2005) of G93A SOD1 transgenic mice delayed the onset of disease and significantly prolonged the survival of the animals indicating that mutant SOD1 does not act via a loss of function but through a toxic gain of function.

That mutant SOD1 causes ALS via toxic gain of function and not by a loss of function or haploinsufficiency is now clear. Exactly how over a hundred different mutations affecting almost all of the coding sequence of a ubiquitously expressed anti-oxidant protein can bring about the progressive death of motor neurons is much less clear.

Clinical features of SOD1-related familial ALS

Familial and sporadic ALS are often clinically indistinguishable. It is not unusual for familial cases to have an earlier onset although this is by no means always the case. Some disease-causing mutations confer an identifiable phenotype which may include a modified prognosis. For example, in A4V (Aoki et al., 1993; Deng et al., 1993) and H48Q (Enayat et al., 1995) SOD1 fALS, disease progression is rapid, leading to death within 2-3 years whereas H46R SOD1 fALS (Aoki et al., 1993; Ratovitski et al., 1999) and G37R SOD1 fALS (Cudkowicz et al., 1997) have an unusually long disease course that may extend up to 17 years. Some ALS-causing mutations confer a susceptibility to non-motor disorders along with ALS. The occurrence of these conditions within a family may provide clues as to the responsible gene.

1.5.2 Chromosome 9 open-reading frame 72 (C9Orf72)-related fALS

Recently the genetic defect responsible for a significant portion of familial ALS, and possibly also a small proportion of sporadic ALS has been discovered on chromosome 9, a locus known to be involved in

familial ALS for over 10 years. The locus at Chr9p21-p22 was first identified by Hosler et al. by linkage analysis of families whose affected members suffer ALS, frontotemporal dementia (FTD) or a combination of both, known as ALS-FTD (Hosler et al., 2000). Whilst others had since confirmed the association of ALS-FTD with this locus (Morita et al., 2006; Vance et al., 2006) it was only very recently discovered that the underlying genetic defect is an expansion of the numbers of a hexamer repeat (GGGGCC) within a non-coding region of C9Orf72, a previously unidentified gene present within the Chr9p locus (DeJesus-Hernandez et al., 2011; Renton et al., 2011). Using repeat-primed PCR in a cohort of ALS-FTD cases and a Finnish ALS cohort, it has been demonstrated that individuals with more than 30 repeats of the non-coding hexamer are likely to develop ALS, ALS-FTD or FTD alone. Results from the study showed that the repeat expansion is the genetic cause of ~40% of fALS and is present in ~7% apparently sporadic ALS cases.

Since publication of the C9Orf72 gene, groups from around the world have sought the expansion of hexamer repeats in their cases (Rademakers, 2012). This has not only confirmed the large proportion of familial cases associated with this genetic change in numerous cohorts from different countries but has also identified expanded hexamer repeats within C9Orf72 in a very small percentage of non-ALS forms of MND. Using repeat-primed PCR, analysis of repeat expansions of C9Orf72 within a large Dutch cohort showed that the repeat expansion was found in ~37% of fALS and ~6% of sALS cases (van Rheenen et al., 2012). This study also showed the C9Orf72 expansion to be associated with ~1% of PLS and PMA. Interestingly, a study conducted on a Japanese cohort of 168 patients (58 familial and 110 sporadic cases), identified expanded hexamer repeats in only ~3.4% of fALS and in no sALS cases at all. The authors suggested that this discrepancy with findings in European and USA cohorts might be accounted for by either low penetrance of C9Orf72 in their Japanese population or else the fact that C9Orf72 repeat expansion-related ALS was rare in the Japanese cohort (Konno et al., 2012; Rademakers, 2012). Since the discovery of the hexamer repeat in C9Orf72, work has begun in earnest to establish the normal function of the gene and what the effects of the expanded intron are. To date no studies have been published.

Other work has been directed towards establishing whether C9Orf72-related ALS has an identifiable clinical and/or pathological phenotype. A recent study in a French ALS cohort showed that C9Orf72-related fALS did have a number of identifiable characteristics (Millecamps et al., 2012). Analysis of genotype-phenotype correlations within the French cohort showed that C9Orf72-related fALS patients had a shorter disease duration, were more likely to develop cognitive impairment and presented more commonly with bulbar onset than non-C9Orf72 fALS and non-C9Orf72 sALS. A similar UK study conducted by Cooper-Knock et al., showed that in a cohort of 563 ALS cases from the North of England revealed 62 cases carrying the C9Orf72 expansion. Of the total 563 cases, C9Orf72 expansion was identified in 43% of fALS patients (27/63) and in 7% of sALS patients (35/500). These cases demonstrated rapid disease progression and had a significantly shorter disease duration

than non-C9Orf72 ALS patients (both sALS and fALS). Of the 62 C9Orf72 cases, in 22 either the patient or a close family relative had dementia (Cooper-Knock et al., 2012).

Recent work suggests that C9Orf72-fALS patients more frequently present with evidence of cognitive impairment than is the case for other forms of fALS. The form of cognitive impairment typically observed in C9Orf72 cases most frequently reflects that observed in FTD. Evidence of a cognitive overlap between ALS and FTD has been demonstrated by neuropsychological testing in studies of families with members presenting with ALS, FTD, or ALS-FTD in whom linkage analyses show the Chr 9 locus to be the genetic cause (Boxer et al., 2011; Gijselinck et al., 2010; Morita et al., 2006). A recent population-based study in an Irish ALS cohort identified cognitive impairment in up to 50% of C9Orf72-related fALS cases compared to only 12% of non-C9Orf72 fALS cases (Byrne et al., 2012). These cases included those with a frank clinical presentation of dementia and those with more subtle sub-clinical deficits identified by neuropsychological testing. Formal neuropsychological testing further demonstrated that patients with C9Orf72 expanded repeats were more likely to present with cognitive deficits typical of the behavioural variant of FTD rather than the language variant. Lastly, neuroimaging using 3T MRI in these patients showed characteristic structural changes in non-motor cortex including areas of the frontal lobes and cingulate gyrus featuring reduced grey-matter volume absent from controls and non-C9Orf72 fALS cases (Byrne et al., 2012). This evidence, taken together with emerging evidence of C9Orf72-specific clinical and pathological phenotypes suggest that the presence of expanded hexamer repeats in C9Orf72 may define a subtype of fALS.

Examination of the pathology of C9Orf72-ALS cohort studied by Cooper-Knock et al. showed TDP43-positive inclusions within motor neurons, p62 reactivity in non-neuronal cells and extra-motor pathology in which similar inclusions were demonstrated within neurons in the frontal cortex and hippocampus (Cooper-Knock et al., 2012). Although TDP43-positive inclusions and p62 immunoreactivity are observed in other forms of ALS (see Section 1.6), the authors concluded that the presence of these inclusions in the CA4 area of the hippocampus was specific to C9Orf72-ALS and that this feature could distinguish C9ORf72 pathology from that of other forms of ALS (Cooper-Knock et al., 2012). Using immunohistochemistry on post-mortem brain tissue from a cohort including both sALS and fALS cases, Brettschneider et al. showed that ubiquilin-2 positive neuronal inclusions were present in the cerebral granular layer and in hippocampal neurons in C9Orf72-related sALS and fALS cases but were absent from non-C9Orf72 cases (Brettschneider et al., 2012). Ubiquilin-2 (*UBQLN2*) is a member of the ubiquitin-like protein family, mutations of which cause a rare form of X-linked ALS (Brettschneider et al., 2012; Deng et al., 2011). The discovery that a significant subset of familial ALS is caused by an expanded hexamer repeat within an intron of C9Orf72 adds another neurodegenerative disorder to the growing family of repeat-expansion disorders. It also provides further support for the idea that some neurodegenerative disorders may have underlying pathogenic mechanisms in common.

1.5.3 FALS associated with RNA processing genes

Mutations in two genes coding proteins known to have roles in RNA processing (amongst other functions) have recently been shown to cause familial ALS. A number of mutations (>15) in the 3' region of TAR DNA binding protein (TDP43) have been shown to be linked to both sporadic and familial ALS cases (Kabashi et al., 2008b; Sreedharan et al., 2008). Mutations (>10) in another RNA processing protein, Fused in sarcoma/Translated in liposarcoma (FUS/TLS) – a functional homolog of TDP43 – have also been shown to cause fALS (Kwiatkowski et al., 2009; Vance et al., 2009). Though the exact role played by the mutant forms of these RNA processing proteins has not yet been elucidated, it has been shown that the mutant forms of the proteins are mislocalized within the cell (Kwiatkowski et al., 2009; Winton et al., 2008) and form characteristic pathological inclusions within motor neurons (Neumann et al., 2006). TDP43 associated fALS cases show TDP43 and ubiquitin-positive neuronal inclusions (Sreedharan et al., 2008), which are negative for SOD1 (Mackenzie et al., 2007). FALS cases associated with mutations to FUS/TLS show FUS-positive motor neuronal cytoplasmic inclusions which are mostly negative for ubiquitin and do not stain for TDP43 (Blair et al., 2010; Vance et al., 2009).

1.5.4 Genetic aetiology in apparently sporadic ALS

There is now evidence that some cases of ALS without an obvious family history have mutations in genes known to cause familial disease. These cases have been termed "apparently sporadic" and may arise due to a number of possible mechanisms including variable penetrance of a pathogenic genetic change or else to modifying effects of other genes on an otherwise pathogenic genetic change. One of the most significant examples of this is the recent discovery of the C9Orf72 expansion repeat (Section 1.5.2) in ~4-7% of sALS cases (Byrne et al., 2012; Konno et al., 2012). There are also similar reports of SOD1 mutations in between 1% and 7% of apparently sporadic ALS patients, the exact frequency varying study to study (Jones et al., 1994; Pasinelli and Brown, 2006; Shaw et al., 1998; Weiss et al., 2006). Mutations in TDP43 and FUS/TLS, each associated with ~5% of fALS have also each been detected in ~1% of apparently sporadic ALS cases (Chio et al., 2011; Ferraiuolo et al., 2011). Mutations in certain other genes, including angiogenin and progranulin (Schymick et al., 2007), have been identified that also, rarely, appear to be associated with sALS cases. Mutations in peripherin have been reported in two sALS patients (Gros-Louis et al., 2006; Schymick et al., 2007). Whether or not these mutations, found in individuals with ALS and no family history, can confidently be said to have caused the disease is far from clear. It seems likely that some will prove to be causative whilst others will not. It can only be speculated whether mutations identified in fALS-associated genes in some apparently sporadic ALS patients might act as predisposing factors, contributing to some extent to disease pathogenesis if not acting as the sole cause of disease.

1.6 Pathological features

Pathologically, ALS is characterized by the loss of UMN in the motor cortex and the loss of LMN in the brainstem and spinal cord. By the time patients become symptomatic it has been estimated that at

least 50% of their vulnerable motor neurons have already been lost. By the time brain and spinal cord from ALS cases comes to autopsy the loss of bulbar and spinal motor neurons is even more profound. Accompanying the loss of motor neurons there is often loss of UMN axons from the anterior and lateral corticospinal tracts accompanied by gliosis. Gliosis (an excess of astrocytes) may also be observed surrounding both spinal motor neurons and upper motor neurons in the motor cortex. Interestingly, motor neurons within the occulomotor, abducens and trochlear nuclei in the brainstem (responsible for eye movements) and Onuf's nucleus in the sacral spinal cord (which innervate the pelvic floor musculature) are spared (Ince et al., 1998).

1.6.1 Proteinaceous inclusions

A pathological hallmark of ALS is the presence of proteinaceous inclusion bodies within motor neurons and surrounding astrocytes (Kato et al., 1999). These inclusions may be found in the cytoplasm, the nucleus or in both. The proteinaceous inclusion bodies in ALS include skein-like inclusions, round compact inclusions, Bunina bodies and Lewy-body like hyaline conglomerates (LBHI). These will each be considered in turn.

Skein-like and round compact inclusions

Neuronal cytoplasmic skein-like and round compact inclusions are a common feature of sALS and mutant TDP43 associated fALS (Piao et al., 2003). They are typically immunopositive for ubiquitin, TDP43 and p62 (an antibody that recognises sequestosome 1, a protein which participates in the ubiquitin-proteasome machinery) and are negative for neurofilaments and SOD1. These inclusions are the most specific molecular marker for ALS and are found in nearly 100% of ALS patients, including non-TDP43-fALS. Similar inclusions have also been reported in spinal cord tissue from clinical variants of ALS including PMA and PLS (Hays, 2006; Wharton and Ince, 2003). They are often accompanied by glial cytoplasmic inclusions which also show TDP43 and p62 immunoreactivity. Some consist of a single intracytoplasmic fibril or a loosely arranged aggregate of fibrils while others are round or irregular dense bodies, with homogenous or fibrillary substructures (Hays, 2006).

Bunina bodies

Bunina bodies are small, eosinophilic inclusions that are predominantly localized to the soma (Bunina, 1962). They are comparatively smaller than the skein-like ALS inclusions and are present in up to 85% of ALS cases, both sporadic and familial (Wood et al., 2003a). They are immunoreactive for the protein cystatin C (Okamoto et al., 1993) but are negative for ubiquitin, TDP43 and p62. They have ultrastructural properties suggestive of a lysosomal origin (Kato, 2008). Bunina bodies are highly specific for ALS and are rare in the motor neurons of patients suffering from other neurological disorders. They do not, however, confer the same degree of diagnostic specificity as ubiquitinated skein-like & round compact inclusions (Hays, 2006; Wharton and Ince, 2003).

Hyaline conglomerate inclusions

Hyaline conglomerate inclusions (HCI) have a glassy appearance (so-termed hyaline) and immunostain positively for neurofilaments (Kondo et al., 1986). They are highly immunoreactive for both medium and heavy chain, phosphorylated and unphosphorylated, neurofilament protein. Occasionally they also stain positively for peripherin (He and Hays, 2004; Reijn et al., 2009). Hyaline conglomerate inclusions are not a common finding in ALS as a whole although they are more common in association with SOD1-related fALS (Bigio et al., 2003). When HCI are present they are predominantly found in the cytoplasm of the soma.

Pathology and immunostaining of proteinaceous inclusions in fALS

The pathobiology of fALS patients is often defined by the specific disease-causing mutation. Mutant SOD1 fALS cases typically show degeneration of the posterior columns of the spinal cord and feature neuronal LBHIs and astrocytic hyaline inclusions that are strongly immunoreactive for wild-type and mutant SOD1 granule-coated fibrils but negative for TDP43 (Mackenzie et al., 2007). These inclusions are sometimes negative for ubiquitin and p62 (Suzuki et al., 2008). Familial ALS cases associated with mutations of the gene for FUS/TLS feature FUS-positive neuronal cytoplasmic inclusions. These inclusions are mostly negative for ubiquitin and are strictly negative for TDP43 (Blair et al., 2010; Vance et al., 2009).

The discovery that TDP43 was the main constituent of ubiquitinated inclusions was the first step in the identification of mutant TDP43-related fALS cases (Neumann et al., 2006). That TDP43 also co-localized with ubiquitinated inclusions in frontotemporal lobar degeneration (FTLD), the most common form of frontotemporal dementia (FTD) led to the recognition that ALS and FTLD had pathology (and in some cases pathogenesis) in common (Neumann et al., 2006). There is now a growing body of evidence arising from these TDP43 pathology findings that suggests that ALS and FTLD can be considered to lie at opposite ends of a common clinico-pathological spectrum, collectively now described as the TDP43 proteinopathies (Lin and Dickson, 2008). The recent discovery of C9orf72-fALS (Section 1.5.2) in which ALS, FTLD and mixed ALS-FTLD cases can exist within one family and result from individuals carrying the same causative mutation reiterates this point.

PATHOGENETIC HYPOTHESES IN ALS

The underlying cause of sporadic ALS is unknown. At present no single hypothesis can by itself explain all the salient features of sALS, namely its adult-onset, the relatively selective loss of both upper and lower motor neurons and the sparing of oculomotor and sacral motor neurons. It seems likely that a combination of pathogenetic mechanisms is likely to bring about motor neuronal death. As has already been discussed (Section 1.2.1), there are few proven risk factors for the development of the disease so

the reason why particular individuals are unlucky enough to develop sALS is also largely unknown. Many authorities favour a multi-hit mechanism by which a combination of genetic background, the effects of ageing and environmental exposures or lifestyle choices tip some individuals into motor neuron degeneration whilst others live on into old age with an adequately functioning motor system.

Multiple hypotheses have been proposed to explain the underlying pathogenesis of ALS. These include oxidative stress, mitochondrial dysfunction, impaired RNA processing, protein aggregation, excitotoxicity and defective axonal transport. There is also evidence for the involvement of non-neuronal cells (Yamanaka et al., 2008) and endoplasmic reticulum-mediated stress (Lautenschlaeger et al., 2012). Each of the major hypotheses is supported by a body of evidence, some of which is presented below. Much of the work supporting these mechanisms of motor neuron degeneration was done in models of SOD1-related fALS. Those mechanisms thought to be of particular relevance to the pathogenesis of SOD1 fALS will be highlighted.

1.7 Oxidative stress

The generation of free radicals and their subsequent metabolism by free radical scavenging enzymes is an integral part of cellular metabolism. The balance between the rate at which free radicals are generated and scavenged is critical and is highly regulated by the cellular anti-oxidant system. Any imbalance in this system such that more free radicals are generated than can be dealt with by cellular anti-oxidants causes oxidative stress (Sies, 1997) and secondary oxidative damage to cellular macromolecules.

1.7.1 Free radicals

The principal free radicals are the superoxide anion ($O_2^{\bullet -}$), the hydroxyl radical ($OH^{\bullet}$) and nitric oxide ($NO^{\bullet}$). Free radicals and their downstream reaction products such as hydrogen peroxide (H_2O_2), peroxynitrite ($ONOO^-$) and hypochlorous acid (HOCl) are collectively known as reactive oxygen species (ROS) (Knight, 1998). Free radicals arise due to the "leak" of electrons from complexes I and III of the electron transport chain during the generation of ATP by oxidative phosphorylation (Turrens, 1997). Excess ROS cause oxidation of proteins, lipids and DNA. Motor neurons are post-mitotic cells and thus are more likely to suffer functional consequences from cumulative oxidative damage if excess ROS are not cleared promptly by anti-oxidants (Imlay, 2003).

1.7.2 Cellular anti-oxidant defence

Cellular anti-oxidant defence comprises 1) anti-oxidant enzymes such as Cu/Zn superoxide dismutase (SOD1), catalase, and peroxidases such as the glutathione peroxidases and peroxiredoxins; 2) heat shock proteins (HSP) that function to repair oxidatively damaged proteins; and 3) other proteins such as albumin and transferrin that reduce the availability of pro-oxidant species such as the transition

metals that are potential generators of the hydroxyl and peroxide ($OOH^{\bullet}$) radicals via the Fenton reaction (Sies, 1997).

$$H_2O_2 + Fe^{2+} \rightarrow OH^{\bullet} + OH^{-} + Fe^{3+}$$
$$Fe^{3+} + H_2O_2 \rightarrow OOH^{\bullet} + Fe^{2+}$$

Superoxide dismutases, including SOD1, catalyze the sequential reduction of two superoxide radicals to H_2O_2:

$$Cu^{2+}\ SOD + O_2^{\bullet -} \rightarrow Cu^{+}\ SOD + O_2$$
$$Cu^{+}\ SOD + O_2^{\bullet -} + 2H^{+} \rightarrow Cu^{2+}\ SOD + H_2O_2$$

Peroxidases including the glutathione peroxidases and the peroxiredoxins then further reduce H_2O_2 to water through a redox-mediated condensation reaction, thereby avoiding the generation of further reactive oxygen species (Sies, 1997).

1.7.3 Oxidative stress and ALS

The discovery in 1993 that mutations to CuZn superoxide dismutase 1 (SOD1), a ubiquitously expressed anti-oxidant enzyme that converted superoxide to hydrogen peroxide, were responsible for ~20% of dominantly inherited familial ALS focused attention on oxidative stress as a possible cause of motor neuronal death in ALS. A raft of studies was carried out which sought evidence of oxidative damage to cellular macromolecules, deficits in cellular anti-oxidant defence and increased ROS generation in the disease.

Evidence of oxidative damage to macromolecules in ALS

Markers of oxidative stress including oxidatively damaged protein, lipid and DNA were found in CNS tissues from ALS patients in several studies (Barber and Shaw, 2010). Elevated levels of 3-nitrotyrosine, a reaction product of peroxynitrite, have been found in spinal motor neurons of both SOD1 fALS and sALS cases (Abe et al., 1995; Abe et al., 1997; Beal et al., 1997). High levels of protein carbonyls (evidence of oxidatively-damaged protein) have also been found in the spinal cords of sALS patients (Shaw et al., 1995b) and the motor cortex of both sALS and fALS patients (Ferrante et al., 1997). The cerebrospinal fluid (CSF) of sALS patients has also been reported to contain high levels of the lipid peroxidation product 4-hydroxy-nonenal (Smith et al., 1998), as well as 3-nitrotyrosine (Tohgi et al., 1999). Simpson et al., showed significantly elevated levels of 4-hydroxy-nonenal in serum and CSF of sALS patients when compared to controls (Simpson et al., 2004). A marker of free radical injury to DNA, 8-hydroxy-2'-deoxyguanosine, was also shown to be present in high levels in sALS motor cortex (Ferrante et al., 1997) and in the spinal cords of sALS and SOD1 fALS patients (Ihara et al., 2005).

Evidence of increased ROS generation in ALS

In two independent studies in G93A and WT SOD1 transgenic mice, Liu et al. and Yim et al. used a spin-trap method to show that G93A mutant SOD1 generates more H_2O_2 than does WT SOD1 (Liu et al., 1998; Yim et al., 1996). Experiments in lymphoblast cell lines derived from both SOD1 fALS and sALS cases using a fluorescent probe assisted ROS assay showed increased generation of intracellular ROS in cells derived from fALS patients when compared to those from sALS patients and normal controls (Said Ahmed et al., 2000). The fALS cases included those caused by 16 different SOD1 mutants and the level of ROS measured among the fALS cases was independent of the causative mutation. A more recent study done in G93A mutant SOD1 transgenic rats produced similar results. Levels of ROS increased by 28% when mitoplasts isolated from non-transgenic rats were exposed to spinal cord preparations made from G93A rats (Ahtoniemi et al., 2008). These studies provide evidence of increased ROS generation by at least some SOD1 mutants known to cause disease in patients.

From the evidence presented it is unarguable that there is oxidative stress in ALS. However, it remains less clear whether or not oxidative stress is a primary cause of motor neuron degeneration or even an important contributing factor. Although several anti-oxidant agents showed promising results in G93A SOD1 transgenic mice, trials of several of these agents in patients failed to increase survival (Dugan et al., 1997; Graf et al., 2005; Louwerse et al., 1995). Whilst there may be many possible explanations for the disappointing performance of anti-oxidant drugs in ALS including poor CNS bio-availability or poor targeting of anti-oxidant therapy, the failure of anti-oxidants significantly to alter the disease course of ALS may be because oxidative stress is not the primary motor neuronal insult in the disease.

1.8 Mitochondrial dysfunction

Mitochondria are membrane-encapsulated organelles with diverse and important roles including the regulation of apoptosis (Strasser et al., 2000), the maintenance of calcium homeostasis (Duchen, 2000) and most importantly the generation of adenosine triphosphate (ATP) (Henze and Martin, 2003). As already discussed in Section 1.7.1, the manufacture of ATP results in the unavoidable generation of free radical species capable of causing oxidative damage to mitochondria and other cellular components (Turrens, 1997). Mitochondria are especially vulnerable to the free radicals they themselves produce due to their close proximity to the site of ROS generation, their lack of catalase, one of the most efficient cellular hydroperoxidases (Mates, 2000; Radi et al., 1991), and the lack of protective histones on mitochondrial DNA (Richter et al., 1988).

1.8.1 Mitochondrial abnormalities in ALS

Mitochondrial abnormalities in ALS include 1) morphological changes, 2) biochemical changes and 3) damage to mitochondrial DNA. These abnormalities are not consistently present in all models of the disease and studies in patients have largely, out of necessity, been performed on post-mortem CNS tissue. For these reasons, it is unclear to what extent the mitochondrial damage that is undoubtedly

seen in ALS is responsible for motor neuronal death or whether it simply reflects collateral damage secondary to a different, primary, pathogenetic mechanism. This uncertainty is reinforced by the disappointing results of trials of therapeutic agents aimed at improving mitochondrial function in ALS (Shefner et al., 2004; Strong and Pattee, 2000).

Morphological abnormalities

Mitochondrial morphological changes have been reported both in ALS patients and in animal and cellular models of the disease. Ultrastructural studies on muscle biopsies from sALS patients revealed increased mitochondrial volume in motor nerve terminals (Siklos et al., 1996). In G93A SOD1 expressing NSC34 cells mitochondria were observed to be vacuolated and swollen (Menzies et al., 2002). Vacuolation of mitochondria has also been observed in some animal models of ALS. Spinal cord motor neurons of G93A mice exhibited fragmented Golgi apparatus and swollen endoplasmic reticulum in addition to mitochondrial vacuolation (Mourelatos et al., 1996). In motor neurons from G93A SOD1 mice, it was observed that vacuole formation within mitochondria correlated with disease progression (Kong and Xu, 1998). However, these morphological changes were not observed in mice expressing SOD1 variants with mutations in the metal binding regions, for example G85R SOD1 mice (Bruijn et al., 1997) and H46R/H48Q SOD1 mice (Wang et al., 2003).

Biochemical abnormalities

The activities of components of the electron transport chain including complex II, complex IV and cytochrome *c* are altered in ALS. In sALS patients, reduction in the activity of complex IV was observed in the spinal cord (Fujita et al., 1996). Using *in situ* histochemical demonstration of enzyme activity, Borthwick et al. showed reduced activity of complex IV and cytochrome *c* in individual spinal motor neurons from post-mortem material of sALS cases (Borthwick et al., 1999). There is, however, some contradictory evidence. Increases in the activity of complexes I, II and III were observed in cerebellum, parietal and motor cortex from SOD1 fALS cases (Browne et al., 1998). Significantly decreased activity of complexes I and III, II and III and complex IV were also observed in brain and spinal cord tissue using direct spectrophotometric assays in 17-week G93A mice compared to non-transgenic mice (Mattiazzi et al., 2002). In NSC34 cells expressing mutant SOD1 (G93A and G37R) complex IV and complex II showed reduced activity compared to vector-only controls and WT-SOD1-expressing cells (Menzies et al., 2002). The studies above differ in detail in the changes in electron transport chain activities they report - quite likely a result of their use of different experimental substrates and different experimental techniques to estimate the activities of various components of the electron transport chain. Despite this, they do without exception identify differences between ALS and controls, suggestive of disrupted function of the electron transport chain in the disease.

In addition to evidence of altered electron transport chain component activities in ALS, more recent studies demonstrate hypermetabolism in the disease. Investigation of resting energy expenditure by

evaluating nutritional intake and body mass index to establish the reduction of fat-free mass showed ALS patients have a higher resting energy expenditure than controls. Indeed, levels of metabolism in ALS patients were ~10% higher on an average (Desport et al., 2001). Similar dysfunctional energy metabolism has been reported in G93A and G86R SOD1 transgenic mice. Using metabolite and hormone assays that included assessments of levels of leptin, insulin and free fatty acid along with glucose intake, Dupuis et al., showed evidence of hypermetabolism in the transgenic mice (Dupuis et al., 2004) which exhibited increased glucose intake and insulin production compared to non-transgenic mice. Furthermore, administration of a fat-enriched diet to SOD1 transgenic mice compensated their high energy consumption, suggesting that an increased metabolic rate was a feature of these SOD1 mice as well as of ALS patients (Dupuis et al., 2004).

There is also evidence of altered handling of calcium by ALS mitochondria. In peripheral blood lymphocytes from sALS patients, cytoplasmic calcium concentrations were higher than those of controls (Curti et al., 1996). A similar effect was also observed in the transgenic mice model of ALS. SH-SY5Y neuroblastoma cells expressing G93A SOD1 were also found to have increased cytosolic calcium compared to non-transgenic cells. The authors suggested defective mitochondrial calcium sequestration due to the presence of mutant SOD1 (Carri et al., 1997).

Genetic abnormalities

Mitochondria house their own genetic material. Mitochondrial DNA (mtDNA) contains 37 genes, most of which encode proteins involved in the normal functioning of mitochondria. Of these 37 genes, 13 encode subunits of the electron transport chain, 22 encode transfer RNA and the remaining two code ribosomal RNA for protein translation (Taanman, 1999). It might be expected, therefore, that alterations in levels or integrity of mtDNA might influence mitochondrial function.

High frequencies of mutations have been observed to occur in mtDNA extracted from ALS brain samples. Dhaliwal et al. compared levels of the 4977 bp "common deletion" of mtDNA in temporal and motor cortex from ALS and control brains. Although rates of the common deletion appeared to be higher in motor cortex than in temporal cortex of both ALS and control cases, this difference was approximately 11-fold higher in ALS brains compared to controls (Dhaliwal and Grewal, 2000). A higher frequency of mtDNA mutations together with decreased quantities of mtDNA were also observed in spinal cord from ALS patients (Wiedemann et al., 2002). Whether or not these changes confer a functional significance is unclear.

1.9 Impaired RNA processing

The identification of TDP43 as a major component of ubiquitinated inclusions, followed by the discovery of *TARDBP* mutations in ~5% of all ALS cases, first raised the possibility that altered RNA metabolism might be important in the pathophysiology of ALS. Causative mutations in other RNA processing genes such as *FUS/TLS*, *ANG* and *SETX* have lent further support to this idea (van

Blitterswijk and Landers, 2010). This section will focus on the mechanisms by which these RNA processing proteins might contribute to disease pathogenesis.

1.9.1 The normal function of TDP43 and FUS/TLS

TDP43 and FUS/TLS are RNA binding proteins that shuttle between the nucleus and cytoplasm. They are believed to influence various facets of RNA processing including transcription, pre mRNA splicing (Buratti and Baralle, 2001; Meissner et al., 2003), spatial and temporal regulation of mRNA translation including mRNA transport, mRNA stability (Gregory et al., 2004) and the transcriptional response to cellular stress (Andersson et al., 2008; Colombrita et al., 2009b).

1.9.2 TDP43 and FUS mutations in ALS

Genetic screening has identified multiple missense mutations localized to the C-terminus of TDP43 in sALS and fALS cases. It has been suggested that these mutations increase the propensity of the protein to misfold and form cellular aggregates, disrupting its normal cellular interactions (Kabashi et al., 2008b; Sreedharan et al., 2008). It is still unknown whether mutations to TDP43 cause ALS via a loss of function or a toxic gain of function secondary to the accumulation of the mutant protein within cytoplasmic aggregates, or both. Recent evidence from transgenic TDP43 and FUS overexpressing animals makes the latter possibility the more likely and has begun to clarify the biology of these proteins. *TARDBP* knock-out mice are embryonically lethal whilst conditional knock-out mice die very quickly after birth suggesting that TDP43 is essential for embryonic development (Chiang et al., 2010; Sephton et al., 2010). Transgenic human mutant TDP43 and mutant FUS overexpressing mice moreover display selective degeneration of motor neurons along with other ALS-like features including the accumulation of protein aggregates similar to those observed in patients (Huang et al., 2011; Kabashi et al., 2010; Wils et al., 2010).

The involvement of TDP43 and FUS/TLS in mRNA transport and the regulation of mRNA spatio-temporal translation may be particularly important to the normal physiology of highly polarized cells such as motor neurons (Colombrita et al., 2011). As such, deficits in these functions might go some way to explain the motor neuronal selectivity of mutant TDP43 and FUS/TLS. Recently, TDP43 and FUS have been shown to be involved in cytoplasmic stress granule dynamics (Bosco et al., 2010; Colombrita et al., 2009a). As stress granules are required for the temporal regulation of protein synthesis during the cellular response to a variety of insults including oxidative, hypoxic and endoplasmic reticulum stress it has been suggested that ALS-causing mutations to TDP43 and FUS might confer a decreased ability to respond to such stressors (Bosco et al., 2010; Gal et al., 2011; Strong and Volkening, 2011).

In conclusion, there remains much to learn about how mutations to these RNA-processing proteins bring about the selective death of motor neurons and ALS. The reiteration of an ALS-like phenotype in

the transgenic overexpressing mice, however, suggests that further progress is likely to be rapid in our understanding of the pathogenesis of this subtype of fALS.

1.10 Protein aggregation

Proteinaceous inclusion bodies are a pathological feature of ALS (Section 1.6), as are they of several other neurodegenerative diseases. The precise mechanism by which they form is still unclear but it is suspected that inclusion body formation is prefaced by the aggregation of protein first into oligomers and then further into insoluble protein complexes (Ross and Poirier, 2004). Although many believe that protein aggregates are inherently toxic to the cell and represent the primary pathogenic event in ALS, others suspect that protein aggregation might instead be a secondary response to another primary insult. In this scenario the formation of protein aggregates is either a compensatory effect that is in some way protective of the cell or else an unimportant epiphenomenon of no functional consequence (Ross and Poirier, 2005).

1.10.1 SOD1 protein aggregation

Proteinaceous inclusions that immunostain positive for SOD1 are a feature of SOD1-related fALS cases and it has been suggested that the aggregation of mutant SOD1 may be an underlying cause of this form of fALS (Wood et al., 2003a). Durham et al. showed that mutant SOD1 cDNA microinjected into cultured murine spinal motor neurons brought about the formation of intracellular aggregates. No aggregates, however, were seen in motor neurons transfected with WT-SOD1 cDNA (Durham et al., 1997). The dorsal root ganglion and hippocampal neurons used as controls in this study, moreover, did not share the same propensity to form aggregates in the presence of mutant SOD1 as did motor neurons. G93A, G85R, and G37R SOD1 transgenic mutant mice have all been shown to contain cytoplasmic protein aggregates in their spinal motor neurons. SOD1 is not present in all of these aggregates, however (Watanabe et al., 2001). Wang et al. demonstrated formation of high molecular weight complexes of mutant SOD1 in the brain and spinal cord of G37R, G85R and G93A mice. Importantly, the quantity of these high molecular weight complexes increased with the age of the mice (Wang et al., 2002).

It has been suggested that ALS-causing mutations of SOD1 generate a less stable SOD1 species than the wild-type protein. The aberrant conformations of 14 variants of mutant SOD1 (including A4V, L38V, G41S, H46R, G72S, D76Y, G85R, D90A, G93A, D124V, D125H, and S134N) have been shown to be responsible for the reduced thermal stability of these species of mutant SOD1 (Rodriguez et al., 2002). These conclusions were drawn from observations of the endothermic energy changes of the enzyme during folding and unfolding using scanning calorimetry. Several hypotheses have been put forward to explain how the formation of SOD1 aggregates might be damaging to the motor neuron. These include the sequestration of important cellular proteins into protein aggregates along with SOD1, bringing about a loss of function, and the overwhelming of the cell's quality-control system for protein leading to an accumulation of misfolded and dysfunctional proteins. Okado-Matsumoto and

Fridovich (2002) showed that aggregating G37R, G93A and G41A SOD1 sequestered heat shock proteins (HSP 70, HSP 27 and HSP 25) in N2a cells leading to a reduction in the levels of these anti-apoptotic factors (Okado-Matsumoto and Fridovich, 2002). Proteasomal activity was shown to be reduced in the presence of mutant SOD1 in a cell-culture model of ALS (Allen et al., 2003), whilst altered expression of constitutive proteasomal subunits and decreased proteasomal activity have also been identified in mutant SOD1 mouse models of ALS (Kabashi et al., 2008a; Kabashi et al., 2004).

1.11 Excitotoxicity

Motor neurons utilize the glutamatergic system, which uses glutamate as its neurotransmitter, to initiate excitatory impulses. Glutamate released from the pre-synaptic nerve terminal, acts at one or more of three ionotrophic receptors the α-amino-3-hydroxy-5-methyl-4-isoxazole propionic acid (AMPA) receptor, the *N*-methyl-D-aspartate (NMDA) receptor and the Kainate (KA) receptor. Of these receptors it is the AMPA receptor that is mainly responsible for triggering the excitatory postsynaptic potential. On glutamate binding the channel opens, there is an influx of Ca^{2+} and Na^{+}, the motor neuron depolarizes and an action potential is triggered. Glutamate also binds to NMDA receptors opening the channel to Ca^{2+} amongst other ions. Glutamatergic stimulation of motor neurons is terminated by removal of glutamate from the synaptic cleft by glutamate re-uptake proteins, principally the excitatory amino acid transporter 2 (EAAT2) present on both neurons and more importantly on surrounding neuroglia. This glutamate is then converted to glutamine. Glutamine taken up by neuroglia is re-released into the synaptic cleft from where it is taken up by the pre-synaptic nerve terminals to be converted back to glutamate as needed (Gleichmann and Mattson, 2011).

Excitotoxicity was a concept introduced in 1978 by Olney and refers to neuronal degeneration caused by over-stimulation of glutamate receptors (Olney, 1982). Excitotoxicity can result from damage to healthy neurons exposed to increased extracellular glutamate or else from damage to more vulnerable neurons exposed to normal extracellular glutamate concentrations (Doble, 1999). Of the two, increased glutamatergic stimulation is considered to be the more relevant to ALS (Heath and Shaw, 2002). Neuronal injury due to excitotoxicity is mainly mediated through excess Ca^{2+} influx via NMDA receptors (Choi, 1987), Ca^{2+} -permeable AMPA receptors (Carriedo et al., 1996) or voltage-gated Ca^{2+} channels. While NMDA receptors are invariably permeable to Ca^{2+} when open, the permeability of AMPA receptors to Ca^{2+} depends on the presence of the GluR2 subunit in the receptor complex (Hume et al., 1991; Verdoorn et al., 1991). The concentration of Ca^{2+} is tightly regulated within neurons. The extracellular free calcium concentration is typically ~1.2 mM whilst the resting cytosolic free calcium concentration is much lower at 100 nM. This difference contributes to the resting potential (Gleichmann and Mattson, 2011). Excess Ca^{2+} influx leads to an increased intracellular Ca^{2+} concentration and Ca^{2+} mislocalization as various cellular organelles, including the mitochondria, sequester the excess Ca^{2+} in an effort to lower cytosolic [Ca^{2+}]. High levels of Ca^{2+} have been suggested to contribute to mitochondrial dysfunction and free radical generation ultimately leading to

neuronal death (Dykens, 1994; Gleichmann and Mattson, 2011). The exact mechanism by which neuronal death is induced after excess Ca^{2+} enters the neuron is not yet clear.

1.11.1 Evidence for excess glutamatergic input to motor neurons in ALS

Abnormal levels of various components of the glutamatergic neurotransmitter system have been reported in ALS patients. Glutamate itself is notoriously difficult to measure but high levels of glutamate have been measured in the CSF of ALS patients (Shaw et al., 1995a). Using HPLC, a large independent study, involving a cohort of 377 ALS patients, also demonstrated elevated CSF glutamate concentrations in ALS patients (Spreux-Varoquaux et al., 2002). An increased glutamate in ALS CSF was not, however, found in all studies (Perry et al., 1990; Rothstein et al., 1992). Increased levels of glutamate dehydrogenase, the enzyme that reversibly converts 2-oxoglutarate into glutamate, have also been observed in post-mortem lumbar spinal cord tissues of ALS patients (Malessa et al., 1991). Couratier et al. found that exposure to CSF from sALS patients was toxic for cultured cortical neurons and that the resultant cell death could be ameliorated by the AMPA receptor blocker 6-cyano-7-nitroquinoxaline-dione disodium (CQNX) (Couratier et al., 1993).

Decreased clearance of extracellular glutamate by the glutamate re-uptake transporter may also result in increased glutamate concentrations, particularly in the synaptic cleft. A selective decrease in the expression of EAAT2 in port-mortem cortex and spinal cord from both familial and sporadic ALS patients was demonstrated using immunohistochemistry (Fray et al., 1998; Rothstein et al., 1995). In contradiction of these findings, EAAT2 mRNA levels were no different in cortical neurons from ALS patients compared to those of controls. The authors of this study suggested that alterations at a protein level but not at an mRNA level could be indicative of post-translational alterations in EAAT2 levels (Bristol and Rothstein, 1996). Others, however, suggested that these apparently conflicting results indicated that there was in fact no deficit in EAAT2 expression in ALS. A later, somewhat controversial study reported different EAAT2 isoforms in brain and spinal cord tissues of sALS patients compared to controls resulting from anomalous mRNA splicing (Lin et al., 1998). Subsequent efforts to reproduce these findings, however, were unsuccessful (Flowers et al., 2001; Jackson et al., 1999).

1.11.2 Evidence for motor neuronal injury due to excitotoxicity in ALS

Motor neuronal vulnerability to AMPA receptor mediated excitotoxicity is evident in both *in vivo* and *in vitro* models of ALS (Nakamura et al., 1994). Motor neurons within cultured organotypic rat spinal cord slices have been reported to be more vulnerable to AMPA receptor mediated excitotoxicity (Rothstein et al., 1993; Saroff et al., 2000). In these two independent studies, spinal cord slices were exposed to increasing concentrations of glutamate. Using biochemical measurements of ChAT and counting, a significant reduction in the loss of motor neurons were observed when exposed to glutamate. This glutamate-mediated toxicity was ameliorated in the presence of AMPA receptor antagonists thus indicating vulnerability of spinal motor neurons to glutamate excitoxicity (Rothstein et

al., 1993; Saroff et al., 2000). Compared with other neurons, motor neurons have higher proportion of Ca^{2+} permeable AMPA receptors in comparison to non-permeable AMPA receptors (Carriedo et al., 2000; Carriedo et al., 1996). The GluR2 subunit content of AMPA receptors is known to regulate their Ca^{2+} permeability (Jia et al., 1996). When knock-out mice lacking the GluR2 subunit of the AMPA receptor were crossed with G93A SOD1 transgenic mice, the dual transgenic offspring had a life span shortened by 15% as well as an accelerated loss of motor neurons compared to their single transgenic G93A SOD1 littermates (Van Damme et al., 2005). This provides further support for the idea that excess Ca^{2+}-permeable AMPA receptors on motor neurons confer a vulnerability that may be relevant to ALS.

In another study of primary murine motor neuronal cultures stably transfected to overexpress G93A, G41R or N139K human mutant SOD1, selective motor neuronal death was demonstrated in response to glutamate (Roy et al., 1998). Glutamate-mediated toxicity in primary motor neurons expressing mutant SOD1 was observed to be inhibited by both CQNX , a general AMPA receptor antagonist, and joro spider toxin, a selective Ca^{2+} permeable antagonist, implicating Ca^{2+} -mediated neuronal injury due to glutamate in the presence of mutant SOD1. In the same study, co-expression of the Ca^{2+} binding protein, calbindin D28K together with various mutant SOD1 species in primary murine motor neurons also ameliorated cell death in mutant SOD1-expressing motor neurons on exposure to glutamate.

Finally, Riluzole is the only drug which delays disease progression in ALS patients (Bensimon et al., 1994; Lacomblez et al., 1996). The principal mechanism of action of Riluzole is to inhibit pre-synaptic glutamate release by disabling voltage-dependent Na^{+} channels on pre-synaptic neurons (Doble, 1996). Riluzole has also been shown to act directly at NMDA and AMPA glutamate receptors present on post-synaptic neurons by binding non-competitively to the receptor thereby blocking glutamate binding (Albo et al., 2004; Doble, 1996). The fact that the only drug currently effective in ALS patients is anti-glutamate in its actions must be considered strong evidence in favour of at least a contribution of excitotoxicity to disease pathogenesis.

1.12 Defective axonal transport

Neurofilaments comprised of light and heavy polypeptide chains together with microtubules are the main components of the neuronal cytoskeleton. The cytoskeleton acts as a platform for the transport of essential proteins and other cargoes from the soma in an anterograde direction down the axon towards the distal end of the neuron and back up the axon in a retrograde direction from the distal end of the neuron towards the soma. The transport of protein cargoes is mediated by molecular motors that utilize the microtubule network. Lumbar motor neurons may have axons over a metre in length – clearly transport of cargoes over this distance represents a significant physiological challenge, and by extension, a potential vulnerability.

1.12.1 Mutations in axonal transport components associated with ALS-like disease

Mutations in the genes encoding neurofilament proteins, molecular motors, and other associated components of the axonal transport system have been implicated in ALS (De Vos et al., 2008). For example, transgenic mice carrying a leucine to proline substitution at codon 394 of the neurofilament light chain (NF-L) subunit, develop a rapidly progressive ALS-like syndrome (Lee et al., 1994). The neurofilament heavy (NF-H) chain subunit has a Lys-Ser-Pro (KSP) repeat region that is of functional importance. Variations in this domain (including insertion of additional repeats) have been found to be associated with ALS cases. These KSP repeat region variations are suggested to alter the function of the domain in such a way as to interfere with normal axonal transport (Figlewicz et al., 1994; Tomkins et al., 1998). Mutations in the heavy chain component of the dynein molecular motor have been introduced into the murine genome as part of a programme of chemical mutagenesis (Hafezparast et al., 2003). The resultant "Legs at Odd Angles" or LOA mice have ALS-like motor and pathological features (Hafezparast et al., 2003; LaMonte et al., 2002). Using multipoint linkage analyses two independent studies have demonstrated that dynactin mutations, potentially leading to disrupted retrograde axonal transport, are associated with familial ALS (Munch et al., 2005; Puls et al., 2003). Both studies showed that the mutant dynactin segregated with affected individuals within a family whilst non-affected individuals did not carry the mutant gene.

High level overexpression of neurofilament light chain (Xu et al., 1993) or neurofilament heavy chain (Cote et al., 1993) in transgenic mice both result in the development of protein aggregates similar to those observed in ALS patients. In addition to the formation of aggregates, axonal swellings, muscle atrophy and axonopathy are also observed in these mice, further reflecting an ALS-like pathology (Cote et al., 1993; Xu et al., 1993).

Effect of mutant SOD1on axonal transport

Tu et al. examined neurofilament assembly in G93A SOD1 transgenic mice and showed that the mice developed neuronal cytoskeletal pathology in the form of hyaline conglomerate-like pathological inclusion bodies similar to those found in ALS patients (Tu et al., 1996). High overexpressing G93A SOD1 transgenic mice demonstrate a significant impairment of retrograde axonal transport (Murakami et al., 2001). Using a different method, Williamson and Cleveland showed reduced transport of protein cargoes, both anterograde and retrograde, of slow axonal transport components (Williamson and Cleveland, 1999). It is thought that accumulation of neurofilaments in axons and cell bodies of motor neurons contributes to impaired retrograde transport in these mice (Rao and Nixon, 2003). Transgenic mice expressing low amounts of G93A SOD1 also developed characteristic neurofilament pathological inclusions, albeit at a later stage than higher mutant SOD1 expressors, as well as other ALS-like features. These low expressing mice also exhibited selective loss of some components required for anterograde fast axonal transport (Zhang et al., 1997). It was also demonstrated that G37R mutant SOD1 transgenic mice exhibit degeneration of mitochondria, membrane vacuolization and axonal degeneration which leads to the development of a severe and progressive ALS-like

phenotype (Wong et al., 1995). Concurrent overexpression of neurofilament heavy chain (NF-H) in G37R SOD1 transgenic mice was observed to at least partially ameliorate the effects of G37R mutant SOD1 (Couillard-Despres et al., 1998) with the dual transgenic mice surviving up to ~65% longer than the single transgenic G37R SOD1 animals. Histological analyses showed that concurrent overexpression of NF-H decreased axonal degeneration leading the authors to suggest that NF-H was acting to protect motor neurons against the toxic effects of G37R mutant SOD1 (Couillard-Despres et al., 1998).

Legs at Odd Angles (LOA) mice carry a mutation to the cytoplasmic dynein heavy chain gene *Dnchc1* and have a disrupted dynein molecular motor resulting in defective retrograde and anterograde axonal transport (Hafezparast et al., 2003; LaMonte et al., 2002). When these mice were crossed with high-expressing G93A SOD1 transgenic mice, their dual G93A/LOA offspring had an increased life span and an almost fully restored axonal transport system (Kieran et al., 2005). The LOA cross appeared to have almost completely ameliorated the retrograde transport impairment typical of the G93A mice. The exact cellular interaction between mutant SOD1 and dynein has not been established but the extension of lifespan in the dual G93A/LOA mice supports the idea that defective axonal transport is at the very least a contributor to motor neuronal death in the G93A SOD1 mouse (Kieran et al., 2005).

THE PEROXIREDOXINS

As has been discussed in Section 1.7, free radicals or reactive oxygen species (ROS) are generated as unavoidable by-products of cellular respiration. Production of ROS in excess of the capability of cellular anti-oxidant defence to respond causes oxidative stress which results in oxidative damage to cellular macromolecules and may ultimately precipitate apoptosis (Boveris et al., 1972; Chance et al., 1979). The superoxide free radical ($O_2^{\bullet -}$) is generated by the electron transport chain and is released from the inner mitochondrial membrane (Han et al., 2001). As superoxide does not readily cross membranes it must be dealt with at its site of generation. Superoxide dismutase 1 (SOD1), present within the mitochondrial intermembrane space as well as the cytosol (Kawamata and Manfredi, 2008), and SOD2 (present within the mitochondria matrix) first convert $O_2^{\bullet -}$ to H_2O_2 via a dismutase reaction. The resultant H_2O_2 must itself be removed if it is not to generate even more reactive free radical species via the Fenton reaction. This step is carried out by one or more hydroperoxidases including catalase, the glutathione peroxidases (GPx) and the peroxiredoxins (Prxs). The various hydroperoxidases differ in their catalytic efficiency, their localization and their relative abundance within cellular compartments. Catalase, for example, is a highly efficient hydroperoxidase ($k = \sim 4 \times 10^8$ $M^{-1} S^{-1}$) but is localized mainly to peroxisomes (De Duve and Baudhuin, 1966) and is not present within mitochondria (Mates, 2000). The peroxiredoxins ($k = \sim 10^5$ $M^{-1} S^{-1}$) and glutathione peroxidases (k =

~10^8 M^{-1} S^{-1}) are less effective than is catalase as hydroperoxidases but there are isoforms of these proteins present in abundance within mitochondrial compartments and within the cytosol enabling them to detoxify H_2O_2 closer to where it is generated (Panfili et al., 1991).

Peroxiredoxins are members of the thioredoxin-fold superfamily and share the family's characteristic thioredoxin fold motif (Schroder and Ponting, 1998). There are six mammalian Prxs classified as thioredoxin-dependent hydroperoxidases that act to reduce H_2O_2 to water, becoming oxidized themselves in the process. Peroxiredoxins are ubiquitously expressed across the tissues of the body with representatives in multiple cellular compartments. They serve effectively to protect cells against free radical injury by reducing hydrogen peroxide, peroxynitrite ($ONOO^-$) and other alkyl hydroperoxides (ROOH) (Bryk et al., 2000). The main substrate of the Prxs is H_2O_2 which they reduce to water through a series of redox reactions which involves a final reduction by a thiol donor that returns the Prxs to their active, reduced state ready to reduce more H_2O_2 (Rhee et al., 2005a).

It has become evident that some members of the Prx family have functions besides anti-oxidant defence. Some eukaryotic Prxs are capable of oxidative inactivation on exposure to excess peroxide conferring a role in the regulation of H_2O_2 signalling. Recent work has also shown that some oxidatively inactivated Prxs can aggregate to form high molecular weight multimers that function as highly efficient molecular chaperones (Rhee and Woo, 2011). The following sections will consider in more detail the classification, functions and biology of the peroxiredoxins. The evidence for the involvement of the Prxs in the pathogenesis of ALS and other neurodegenerative diseases will then be considered.

1.13 Classification

In mammals, six peroxiredoxins (Prx 1-6) have been identified and characterized (Table 1.3). Broadly, these peroxiredoxins are categorized into two groups according to the number of conserved cysteine residues present (Rhee et al., 2001). All six forms of Prx have at least one conserved cysteine residue in their polypeptide chain. Peroxiredoxin 6 has only one conserved cysteine residue and is the only 1-cys peroxiredoxin. Peroxiredoxins 1-5 have two conserved cysteine residues and are therefore classified as 2-cys peroxiredoxins.

1.13.1 Two-cys peroxiredoxins

The 2-cys Prxs are so-named so because they contain 2 conserved cysteine residues, one at each terminus. The cysteine at the N-terminus is referred to as the active cysteine or the peroxidatic cysteine (Cp) as it is the residue that actively initiates catalysis of H_2O_2 and other alkyl hydroperoxides. By doing so, its thiol (SH) is oxidized to cysteine-sulfenic acid (SOH). The C-terminus cysteine is called the resolving cysteine (Cr). This cysteine is involved in the reduction of the oxidized Prx back to its active reduced form thereby completing the reduction reaction. The 2-cys Prxs may be further divided

into typical 2-cys Prxs and atypical 2-cys Prxs based on the manner in which their reduced state is regained (Rhee and Woo, 2011; Wood et al., 2003c).

Peroxiredoxin	Sub-family	Protein length (aa)	Cellular localization	Expression in the nervous system (Goemaere and Knoops, 2012; Jin et al., 2005)
Prx 1	Typical 2-cys	199	Cytosol and nucleus	Microglia and oligodendrocytes
Prx 2	Typical 2-cys	198	Cytosol and mitochondria	Neurons
Prx 3	Typical 2-cys	256	Exclusively mitochondrial matrix	Neurons
Prx 4	Typical 2-cys	271	Secreted protein Golgi and cytosol	Oligodendrocytes and neurons
Prx 5	Atypical 2-cys	214	Mitochondria, cytosol and peroxisomes	Abundant in neurons
Prx 6	One-cys	224	Cytosol	Abundant in astrocytes

Table 1.3: *The six mammalian peroxiredoxins.*

Typical 2-cys peroxiredoxins (Prxs 1-4)

In mammals peroxiredoxins 1-4 are classified as typical 2-cys Prxs and share more than 70% sequence homology with one another. The majority of these conserved sequences are located in the region surrounding the Cp and Cr. Typical 2-cys Prxs function as obligate homodimers. Using X-ray crystallography it has been demonstrated that the individual subunits of these homodimers are orientated in opposite directions to each another (Chae et al., 1994b). Hence, during the reduction of H_2O_2, the Cp of one subunit is reduced by the Cr of the other subunit. Once the Cp of one subunit is oxidized by reaction with H_2O_2 forming cysteine-sulfenic acid (SOH), its sulphur then is reduced by the Cr of the other subunit, resulting in the formation of an *inter*-molecular disulphide bond between the two monomers. The Prx monomer, oxidized at this stage, is enzymatically inactive in that there are no free electrons to further react without the use of high energy. The oxidized Prx is recycled back to its native reduced form by thioredoxin (Trx) which serves as an electron donor (Chae et al., 1994a). Thioredoxin reduces the disulphide bond back to a thiol group by donating electrons. The oxidized Trx is in turn reduced back to its functional reduced form by thioredoxin reductase (TrxR) using electrons donated by NADPH completing the reaction cycle. This series of redox reactions is summarized in Figure 1.3.

Typical 2-cys Prxs are ubiquitously expressed throughout the body and are found in most intracellular compartments. All four typical 2-cys Prxs are expressed within the central nervous system. While Prxs 2, 3 and 4 are expressed within neurons, Prx 1 is abundantly expressed in astrocytes. Oligodendrocytes have been shown to express Prx 1 and Prx 4 (Goemaere and Knoops, 2012; Jin et al., 2005). Prx 4 is a secreted protein which is also found in the cytosol. Prxs 1 and 2 are found in the nucleus and the cytosol, while Prx 3 is exclusively localized to the mitochondria (Goemaere and Knoops, 2012; Jin et al., 2005). Prx 3 lies within the mitochondrial matrix in close proximity to the electron transport chain, the major producer of superoxide, hydrogen peroxide and other free-radical species. Prx 3 forms the first line of defence against free radicals generated within mitochondria together with Thioredoxin 2 (Spyrou et al., 1997) and Thioredoxin reductase 2 (Lee et al., 1999), the mitochondrial electron donors that return Prx 3 to its reduced, active state.

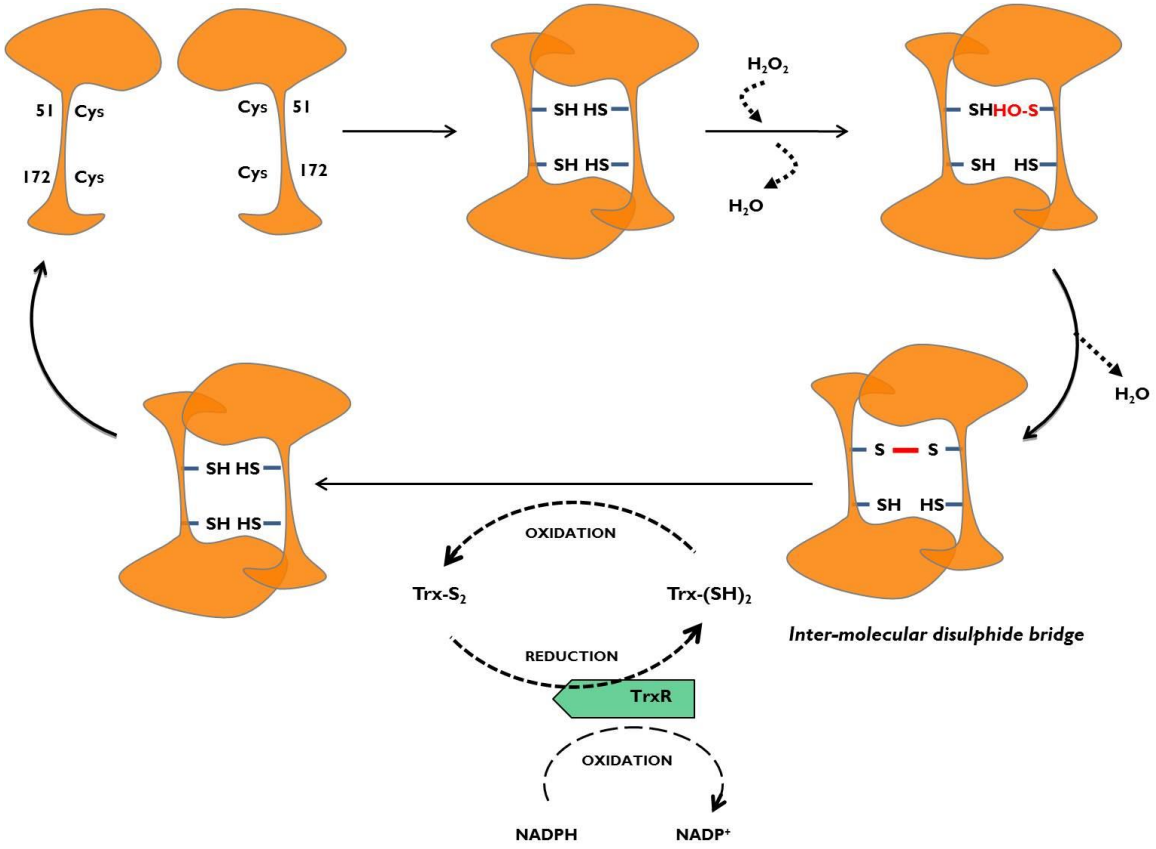

Figure 1.3: *Schematic showing the catalytic cycle of the typical 2-cys peroxiredoxins (Prxs 1-4). Image drawn based on information obtained from Rhee (Rhee and Woo, 2011). Trx – Thioredoxin, TrxR – Thioredoxin reductase.*

Atypical 2-cys peroxiredoxin (Prx 5)

Peroxiredoxin 5 is the only atypical 2-cys peroxiredoxin in mammals and was identified and characterized by Knoop and colleagues (Knoops et al., 1999). In the CNS, Prx 5 is expressed only in neurons. It shares only ~10 % of its overall sequence with the other Prx enzymes (Knoops et al., 2011). Similar to the typical 2-cys Prxs, Prx 5 contains two reactive cysteine residues along its polypeptide chain with only the N-terminal cysteine (Cp) nested within the conserved sequence

KGKYVVLFFYPLDFTFVCP that is shared by all the other 2-cys Prxs (Prx 1-4) (Knoops et al., 2011). The sequence around its C-terminal cysteine (Cr) is not in common with the typical 2-cys Prxs.

Prx 5 is categorized as a 2-cys peroxiredoxin because its hydroperoxidase function is dependent upon its two cysteine residues (Rhee and Woo, 2011). The mechanism by which these two cysteines reduce hydrogen peroxide, however, is different to that of the typical 2-cys Prxs. Although Prx 5 shares the basic H_2O_2 reduction mechanism of the typical 2-cys Prxs, it functions as a monomer (Seo et al., 2000). After initial oxidation of its Cp, return of inactive Prx 5 to its active form is achieved by formation of an *intra*-molecular disulfide bridge between the Cp and Cr of a single Prx 5 subunit rather than an *inter*-molecular disulfide bond between those of two separate monomers as is the case for the typical 2-cys Prxs. Prx 5 regeneration is dependent on the Trx and TrxR reduction system in the same way as is the regeneration of the typical 2-cys Prxs (Figure 1.4). Although regeneration of oxidized Prx 5 is thought by most to involve only one monomer, recent evidence suggests that an intermediate *inter*-molecular disulphide bridge may form between two oxidized Prx 5 subunits prior to shifting and rearrangement of the bonds to form the *intra*-molecular bridge within each monomer pre-reactivation (Evrard et al., 2004).

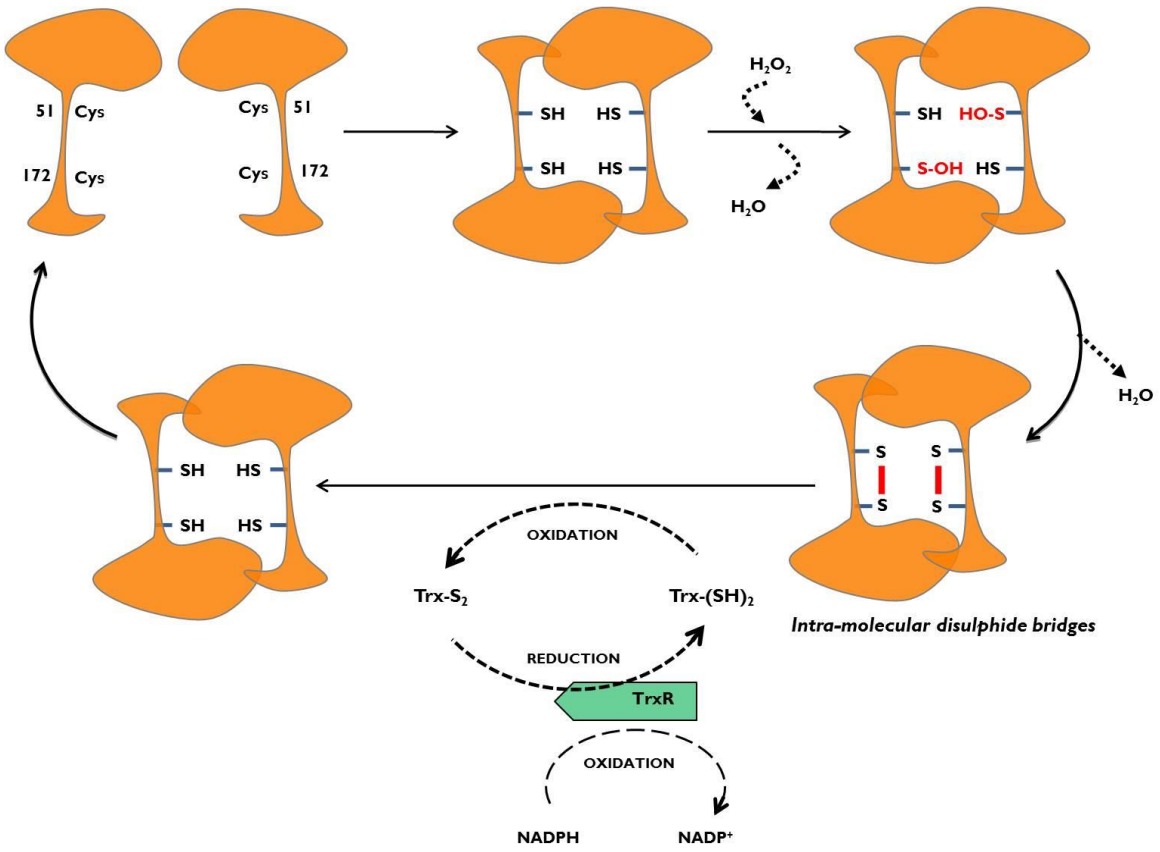

Figure 1.4: *Schematic showing the catalytic cycle of Prx 5, the only atypical 2-cys peroxiredoxin. Image drawn based on information obtained from Rhee (Rhee and Woo, 2011). Trx – Thioredoxin, TrxR – Thioredoxin reductase.*

1.13.2 One-cys peroxiredoxin (Prx 6)

Peroxiredoxin 6 is the only 1-cys mammalian Prx. Unlike the 2-cys Prxs, Prx 6 contains a single conserved cysteine residue – its active cysteine (Cp) (Choi et al., 1998). Prx 6 is a cytosolic peroxidase and within the CNS is it expressed only in astrocytes (Goemaere and Knoops, 2012).The catalytic mechanism of Prx 6 is poorly understood. Although it is evident that peroxide reduction is brought about by its single cysteine (Cp), the mechanisms by which oxidized Prx 6 is returned to its active, reduced form are still unclear. The regeneration mechanism of Prx 6 does not involve the Trx/TrxR system used by the 2-cys Prxs but is instead hypothesized to use another thiol-containing reductant (Manevich et al., 2004; Monteiro et al., 2007).

1.14 Overoxidation of the typical 2-cys peroxiredoxins and their regeneration

There is now substantial evidence for the overoxidation of some mammalian peroxiredoxins, as reviewed by Kang (Kang et al., 2005). It has been found that members of the typical 2-cys Prx subfamily have the ability to form sulfinic (SO_2H) and sulfonic acids (SO_3H) at the Cp resulting from the further oxidation of the cys-sulfenic acid (SOH) form of the protein formed during its catalytic cycle. It is thought that delay in the formation of the intermolecular disulfide bond between two 2-cys Prx monomers during catalysis (Figs.1.3 and 1.4) provides an opportunity for further oxidation of the cys-sulfenic acid to a cys-sulfinic (SO_2H) acid rather than its reduction (Rhee et al., 2005a). Further encounters with peroxide can overoxidize the cys-sulfinic form of the 2-cys Prx to a still more oxidized form, a cys-sulfonic acid (SO_3H). The cys-sulfenic and cys-sulfonic forms of the 2-cys Prxs are inactive as hydroperoxidases, but can aggregate together to form multimers with a protein chaperone function (discussed in Section 1.15.2).

Sequence homology searches have indicated a C-terminus four-residue domain comprising Glycine (Gly) and Leucine (Leu), in the order Gly-Gly-Leu-Gly (GGLG), and a conserved tyrosine-phenylalanine (YF) motif that is present almost without exception in only eukaryotic Prxs (Chuang et al., 2006; Pascual et al., 2010). In mammals these motifs, positioned near the carboxy terminus, are thought to mediate the oxidative inactivation of the typical 2-cys Prxs. It has been hypothesized that the presence of these motifs hinders the ability of the Cr to reduce the formed cys-sulfenic acid (SOH) to its thiol state, thus allowing further oxidation of the Prxs in the presence of excess hydrogen peroxide or other peroxide substrates (Koo et al., 2002; Wood et al., 2003b).

1.14.1 Regeneration of the typical 2-cys peroxiredoxins

Overoxidized 2-cys Prxs ($PrxSO_{2/3}$) cannot be reduced by the usual thioredoxin/thioredoxin reductase mechanism nor do they readily spontaneously revert to a less oxidized form (Yang et al., 2002). Although 2-cys Prx overoxidation was originally thought to be irreversible, more recent work on oxidatively-inactivated typical 2-cys Prxs has shown that overoxidation is, in some cases, reversible (Woo et al., 2003). Using immunoblotting and activity assays on HeLa cells expressing recombinant Prx 1, reduction of this overoxidized typical 2-cys Prx back to its reduced form with hydroperoxidase

activity was shown to be mediated by Sulfiredoxin 1 (Srx 1) (Chang et al., 2004). The overoxidation of the 2-cys Prxs and their regeneration is illustrated in Figure 1.5.

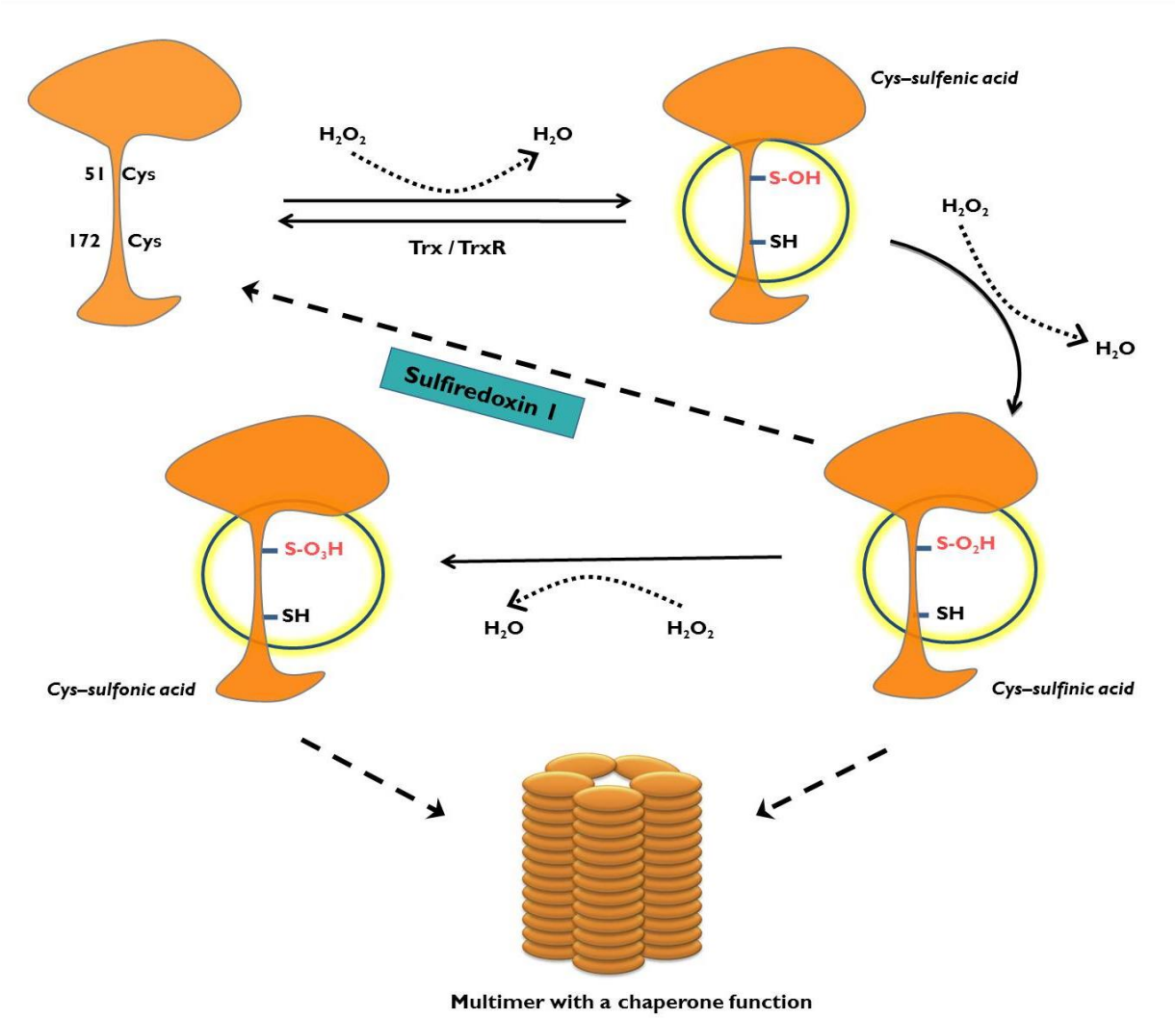

Figure 1.5: *Schematic showing the overoxidation and regeneration of typical 2-cys peroxiredoxins along with the formation of multimeric chaperones from the overoxidized forms. Image drawn from information obtained from Rhee (Rhee and Woo, 2011).*

The reducing mechanism of Srx 1 is specific for sulfinylated forms of typical 2-cys Prxs (Woo et al., 2005) and is dependent on a thiol donor (a free organosulphur compound containing a functional sulfhydryl (-SH) group), ATP and Mg^{2+} ions (Biteau et al., 2003; Jonsson et al., 2005). Using recombinant forms of 2-cys Prxs that were overoxidized *in vitro,* Woo et al. demonstrated that Srx 1 was able to reduce overoxidized typical 2-cys Prxs but not Prx 5 or Prx 6 (Woo et al., 2005). Although in this study reduction of overoxidized Prx 3 and Prx 4 could not be fully attributed to Srx 1 (Woo et al., 2005), it has since been shown that Srx 1 does serve as a regenerator of overoxidized Prx 3, the most important mitochondrial Prx. Using FLAG-tagged Srx1, translocation of Srx 1 into mitochondria in response to localized oxidative stress was demonstrated in HeLa cells (Noh et al., 2009). Western blotting of mitochondrially-enriched preparations showed that increased

mitochondrially-targeted Srx 1coincided with decreased overoxidized Prx 3 after an oxidative insult, suggesting that Srx 1 might catalyze the regeneration of overoxidized Prx 3. An earlier study using bone marrow-derived macrophages from Srx-deficient mice has also demonstrated that Srx 1 plays a crucial role in the reduction of the sulfinic form of Prx 3 as well as sulfinic forms of Prx I and II (Diet et al., 2007). It is now thought that Srx 1 mediates the reduction of overoxidized 2-cys Prxs through formation of a sulfinic phosphoryl ester intermediate which generates cysteine-sulfenic acid (SOH), the physiologically oxidized Prx substrate able to be further reduced by Trx/TrxR using NADPH (Jeong et al., 2006; Rhee et al., 2007).

Transcriptional control of Sulfiredoxin 1

It has been recently shown that Srx 1 transcription is regulated by two transcription factors – Activator protein-1 (AP-1) and Nuclear factor erythroid 2-related factor (Nrf 2) (Soriano et al., 2009a). AP-1 acts via specific AP-1 binding sites whilst Nrf 2 acts at an anti-oxidant response element (ARE), both located in the 5' UTR of the Srx 1 gene. Both these transcription factors induce expression of Srx 1 in the presence of oxidative stress (Figure 1.6). Under conditions of oxidative stress Trx unbinds from apoptosis signalling kinase 1 (ASK 1) leading to its activation. Activated ASK1 activates c-jun N-terminal kinases (JNK) by phosphorylation and by so doing initiates a phosphorylation cascade that results in the activation of c-jun by double phosphorylation. Activated c-jun then heterodimerizes with c-fos to form the AP-1 transcription factor (Hess et al., 2004). AP-1 then brings about the induction of Srx 1 by binding to three AP-1 sites in its 5' UTR (Papadia et al., 2008).

Independently, oxidative stress releases Kelch-like ECH associated-protein 1 (Keap 1) which is bound to Nrf 2 in the cytoplasm. Nrf 2 is a tightly regulated stress-response transcription factor that is constantly targeted for ubiquitin-mediated proteasomal degradation when bound to Keap 1 (Lee et al., 2005). Once released from Keap 1, Nrf 2 translocates to the nucleus, binds to small Maf proteins and, acting via the ARE, brings about the induction of Srx 1 (Papadia et al., 2008; Soriano et al., 2009a). Lastly, in cortical neurons Srx 1 levels are also regulated by synaptic activity at NMDA receptors (Papadia et al., 2008). This is discussed in more detail in Section 1.15.3.

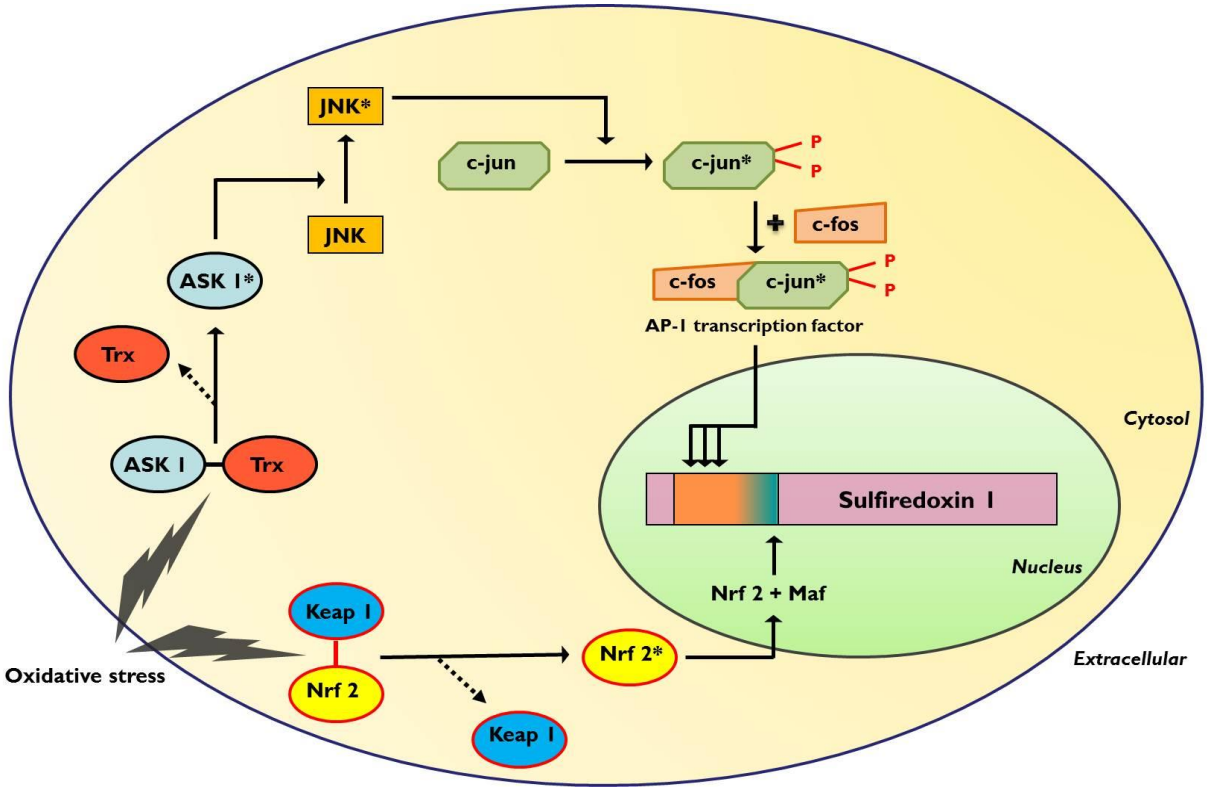

Figure 1.6: *Schematic showing the Sulfiredoxin 1 induction signalling cascade. * = activated species. Figure drawn from information obtained from Papadia and Soriano (Papadia et al., 2008; Soriano et al., 2009a).*

Budanov published work in 2004 that suggested that Sestrin 2 (Sesn 2), a redox-enzyme and p53 modulated protein, was also able to return overoxidized (sulfinylated) 2-cys Prxs to their reduced, active state (Budanov et al., 2004). Knock-out experiments conducted in RKO cells (a human colon carcinoma cell line) showed that depleted levels of Sestrin 1 or 2 generated increased levels of ROS pre-and post-H_2O_2 treatment. In contrast, overexpression of Sestrin 1 or 2 markedly reduced intracellular ROS generation. Papadia et al. identified *SESN 2* as a late-response gene that is activated (and regulated) by CAAT- enhancer binding protein transcription factor (C/EBPβ) in response to oxidative stress (Papadia et al., 2008). The same authors demonstrated that induction of Sesn 2 reduced levels of overoxidized two-cys Prxs *in vivo* (Papadia et al., 2008; Soriano et al., 2009b). Subsequently, conflicting evidence has emerged that Sesn 2 may not be an active regenerator of overoxidized typical two-cys Prxs (Woo et al., 2009). Co-immunoprecipitation using hemagglutinin epitope tagged Srx 1 and Sesn 2 demonstrated that reduction of overoxidized recombinant Prx 1 *in vitro* occurred only in the presence of Srx 1 and not in the presence of Sesn 2. Furthermore, overexpression of Sesn 2 in HeLa and A549 mammalian cell lines, did not affect the reduction of overoxidized typical 2-cys Prxs. In contrast, the reduction of $PrxSO_{2/3}$ was increased by the overexpression of Srx 1 in the same cell lines. This confirmed that reduction of $PrxSO_{2/3}$ was not influenced by levels of Sesn 2. Lastly, the effects of Sesn 2 on overoxidized typical 2-cys Prxs were studied using Sesn 2 knock-out mice. It was demonstrated that mouse embryonic fibroblasts from Sesn 2 knock-out and wild-type mice, subjected to H_2O_2 exposure and allowed to recover, showed no

difference in the rate of reduction of $PrxSO_{2/3}$. The authors concluded that Sesn 2 does not influence $PrxSO_{2/3}$ levels (Woo et al., 2009). On the balance of current evidence it seem likely that Srx 1 is the main regenerator of overoxidized 2-cys Prxs (Rhee et al., 2007) whilst a similar role for Sestrin 2 seems much less likely.

1.15 Functions of overoxidized typical 2-cys peroxiredoxins

Peroxiredoxins are found in all organisms but interestingly, oxidative inactivation of typical 2-cys Prxs through overoxidation of their thiol group is seen chiefly in eukaryotes but hardly ever in prokaryotes (Rhee et al., 2005a). In prokaryotes, the main role of the Prxs is defence against H_2O_2 released by other microorganisms or by the peroxide bursts of phagocytic cells within host animals (Wood et al., 2003b). Given this role in self-defence it is perhaps unsurprisingly that prokaryotic Prxs are highly resistant to oxidative inactivation (Yang et al., 2002). In contrast, eukaryotic 2-cys Prxs have evolved the capacity for oxidative inactivation and by doing so facilitated the development of a role for H_2O_2 in cell signalling. Sequence analyses of prokaryotic and eukaryotic Prxs demonstrate the structural changes that have developed through evolution allowing eukaryotic Prxs to become overoxidized. These changes have subsequently become highly conserved in eukaryotic typical 2-cys peroxiredoxins (Hall et al., 2009).

1.15.1 Hydrogen peroxide as a cellular messenger

Hydrogen peroxide is a source of highly reactive hydroxyl free radicals generated via the Fenton reaction (Chance et al., 1979). Previously it was thought of as an exclusively harmful by-product of the activities of the electron transport chain capable of causing oxidative damage to macromolecules if not dealt with quickly by the cell's anti-oxidant defence systems. Indeed, each compartment of the cell contains a number of hydroperoxidases capable of detoxifying H_2O_2 to water. These include catalase and the various glutathione peroxidases in addition to the Prxs (Barber and Shaw, 2010). These hydroperoxidases are essential for protecting cellular macromolecules from oxidative damage caused by H_2O_2 present in excess. The relative importance of each hydroperoxidase to this role is dependent upon intracellular localization, relative abundance and how effective each is as a hydroperoxidase. The 2-cys Prxs were earlier thought to be the least effective of the hydroperoxidases – more recent work suggests that their hydroperoxidase activity is greater than was previously thought (Woo et al., 2009). This, together with their abundance within some intracellular compartments, has brought about a re-evaluation of their relative importance as hydroperoxidases. For example, the mitochondrial matrix is subject to particularly high levels of H_2O_2 due to its proximity to components of the electron transport chain that generate superoxide. Despite this there is no catalase, a highly efficient hydroperoxidase, within this compartment. Peroxiredoxin 3, however, is present in abundance (Goemaere and Knoops, 2012) and is thought to provide the main protection against oxidative damage from H_2O_2 within the mitochondrial matrix.

Although it is certainly the case that H_2O_2 present in excess is a source of oxidative damage, H_2O_2 plays other more constructive roles within the cell. In addition to the beneficial antimicrobial effects of H_2O_2 released by phagocytic cells as part of the immune response to infection (Lambeth, 2004), there is now increasing evidence to suggest that H_2O_2 may mediate diverse intracellular processes by acting as an intracellular messenger. This role in signal transduction is reliant upon the tight control of local levels of H_2O_2 within the cell - something now believed to be mediated by the mammalian 2-cys Prxs facilitated by their capacity for inactivation by overoxidation (Rhee, 2006; Rhee et al., 2005b). Hydrogen peroxide is produced at the cell membrane in response to external stimuli including cytokines (Meier et al., 1989), hormones, peptide growth factors (Shibanuma et al., 1991) and neurotransmitters (Yao et al., 1999). This H_2O_2 may then bring about downstream effects by its modulation of the activities of numerous groups of proteins including transcription factors, phospholipases, protein kinases, phosphatases, ion channels and G-proteins (Rhee, 2006). Whether or not local bursts of H_2O_2 produced in cell-signalling go on to mediate these downstream effects or are simply converted to water depends upon the local concentration and hydroperoxidase activity of the 2-cys Prxs in a process described by the floodgate hypothesis (discussed below).

Floodgate hypothesis

The floodgate hypothesis was put forward to explain the role of the typical 2-cys Prxs in maintaining a balance between reduction of potentially damaging excess H_2O_2 and allowing the regulated release of local bursts of H_2O_2 for the purposes of cell signalling (Rhee et al., 2005b). Within cells, the levels of cytosolic typical 2-cys Prxs are tightly regulated. During a peroxide burst, if typical 2-cys Prxs in the locality are present at low levels they will be rapidly overoxidized and inactivated. This inactivation allows local H_2O_2 levels to increase and H_2O_2 may then serve as an intracellular signal in the window of opportunity provided by inactive 2-cys Prxs. The floodgate now open, reverts to its original closed state by the removal of the H_2O_2 by other cytosolic peroxidases such as catalase and the glutathione peroxidases. The regeneration of overoxidized typical 2-cys Prxs takes hours (Soriano et al., 2008), as does *de novo* Prx synthesis. The system is reset with the eventual regeneration of reduced 2-cys Prxs by active regenerators of overoxidized 2-cys Prxs such as Sulfiredoxin 1. If on the other hand, levels of the typical 2-cys Prxs in the neighbourhood of the peroxide burst are high at the outset these Prxs may reduce almost all of the H_2O_2 released by the signal burst providing no opportunity for H_2O_2 to act a cellular messenger. A schematic of the floodgate hypothesis is provided in Figure 1.7.

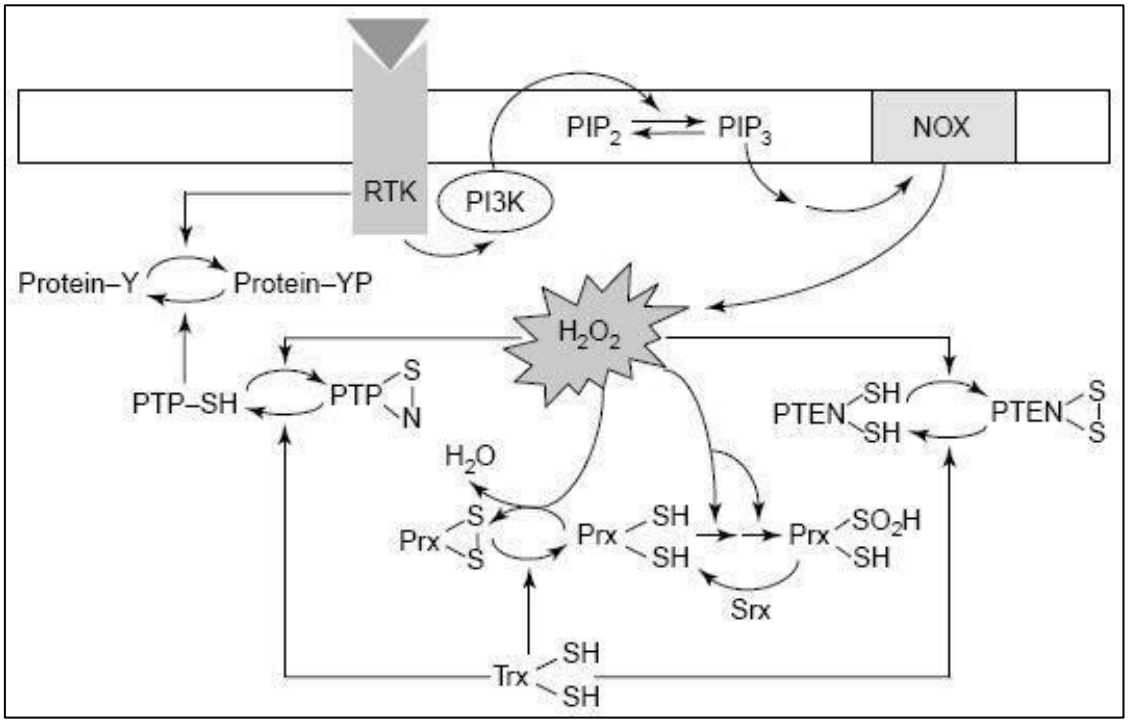

Figure 1.7: *The floodgate hypothesis. Activation of receptor tyrosine kinases (RTK) and phosphatidylinositol 3-kinase (PI3K), via an external stimulus, results in conversion of phosphatidylinositol 4,5-bisphosphate (PIP2) to phosphatidylinositol 3,4,5-triphosphate (PIP3) by phosphorylation. Activation of NADPH oxidase (NOX) by PIP3 results in production of H_2O_2. Locally present typical 2-cys Prxs are oxidatively inactivated as a consequence of the peroxide burst leading to rising local levels of H_2O_2. The floodgate at this stage is said to be open and allows H_2O_2-mediated cell signalling. Effects of the H_2O_2 burst are also seen on protein tyrosine phosphatases (PTP) and phosphatidylinositol 3,4,5-triphosphate 3-phosphatase (PTEN). Excess H_2O_2 is gradually cleared by other cellular peroxidases bringing signalling to an end. The overoxidized Prxs are returned to their reduced state and the floodgate is closed. Image reproduced from Rhee (Rhee et al., 2005b) with permission from Elsevier.*

Recently, Woo et al. demonstrated that Prx I is locally inactivated to promote H_2O_2-mediated signalling at the cell membrane, whereas in the rest of the cell H_2O_2 is eliminated by other peroxiredoxins (Woo et al., 2010). In NIH 3T3 cells, using Prx I transiently phosphorylated at tyrosine-194 in response to epidermal growth factor (EGF) and platelet-derived growth factor (PDGF), oxidative inactivation of Prx I was achieved. This localized inactivation of Prx I allowed for the transient accumulation of H_2O_2 around the cell membrane, where signalling components are concentrated. Prx 2 on the other hand was resistant to phosphorylation and thereby less susceptible to inactivation by overoxidation, serving to prevent the toxic accumulation of H_2O_2 elsewhere. Prx 2 was, however, oxidatively inactivated if exposed continuously to oxidative stress (Woo et al., 2010). This differential susceptibility of Prx I and Prx 2 to inactivation by phosphorylation and overoxidation suggests distinctive roles for these two members of the typical 2-cys Prx family in the facilitation of cell signalling.

1.15.2 Chaperone activity of overoxidized typical 2-cys peroxiredoxins

An important structural feature of the peroxiredoxins is their thioredoxin fold motif (Schroder and Ponting, 1998). Other proteins which contain a thioredoxin fold such as HSP33 (Jakob et al., 1999) and Protein disulphide isomerase (Wang, 2002) are known to function as molecular chaperones. This sequence homology with known protein chaperones suggested a possible role for the peroxiredoxins in the monitoring of misfolded proteins under conditions of oxidative stress.

In yeast under conditions of oxidative stress and heat shock, Prx 1 and 2 were shown to become overoxidized and form high molecular weight complexes (Jang et al., 2004). These complexes had a molecular mass ~10-50 times that of the single subunit and were shown to act as molecular chaperones. In this overoxidized multimeric form, Prx 1 and 2 lost their hydroperoxidase activity. In contrast, reduced Prx 1 and 2 homodimers did not exhibit any chaperone-like ability. Moon *et al.,* working in HeLa cells, showed that under conditions of oxidative stress Prx 2 formed a high molecular weight complex able to function as a protein chaperone. Removal of the source of oxidative stress resulted in the dissociation of the chaperone back to individual homodimers that reverted back to active hydroperoxidases via a chaperone-to-peroxidase switch. The functional switching from peroxidase to chaperone function of Prx 2 was shown to be dependent upon the oxidation state of the Cp and a C-terminus YF domain (Moon et al., 2005). Although Koo et al. demonstrated the importance of this domain in mediating the oxidative inactivation of Prxs (Koo et al., 2002), the idea of this domain acting as a molecular redox switch only emerged later on (Rhee et al., 2005a). Whilst human Prx 3 can become overoxidized and is a substrate for sulfiredoxin 1, overoxidized human Prx 3 has yet to be shown to have a chaperone function.

1.15.3 Activity-mediated regulation of the overoxidized typical 2-cys peroxiredoxins

An important recent study in rat cortical neurons demonstrated regulation of anti-oxidant defence by synaptic activity – that is, synaptic activity served to bolster anti-oxidant defence (Papadia et al., 2008). This activity-dependent upregulation of anti-oxidant defence is mediated by glutamatergic N-methyl-D-aspartate (NMDA) receptors via alterations in the level and activity of proteins that regulate the peroxidase activity of the typical 2-cys Prxs and those that regenerate the overoxidized species. First, synaptic activity via NMDA receptors upregulated levels of the Prx regenerator sulfiredoxin 1 and the putative regenerator sestrin 2 via their respective transcription factors AP-1 and C/EBPβ. NMDA-mediated synaptic activity also negatively regulated the transcription of the thioredoxin inhibitor, thioredoxin-interacting protein (Txnip), thereby increasing Trx activity within cells. Taken together, these changes were shown to increase the availability of reduced typical 2-cys Prxs able to act as hydroperoxidases as synaptic activity at the cell membrane increased, protecting the neuron from free radical damage from H_2O_2 (depicted in Figure 1.8). Furthermore, quantitative polymerized chain reaction (Q-PCR) analyses of post-mortem cortices of individuals aged between 81-95 yrs and between 25-37 yrs showed increased levels of Txnip mRNA in post-mortem cortex from older individuals indicating that with age there could be a reduction in Prx-mediated anti-oxidant defence.

The authors suggested that this regulatory system was one way in which a neuron's pattern of activity could influence the extent of cumulative oxidative damage incurred over time. They also hypothesized that such a mechanism might underlie the onset in middle age of neurodegenerative diseases including ALS, Alzheimer's disease and Parkinson's disease (Papadia et al., 2008). Given the high levels of electrical activity of motor neurons it would be interesting to know whether this, or a similar, system was present in this cell type and, if so, whether any deficit might exist in ALS. Such a deficit could potentially provide an explanation for the selectivity for motor neurons of ALS and the adult-onset of the disease, features that, to date, remain unexplained.

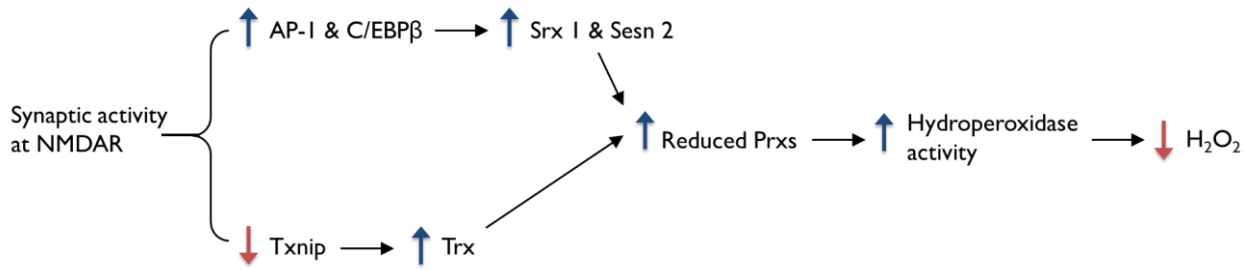

Figure 1.8: *Schematic showing how synaptic activity regulates the oxidation state of typical 2-cys Prxs leading to increased protection against free radical damage as neuronal synaptic activity mediated at NMDA receptors increases. Figure drawn from information obtained from Papadia (Papadia et al., 2008).*

1.15.4 Circadian rhythms and the 2-cys peroxiredoxins

Typical 2-cys peroxiredoxins have very recently been shown to exhibit endogenously regulated circadian redox rhythms. Experiments conducted in red blood cells (RBCs) obtained from healthy volunteers demonstrated that typical 2-cys Prxs were present in dimerized forms (their physiologically oxidized state) and overoxidized forms ($PrxSO_{2/3}$) at regular intervals over each 24 hour period (O'Neill and Reddy, 2011). Given that RBCs lack a nucleus, it is apparent that Prx circadian rhythms are independent of any transcriptional circadian pattern. To verify that contaminating white blood cells were not regulating the Prx circadian redox cycle via transcription-by-proxy, experiments were repeated in the presence of transcription- and translation-blocking agents. The transcriptional independence of the observed Prx circadian cycling was confirmed. Prx circadian redox rhythms were also shown to be independent of light and temperature indicating the presence of an innate cellular clock.

When similar experiments were conducted in nucleated NIH3T3 cells and mouse embryonic fibroblasts, a rhythmic cycling of levels of overoxidized 2-cys Prxs similar to that observed in anuclear cells was observed. Furthermore, mouse embryonic fibroblasts from mice lacking clock genes (*Cry1-/- & Cry2 -/-)* also exhibited redox cycles similar to those of control mice (O'Neill and Reddy, 2011). Taken together these results indicate that the oxidation state of the typical 2-cys Prxs is regulated by an as yet unidentified innate clock that is independent of transcription, translation and external stimuli.

The authors hypothesized that the redox rhythms of typical 2-cys Prxs play a role in regulating transcription/translation feedback loops within cells (O'Neill et al., 2011). To what extent this new feature of Prx biology interacts with the other known functions of 2-cys Prxs such as anti-oxidant defence and their functions as protein chaperones and mediators of H_2O_2 signalling remains to be seen.

1.16 Peroxiredoxins and neurodegenerative diseases

Alterations in the levels of peroxiredoxins have been observed in several neurodegenerative disorders. This evidence will be surveyed in the following sections with particular attention paid to studies suggestive of involvement of the Prxs in the pathogenesis of ALS.

1.16.1 Peroxiredoxins and ALS

Proteomic analysis of the cytosol of NSC34 cells stably transfected with various species of mutant human SOD1, a well-characterized cellular model of fALS (see Chapter 2, Section 2.3), showed increased levels of Prx 1 in cells expressing G93A or G37R SOD1 when compared to WT or empty vector cells (Allen et al., 2003). Kirby et al. carried out gene expression studies of NSC34 cells stably expressing G93A mutant SOD1 and showed changes in the level of several Prxs at an mRNA level when compared to controls. In comparison to vector-only control cells, there was a 1.96-fold increase in Prx 2 mRNA levels while those of Prx 3 and Prx 4 were decreased by a factor of 4.8 and 2.4 respectively (Kirby et al., 2005). These findings were also reflected at a protein level. Proteomic analysis of mitochondrially-enriched fractions of the same NSC34 cell model with subsequent confirmation by Western blotting showed the expression of Prx 3 to be decreased and that of Prx 2 increased in the presence of mutant SOD1. A reduction in Prx 3 was then demonstrated by Western blotting of mitochondrially-enriched preparations of spinal cord homogenates from 90 day old G93A SOD1 transgenic mice when compared to non-transgenic littermates and age-matched mice overexpressing human WT-SOD1. Furthermore, Q-PCR of mRNA extracted from laser-capture microdissected motor neurons from post-mortem spinal cord from both sALS and SOD1 fALS patients also showed decreased levels of Prx 3 mRNA, mirroring the results obtained in the cell model and G93A transgenic mice (Wood-Allum et al., 2006). In an independent proteomic study of mitochondrially-enriched preparations of NSC34 cells expressing G93A mutant human SOD1, Fukada et al. also confirmed a decrease in Prx 3 levels in the presence of the mutant SOD1 compared to cells expressing WT human SOD1 (Fukada et al., 2004). Ferraiuolo et al. showed a 2.12-fold decrease of Prx 2 at mRNA in laser-capture microdissected spinal cord motor neurons of 120 day-old G93A mice compared to non-transgenic littermates (Ferraiuolo et al., 2007). Whilst the findings of these studies in different models of SOD1 fALS at various timepoints in the disease course are not entirely consistent with one another, the recurrence of alterations in the levels of various 2-cys Prxs in the presence of mutant SOD1 suggests dysregulation of this component of anti-oxidant defence in ALS.

Neuropathological evidence

There is also evidence from immunohistochemical studies of post-mortem central nervous system (CNS) tissue from patients with SOD1-related familial ALS. Analyses of motor neuron-specific Lewy-body like hyaline conglomerate inclusions from A126V SOD1-fALS patients showed that these proteinaceous inclusions immunostained positive for Prx 2. These findings were replicated in two different mutant SOD1 transgenic mice (H46R and G93A). The presence of Prx 2 in these proteinaceous inclusion bodies, highly characteristic of ALS, does not prove an active role for the 2-cys Prxs in disease pathogenesis but nevertheless there are now other examples where this has turned out to be the case (e.g., TDP43). The authors suggest that their findings further implicate the peroxiredoxins and suggest redox-dysfunction in SOD1 ALS (Kato et al., 2004). In a follow-up study that included sALS patients, immunohistochemistry of spinal cord motor neurons showed that Prx 2 expression was decreased in neurons affected by the disease but was increased in the surviving ones, findings interpreted by the authors as indicating that after an initial attempt at compensation (the increased Prx 2), eventual impairment of anti-oxidant defence may occur with disease progression, eventually contributing to neuronal death (Kato et al., 2005).

1.16.2 Peroxiredoxins and other neurodegenerative disorders

Alterations in levels of the Prxs have also been reported in other neurodegenerative diseases including Alzheimer's disease (AD), Down's syndrome, and Parkinson's disease (PD). To what extent these changes confer important changes in functionality is unclear although the consistency between studies suggests they are unlikely to be artefactual. Further investigation of this at a biochemical level in post-mortem tissue from patients is, however, likely to be difficult.

Alzheimer's disease (AD)

Proteomic analysis using 2-D gel electrophoresis coupled with MALDI-MS of frontal cortex and cerebellum from Down's syndrome and AD patients showed changes in the levels of Prx 2 and 3 (Krapfenbauer et al., 2003). Down's syndrome is a chromosomal disorder whose sufferers commonly develop an Alzheimer's like dementia at a young age (30-35 years) (Ness et al., 2012; Zigman and Lott, 2007). In the Krapfenbauer study, levels of Prx 2 were observed to be significantly increased in frontal cortex of patients with both Down's syndrome and Alzheimer's disease when compared to controls. Additionally, levels of Prx 3 were observed to be significantly decreased in frontal cortex of Down's syndrome patients. Similar changes were also reported in an earlier proteomic study of brain samples from AD and Down's syndrome cases which once again showed statistically significant increases in Prx 2 and decreases in Prx 3 (Kim et al., 2001). However, in contrast to the findings of Krapfenbauer et al., Kim et al. also showed significantly increased levels of Prx 1 in AD and Down's syndrome patients compared to controls (Kim et al., 2001). In another recent study, levels of Prx 2 were observed to be elevated in hippocampal and temporal cortex from AD patients compared to controls (Yao et al., 2007). These authors went on to investigate the cause of this using an amyloid precursor protein (APP) transgenic mouse model of Alzheimer's disease, that overexpressed amyloid beta and amyloid

binding alcohol dehydrogenase (ABAD). They demonstrated that Prx 2 levels were dependent upon interactions between amyloid beta and ABAD. Using 2-D electrophoresis and immunoblotting, the authors further demonstrated upregulation of Prx 2 in hippocampus and cerebral cortex (Yao et al., 2007). An amyloid beta (Aβ) resistant nerve cell model of AD was also shown to have increased resistance to the toxicity conferred by Aβ in the presence of high levels of Prx 1, correlating with the increased levels of Prx 1 (in its reduced state) found in the brain tissue of AD patients compared to controls. High levels of oxidized Prx 2 were also observed in brain tissue from AD patients (Cumming et al., 2007).

Parkinson's disease (PD)

A study by Basso et al. in PD brain tissue using 2-D electrophoresis and MALDI-MS to perform proteomic analyses of substantia nigra samples from post-mortem PD and control brain showed significantly increased levels of Prx 2 in the PD samples compared to controls (Basso et al., 2004). In another study, brain tissue from PD patients was shown to have increased levels of nitrosylated Prx 2 compared to controls. Nitrosylation of the sulphur at the reactive sites (Cp and Cr) by reaction with peroxynitrite was shown to ablate the enzyme's anti-oxidant function resulting in oxidative stress (Fang et al., 2007). The loss of Prx 2 hydroperoxidase activity was demonstrated in neuronal SH-SY5Y cells and in primary neuronal cultures that were exposed to nitric oxide synthase (NOS). Upon inhibiting the action of NOS, the hydroperoxidase function of Prx 2 was restored. These findings were consistent in dopaminergic SH-SY5Y cells, a cell model of PD (Fang et al., 2007).

Using a proteomic approach, Lee et al. investigated changes in protein expression and post-translational modification after drug treatment of MN9D dopaminergic neuronal cells, a cellular model of PD (Lee et al., 2008). The expression of Prx 1, 2 and 6 was found to be significantly altered following treatment with 6-hydroxydopamine (6-OHDA) – a neurotoxin that selectively depletes dopaminergic neurons. In the case of Prx 1, 6-OHDA-induced Prx 1 overoxidation was confirmed by an acidic shift in the position of the Prx 1 spot on 2D gels prepared from treated MN9D lysates when compared to those made from control lysates. Addition of the anti-oxidant agent *N*-acetylcysteine blocked the oxidative inactivation of Prx 1 suggesting that ROS generated by 6-OHDA induced the overoxidation of Prx 1 (Lee et al., 2008).

The evidence presented here indicates that the levels and post-translational modification of the peroxiredoxins are altered in CNS tissue in neurodegenerative diseases where there is evidence of oxidative stress and protein misfolding, ALS included. This work was directed at investigating the possibility that this versatile group of anti-oxidants might play a role in the pathogenesis of ALS. The rationale, aims and experimental approach adopted are considered next.

1.17 Rationale

As has been discussed, the peroxiredoxins are a highly conserved group of hydroperoxidases expressed throughout the CNS with representatives in multiple cellular compartments. In addition to their ability to detoxify H_2O_2 to water, giving them a central role in anti-oxidant defence, the capacity of eukaryotic 2-cys Prxs to become oxidatively inactivated has conferred other functions. These include the ability, when overoxidized, to coalesce into multimeric structures able to function as protein chaperones and the capacity to modulate the response of H_2O_2 signaling pathways to incoming stimuli. Given strong evidence for the involvement of oxidative stress, mitochondrial dysfunction and protein aggregation in the pathogenesis of ALS these interchangeable Prx functions appeared likely to be relevant. Together with changes in Prx levels observed in ALS patients and models of the disease as well as in related neurodegenerative disorders and the fact that synaptic activity of cortical neurons can influence the degree to which the 2-cys Prxs are overoxidized it seemed plausible that the Prxs might play a role in the pathogenesis of ALS. In my work I focused on those typical 2-cys Prxs that are expressed in neurons – Prx 2, 3 and 4. Of the three, my primary focus was on Prx 2 and Prx 3, both of which are expressed abundantly in neurons. Prx 3 was of particular interest as it is the only peroxiredoxin exclusively found within the mitochondrial matrix, the frontline of ROS generation.

1.18 Hypothesis, aims & objectives

1.18.1 Hypothesis

We hypothesized that in the light of known oxidative stress in ALS the typical 2-cys Prxs might exist in a more oxidized state in ALS than in health. As overoxidation inactivates the typical 2-cys Prxs as hydroperoxidases we further hypothesized that excess typical 2-cys Prx overoxidation might contribute to disease pathogenesis by reducing the anti-oxidant capacity of the cell, especially in those compartments where the contribution of the Prxs to overall hydroperoxidase activity was the greatest, for example the mitochondrial matrix. As overoxidation is also thought to operate as a redox switch converting 2-cys Prxs from hydroperoxidases to protein chaperones we also hoped to investigate the possibility that increased typical 2-cys Prx overoxidation might represent a compensatory response to conditions of oxidative stress in ALS.

1.18.2 Aims & objectives

The primary aim of this work was to establish whether or not excess overoxidized 2-cys Prxs could be detected in ALS. I planned to investigate this in our cellular and murine models of SOD1-related fALS. I next aimed to establish whether or not recovery of overoxidized 2-cys Prxs was defective in ALS. Were excess typical 2-cys Prx overoxidized or defective recovery of overoxidized Prxs demonstrated in the disease state, I aimed to investigate the functional consequences of this and explore whether manipulation of the oxidation state of the 2-cys Prxs might impact positively upon cellular viability with a view to establishing if this pathway might represent a therapeutic target.

1.19 Experimental approach

In order to establish whether or not the 2-cys Prxs were present in a more oxidized state in ALS, I looked at two cellular models of the disease. I investigated fibroblasts obtained from patients suffering from familial ALS due to mutations in SOD1 and TDP43 and compared them with fibroblasts obtained from healthy age- and sex-matched controls. Alterations in the levels of overoxidized 2-cys Prxs between control and patient fibroblasts were examined at a protein level by Western blotting. The response of these cells to exogenously applied H_2O_2 was then examined in the same way. Finally, the time required for the recovery of overoxidized 2-cys Prxs after application of H_2O_2 was determined. Levels of overoxidized 2-cys Prxs and the proteins involved in the regeneration of reduced 2-cys Prxs were measured in these samples. In order to extend my work into a more motor neuronal system, I went on to test my hypotheses in NSC34 cells, a well-established immortalized murine motor neuronal cell line stably transfected to express various species of mutant human SOD1 known to cause fALS in patients. Lastly, levels of overoxidized 2-cys Prxs and related proteins were measured in spinal cord and brain tissue from G93A-SOD1 overexpressing transgenic mice.

REFERENCES

Abe, K., Pan, L.H., Watanabe, M., Kato, T., and Itoyama, Y. (1995). Induction of nitrotyrosine-like immunoreactivity in the lower motor neuron of amyotrophic lateral sclerosis. Neurosci Lett *199*, 152-154.

Abe, K., Pan, L.H., Watanabe, M., Konno, H., Kato, T., and Itoyama, Y. (1997). Upregulation of protein-tyrosine nitration in the anterior horn cells of amyotrophic lateral sclerosis. Neurol Res *19*, 124-128.

Adams, C.R., Ziegler, D.K., and Lin, J.T. (1983). Mercury intoxication simulating amyotrophic lateral sclerosis. Jama *250*, 642-643.

Ahtoniemi, T., Jaronen, M., Keksa-Goldsteine, V., Goldsteins, G., and Koistinaho, J. (2008). Mutant SOD1 from spinal cord of G93A rats is destabilized and binds to inner mitochondrial membrane. Neurobiol Dis *32*, 479-485.

Albo, F., Pieri, M., and Zona, C. (2004). Modulation of AMPA receptors in spinal motor neurons by the neuroprotective agent riluzole. J Neurosci Res *78*, 200-207.

Allen, S., Heath, P.R., Kirby, J., Wharton, S.B., Cookson, M.R., Menzies, F.M., Banks, R.E., and Shaw, P.J. (2003). Analysis of the cytosolic proteome in a cell culture model of familial amyotrophic lateral sclerosis reveals alterations to the proteasome, antioxidant defenses, and nitric oxide synthetic pathways. Journal of Biological Chemistry *278*, 6371-6383.

Alonso, A., Logroscino, G., and Hernan, M.A. (2010a). Smoking and the risk of amyotrophic lateral sclerosis: a systematic review and meta-analysis. Journal of Neurology, Neurosurgery, and Psychiatry *81*, 1249-1252.

Alonso, A., Logroscino, G., Jick, S.S., and Hernan, M.A. (2010b). Association of smoking with amyotrophic lateral sclerosis risk and survival in men and women: a prospective study. BMC Neurol *10*, 6.

ALSOD website (accessed on 15th Oct 2012). http://alsod.iop.kcl.ac.uk/Overview/gene.aspx?gene_id=SOD1 , SOD1 mutations associated with ALS.

Andersen, P.M. (2006). Amyotrophic lateral sclerosis associated with mutations in the CuZn superoxide dismutase gene. Curr Neurol Neurosci Rep *6*, 37-46.

Andersen, P.M. (2012). Mutation in C9orf72 changes the boundaries of ALS and FTD. Lancet Neurol *11*, 205-207.

Andersen, P.M., Nilsson, P., Ala-Hurula, V., Keranen, M.L., Tarvainen, I., Haltia, T., Nilsson, L., Binzer, M., Forsgren, L., and Marklund, S.L. (1995). Amyotrophic lateral sclerosis associated with homozygosity for an Asp90Ala mutation in CuZn-superoxide dismutase. Nat Genet *10*, 61-66.

Andersson, M.K., Stahlberg, A., Arvidsson, Y., Olofsson, A., Semb, H., Stenman, G., Nilsson, O., and Aman, P. (2008). The multifunctional FUS, EWS and TAF15 proto-oncoproteins show cell type-specific expression patterns and involvement in cell spreading and stress response. BMC Cell Biol *9*, 37.

Aoki, M., Ogasawara, M., Matsubara, Y., Narisawa, K., Nakamura, S., Itoyama, Y., and Abe, K. (1993). Mild ALS in Japan associated with novel SOD mutation. Nat Genet *5*, 323-324.

Armon, C. (2003). An evidence-based medicine approach to the evaluation of the role of exogenous risk factors in sporadic amyotrophic lateral sclerosis. Neuroepidemiology *22*, 217-228.

Armon, C. (2009). Smoking may be considered an established risk factor for sporadic ALS. Neurology *73*, 1693-1698.

Azzouz, M., Poindron, P., Guettier, S., Leclerc, N., Andres, C., Warter, J.M., and Borg, J. (2000). Prevention of mutant SOD1 motoneuron degeneration by copper chelators in vitro. J Neurobiol *42*, 49-55.

Barber, S.C., and Shaw, P.J. (2010). Oxidative stress in ALS: key role in motor neuron injury and therapeutic target. Free Radical Biology & Medicine *48*, 629-641.

Basso, M., Giraudo, S., Corpillo, D., Bergamasco, B., Lopiano, L., and Fasano, M. (2004). Proteome analysis of human substantia nigra in Parkinson's disease. Proteomics *4*, 3943-3952.

Beal, M.F., Ferrante, R.J., Browne, S.E., Matthews, R.T., Kowall, N.W., and Brown, R.H., Jr. (1997). Increased 3-nitrotyrosine in both sporadic and familial amyotrophic lateral sclerosis. Ann Neurol *42*, 644-654.

Bensimon, G., Lacomblez, L., and Meininger, V. (1994). A controlled trial of riluzole in amyotrophic lateral sclerosis. ALS/Riluzole Study Group. N Engl J Med *330*, 585-591.

Bigio, E.H., Lipton, A.M., White, C.L., 3rd, Dickson, D.W., and Hirano, A. (2003). Frontotemporal and motor neurone degeneration with neurofilament inclusion bodies: additional evidence for overlap between FTD and ALS. Neuropathol Appl Neurobiol *29*, 239-253.

Biteau, B., Labarre, J., and Toledano, M.B. (2003). ATP-dependent reduction of cysteine-sulphinic acid by S. cerevisiae sulphiredoxin. Nature *425*, 980-984.

Blair, I.P., Williams, K.L., Warraich, S.T., Durnall, J.C., Thoeng, A.D., Manavis, J., Blumbergs, P.C., Vucic, S., Kiernan, M.C., and Nicholson, G.A. (2010). FUS mutations in amyotrophic lateral sclerosis: clinical, pathological, neurophysiological and genetic analysis. Journal of Neurology, Neurosurgery, and Psychiatry *81*, 639-645.

Borchelt, D.R., Lee, M.K., Slunt, H.S., Guarnieri, M., Xu, Z.S., Wong, P.C., Brown, R.H., Jr., Price, D.L., Sisodia, S.S., and Cleveland, D.W. (1994). Superoxide dismutase 1 with mutations linked to familial amyotrophic lateral sclerosis possesses significant activity. Proc Natl Acad Sci U S A *91*, 8292-8296.

Borthwick, G.M., Johnson, M.A., Ince, P.G., Shaw, P.J., and Turnbull, D.M. (1999). Mitochondrial enzyme activity in amyotrophic lateral sclerosis: implications for the role of mitochondria in neuronal cell death. Ann Neurol *46*, 787-790.

Bosco, D.A., Lemay, N., Ko, H.K., Zhou, H., Burke, C., Kwiatkowski, T.J., Jr., Sapp, P., McKenna-Yasek, D., Brown, R.H., Jr., and Hayward, L.J. (2010b). Mutant FUS proteins that cause amyotrophic lateral sclerosis incorporate into stress granules. Hum Mol Genet *19*, 4160-4175.

Bourke, S.C., Tomlinson, M., Williams, T.L., Bullock, R.E., Shaw, P.J., and Gibson, G.J. (2006). Effects of non-invasive ventilation on survival and quality of life in patients with amyotrophic lateral sclerosis: a randomised controlled trial. Lancet Neurol *5*, 140-147.

Boveris, A., Oshino, N., and Chance, B. (1972). The cellular production of hydrogen peroxide. Biochem J *128*, 617-630.

Boxer, A.L., Mackenzie, I.R., Boeve, B.F., Baker, M., Seeley, W.W., Crook, R., Feldman, H., Hsiung, G.Y., Rutherford, N., Laluz, V.*, et al.* (2011). Clinical, neuroimaging and neuropathological features of a new chromosome 9p-linked FTD-ALS family. J Neurol Neurosurg Psychiatry *82*, 196-203.

Brettschneider, J., Van Deerlin, V.M., Robinson, J.L., Kwong, L., Lee, E.B., Ali, Y.O., Safren, N., Monteiro, M.J., Toledo, J.B., Elman, L.*, et al.* (2012). Pattern of ubiquilin pathology in ALS and FTLD indicates presence of C9ORF72 hexanucleotide expansion. Acta Neuropathol *123*, 825-839.

Bristol, L.A., and Rothstein, J.D. (1996). Glutamate transporter gene expression in amyotrophic lateral sclerosis motor cortex. Ann Neurol *39*, 676-679.

Brooks, B.R., Miller, R.G., Swash, M., and Munsat, T.L. (2000). El Escorial revisited: revised criteria for the diagnosis of amyotrophic lateral sclerosis. Amyotroph Lateral Scler Other Motor Neuron Disord *1*, 293-299.

Browne, S.E., Bowling, A.C., Baik, M.J., Gurney, M., Brown, R.H., Jr., and Beal, M.F. (1998). Metabolic dysfunction in familial, but not sporadic, amyotrophic lateral sclerosis. J Neurochem *71*, 281-287.

Bruijn, L.I., Becher, M.W., Lee, M.K., Anderson, K.L., Jenkins, N.A., Copeland, N.G., Sisodia, S.S., Rothstein, J.D., Borchelt, D.R., Price, D.L., *et al.* (1997). ALS-linked SOD1 mutant G85R mediates damage to astrocytes and promotes rapidly progressive disease with SOD1-containing inclusions. Neuron *18*, 327-338.

Bruyn, R.P., Koelman, J.H., Troost, D., and de Jong, J.M. (1995). Motor neuron disease (amyotrophic lateral sclerosis) arising from longstanding primary lateral sclerosis. J Neurol Neurosurg Psychiatry *58*, 742-744.

Bryk, R., Griffin, P., and Nathan, C. (2000). Peroxynitrite reductase activity of bacterial peroxiredoxins. Nature *407*, 211-215.

Budanov, A.V., Sablina, A.A., Feinstein, E., Koonin, E.V., and Chumakov, P.M. (2004). Regeneration of peroxiredoxins by p53-regulated sestrins, homologs of bacterial AhpD. Science *304*, 596-600.

Bunina, T.L. (1962). [On intracellular inclusions in familial amyotrophic lateral sclerosis.]. Zh Nevropatol Psikhiatr Im S S Korsakova *62*, 1293-1299.

Buratti, E., and Baralle, F.E. (2001). Characterization and functional implications of the RNA binding properties of nuclear factor TDP-43, a novel splicing regulator of CFTR exon 9. J Biol Chem *276*, 36337-36343.

Byrne, S., Elamin, M., Bede, P., Shatunov, A., Walsh, C., Corr, B., Heverin, M., Jordan, N., Kenna, K., Lynch, C., *et al.* (2012). Cognitive and clinical characteristics of patients with amyotrophic lateral sclerosis carrying a C9orf72 repeat expansion: a population-based cohort study. Lancet neurology.

Carri, M.T., Ferri, A., Battistoni, A., Famhy, L., Gabbianelli, R., Poccia, F., and Rotilio, G. (1997). Expression of a Cu,Zn superoxide dismutase typical of familial amyotrophic lateral sclerosis induces mitochondrial alteration and increase of cytosolic Ca2+ concentration in transfected neuroblastoma SH-SY5Y cells. FEBS Lett *414*, 365-368.

Carriedo, S.G., Sensi, S.L., Yin, H.Z., and Weiss, J.H. (2000). AMPA exposures induce mitochondrial Ca(2+) overload and ROS generation in spinal motor neurons in vitro. J Neurosci *20*, 240-250.

Carriedo, S.G., Yin, H.Z., and Weiss, J.H. (1996). Motor neurons are selectively vulnerable to AMPA/kainate receptor-mediated injury in vitro. J Neurosci *16*, 4069-4079.

Chad, D.A. (2006). Classification, diagnosis, and presentation of diagnosis of ALS. In Amyotrophic lateral sclerosis, H. Mitsumoto, S. Przedborski, and P.H. Gordon, eds. (New York: Taylor & Francis Group), pp. 201-225.

Chae, H.Z., Chung, S.J., and Rhee, S.G. (1994a). Thioredoxin-dependent peroxide reductase from yeast. J Biol Chem *269*, 27670-27678.

Chae, H.Z., Uhm, T.B., and Rhee, S.G. (1994b). Dimerization of thiol-specific antioxidant and the essential role of cysteine 47. Proc Natl Acad Sci U S A *91*, 7022-7026.

Chance, B., Sies, H., and Boveris, A. (1979). Hydroperoxide metabolism in mammalian organs. Physiol Rev *59*, 527-605.

Chance, P.F., Rabin, B.A., Ryan, S.G., Ding, Y., Scavina, M., Crain, B., Griffin, J.W., and Cornblath, D.R. (1998). Linkage of the gene for an autosomal dominant form of juvenile amyotrophic lateral sclerosis to chromosome 9q34. American Journal of Human Genetics *62*, 633-640.

Chang, T.S., Jeong, W., Woo, H.A., Lee, S.M., Park, S., and Rhee, S.G. (2004). Characterization of mammalian sulfiredoxin and its reactivation of hyperoxidized peroxiredoxin through reduction of cysteine sulfinic acid in the active site to cysteine. J Biol Chem *279*, 50994-51001.

Chavada, G., El-Nayal, A., Lee, F., Webber, S.J., McAlindon, M., Walsh, T., Hollinger, H., McDermott, C.J., and Shaw, P.J. (2010). Evaluation of two different methods for per-oral gastrostomy tube placement in patients with motor neuron disease (MND): PIG versus PEG procedures. Amyotroph Lateral Scler *11*, 531-536.

Chen, Y.Z., Bennett, C.L., Huynh, H.M., Blair, I.P., Puls, I., Irobi, J., Dierick, I., Abel, A., Kennerson, M.L., Rabin, B.A.*, et al.* (2004). DNA/RNA helicase gene mutations in a form of juvenile amyotrophic lateral sclerosis (ALS4). Am J Hum Genet *74*, 1128-1135.

Cheramy, A., Barbeito, L., Godeheu, G., and Glowinski, J. (1992). Riluzole inhibits the release of glutamate in the caudate nucleus of the cat in vivo. Neurosci Lett *147*, 209-212.

Chiang, P.M., Ling, J., Jeong, Y.H., Price, D.L., Aja, S.M., and Wong, P.C. (2010). Deletion of TDP-43 down-regulates Tbc1d1, a gene linked to obesity, and alters body fat metabolism. Proceedings of the National Academy of Sciences of the United States of America *107*, 16320-16324.

Chio, A., Benzi, G., Dossena, M., Mutani, R., and Mora, G. (2005). Severely increased risk of amyotrophic lateral sclerosis among Italian professional football players. Brain *128*, 472-476.

Chio, A., Calvo, A., Moglia, C., Ossola, I., Brunetti, M., Sbaiz, L., Lai, S.L., Abramzon, Y., Traynor, B.J., and Restagno, G. (2011). A de novo missense mutation of the FUS gene in a "true" sporadic ALS case. Neurobiol Aging *32*, 553 e523-556.

Choi, D.W. (1987). Ionic dependence of glutamate neurotoxicity. J Neurosci *7*, 369-379.

Choi, H.J., Kang, S.W., Yang, C.H., Rhee, S.G., and Ryu, S.E. (1998). Crystal structure of a novel human peroxidase enzyme at 2.0 A resolution. Nat Struct Biol *5*, 400-406.

Chow, C.Y., Landers, J.E., Bergren, S.K., Sapp, P.C., Grant, A.E., Jones, J.M., Everett, L., Lenk, G.M., McKenna-Yasek, D.M., Weisman, L.S.*, et al.* (2009). Deleterious variants of FIG4, a phosphoinositide phosphatase, in patients with ALS. American Journal of Human Genetics *84*, 85-88.

Chuang, M.H., Wu, M.S., Lo, W.L., Lin, J.T., Wong, C.H., and Chiou, S.H. (2006). The antioxidant protein alkylhydroperoxide reductase of Helicobacter pylori switches from a peroxide reductase to a molecular chaperone function. Proceedings of the National Academy of Sciences of the United States of America *103*, 2552-2557.

Clement, A.M., Nguyen, M.D., Roberts, E.A., Garcia, M.L., Boillee, S., Rule, M., McMahon, A.P., Doucette, W., Siwek, D., Ferrante, R.J.*, et al.* (2003). Wild-type nonneuronal cells extend survival of SOD1 mutant motor neurons in ALS mice. Science *302*, 113-117.

Colombrita, C., Onesto, E., Tiloca, C., Ticozzi, N., Silani, V., and Ratti, A. (2011). RNA-binding proteins and RNA metabolism: a new scenario in the pathogenesis of Amyotrophic lateral sclerosis. Arch Ital Biol *149*, 83-99.

Colombrita, C., Zennaro, E., Fallini, C., Weber, M., Sommacal, A., Buratti, E., Silani, V., and Ratti, A. (2009a). TDP-43 is recruited to stress granules in conditions of oxidative insult. J Neurochem *111*, 1051-1061.

Colombrita, C., Zennaro, E., Fallini, C., Weber, M., Sommacal, A., Buratti, E., Silani, V., and Ratti, A. (2009b). TDP-43 is recruited to stress granules in conditions of oxidative insult. Journal of neurochemistry *111*, 1051-1061.

Cooper-Knock, J., Hewitt, C., Highley, J.R., Brockington, A., Milano, A., Man, S., Martindale, J., Hartley, J., Walsh, T., Gelsthorpe, C.*, et al.* (2012). Clinico-pathological features in amyotrophic lateral sclerosis with expansions in C9ORF72. Brain *135*, 751-764.

Corson, L.B., Strain, J.J., Culotta, V.C., and Cleveland, D.W. (1998). Chaperone-facilitated copper binding is a property common to several classes of familial amyotrophic lateral sclerosis-linked superoxide dismutase mutants. Proc Natl Acad Sci U S A *95*, 6361-6366.

Cote, F., Collard, J.F., and Julien, J.P. (1993). Progressive neuronopathy in transgenic mice expressing the human neurofilament heavy gene: a mouse model of amyotrophic lateral sclerosis. Cell *73*, 35-46.

Couillard-Despres, S., Zhu, Q., Wong, P.C., Price, D.L., Cleveland, D.W., and Julien, J.P. (1998). Protective effect of neurofilament heavy gene overexpression in motor neuron disease induced by mutant superoxide dismutase. Proc Natl Acad Sci U S A *95*, 9626-9630.

Couratier, P., Hugon, J., Sindou, P., Vallat, J.M., and Dumas, M. (1993). Cell culture evidence for neuronal degeneration in amyotrophic lateral sclerosis being linked to glutamate AMPA/kainate receptors. Lancet *341*, 265-268.

Cudkowicz, M.E., McKenna-Yasek, D., Sapp, P.E., Chin, W., Geller, B., Hayden, D.L., Schoenfeld, D.A., Hosler, B.A., Horvitz, H.R., and Brown, R.H. (1997). Epidemiology of mutations in superoxide dismutase in amyotrophic lateral sclerosis. Ann Neurol *41*, 210-221.

Cudkowicz, M.E., Shefner, J.M., Schoenfeld, D.A., Brown, R.H., Jr., Johnson, H., Qureshi, M., Jacobs, M., Rothstein, J.D., Appel, S.H., Pascuzzi, R.M.*, et al.* (2003). A randomized, placebo-controlled trial of topiramate in amyotrophic lateral sclerosis. Neurology *61*, 456-464.

Cumming, R.C., Dargusch, R., Fischer, W.H., and Schubert, D. (2007). Increase in expression levels and resistance to sulfhydryl oxidation of peroxiredoxin isoforms in amyloid beta-resistant nerve cells. J Biol Chem *282*, 30523-30534.

Curti, D., Malaspina, A., Facchetti, G., Camana, C., Mazzini, L., Tosca, P., Zerbi, F., and Ceroni, M. (1996). Amyotrophic lateral sclerosis: oxidative energy metabolism and calcium homeostasis in peripheral blood lymphocytes. Neurology *47*, 1060-1064.

Dal Canto, M.C., and Gurney, M.E. (1995). Neuropathological changes in two lines of mice carrying a transgene for mutant human Cu,Zn SOD, and in mice overexpressing wild type human SOD: a model of familial amyotrophic lateral sclerosis (FALS). Brain Res *676*, 25-40.

Davenport, R.J., Swingler, R.J., Chancellor, A.M., and Warlow, C.P. (1996). Avoiding false positive diagnoses of motor neuron disease: lessons from the Scottish Motor Neuron Disease Register. J Neurol Neurosurg Psychiatry *60*, 147-151.

de Carvalho, M., Dengler, R., Eisen, A., England, J.D., Kaji, R., Kimura, J., Mills, K., Mitsumoto, H., Nodera, H., Shefner, J.*, et al.* (2008). Electrodiagnostic criteria for diagnosis of ALS. Clin Neurophysiol *119*, 497-503.

de Carvalho, M., and Swash, M. (2004). Cramps, muscle pain, and fasciculations: not always benign? Neurology *63*, 721-723.

De Duve, C., and Baudhuin, P. (1966). Peroxisomes (microbodies and related particles). Physiol Rev *46*, 323-357.

De Vos, K.J., Grierson, A.J., Ackerley, S., and Miller, C.C. (2008). Role of axonal transport in neurodegenerative diseases. Annu Rev Neurosci *31*, 151-173.

DeJesus-Hernandez, M., Mackenzie, I.R., Boeve, B.F., Boxer, A.L., Baker, M., Rutherford, N.J., Nicholson, A.M., Finch, N.A., Flynn, H., Adamson, J., *et al.* (2011). Expanded GGGGCC hexanucleotide repeat in noncoding region of C9ORF72 causes chromosome 9p-linked FTD and ALS. Neuron *72*, 245-256.

Deng, H.X., Chen, W., Hong, S.T., Boycott, K.M., Gorrie, G.H., Siddique, N., Yang, Y., Fecto, F., Shi, Y., Zhai, H., *et al.* (2011). Mutations in UBQLN2 cause dominant X-linked juvenile and adult-onset ALS and ALS/dementia. Nature *477*, 211-215.

Deng, H.X., Hentati, A., Tainer, J.A., Iqbal, Z., Cayabyab, A., Hung, W.Y., Getzoff, E.D., Hu, P., Herzfeldt, B., Roos, R.P., *et al.* (1993). Amyotrophic lateral sclerosis and structural defects in Cu,Zn superoxide dismutase. Science *261*, 1047-1051.

Desport, J.C., Preux, P.M., Magy, L., Boirie, Y., Vallat, J.M., Beaufrere, B., and Couratier, P. (2001). Factors correlated with hypermetabolism in patients with amyotrophic lateral sclerosis. Am J Clin Nutr *74*, 328-334.

Dhaliwal, G.K., and Grewal, R.P. (2000). Mitochondrial DNA deletion mutation levels are elevated in ALS brains. Neuroreport *11*, 2507-2509.

Diet, A., Abbas, K., Bouton, C., Guillon, B., Tomasello, F., Fourquet, S., Toledano, M.B., and Drapier, J.C. (2007). Regulation of peroxiredoxins by nitric oxide in immunostimulated macrophages. The Journal of Biological Chemistry *282*, 36199-36205.

Doble, A. (1996). The pharmacology and mechanism of action of riluzole. Neurology *47*, S233-241.

Doble, A. (1999). The role of excitotoxicity in neurodegenerative disease: implications for therapy. Pharmacol Ther *81*, 163-221.

Duchen, M.R. (2000). Mitochondria and calcium: from cell signalling to cell death. J Physiol *529 Pt 1*, 57-68.

Dugan, L.L., Turetsky, D.M., Du, C., Lobner, D., Wheeler, M., Almli, C.R., Shen, C.K., Luh, T.Y., Choi, D.W., and Lin, T.S. (1997). Carboxyfullerenes as neuroprotective agents. Proc Natl Acad Sci U S A *94*, 9434-9439.

Dupuis, L., Oudart, H., Rene, F., Gonzalez de Aguilar, J.L., and Loeffler, J.P. (2004). Evidence for defective energy homeostasis in amyotrophic lateral sclerosis: benefit of a high-energy diet in a transgenic mouse model. Proc Natl Acad Sci U S A *101*, 11159-11164.

Durham, H.D., Roy, J., Dong, L., and Figlewicz, D.A. (1997). Aggregation of mutant Cu/Zn superoxide dismutase proteins in a culture model of ALS. J Neuropathol Exp Neurol *56*, 523-530.

Dykens, J.A. (1994). Isolated cerebral and cerebellar mitochondria produce free radicals when exposed to elevated CA2+ and Na+: implications for neurodegeneration. J Neurochem *63*, 584-591.

Elden, A.C., Kim, H.J., Hart, M.P., Chen-Plotkin, A.S., Johnson, B.S., Fang, X., Armakola, M., Geser, F., Greene, R., Lu, M.M., *et al.* (2010). Ataxin-2 intermediate-length polyglutamine expansions are associated with increased risk for ALS. Nature *466*, 1069-1075.

Enayat, Z.E., Orrell, R.W., Claus, A., Ludolph, A., Bachus, R., Brockmuller, J., Ray-Chaudhuri, K., Radunovic, A., Shaw, C., Wilkinson, J., *et al.* (1995). Two novel mutations in the gene for copper zinc superoxide dismutase in UK families with amyotrophic lateral sclerosis. Hum Mol Genet *4*, 1239-1240.

Evrard, C., Capron, A., Marchand, C., Clippe, A., Wattiez, R., Soumillion, P., Knoops, B., and Declercq, J.P. (2004). Crystal structure of a dimeric oxidized form of human peroxiredoxin 5. J Mol Biol *337*, 1079-1090.

Fang, J., Nakamura, T., Cho, D.H., Gu, Z., and Lipton, S.A. (2007). S-nitrosylation of peroxiredoxin 2 promotes oxidative stress-induced neuronal cell death in Parkinson's disease. Proceedings of the National Academy of Sciences of the United States of America *104*, 18742-18747.

Ferraiuolo, L., Heath, P.R., Holden, H., Kasher, P., Kirby, J., and Shaw, P.J. (2007). Microarray analysis of the cellular pathways involved in the adaptation to and progression of motor neuron injury in the SOD1 G93A mouse model of familial ALS. J Neurosci *27*, 9201-9219.

Ferraiuolo, L., Kirby, J., Grierson, A.J., Sendtner, M., and Shaw, P.J. (2011). Molecular pathways of motor neuron injury in amyotrophic lateral sclerosis. Nat Rev Neurol *7*, 616-630.

Ferrante, R.J., Browne, S.E., Shinobu, L.A., Bowling, A.C., Baik, M.J., MacGarvey, U., Kowall, N.W., Brown, R.H., Jr., and Beal, M.F. (1997). Evidence of increased oxidative damage in both sporadic and familial amyotrophic lateral sclerosis. J Neurochem *69*, 2064-2074.

Figlewicz, D.A., Krizus, A., Martinoli, M.G., Meininger, V., Dib, M., Rouleau, G.A., and Julien, J.P. (1994). Variants of the heavy neurofilament subunit are associated with the development of amyotrophic lateral sclerosis. Hum Mol Genet *3*, 1757-1761.

Flowers, J.M., Powell, J.F., Leigh, P.N., Andersen, P., and Shaw, C.E. (2001). Intron 7 retention and exon 9 skipping EAAT2 mRNA variants are not associated with amyotrophic lateral sclerosis. Ann Neurol *49*, 643-649.

Fray, A.E., Ince, P.G., Banner, S.J., Milton, I.D., Usher, P.A., Cookson, M.R., and Shaw, P.J. (1998). The expression of the glial glutamate transporter protein EAAT2 in motor neuron disease: an immunohistochemical study. Eur J Neurosci *10*, 2481-2489.

Fujita, K., Yamauchi, M., Shibayama, K., Ando, M., Honda, M., and Nagata, Y. (1996). Decreased cytochrome c oxidase activity but unchanged superoxide dismutase and glutathione peroxidase activities in the spinal cords of patients with amyotrophic lateral sclerosis. J Neurosci Res *45*, 276-281.

Fukada, K., Zhang, F., Vien, A., Cashman, N.R., and Zhu, H. (2004). Mitochondrial proteomic analysis of a cell line model of familial amyotrophic lateral sclerosis. Mol Cell Proteomics *3*, 1211-1223.

Furby, A., Beauvais, K., Kolev, I., Rivain, J.G., and Sebille, V. (2010). Rural environment and risk factors of amyotrophic lateral sclerosis: a case-control study. Journal of Neurology *257*, 792-798.

Gal, J., Zhang, J., Kwinter, D.M., Zhai, J., Jia, H., Jia, J., and Zhu, H. (2011). Nuclear localization sequence of FUS and induction of stress granules by ALS mutants. Neurobiology of Aging *32*, 2323 e2327-2340.

Gallagher, J.P., and Sanders, M. (1987). Trauma and amyotrophic lateral sclerosis: a report of 78 patients. Acta Neurol Scand *75*, 145-150.

Ganesalingam, J., and Bowser, R. (2010). The application of biomarkers in clinical trials for motor neuron disease. Biomark Med *4*, 281-297.

Gijselinck, I., Engelborghs, S., Maes, G., Cuijt, I., Peeters, K., Mattheijssens, M., Joris, G., Cras, P., Martin, J.J., De Deyn, P.P., *et al.* (2010). Identification of 2 Loci at chromosomes 9 and 14 in a multiplex family with frontotemporal lobar degeneration and amyotrophic lateral sclerosis. Arch Neurol *67*, 606-616.

Gleichmann, M., and Mattson, M.P. (2011). Neuronal calcium homeostasis and dysregulation. Antioxid Redox Signal *14*, 1261-1273.

Goemaere, J., and Knoops, B. (2012). Peroxiredoxin distribution in the mouse brain with emphasis on neuronal populations affected in neurodegenerative disorders. The Journal of Comparative Neurology *520*, 258-280.

Gordon, P.H., Cheng, B., Katz, I.B., Pinto, M., Hays, A.P., Mitsumoto, H., and Rowland, L.P. (2006). The natural history of primary lateral sclerosis. Neurology *66*, 647-653.

Graf, M., Ecker, D., Horowski, R., Kramer, B., Riederer, P., Gerlach, M., Hager, C., Ludolph, A.C., Becker, G., Osterhage, J.*, et al.* (2005). High dose vitamin E therapy in amyotrophic lateral sclerosis as add-on therapy to riluzole: results of a placebo-controlled double-blind study. J Neural Transm *112*, 649-660.

Greenway, M.J., Andersen, P.M., Russ, C., Ennis, S., Cashman, S., Donaghy, C., Patterson, V., Swingler, R., Kieran, D., Prehn, J.*, et al.* (2006). ANG mutations segregate with familial and 'sporadic' amyotrophic lateral sclerosis. Nature genetics *38*, 411-413.

Gregory, R.I., Yan, K.P., Amuthan, G., Chendrimada, T., Doratotaj, B., Cooch, N., and Shiekhattar, R. (2004). The Microprocessor complex mediates the genesis of microRNAs. Nature *432*, 235-240.

Gros-Louis, F., Gaspar, C., and Rouleau, G.A. (2006). Genetics of familial and sporadic amyotrophic lateral sclerosis. Biochim Biophys Acta *1762*, 956-972.

Gurney, M.E., Cutting, F.B., Zhai, P., Doble, A., Taylor, C.P., Andrus, P.K., and Hall, E.D. (1996). Benefit of vitamin E, riluzole, and gabapentin in a transgenic model of familial amyotrophic lateral sclerosis. Ann Neurol *39*, 147-157.

Gurney, M.E., Pu, H., Chiu, A.Y., Dal Canto, M.C., Polchow, C.Y., Alexander, D.D., Caliendo, J., Hentati, A., Kwon, Y.W., Deng, H.X.*, et al.* (1994). Motor neuron degeneration in mice that express a human Cu,Zn superoxide dismutase mutation. Science *264*, 1772-1775.

Hadano, S., Hand, C.K., Osuga, H., Yanagisawa, Y., Otomo, A., Devon, R.S., Miyamoto, N., Showguchi-Miyata, J., Okada, Y., Singaraja, R.*, et al.* (2001). A gene encoding a putative GTPase regulator is mutated in familial amyotrophic lateral sclerosis 2. Nat Genet *29*, 166-173.

Hafezparast, M., Klocke, R., Ruhrberg, C., Marquardt, A., Ahmad-Annuar, A., Bowen, S., Lalli, G., Witherden, A.S., Hummerich, H., Nicholson, S.*, et al.* (2003). Mutations in dynein link motor neuron degeneration to defects in retrograde transport. Science *300*, 808-812.

Hall, A., Karplus, P.A., and Poole, L.B. (2009). Typical 2-Cys peroxiredoxins--structures, mechanisms and functions. The FEBS journal *276*, 2469-2477.

Han, D., Williams, E., and Cadenas, E. (2001). Mitochondrial respiratory chain-dependent generation of superoxide anion and its release into the intermembrane space. Biochem J *353*, 411-416.

Hand, C.K., Khoris, J., Salachas, F., Gros-Louis, F., Lopes, A.A., Mayeux-Portas, V., Brewer, C.G., Brown, R.H., Jr., Meininger, V., Camu, W.*, et al.* (2002). A novel locus for familial amyotrophic lateral sclerosis, on chromosome 18q. Am J Hum Genet *70*, 251-256.

Harwood, C.A., McDermott, C.J., and Shaw, P.J. (2009). Physical activity as an exogenous risk factor in motor neuron disease (MND): a review of the evidence. Amyotroph Lateral Scler *10*, 191-204.

Hays, A.P. (2006). The Pathology of Amyotrophic Lateral Sclerosis. In Amyotrophic lateral sclerosis, H. Mitsumoto, S. Przedborski, and P.H. Gordon, eds. (New York: Taylor & Francis Group), pp. 43-80.

He, C.Z., and Hays, A.P. (2004). Expression of peripherin in ubiquinated inclusions of amyotrophic lateral sclerosis. Journal of the Neurological Sciences *217*, 47-54.

Heath, P.R., and Shaw, P.J. (2002). Update on the glutamatergic neurotransmitter system and the role of excitotoxicity in amyotrophic lateral sclerosis. Muscle Nerve *26*, 438-458.

Hentati, A., Bejaoui, K., Pericak-Vance, M.A., Hentati, F., Speer, M.C., Hung, W.Y., Figlewicz, D.A., Haines, J., Rimmler, J., Ben Hamida, C., *et al.* (1994). Linkage of recessive familial amyotrophic lateral sclerosis to chromosome 2q33-q35. Nat Genet *7*, 425-428.

Hentati, A., Ouahchi, K., Pericak-Vance, M.A., Nijhawan, D., Ahmad, A., Yang, Y., Rimmler, J., Hung, W., Schlotter, B., Ahmed, A., *et al.* (1998). Linkage of a commoner form of recessive amyotrophic lateral sclerosis to chromosome 15q15-q22 markers. Neurogenetics *2*, 55-60.

Henze, K., and Martin, W. (2003). Evolutionary biology: essence of mitochondria. Nature *426*, 127-128.

Hess, J., Angel, P., and Schorpp-Kistner, M. (2004). AP-1 subunits: quarrel and harmony among siblings. Journal of Cell Science *117*, 5965-5973.

Hosler, B.A., Siddique, T., Sapp, P.C., Sailor, W., Huang, M.C., Hossain, A., Daube, J.R., Nance, M., Fan, C., Kaplan, J., *et al.* (2000). Linkage of familial amyotrophic lateral sclerosis with frontotemporal dementia to chromosome 9q21-q22. Jama *284*, 1664-1669.

Huang, C., Zhou, H., Tong, J., Chen, H., Liu, Y.J., Wang, D., Wei, X., and Xia, X.G. (2011). FUS transgenic rats develop the phenotypes of amyotrophic lateral sclerosis and frontotemporal lobar degeneration. PLoS Genet *7*, e1002011.

Hume, R.I., Dingledine, R., and Heinemann, S.F. (1991). Identification of a site in glutamate receptor subunits that controls calcium permeability. Science *253*, 1028-1031.

Hutton, M., Lendon, C.L., Rizzu, P., Baker, M., Froelich, S., Houlden, H., Pickering-Brown, S., Chakraverty, S., Isaacs, A., Grover, A., *et al.* (1998). Association of missense and 5'-splice-site mutations in tau with the inherited dementia FTDP-17. Nature *393*, 702-705.

Ihara, Y., Nobukuni, K., Takata, H., and Hayabara, T. (2005). Oxidative stress and metal content in blood and cerebrospinal fluid of amyotrophic lateral sclerosis patients with and without a Cu, Zn-superoxide dismutase mutation. Neurol Res *27*, 105-108.

Imlay, J.A. (2003). Pathways of oxidative damage. Annu Rev Microbiol *57*, 395-418.

Ince, P.G., Evans, J., Knopp, M., Forster, G., Hamdalla, H.H., Wharton, S.B., and Shaw, P.J. (2003). Corticospinal tract degeneration in the progressive muscular atrophy variant of ALS. Neurology *60*, 1252-1258.

Ince, P.G., Lowe, J., and Shaw, P.J. (1998). Amyotrophic lateral sclerosis: current issues in classification, pathogenesis and molecular pathology. Neuropathol Appl Neurobiol *24*, 104-117.

Jaarsma, D., Haasdijk, E.D., Grashorn, J.A., Hawkins, R., van Duijn, W., Verspaget, H.W., London, J., and Holstege, J.C. (2000). Human Cu/Zn superoxide dismutase (SOD1) overexpression in mice causes mitochondrial vacuolization, axonal degeneration, and premature motoneuron death and accelerates motoneuron disease in mice expressing a familial amyotrophic lateral sclerosis mutant SOD1. Neurobiol Dis *7*, 623-643.

Jackson, M., Steers, G., Leigh, P.N., and Morrison, K.E. (1999). Polymorphisms in the glutamate transporter gene EAAT2 in European ALS patients. J Neurol *246*, 1140-1144.

Jafari, H., Couratier, P., and Camu, W. (2001). Motor neuron disease after electric injury. J Neurol Neurosurg Psychiatry *71*, 265-267.

Jakob, U., Muse, W., Eser, M., and Bardwell, J.C. (1999). Chaperone activity with a redox switch. Cell *96*, 341-352.

Jang, H.H., Lee, K.O., Chi, Y.H., Jung, B.G., Park, S.K., Park, J.H., Lee, J.R., Lee, S.S., Moon, J.C., Yun, J.W., *et al.* (2004). Two enzymes in one; two yeast peroxiredoxins display oxidative stress-dependent switching from a peroxidase to a molecular chaperone function. Cell *117*, 625-635.

Jeong, W., Park, S.J., Chang, T.S., Lee, D.Y., and Rhee, S.G. (2006). Molecular mechanism of the reduction of cysteine sulfinic acid of peroxiredoxin to cysteine by mammalian sulfiredoxin. The Journal of Biological Chemistry *281*, 14400-14407.

Jia, Z., Agopyan, N., Miu, P., Xiong, Z., Henderson, J., Gerlai, R., Taverna, F.A., Velumian, A., MacDonald, J., Carlen, P., *et al.* (1996). Enhanced LTP in mice deficient in the AMPA receptor GluR2. Neuron *17*, 945-956.

Jin, M.H., Lee, Y.H., Kim, J.M., Sun, H.N., Moon, E.Y., Shong, M.H., Kim, S.U., Lee, S.H., Lee, T.H., Yu, D.Y., *et al.* (2005). Characterization of neural cell types expressing peroxiredoxins in mouse brain. Neurosci Lett *381*, 252-257.

Johnson, J.O., Mandrioli, J., Benatar, M., Abramzon, Y., Van Deerlin, V.M., Trojanowski, J.Q., Gibbs, J.R., Brunetti, M., Gronka, S., Wuu, J., *et al.* (2010). Exome sequencing reveals VCP mutations as a cause of familial ALS. Neuron *68*, 857-864.

Jones, C.T., Swingler, R.J., and Brock, D.J. (1994). Identification of a novel SOD1 mutation in an apparently sporadic amyotrophic lateral sclerosis patient and the detection of Ile113Thr in three others. Hum Mol Genet *3*, 649-650.

Jonsson, P.A., Backstrand, A., Andersen, P.M., Jacobsson, J., Parton, M., Shaw, C., Swingler, R., Shaw, P.J., Robberecht, W., Ludolph, A.C., *et al.* (2002). CuZn-superoxide dismutase in D90A heterozygotes from recessive and dominant ALS pedigrees. Neurobiol Dis *10*, 327-333.

Jonsson, T.J., Murray, M.S., Johnson, L.C., Poole, L.B., and Lowther, W.T. (2005). Structural basis for the retroreduction of inactivated peroxiredoxins by human sulfiredoxin. Biochemistry *44*, 8634-8642.

Joyce, P.I., Fratta, P., Fisher, E.M., and Acevedo-Arozena, A. (2011). SOD1 and TDP-43 animal models of amyotrophic lateral sclerosis: recent advances in understanding disease toward the development of clinical treatments. Mamm Genome *22*, 420-448.

Kabashi, E., Agar, J.N., Hong, Y., Taylor, D.M., Minotti, S., Figlewicz, D.A., and Durham, H.D. (2008a). Proteasomes remain intact, but show early focal alteration in their composition in a mouse model of amyotrophic lateral sclerosis. Journal of Neurochemistry *105*, 2353-2366.

Kabashi, E., Agar, J.N., Taylor, D.M., Minotti, S., and Durham, H.D. (2004). Focal dysfunction of the proteasome: a pathogenic factor in a mouse model of amyotrophic lateral sclerosis. Journal of Neurochemistry *89*, 1325-1335.

Kabashi, E., Lin, L., Tradewell, M.L., Dion, P.A., Bercier, V., Bourgouin, P., Rochefort, D., Bel Hadj, S., Durham, H.D., Vande Velde, C., *et al.* (2010). Gain and loss of function of ALS-related mutations of TARDBP (TDP-43) cause motor deficits in vivo. Human molecular genetics *19*, 671-683.

Kabashi, E., Valdmanis, P.N., Dion, P., Spiegelman, D., McConkey, B.J., Vande Velde, C., Bouchard, J.P., Lacomblez, L., Pochigaeva, K., Salachas, F., *et al.* (2008b). TARDBP mutations in individuals with sporadic and familial amyotrophic lateral sclerosis. Nat Genet *40*, 572-574.

Kaji, R., Izumi, Y., Adachi, Y., and Kuzuhara, S. (2012). ALS-parkinsonism-dementia complex of Kii and other related diseases in Japan. Parkinsonism Relat Disord *18 Suppl 1*, S190-191.

Kamel, F., Umbach, D.M., Munsat, T.L., Shefner, J.M., and Sandler, D.P. (1999). Association of cigarette smoking with amyotrophic lateral sclerosis. Neuroepidemiology *18*, 194-202.

Kang, S.W., Rhee, S.G., Chang, T.S., Jeong, W., and Choi, M.H. (2005). 2-Cys peroxiredoxin function in intracellular signal transduction: therapeutic implications. Trends Mol Med *11*, 571-578.

Kaspar, B.K., Llado, J., Sherkat, N., Rothstein, J.D., and Gage, F.H. (2003). Retrograde viral delivery of IGF-1 prolongs survival in a mouse ALS model. Science *301*, 839-842.

Kato, S. (2008). Amyotrophic lateral sclerosis models and human neuropathology: similarities and differences. Acta Neuropathologica *115*, 97-114.

Kato, S., Kato, M., Abe, Y., Matsumura, T., Nishino, T., Aoki, M., Itoyama, Y., Asayama, K., Awaya, A., Hirano, A., *et al.* (2005). Redox system expression in the motor neurons in amyotrophic lateral sclerosis (ALS): immunohistochemical studies on sporadic ALS, superoxide dismutase 1 (SOD1)-mutated familial ALS, and SOD1-mutated ALS animal models. Acta Neuropathol (Berl) *110*, 101-112.

Kato, S., Saeki, Y., Aoki, M., Nagai, M., Ishigaki, A., Itoyama, Y., Kato, M., Asayama, K., Awaya, A., Hirano, A.*, et al.* (2004). Histological evidence of redox system breakdown caused by superoxide dismutase 1 (SOD1) aggregation is common to SOD1-mutated motor neurons in humans and animal models. Acta Neuropathology (Berlin) *107*, 149-158.

Kato, S., Saito, M., Hirano, A., and Ohama, E. (1999). Recent advances in research on neuropathological aspects of familial amyotrophic lateral sclerosis with superoxide dismutase 1 gene mutations: neuronal Lewy body-like hyaline inclusions and astrocytic hyaline inclusions. Histol Histopathol *14*, 973-989.

Kawamata, H., and Manfredi, G. (2008). Different regulation of wild-type and mutant Cu,Zn superoxide dismutase localization in mammalian mitochondria. Hum Mol Genet *17*, 3303-3317.

Kieran, D., Hafezparast, M., Bohnert, S., Dick, J.R., Martin, J., Schiavo, G., Fisher, E.M., and Greensmith, L. (2005). A mutation in dynein rescues axonal transport defects and extends the life span of ALS mice. J Cell Biol *169*, 561-567.

Kim, S.H., Fountoulakis, M., Cairns, N., and Lubec, G. (2001). Protein levels of human peroxiredoxin subtypes in brains of patients with Alzheimer's disease and Down syndrome. J Neural Transm Suppl, 223-235.

Kirby, J., Halligan, E., Baptista, M.J., Allen, S., Heath, P.R., Holden, H., Barber, S.C., Loynes, C.A., Wood-Allum, C.A., Lunec, J.*, et al.* (2005). Mutant SOD1 alters the motor neuronal transcriptome: implications for familial ALS. Brain *128*, 1686-1706.

Knight, J.A. (1998). Free radicals: their history and current status in aging and disease. Ann Clin Lab Sci *28*, 331-346.

Knoops, B., Clippe, A., Bogard, C., Arsalane, K., Wattiez, R., Hermans, C., Duconseille, E., Falmagne, P., and Bernard, A. (1999). Cloning and characterization of AOEB166, a novel mammalian antioxidant enzyme of the peroxiredoxin family. J Biol Chem *274*, 30451-30458.

Knoops, B., Goemaere, J., Van der Eecken, V., and Declercq, J.P. (2011). Peroxiredoxin 5: structure, mechanism, and function of the mammalian atypical 2-Cys peroxiredoxin. Antioxid Redox Signal *15*, 817-829.

Kondo, A., Iwaki, T., Tateishi, J., Kirimoto, K., Morimoto, T., and Oomura, I. (1986). Accumulation of neurofilaments in a sporadic case of amyotrophic lateral sclerosis. Jpn J Psychiatry Neurol *40*, 677-684.

Kong, J., and Xu, Z. (1998). Massive mitochondrial degeneration in motor neurons triggers the onset of amyotrophic lateral sclerosis in mice expressing a mutant SOD1. J Neurosci *18*, 3241-3250.

Konno, T., Shiga, A., Tsujino, A., Sugai, A., Kato, T., Kanai, K., Yokoseki, A., Eguchi, H., Kuwabara, S., Nishizawa, M., *et al.* (2012). Japanese amyotrophic lateral sclerosis patients with GGGGCC hexanucleotide repeat expansion in C9ORF72. J Neurol Neurosurg Psychiatry.

Koo, K.H., Lee, S., Jeong, S.Y., Kim, E.T., Kim, H.J., Kim, K., Song, K., and Chae, H.Z. (2002). Regulation of thioredoxin peroxidase activity by C-terminal truncation. Arch Biochem Biophys *397*, 312-318.

Krapfenbauer, K., Engidawork, E., Cairns, N., Fountoulakis, M., and Lubec, G. (2003). Aberrant expression of peroxiredoxin subtypes in neurodegenerative disorders. Brain Res *967*, 152-160.

Kuzuhara, S. (2007). [ALS-parkinsonism-dementia complex of the Kii peninsula of Japan (Muro disease). Historical review, epidemiology and concept]. Rinsho Shinkeigaku *47*, 962-965.

Kwiatkowski, T.J., Jr., Bosco, D.A., Leclerc, A.L., Tamrazian, E., Vanderburg, C.R., Russ, C., Davis, A., Gilchrist, J., Kasarskis, E.J., Munsat, T., *et al.* (2009). Mutations in the FUS/TLS gene on chromosome 16 cause familial amyotrophic lateral sclerosis. Science *323*, 1205-1208.

Lacomblez, L., Bensimon, G., Leigh, P.N., Guillet, P., and Meininger, V. (1996). Dose-ranging study of riluzole in amyotrophic lateral sclerosis. Amyotrophic Lateral Sclerosis/Riluzole Study Group II. Lancet *347*, 1425-1431.

Lai, E.C., Felice, K.J., Festoff, B.W., Gawel, M.J., Gelinas, D.F., Kratz, R., Murphy, M.F., Natter, H.M., Norris, F.H., and Rudnicki, S.A. (1997). Effect of recombinant human insulin-like growth factor-I on progression of ALS. A placebo-controlled study. The North America ALS/IGF-I Study Group. Neurology *49*, 1621-1630.

Lambeth, J.D. (2004). NOX enzymes and the biology of reactive oxygen. Nat Rev Immunol *4*, 181-189.

LaMonte, B.H., Wallace, K.E., Holloway, B.A., Shelly, S.S., Ascano, J., Tokito, M., Van Winkle, T., Howland, D.S., and Holzbaur, E.L. (2002). Disruption of dynein/dynactin inhibits axonal transport in motor neurons causing late-onset progressive degeneration. Neuron *34*, 715-727.

Lautenschlaeger, J., Prell, T., and Grosskreutz, J. (2012). Endoplasmic reticulum stress and the ER mitochondrial calcium cycle in amyotrophic lateral sclerosis. Amyotroph Lateral Scler *13*, 166-177.

Lee, J.M., Li, J., Johnson, D.A., Stein, T.D., Kraft, A.D., Calkins, M.J., Jakel, R.J., and Johnson, J.A. (2005). Nrf2, a multi-organ protector? Faseb J *19*, 1061-1066.

Lee, M.K., Marszalek, J.R., and Cleveland, D.W. (1994). A mutant neurofilament subunit causes massive, selective motor neuron death: implications for the pathogenesis of human motor neuron disease. Neuron *13*, 975-988.

Lee, S.R., Kim, J.R., Kwon, K.S., Yoon, H.W., Levine, R.L., Ginsburg, A., and Rhee, S.G. (1999). Molecular cloning and characterization of a mitochondrial selenocysteine-containing thioredoxin reductase from rat liver. The Journal of Biological Chemistry *274*, 4722-4734.

Lee, Y.M., Park, S.H., Shin, D.I., Hwang, J.Y., Park, B., Park, Y.J., Lee, T.H., Chae, H.Z., Jin, B.K., Oh, T.H., *et al.* (2008). Oxidative modification of peroxiredoxin is associated with drug-induced apoptotic signaling in experimental models of Parkinson disease. The Journal of Biological Chemistry *283*, 9986-9998.

Lin, C.L., Bristol, L.A., Jin, L., Dykes-Hoberg, M., Crawford, T., Clawson, L., and Rothstein, J.D. (1998). Aberrant RNA processing in a neurodegenerative disease: the cause for absent EAAT2, a glutamate transporter, in amyotrophic lateral sclerosis. Neuron *20*, 589-602.

Lin, W.L., and Dickson, D.W. (2008). Ultrastructural localization of TDP-43 in filamentous neuronal inclusions in various neurodegenerative diseases. Acta neuropathologica *116*, 205-213.

Liu, R., Althaus, J.S., Ellerbrock, B.R., Becker, D.A., and Gurney, M.E. (1998). Enhanced oxygen radical production in a transgenic mouse model of familial amyotrophic lateral sclerosis. Ann Neurol *44*, 763-770.

Louwerse, E.S., Weverling, G.J., Bossuyt, P.M., Meyjes, F.E., and de Jong, J.M. (1995). Randomized, double-blind, controlled trial of acetylcysteine in amyotrophic lateral sclerosis. Arch Neurol *52*, 559-564.

Mackenzie, I.R., Bigio, E.H., Ince, P.G., Geser, F., Neumann, M., Cairns, N.J., Kwong, L.K., Forman, M.S., Ravits, J., Stewart, H.*, et al.* (2007). Pathological TDP-43 distinguishes sporadic amyotrophic lateral sclerosis from amyotrophic lateral sclerosis with SOD1 mutations. Annals of Neurology *61*, 427-434.

Malessa, S., Leigh, P.N., Bertel, O., Sluga, E., and Hornykiewicz, O. (1991). Amyotrophic lateral sclerosis: glutamate dehydrogenase and transmitter amino acids in the spinal cord. J Neurol Neurosurg Psychiatry *54*, 984-988.

Manevich, Y., Feinstein, S.I., and Fisher, A.B. (2004). Activation of the antioxidant enzyme 1-CYS peroxiredoxin requires glutathionylation mediated by heterodimerization with pi GST. Proceedings of the National Academy of Sciences of the United States of America *101*, 3780-3785.

Martin, D., Thompson, M.A., and Nadler, J.V. (1993). The neuroprotective agent riluzole inhibits release of glutamate and aspartate from slices of hippocampal area CA1. Eur J Pharmacol *250*, 473-476.

Maruyama, H., Morino, H., Ito, H., Izumi, Y., Kato, H., Watanabe, Y., Kinoshita, Y., Kamada, M., Nodera, H., Suzuki, H.*, et al.* (2010). Mutations of optineurin in amyotrophic lateral sclerosis. Nature *465*, 223-226.

Mates, J.M. (2000). Effects of antioxidant enzymes in the molecular control of reactive oxygen species toxicology. Toxicology *153*, 83-104.

Mattiazzi, M., D'Aurelio, M., Gajewski, C.D., Martushova, K., Kiaei, M., Beal, M.F., and Manfredi, G. (2002). Mutated human SOD1 causes dysfunction of oxidative phosphorylation in mitochondria of transgenic mice. J Biol Chem *277*, 29626-29633.

Mazzini, L., Mareschi, K., Ferrero, I., Vassallo, E., Oliveri, G., Nasuelli, N., Oggioni, G.D., Testa, L., and Fagioli, F. (2008). Stem cell treatment in Amyotrophic Lateral Sclerosis. J Neurol Sci *265*, 78-83.

McDermott, C.J., and Shaw, P.J. (2008). Diagnosis and management of motor neurone disease. BMJ *336*, 658-662.

Meier, B., Radeke, H.H., Selle, S., Younes, M., Sies, H., Resch, K., and Habermehl, G.G. (1989). Human fibroblasts release reactive oxygen species in response to interleukin-1 or tumour necrosis factor-alpha. Biochem J *263*, 539-545.

Meissner, M., Lopato, S., Gotzmann, J., Sauermann, G., and Barta, A. (2003). Proto-oncoprotein TLS/FUS is associated to the nuclear matrix and complexed with splicing factors PTB, SRm160, and SR proteins. Exp Cell Res *283*, 184-195.

Menzies, F.M., Cookson, M.R., Taylor, R.W., Turnbull, D.M., Chrzanowska-Lightowlers, Z.M., Dong, L., Figlewicz, D.A., and Shaw, P.J. (2002). Mitochondrial dysfunction in a cell culture model of familial amyotrophic lateral sclerosis. Brain *125*, 1522-1533.

Millecamps, S., Boillee, S., Le Ber, I., Seilhean, D., Teyssou, E., Giraudeau, M., Moigneu, C., Vandenberghe, N., Danel-Brunaud, V., Corcia, P.*, et al.* (2012). Phenotype difference between ALS patients with expanded repeats in C9ORF72 and patients with mutations in other ALS-related genes. J Med Genet *49*, 258-263.

Miller, R.G., Mitchell, J.D., Lyon, M., and Moore, D.H. (2009). Riluzole for amyotrophic lateral sclerosis (ALS)/ motor neuron disease (MND). Cochrane Database Syst Rev.

Miller, R.G., Moore, D.H., 2nd, Gelinas, D.F., Dronsky, V., Mendoza, M., Barohn, R.J., Bryan, W., Ravits, J., Yuen, E., Neville, H., *et al.* (2001). Phase III randomized trial of gabapentin in patients with amyotrophic lateral sclerosis. Neurology *56*, 843-848.

MNDA website (accessed on 20th Oct 2012). http://www.mndassociation.org/research/research_explained/treatment_trials/index.html.

Monteiro, G., Horta, B.B., Pimenta, D.C., Augusto, O., and Netto, L.E. (2007). Reduction of 1-Cys peroxiredoxins by ascorbate changes the thiol-specific antioxidant paradigm, revealing another function of vitamin C. Proc Natl Acad Sci U S A *104*, 4886-4891.

Moon, J.C., Hah, Y.S., Kim, W.Y., Jung, B.G., Jang, H.H., Lee, J.R., Kim, S.Y., Lee, Y.M., Jeon, M.G., Kim, C.W., *et al.* (2005). Oxidative stress-dependent structural and functional switching of a human 2-Cys peroxiredoxin isotype II that enhances HeLa cell resistance to H2O2-induced cell death. J Biol Chem *280*, 28775-28784.

Morita, M., Al-Chalabi, A., Andersen, P.M., Hosler, B., Sapp, P., Englund, E., Mitchell, J.E., Habgood, J.J., de Belleroche, J., Xi, J., *et al.* (2006). A locus on chromosome 9p confers susceptibility to ALS and frontotemporal dementia. Neurology *66*, 839-844.

Mourelatos, Z., Gonatas, N.K., Stieber, A., Gurney, M.E., and Dal Canto, M.C. (1996). The Golgi apparatus of spinal cord motor neurons in transgenic mice expressing mutant Cu,Zn superoxide dismutase becomes fragmented in early, preclinical stages of the disease. Proc Natl Acad Sci U S A *93*, 5472-5477.

Munch, C., Rosenbohm, A., Sperfeld, A.D., Uttner, I., Reske, S., Krause, B.J., Sedlmeier, R., Meyer, T., Hanemann, C.O., Stumm, G., *et al.* (2005). Heterozygous R1101K mutation of the DCTN1 gene in a family with ALS and FTD. Ann Neurol *58*, 777-780.

Murakami, T., Nagano, I., Hayashi, T., Manabe, Y., Shoji, M., Setoguchi, Y., and Abe, K. (2001). Impaired retrograde axonal transport of adenovirus-mediated E. coli LacZ gene in the mice carrying mutant SOD1 gene. Neurosci Lett *308*, 149-152.

Nakamura, R., Kamakura, K., and Kwak, S. (1994). Late-onset selective neuronal damage in the rat spinal cord induced by continuous intrathecal administration of AMPA. Brain Res *654*, 279-285.

Nelson, L.M., McGuire, V., Longstreth, W.T., Jr., and Matkin, C. (2000). Population-based case-control study of amyotrophic lateral sclerosis in western Washington State. I. Cigarette smoking and alcohol consumption. American journal of epidemiology *151*, 156-163.

Ness, S., Rafii, M., Aisen, P., Krams, M., Silverman, W., and Manji, H. (2012). Down's syndrome and Alzheimer's disease: towards secondary prevention. Nature reviews Drug discovery *11*, 655-656.

Neumann, M., Sampathu, D.M., Kwong, L.K., Truax, A.C., Micsenyi, M.C., Chou, T.T., Bruce, J., Schuck, T., Grossman, M., Clark, C.M., *et al.* (2006). Ubiquitinated TDP-43 in frontotemporal lobar degeneration and amyotrophic lateral sclerosis. Science *314*, 130-133.

NICE website (accessed on 16th Sept 2012). http://publications.nice.org.uk/guidance-on-the-use-of-riluzole-rilutek-for-the-treatment-of-motor-neurone-disease-ta20. NICE guidelines on the use of Riluzole.

Nishimura, A.L., Mitne-Neto, M., Silva, H.C., Oliveira, J.R., Vainzof, M., and Zatz, M. (2004). A novel locus for late onset amyotrophic lateral sclerosis/motor neurone disease variant at 20q13. J Med Genet *41*, 315-320.

Noh, Y.H., Baek, J.Y., Jeong, W., Rhee, S.G., and Chang, T.S. (2009). Sulfiredoxin Translocation into Mitochondria Plays a Crucial Role in Reducing Hyperoxidized Peroxiredoxin III. J Biol Chem *284*, 8470-8477.

O'Neill, J.S., and Reddy, A.B. (2011). Circadian clocks in human red blood cells. Nature *469*, 498-503.

O'Neill, J.S., van Ooijen, G., Dixon, L.E., Troein, C., Corellou, F., Bouget, F.Y., Reddy, A.B., and Millar, A.J. (2011). Circadian rhythms persist without transcription in a eukaryote. Nature *469*, 554-558.

Okado-Matsumoto, A., and Fridovich, I. (2002). Amyotrophic lateral sclerosis: a proposed mechanism. Proc Natl Acad Sci U S A *99*, 9010-9014.

Okamoto, K., Hirai, S., Amari, M., Watanabe, M., and Sakurai, A. (1993). Bunina bodies in amyotrophic lateral sclerosis immunostained with rabbit anti-cystatin C serum. Neuroscience Letters *162*, 125-128.

Olney, J.W. (1982). The toxic effects of glutamate and related compounds in the retina and the brain. Retina *2*, 341-359.

Orlacchio, A., Babalini, C., Borreca, A., Patrono, C., Massa, R., Basaran, S., Munhoz, R.P., Rogaeva, E.A., St George-Hyslop, P.H., Bernardi, G.*, et al.* (2010). SPATACSIN mutations cause autosomal recessive juvenile amyotrophic lateral sclerosis. Brain : A Journal of Neurology *133*, 591-598.

Panfili, E., Sandri, G., and Ernster, L. (1991). Distribution of glutathione peroxidases and glutathione reductase in rat brain mitochondria. FEBS letters *290*, 35-37.

Panzeri, C., De Palma, C., Martinuzzi, A., Daga, A., De Polo, G., Bresolin, N., Miller, C.C., Tudor, E.L., Clementi, E., and Bassi, M.T. (2006). The first ALS2 missense mutation associated with JPLS reveals new aspects of alsin biological function. Brain : A Journal of Neurology *129*, 1710-1719.

Papadia, S., Soriano, F.X., Leveille, F., Martel, M.A., Dakin, K.A., Hansen, H.H., Kaindl, A., Sifringer, M., Fowler, J., Stefovska, V.*, et al.* (2008). Synaptic NMDA receptor activity boosts intrinsic antioxidant defenses. Nat Neurosci *11*, 476-487.

Pascual, M.B., Mata-Cabana, A., Florencio, F.J., Lindahl, M., and Cejudo, F.J. (2010). Overoxidation of 2-Cys peroxiredoxin in prokaryotes: cyanobacterial 2-Cys peroxiredoxins sensitive to oxidative stress. The Journal of Biological Chemistry *285*, 34485-34492.

Pasinelli, P., and Brown, R.H. (2006). Molecular biology of amyotrophic lateral sclerosis: insights from genetics. Nat Rev Neurosci *7*, 710-723.

Perry, T.L., Krieger, C., Hansen, S., and Eisen, A. (1990). Amyotrophic lateral sclerosis: amino acid levels in plasma and cerebrospinal fluid. Ann Neurol *28*, 12-17.

Piao, Y.S., Wakabayashi, K., Kakita, A., Yamada, M., Hayashi, S., Morita, T., Ikuta, F., Oyanagi, K., and Takahashi, H. (2003). Neuropathology with clinical correlations of sporadic amyotrophic lateral sclerosis: 102 autopsy cases examined between 1962 and 2000. Brain Pathol *13*, 10-22.

Plato, C.C., Garruto, R.M., Galasko, D., Craig, U.K., Plato, M., Gamst, A., Torres, J.M., and Wiederholt, W. (2003). Amyotrophic lateral sclerosis and parkinsonism-dementia complex of Guam: changing incidence rates during the past 60 years. Am J Epidemiol *157*, 149-157.

Puls, I., Jonnakuty, C., LaMonte, B.H., Holzbaur, E.L., Tokito, M., Mann, E., Floeter, M.K., Bidus, K., Drayna, D., Oh, S.J.*, et al.* (2003). Mutant dynactin in motor neuron disease. Nat Genet *33*, 455-456.

Qureshi, M.M., Hayden, D., Urbinelli, L., Ferrante, K., Newhall, K., Myers, D., Hilgenberg, S., Smart, R., Brown, R.H., and Cudkowicz, M.E. (2006). Analysis of factors that modify susceptibility and rate of progression in amyotrophic lateral sclerosis (ALS). Amyotroph Lateral Scler *7*, 173-182.

Raaphorst, J., de Visser, M., van Tol, M.J., Linssen, W.H., van der Kooi, A.J., de Haan, R.J., van den Berg, L.H., and Schmand, B. (2011). Cognitive dysfunction in lower motor neuron disease: executive and memory deficits in progressive muscular atrophy. Journal of Neurology, Neurosurgery, and Psychiatry *82*, 170-175.

Rademakers, R. (2012). C9orf72 repeat expansions in patients with ALS and FTD. Lancet Neurol *11*, 297-298.

Radi, R., Turrens, J.F., Chang, L.Y., Bush, K.M., Crapo, J.D., and Freeman, B.A. (1991). Detection of catalase in rat heart mitochondria. J Biol Chem *266*, 22028-22034.

Ralph, G.S., Radcliffe, P.A., Day, D.M., Carthy, J.M., Leroux, M.A., Lee, D.C., Wong, L.F., Bilsland, L.G., Greensmith, L., Kingsman, S.M.*, et al.* (2005). Silencing mutant SOD1 using RNAi protects against neurodegeneration and extends survival in an ALS model. Nat Med *11*, 429-433.

Rao, M.V., and Nixon, R.A. (2003). Defective neurofilament transport in mouse models of amyotrophic lateral sclerosis: a review. Neurochem Res *28*, 1041-1047.

Raoul, C., Abbas-Terki, T., Bensadoun, J.C., Guillot, S., Haase, G., Szulc, J., Henderson, C.E., and Aebischer, P. (2005). Lentiviral-mediated silencing of SOD1 through RNA interference retards disease onset and progression in a mouse model of ALS. Nat Med *11*, 423-428.

Ratovitski, T., Corson, L.B., Strain, J., Wong, P., Cleveland, D.W., Culotta, V.C., and Borchelt, D.R. (1999). Variation in the biochemical/biophysical properties of mutant superoxide dismutase 1 enzymes and the rate of disease progression in familial amyotrophic lateral sclerosis kindreds. Hum Mol Genet *8*, 1451-1460.

Reaume, A.G., Elliott, J.L., Hoffman, E.K., Kowall, N.W., Ferrante, R.J., Siwek, D.F., Wilcox, H.M., Flood, D.G., Beal, M.F., Brown, R.H., Jr.*, et al.* (1996). Motor neurons in Cu/Zn superoxide dismutase-deficient mice develop normally but exhibit enhanced cell death after axonal injury. Nat Genet *13*, 43-47.

Reijn, T.S., Abdo, W.F., Schelhaas, H.J., and Verbeek, M.M. (2009). CSF neurofilament protein analysis in the differential diagnosis of ALS. Journal of Neurology *256*, 615-619.

Renton, A.E., Majounie, E., Waite, A., Simon-Sanchez, J., Rollinson, S., Gibbs, J.R., Schymick, J.C., Laaksovirta, H., van Swieten, J.C., Myllykangas, L.*, et al.* (2011). A hexanucleotide repeat expansion in C9ORF72 is the cause of chromosome 9p21-linked ALS-FTD. Neuron *72*, 257-268.

Rhee, S.G. (2006). Cell signaling. H2O2, a necessary evil for cell signaling. Science *312*, 1882-1883.

Rhee, S.G., Chae, H.Z., and Kim, K. (2005a). Peroxiredoxins: a historical overview and speculative preview of novel mechanisms and emerging concepts in cell signaling. Free Radic Biol Med *38*, 1543-1552.

Rhee, S.G., Jeong, W., Chang, T.S., and Woo, H.A. (2007). Sulfiredoxin, the cysteine sulfinic acid reductase specific to 2-Cys peroxiredoxin: its discovery, mechanism of action, and biological significance. Kidney Int Suppl, S3-8.

Rhee, S.G., Kang, S.W., Chang, T.S., Jeong, W., and Kim, K. (2001). Peroxiredoxin, a novel family of peroxidases. IUBMB Life *52*, 35-41.

Rhee, S.G., Kang, S.W., Jeong, W., Chang, T.S., Yang, K.S., and Woo, H.A. (2005b). Intracellular messenger function of hydrogen peroxide and its regulation by peroxiredoxins. Curr Opin Cell Biol *17*, 183-189.

Rhee, S.G., and Woo, H.A. (2011). Multiple functions of peroxiredoxins: peroxidases, sensors and regulators of the intracellular messenger HO, and protein chaperones. Antioxid Redox Signal *15*, 781-794.

Richter, C., Park, J.W., and Ames, B.N. (1988). Normal oxidative damage to mitochondrial and nuclear DNA is extensive. Proc Natl Acad Sci U S A *85*, 6465-6467.

Rodriguez, J.A., Valentine, J.S., Eggers, D.K., Roe, J.A., Tiwari, A., Brown, R.H., Jr., and Hayward, L.J. (2002). Familial amyotrophic lateral sclerosis-associated mutations decrease the thermal stability of distinctly metallated species of human copper/zinc superoxide dismutase. J Biol Chem *277*, 15932-15937.

Rosen, D.R., Siddique, T., Patterson, D., Figlewicz, D.A., Sapp, P., Hentati, A., Donaldson, D., Goto, J., O'Regan, J.P., Deng, H.X., *et al.* (1993). Mutations in Cu/Zn superoxide dismutase gene are associated with familial amyotrophic lateral sclerosis. Nature *362*, 59-62.

Ross, C.A., and Poirier, M.A. (2004). Protein aggregation and neurodegenerative disease. Nat Med *10 Suppl*, S10-17.

Ross, C.A., and Poirier, M.A. (2005). Opinion: What is the role of protein aggregation in neurodegeneration? Nat Rev Mol Cell Biol *6*, 891-898.

Rothstein, J.D., Jin, L., Dykes-Hoberg, M., and Kuncl, R.W. (1993). Chronic inhibition of glutamate uptake produces a model of slow neurotoxicity. Proc Natl Acad Sci U S A *90*, 6591-6595.

Rothstein, J.D., Martin, L.J., and Kuncl, R.W. (1992). Decreased glutamate transport by the brain and spinal cord in amyotrophic lateral sclerosis. N Engl J Med *326*, 1464-1468.

Rothstein, J.D., Van Kammen, M., Levey, A.I., Martin, L.J., and Kuncl, R.W. (1995). Selective loss of glial glutamate transporter GLT-1 in amyotrophic lateral sclerosis. Ann Neurol *38*, 73-84.

Rowland, L.P. (2003). Clinical aspects of sporadic amyotrophic lateral sclerosis/motor neuron disease. In Motor Neuron Disorders, P.J. Shaw, and M.J. Strong, eds. (Philadelphia: Butterworth Heineman), pp. 111-143.

Rowland, L.P., and Shneider, N.A. (2001). Amyotrophic lateral sclerosis. N Engl J Med *344*, 1688-1700.

Roy, J., Minotti, S., Dong, L., Figlewicz, D.A., and Durham, H.D. (1998). Glutamate potentiates the toxicity of mutant Cu/Zn-superoxide dismutase in motor neurons by postsynaptic calcium-dependent mechanisms. J Neurosci *18*, 9673-9684.

Ruddy, D.M., Parton, M.J., Al-Chalabi, A., Lewis, C.M., Vance, C., Smith, B.N., Leigh, P.N., Powell, J.F., Siddique, T., Meyjes, E.P., *et al.* (2003). Two families with familial amyotrophic lateral sclerosis are linked to a novel locus on chromosome 16q. Am J Hum Genet *73*, 390-396.

Said Ahmed, M., Hung, W.Y., Zu, J.S., Hockberger, P., and Siddique, T. (2000). Increased reactive oxygen species in familial amyotrophic lateral sclerosis with mutations in SOD1. J Neurol Sci *176*, 88-94.

Sapp, P.C., Hosler, B.A., McKenna-Yasek, D., Chin, W., Gann, A., Genise, H., Gorenstein, J., Huang, M., Sailer, W., Scheffler, M., *et al.* (2003). Identification of two novel loci for dominantly inherited familial amyotrophic lateral sclerosis. Am J Hum Genet *73*, 397-403.

Saroff, D., Delfs, J., Kuznetsov, D., and Geula, C. (2000). Selective vulnerability of spinal cord motor neurons to non-NMDA toxicity. Neuroreport *11*, 1117-1121.

Schroder, E., and Ponting, C.P. (1998). Evidence that peroxiredoxins are novel members of the thioredoxin fold superfamily. Protein Sci *7*, 2465-2468.

Schwarz, S., Husstedt, I., Bertram, H.P., and Kuchelmeister, K. (1996). Amyotrophic lateral sclerosis after accidental injection of mercury. J Neurol Neurosurg Psychiatry *60*, 698.

Schymick, J.C., Talbot, K., and Traynor, B.J. (2007). Genetics of sporadic amyotrophic lateral sclerosis. Hum Mol Genet *16 Spec No. 2*, R233-242.

Seo, M.S., Kang, S.W., Kim, K., Baines, I.C., Lee, T.H., and Rhee, S.G. (2000). Identification of a new type of mammalian peroxiredoxin that forms an intramolecular disulfide as a reaction intermediate. J Biol Chem *275*, 20346-20354.

Sephton, C.F., Good, S.K., Atkin, S., Dewey, C.M., Mayer, P., 3rd, Herz, J., and Yu, G. (2010). TDP-43 is a developmentally regulated protein essential for early embryonic development. The Journal of Biological Chemistry *285*, 6826-6834.

Shaw, C.E., Enayat, Z.E., Chioza, B.A., Al-Chalabi, A., Radunovic, A., Powell, J.F., and Leigh, P.N. (1998). Mutations in all five exons of SOD-1 may cause ALS. Ann Neurol *43*, 390-394.

Shaw, P.J. (2005). Molecular and cellular pathways of neurodegeneration in motor neurone disease. J Neurol Neurosurg Psychiatry *76*, 1046-1057.

Shaw, P.J., Forrest, V., Ince, P.G., Richardson, J.P., and Wastell, H.J. (1995a). CSF and plasma amino acid levels in motor neuron disease: elevation of CSF glutamate in a subset of patients. Neurodegeneration *4*, 209-216.

Shaw, P.J., Ince, P.G., Falkous, G., and Mantle, D. (1995b). Oxidative damage to protein in sporadic motor neuron disease spinal cord. Ann Neurol *38*, 691-695.

Shefner, J.M., Cudkowicz, M.E., Schoenfeld, D., Conrad, T., Taft, J., Chilton, M., Urbinelli, L., Qureshi, M., Zhang, H., Pestronk, A.*, et al.* (2004). A clinical trial of creatine in ALS. Neurology *63*, 1656-1661.

Shibanuma, M., Kuroki, T., and Nose, K. (1991). Release of H2O2 and phosphorylation of 30 kilodalton proteins as early responses of cell cycle-dependent inhibition of DNA synthesis by transforming growth factor beta 1. Cell Growth Differ *2*, 583-591.

Siddique, T., Figlewicz, D.A., Pericak-Vance, M.A., Haines, J.L., Rouleau, G., Jeffers, A.J., Sapp, P., Hung, W.Y., Bebout, J., McKenna-Yasek, D.*, et al.* (1991). Linkage of a gene causing familial amyotrophic lateral sclerosis to chromosome 21 and evidence of genetic-locus heterogeneity. N Engl J Med *324*, 1381-1384.

Siddique, T., Hong, S.T., Brooks, B.R., Hung, W., Siddique, N.A., Rimmler, J., Kaplan, J., Haines, J.L., Brown, R.H., and Pericak-Vance, M. (1998). X-linked dominant locus for late-onset familial amyotrophic lateral sclerosis. American Journal of Human Genetics *Suppl 63*, A308.

Sies, H. (1997). Oxidative stress: oxidants and antioxidants. Exp Physiol *82*, 291-295.

Siklos, L., Engelhardt, J., Harati, Y., Smith, R.G., Joo, F., and Appel, S.H. (1996). Ultrastructural evidence for altered calcium in motor nerve terminals in amyotropic lateral sclerosis. Ann Neurol *39*, 203-216.

Simpson, E.P., Henry, Y.K., Henkel, J.S., Smith, R.G., and Appel, S.H. (2004). Increased lipid peroxidation in sera of ALS patients: a potential biomarker of disease burden. Neurology *62*, 1758-1765.

Smith, R.G., Henry, Y.K., Mattson, M.P., and Appel, S.H. (1998). Presence of 4-hydroxynonenal in cerebrospinal fluid of patients with sporadic amyotrophic lateral sclerosis. Ann Neurol *44*, 696-699.

Soriani, M.H., and Desnuelle, C. (2009). [Epidemiology of amyotrophic lateral sclerosis]. Rev Neurol (Paris) *165*, 627-640.

Soriano, F.X., Baxter, P., Murray, L.M., Sporn, M.B., Gillingwater, T.H., and Hardingham, G.E. (2009a). Transcriptional regulation of the AP-1 and Nrf2 target gene sulfiredoxin. Mol Cells *27*, 279-282.

Soriano, F.X., Leveille, F., Papadia, S., Higgins, L.G., Varley, J., Baxter, P., Hayes, J.D., and Hardingham, G.E. (2008). Induction of sulfiredoxin expression and reduction of peroxiredoxin hyperoxidation by the neuroprotective Nrf2 activator 3H-1,2-dithiole-3-thione. J Neurochem *107*, 533-543.

Soriano, F.X., Papadia, S., Bell, K.F., and Hardingham, G.E. (2009b). Role of histone acetylation in the activity-dependent regulation of sulfiredoxin and sestrin 2. Epigenetics *4*, 152-158.

Spreux-Varoquaux, O., Bensimon, G., Lacomblez, L., Salachas, F., Pradat, P.F., Le Forestier, N., Marouan, A., Dib, M., and Meininger, V. (2002). Glutamate levels in cerebrospinal fluid in amyotrophic lateral sclerosis: a reappraisal using a new HPLC method with coulometric detection in a large cohort of patients. J Neurol Sci *193*, 73-78.

Spyrou, G., Enmark, E., Miranda-Vizuete, A., and Gustafsson, J. (1997). Cloning and expression of a novel mammalian thioredoxin. The Journal of Biological Chemistry *272*, 2936-2941.

Sreedharan, J., Blair, I.P., Tripathi, V.B., Hu, X., Vance, C., Rogelj, B., Ackerley, S., Durnall, J.C., Williams, K.L., Buratti, E.*, et al.* (2008). TDP-43 mutations in familial and sporadic amyotrophic lateral sclerosis. Science *319*, 1668-1672.

Strasser, A., O'Connor, L., and Dixit, V.M. (2000). Apoptosis signaling. Annu Rev Biochem *69*, 217-245.

Strong, M.J., and Gordon, P.H. (2005). Primary lateral sclerosis, hereditary spastic paraplegia and amyotrophic lateral sclerosis: discrete entities or spectrum? Amyotroph Lateral Scler Other Motor Neuron Disord *6*, 8-16.

Strong, M.J., and Pattee, G.L. (2000). Creatine and coenzyme Q10 in the treatment of ALS. Amyotroph Lateral Scler Other Motor Neuron Disord *1 Suppl 4*, 17-20.

Strong, M.J., and Volkening, K. (2011). TDP-43 and FUS/TLS: sending a complex message about messenger RNA in amyotrophic lateral sclerosis? The FEBS journal *278*, 3569-3577.

Suzuki, M., Irie, T., Watanabe, T., Mikami, H., Yamazaki, T., Oyanagi, K., and Ono, S. (2008). Familial amyotrophic lateral sclerosis with Gly93Ser mutation in Cu/Zn superoxide dismutase: a clinical and neuropathological study. Journal of the Neurological Sciences *268*, 140-144.

Swash, M. (2003). Clinical principles in the diagnosis of motor neuron disorders. In Motor Neuron Disorders, P.J. Shaw, and M.J. Strong, eds. (Philadelphia: Butterworth Heineman), pp. 3-15.

Taanman, J.W. (1999). The mitochondrial genome: structure, transcription, translation and replication. Biochim Biophys Acta *1410*, 103-123.

Talbot, K. (2002). Motor neurone disease. Postgrad Med J *78*, 513-519.

Tartaglia, M.C., Rowe, A., Findlater, K., Orange, J.B., Grace, G., and Strong, M.J. (2007). Differentiation between primary lateral sclerosis and amyotrophic lateral sclerosis: examination of symptoms and signs at disease onset and during follow-up. Archives of neurology *64*, 232-236.

The BDNF Study Group (1999). A controlled trial of recombinant methionyl human BDNF in ALS: The BDNF Study Group (Phase III). Neurology *52*, 1427-1433.

Thornton, F.J., Fotheringham, T., Alexander, M., Hardiman, O., McGrath, F.P., and Lee, M.J. (2002). Amyotrophic lateral sclerosis: enteral nutrition provision--endoscopic or radiologic gastrostomy? Radiology *224*, 713-717.

Tohgi, H., Abe, T., Yamazaki, K., Murata, T., Ishizaki, E., and Isobe, C. (1999). Remarkable increase in cerebrospinal fluid 3-nitrotyrosine in patients with sporadic amyotrophic lateral sclerosis. Ann Neurol *46*, 129-131.

Tomkins, J., Usher, P., Slade, J.Y., Ince, P.G., Curtis, A., Bushby, K., and Shaw, P.J. (1998). Novel insertion in the KSP region of the neurofilament heavy gene in amyotrophic lateral sclerosis (ALS). Neuroreport *9*, 3967-3970.

Tsermentseli, S., Leigh, P.N., and Goldstein, L.H. (2012). The anatomy of cognitive impairment in amyotrophic lateral sclerosis: more than frontal lobe dysfunction. Cortex; A Journal devoted to the study of the Nervous System and Behavior *48*, 166-182.

Tu, P.H., Raju, P., Robinson, K.A., Gurney, M.E., Trojanowski, J.Q., and Lee, V.M. (1996). Transgenic mice carrying a human mutant superoxide dismutase transgene develop neuronal cytoskeletal pathology resembling human amyotrophic lateral sclerosis lesions. Proc Natl Acad Sci U S A *93*, 3155-3160.

Turner, B.J., and Talbot, K. (2008). Transgenics, toxicity and therapeutics in rodent models of mutant SOD1-mediated familial ALS. Progress in Neurobiology *85*, 94-134.

Turrens, J.F. (1997). Superoxide production by the mitochondrial respiratory chain. Biosci Rep *17*, 3-8.

Valentine, J.S., and Hart, P.J. (2003). Misfolded CuZnSOD and amyotrophic lateral sclerosis. Proc Natl Acad Sci U S A *100*, 3617-3622.

van Blitterswijk, M., and Landers, J.E. (2010). RNA processing pathways in amyotrophic lateral sclerosis. Neurogenetics *11*, 275-290.

Van Damme, P., Braeken, D., Callewaert, G., Robberecht, W., and Van Den Bosch, L. (2005). GluR2 deficiency accelerates motor neuron degeneration in a mouse model of amyotrophic lateral sclerosis. J Neuropathol Exp Neurol *64*, 605-612.

van Rheenen, W., van Blitterswijk, M., Huisman, M.H., Vlam, L., van Doormaal, P.T., Seelen, M., Medic, J., Dooijes, D., de Visser, M., van der Kooi, A.J., *et al.* (2012). Hexanucleotide repeat expansions in C9ORF72 in the spectrum of motor neuron diseases. Neurology *79*, 878-882.

Vanacore, N., Cocco, P., Fadda, D., and Dosemeci, M. (2010). Job strain, hypoxia and risk of amyotrophic lateral sclerosis: Results from a death certificate study. Amyotroph Lateral Scler *11*, 430-434.

Vance, C., Al-Chalabi, A., Ruddy, D., Smith, B.N., Hu, X., Sreedharan, J., Siddique, T., Schelhaas, H.J., Kusters, B., Troost, D., *et al.* (2006). Familial amyotrophic lateral sclerosis with frontotemporal dementia is linked to a locus on chromosome 9p13.2-21.3. Brain *129*, 868-876.

Vance, C., Rogelj, B., Hortobagyi, T., De Vos, K.J., Nishimura, A.L., Sreedharan, J., Hu, X., Smith, B., Ruddy, D., Wright, P., *et al.* (2009). Mutations in FUS, an RNA processing protein, cause familial amyotrophic lateral sclerosis type 6. Science *323*, 1208-1211.

Veldink, J.H., Kalmijn, S., Groeneveld, G.J., Titulaer, M.J., Wokke, J.H., and van den Berg, L.H. (2005). Physical activity and the association with sporadic ALS. Neurology *64*, 241-245.

Verdoorn, T.A., Burnashev, N., Monyer, H., Seeburg, P.H., and Sakmann, B. (1991). Structural determinants of ion flow through recombinant glutamate receptor channels. Science *252*, 1715-1718.

Visser, J., de Jong, J.M., and de Visser, M. (2008). The history of progressive muscular atrophy: syndrome or disease? Neurology *70*, 723-727.

Wang, C.C. (2002). Protein disulfide isomerase as an enzyme and a chaperone in protein folding. Methods Enzymol *348*, 66-75.

Wang, H., O'Reilly, E.J., Weisskopf, M.G., Logroscino, G., McCullough, M.L., Thun, M.J., Schatzkin, A., Kolonel, L.N., and Ascherio, A. (2011). Smoking and risk of amyotrophic lateral sclerosis: a pooled analysis of 5 prospective cohorts. Archives of neurology *68*, 207-213.

Wang, J., Slunt, H., Gonzales, V., Fromholt, D., Coonfield, M., Copeland, N.G., Jenkins, N.A., and Borchelt, D.R. (2003). Copper-binding-site-null SOD1 causes ALS in transgenic mice: aggregates of non-native SOD1 delineate a common feature. Hum Mol Genet *12*, 2753-2764.

Wang, J., Xu, G., and Borchelt, D.R. (2002). High molecular weight complexes of mutant superoxide dismutase 1: age-dependent and tissue-specific accumulation. Neurobiol Dis *9*, 139-148.

Watanabe, M., Dykes-Hoberg, M., Culotta, V.C., Price, D.L., Wong, P.C., and Rothstein, J.D. (2001). Histological evidence of protein aggregation in mutant SOD1 transgenic mice and in amyotrophic lateral sclerosis neural tissues. Neurobiol Dis *8*, 933-941.

Weiss, M.D., Ravits, J.M., Schuman, N., and Carter, G.T. (2006). A4V superoxide dismutase mutation in apparently sporadic ALS resembling neuralgic amyotrophy. Amyotroph Lateral Scler *7*, 61-63.

Wharton, S.B., and Ince, P.G. (2003). Pathology of motor neuron diorders. In Motor Neuron Disorders, P.J. Shaw, and M.J. Strong, eds. (Philadelphia: Butterworth Heineman), pp. 17-49.

Wiedemann, F.R., Manfredi, G., Mawrin, C., Beal, M.F., and Schon, E.A. (2002). Mitochondrial DNA and respiratory chain function in spinal cords of ALS patients. J Neurochem *80*, 616-625.

Williamson, T.L., and Cleveland, D.W. (1999). Slowing of axonal transport is a very early event in the toxicity of ALS-linked SOD1 mutants to motor neurons. Nat Neurosci *2*, 50-56.

Wils, H., Kleinberger, G., Janssens, J., Pereson, S., Joris, G., Cuijt, I., Smits, V., Ceuterick-de Groote, C., Van Broeckhoven, C., and Kumar-Singh, S. (2010). TDP-43 transgenic mice develop spastic paralysis and neuronal inclusions characteristic of ALS and frontotemporal lobar degeneration. Proceedings of the National Academy of Sciences of the United States of America *107*, 3858-3863.

Winton, M.J., Igaz, L.M., Wong, M.M., Kwong, L.K., Trojanowski, J.Q., and Lee, V.M. (2008). Disturbance of nuclear and cytoplasmic TAR DNA-binding protein (TDP-43) induces disease-like redistribution, sequestration, and aggregate formation. J Biol Chem *283*, 13302-13309.

Wong, P.C., Pardo, C.A., Borchelt, D.R., Lee, M.K., Copeland, N.G., Jenkins, N.A., Sisodia, S.S., Cleveland, D.W., and Price, D.L. (1995). An adverse property of a familial ALS-linked SOD1 mutation causes motor neuron disease characterized by vacuolar degeneration of mitochondria. Neuron *14*, 1105-1116.

Woo, H.A., Bae, S.H., Park, S., and Rhee, S.G. (2009). Sestrin 2 is not a reductase for cysteine sulfinic acid of peroxiredoxins. Antioxid Redox Signal *11*, 739-745.

Woo, H.A., Jeong, W., Chang, T.S., Park, K.J., Park, S.J., Yang, J.S., and Rhee, S.G. (2005). Reduction of cysteine sulfinic acid by sulfiredoxin is specific to 2-cys peroxiredoxins. J Biol Chem *280*, 3125-3128.

Woo, H.A., Kang, S.W., Kim, H.K., Yang, K.S., Chae, H.Z., and Rhee, S.G. (2003). Reversible oxidation of the active site cysteine of peroxiredoxins to cysteine sulfinic acid. Immunoblot detection with antibodies specific for the hyperoxidized cysteine-containing sequence. J Biol Chem *278*, 47361-47364.

Woo, H.A., Yim, S.H., Shin, D.H., Kang, D., Yu, D.Y., and Rhee, S.G. (2010). Inactivation of peroxiredoxin I by phosphorylation allows localized H(2)O(2) accumulation for cell signaling. Cell *140*, 517-528.

Wood-Allum, C.A., Barber, S.C., Kirby, J., Heath, P., Holden, H., Mead, R., Higginbottom, A., Allen, S., Beaujeux, T., Alexson, S.E., *et al.* (2006). Impairment of mitochondrial anti-oxidant defence in SOD1-related motor neuron injury and amelioration by ebselen. Brain *129*, 1693-1709.

Wood-Allum, C.A., and Shaw, P.J. (2006). Clinical Review of Motor Neurone Disease,. In General Practitioner Newspaper March 24th & 31st

Wood, J.D., Beaujeux, T.P., and Shaw, P.J. (2003a). Protein aggregation in motor neurone disorders. Neuropathol Appl Neurobiol *29*, 529-545.

Wood, Z.A., Poole, L.B., and Karplus, P.A. (2003b). Peroxiredoxin evolution and the regulation of hydrogen peroxide signaling. Science *300*, 650-653.

Wood, Z.A., Schroder, E., Robin Harris, J., and Poole, L.B. (2003c). Structure, mechanism and regulation of peroxiredoxins. Trends Biochem Sci *28*, 32-40.

Xu, Z., Cork, L.C., Griffin, J.W., and Cleveland, D.W. (1993). Increased expression of neurofilament subunit NF-L produces morphological alterations that resemble the pathology of human motor neuron disease. Cell *73*, 23-33.

Yamanaka, K., Boillee, S., Roberts, E.A., Garcia, M.L., McAlonis-Downes, M., Mikse, O.R., Cleveland, D.W., and Goldstein, L.S. (2008). Mutant SOD1 in cell types other than motor neurons and oligodendrocytes accelerates onset of disease in ALS mice. Proc Natl Acad Sci U S A *105*, 7594-7599.

Yang, K.S., Kang, S.W., Woo, H.A., Hwang, S.C., Chae, H.Z., Kim, K., and Rhee, S.G. (2002). Inactivation of human peroxiredoxin I during catalysis as the result of the oxidation of the catalytic site cysteine to cysteine-sulfinic acid. J Biol Chem *277*, 38029-38036.

Yang, Y., Hentati, A., Deng, H.X., Dabbagh, O., Sasaki, T., Hirano, M., Hung, W.Y., Ouahchi, K., Yan, J., Azim, A.C.*, et al.* (2001). The gene encoding alsin, a protein with three guanine-nucleotide exchange factor domains, is mutated in a form of recessive amyotrophic lateral sclerosis. Nat Genet *29*, 160-165.

Yao, J., Taylor, M., Davey, F., Ren, Y., Aiton, J., Coote, P., Fang, F., Chen, J.X., Yan, S.D., and Gunn-Moore, F.J. (2007). Interaction of amyloid binding alcohol dehydrogenase/Abeta mediates up-regulation of peroxiredoxin II in the brains of Alzheimer's disease patients and a transgenic Alzheimer's disease mouse model. Mol Cell Neurosci *35*, 377-382.

Yao, Z., Tong, J., Tan, X., Li, C., Shao, Z., Kim, W.C., vanden Hoek, T.L., Becker, L.B., Head, C.A., and Schumacker, P.T. (1999). Role of reactive oxygen species in acetylcholine-induced preconditioning in cardiomyocytes. Am J Physiol *277*, H2504-2509.

Yase, Y., Yoshida, S., Kihira, T., Wakayama, I., and Komoto, J. (2001). Kii ALS dementia. Neuropathology *21*, 105-109.

Yim, M.B., Kang, J.H., Yim, H.S., Kwak, H.S., Chock, P.B., and Stadtman, E.R. (1996). A gain-of-function of an amyotrophic lateral sclerosis-associated Cu,Zn-superoxide dismutase mutant: An enhancement of free radical formation due to a decrease in Km for hydrogen peroxide. Proc Natl Acad Sci U S A *93*, 5709-5714.

Zhang, B., Tu, P., Abtahian, F., Trojanowski, J.Q., and Lee, V.M. (1997). Neurofilaments and orthograde transport are reduced in ventral root axons of transgenic mice that express human SOD1 with a G93A mutation. J Cell Biol *139*, 1307-1315.

Zigman, W.B., and Lott, I.T. (2007). Alzheimer's disease in Down syndrome: neurobiology and risk. Ment Retard Dev Disabil Res Rev *13*, 237-246.

2. METHODS

EXPERIMENTAL SUBSTRATES

2.1 HEK293 cells

The Human Embryonic Kidney cell line (HEK293) is an immortalized cell line generated by the transfection of sheared adenovirus DNA into human embryonic kidney cells (Graham et al., 1977). HEK293 cells are robust, easy to culture and fast-growing. HEK293 cells, originally purchased from Life Technologies (Paisley, UK), are maintained in culture by members of our department and previously frozen-down cells between passages 6-10 were available for resuscitation (see Sections 2.8 and 2.9). These cells were used for the purpose of working up new antibodies and experimental protocols.

MODELS OF ALS USED AS EXPERIMENTAL SUBSTRATES

ALS is a disease largely of motor neurons. The motor neurons affected in ALS are the upper motor neurons in the motor cortex serving bulbar, respiratory and limb muscles and the lower motor neurons in the brain stem nuclei serving the bulbar musculature along with motor neurons in the anterior spinal cord serving limb and respiratory muscles. These cells are not accessible in life in patients or in healthy controls. Biopsy of motor cortex or spinal cord in life for research purposes would likely result in irreversible neurological damage and would be ethically unacceptable, notwithstanding the risks of general anaesthetic and neurosurgery. Although post-mortem tissue is available for research purposes, the use of this material has many limitations including frequently lengthy post-mortem delays prior to harvest of CNS tissue. The fact that human motor neurons are inaccessible during life has made it essential to develop disease models featuring living cells that recapitulate at least partially the pathogenesis of ALS. The next sections will discuss the ALS models used in this work along with the advantages and disadvantages of their use.

2.2 Human fibroblasts

Fibroblasts are connective tissue cells present in the mesodermal layer of the skin. Damage to skin induces fibrocyte formation and mitosis in fibroblasts (Villegas and McPhaul, 2005) enabling skin biopsies to serve as a primary source of these cells. Cultivating fibroblasts in a medium containing epidermal growth factor allows them to be maintained in a replicative state *in vitro* (Shiraha et al., 2000) allowing fibroblasts obtained from individual patients to be maintained in ongoing culture (West et al., 1989).

2.2.1 Rationale for the use of human ALS fibroblasts to model ALS

The replication of cultured fibroblasts and their ease of culture in the laboratory makes them a convenient, readily renewable and relatively homogeneous resource to work with. Fibroblasts from ALS patients carrying mutations responsible for their disease will express these mutant genes as the

genes found to cause inherited ALS have, to date, been found to be ubiquitously expressed across tissues, including in the skin. It is likely, although not certain, that any modifier genes modulating the manifestation of ALS in an individual ALS patient will also be represented in the fibroblasts obtained from their donated skin biopsy. Skin biopsies may be readily obtained from patients with sporadic ALS generating a cell culture model of the most prevalent form of the disease. All other cellular models of ALS can only model the familial form of the disease. They either comprise embryonic motor neurons obtained from a transgenic animal model (e.g., primary murine motor neurons grown up from embryonic SOD1 transgenic mouse spinal cord tissue) or else "motor neuronal" cells with a variably motor neuron-like phenotype into which are transfected mutant genes known to be responsible for various forms of inherited ALS in patients.

There is precedence for the use of fibroblasts from patients with other neurodegenerative diseases in basic research. In these conditions findings initially observed in fibroblasts have been shown to be reiterated in the relevant CNS tissue (Hein et al., 2010; Ito et al., 1994; Mendonsa et al., 2009). Previous work published by others in ALS fibroblasts bears out the validity of this principle in ALS (see Section 2.2.2). As with all models of neurodegenerative disease, the use of human fibroblasts obtained from patients confers both advantages and disadvantages. These are considered next. The means by which our fibroblasts were obtained is discussed in Section 2.2.3.

2.2.2 Advantages and disadvantages of human ALS fibroblasts as a model of ALS

Advantages

- Fibroblasts are of human origin and may be obtained directly from both sporadic and familial ALS patients (sporadic/familial) as well as healthy controls via a relatively simple skin biopsy procedure. The tissue from patients is, by definition, obtained at a time when the individual is manifesting the disease.
- In contrast to overexpressing transgenic mouse models and transfected cellular models of ALS which often carry multiple copies of the mutant human gene, fibroblasts obtained from fALS patients carry only a single copy. As such these fibroblasts represent a more physiological cellular model of ALS.
- Cultured fibroblasts can be re-differentiated into motor neurons through a series of genetic reprogramming steps starting with the generation of pluripotent stem cells. These may then be encouraged to generate both motor neurons and their surrounding glia by culture in highly selective media. The fact that fibroblasts may be converted to motor neurons emphasizes what the two cell types have in common (Dimos et al., 2008).
- Importantly, the results of previous work in ALS fibroblasts has reflected already known pathogenic mechanisms observed in patient motor neurons and in other models of the disease (Aguirre et al., 1998; Robberecht, 2000).

- Fibroblasts are robust, quickly growing and a homogenous population of cells. As such they represent an economical cell-culture model of ALS.

Disadvantages

- Fibroblasts are skin cells and as such differ in fundamental ways from motor neurons. First, unlike post-mitotic motor neurons, fibroblasts are replicative. Second, fibroblasts lack the macroscopic scale of many motor neurons and the maintenance and transport demands that are a consequence of an axon up to a metre in length. The chief role of spinal motor neurons is to receive, modulate and transmit electrical impulses descending from the motor cortex to the neuromuscular junction. The cellular apparatus and biochemistry needed to support this role is entirely absent from fibroblasts.
- Once stabilized in culture, fibroblasts from any one individual represent a homogenous cell population. The fact that they are obtained from individual people, however, means that their genome, transcriptome and proteome will be unique in at least some aspects and therefore inherently variable cell line to cell line. This is true both of patient and control fibroblast lines.
- Cultured fibroblasts as is the case for NSC34 cells, discussed next, cannot model the effects of the physical and functional interactions of other cell types that surround and synapse with motor neurons.
- Lastly, senescence limits the use of cultured fibroblasts (Shiraha et al., 2000). Consistent results are produced when experiments are conducted during the replicative phase of the fibroblasts but with each cell cycle, dysregulation of antioxidant pathways have been observed (Hayflick and Moorhead, 1961; Hutter et al., 2004). This makes the use of fibroblasts at advanced passage numbers inadvisable.

2.2.3 Preparation of human fibroblast cultures

Fibroblasts were obtained from skin biopsies donated by SOD1-ALS patients, TDP43-ALS patients and by age- and sex-matched healthy controls (see Table 2.1). Human fibroblast cultures (with one exception, detailed in Table 2.1) were established in the Metabolic Biochemistry and Tissue Culture Unit of the Sheffield Children's NHS Foundation Trust before transfer to our laboratory where they were maintained in culture (see Section 2.6).

Subject	Mutation	Sex	Age (yr)
Control 1	-----	Male	45
Control 4	-----	Male	55
Control 8	-----	Female	42
Control 11	-----	Male	58
Patient 28	SOD1 I113T	Male	62
Patient 91	SOD1 I113T	Male	62
Dutch Patient*	SOD1 I113T	Male	61
Patient 48	TDP-43 A321V	Female	43
Patient 51	TDP-43 M337V	Male	66
Patient 55	TDP-43 G287S	Male	60

Table 2.1: *Table showing the age and sex of the individuals who donated control and patient fibroblasts. *Fibroblasts from one I113T SOD1-ALS patient were the kind gift of Professor Frank Bass, University of Amsterdam, Netherlands, and were used with his permission.*

Informed consent and skin biopsies were taken by the MND Specialist Nurses and neurology clinical team caring for the patient. Briefly, skin biopsies were collected from the forearm of the subject under sterile conditions and were placed in 5 ml of Dulbecco's Modified Eagle Media (DMEM) (Gibco, Paisley, Scotland, UK). All work from this point was carried out by the staff of the Metabolic Biochemistry and Tissue Culture Unit at the Sheffield Children's NHS Foundation Trust. The biopsy was dissected using sterile surgical blades and explants were trapped under a coverslip placed on the flat base of a Nunc tube (Nalge Nunc International, Rochester, USA) using a sterilised glass pipette. The samples were incubated with 3 ml of fibroblast culture medium (Section 2.20) in an incubator with a humidified atmosphere maintained at 37˚C and containing 5% CO_2 (Incusafe™, Sanyo, Japan). Following outgrowth of fibroblasts from the explanted tissue and coverage of both sides of the coverslip, the fibroblasts were released into solution using Trypsin-EDTA and transferred to T-25 culture flasks for ongoing culture.

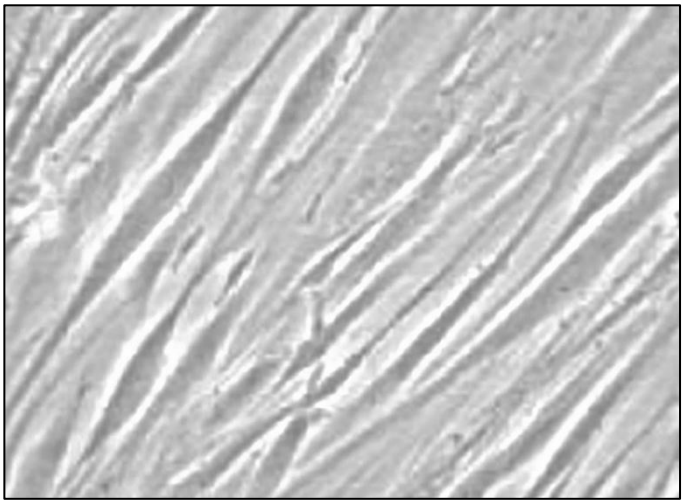

Figure 2.1: *Human fibroblasts growing in culture. Once seeded in a culture flask fibroblasts develop an elongated cell shape over a period of 2-4 days (with thanks to Laura Ferraiuolo).*

2.3 NSC34 cells

2.3.1 Generation and phenotype of motor neuronal NSC34 cells

The NSC34 cells (Fig. 2.2) used in this work were originally the kind gift of Dr. Neil Cashman (University of Toronto, Canada) to Professor Pamela Shaw. NSC34 cells are an immortalized motor neuronal cell line generated by the fusion of the N18TGT neuroblastoma cell line with 12-14 day motor neuron-enriched embryonic murine spinal cord cultures using a polyethylene glycol-mediated fusion technique (Cashman et al., 1992).

The resultant fused hybrid cells were then screened to identify the clones that had retained the most motor neuronal characteristics. The screening selection included both morphological and physiological properties characteristic of motor neurons. The clone ultimately selected by this process (NSC34) displayed many morphological characteristics typical of motor neurons in culture in that they were adherent to the culture substrate, were multipolar in shape and when allowed to grow in culture extended out long terminal processes. They were also able to synthesize and store Acetyl Choline (ACh) and expressed Choline Acetyl Transferase (ChAT). It was also observed that after reseeding of the culture flask NSC34 cells exhibited a sequential pattern of neurofilament protein expression that reiterated motor neuron development that was observed during *in vivo,* i.e., initial expression of vimentin, followed by expression of all 3 neurofilament proteins then, finally, loss of vimentin expression. NSC-34 cells co-cultured with neonatal mouse forelimb myotubes grew in close association with the myotube surface and were able to support action potentials that induced myotube twitches. Additionally, clustering of ACh receptors was observed in those areas of the myotube membrane closely associated with the NSC34 cells suggestive of the first stages of neuromuscular junction formation. Electrophysiological studies using ion-channel blocking agents, moreover, identified inward Na^+ and Ca^+ currents and an outward K^+ current similar to those observed in cultured spinal motor neurons (Durham et al., 1993).

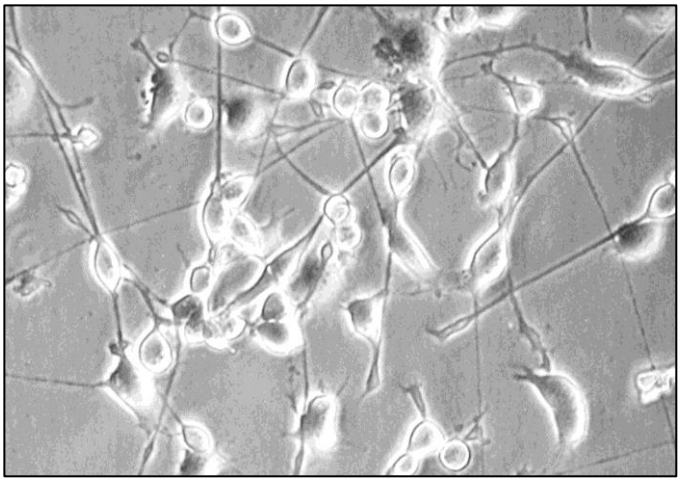

Figure 2.2: *NSC34 cells growing in culture. Once seeded in a culture flask cells develop an increasingly motor neuronal phenotype over a period of 3-4 days extending out long slender cell processes (with thanks to Fiona Menzies).*

2.3.2 Advantages and disadvantages of NSC34 cells as a model of human ALS

Advantages

- Immortalized NSC34 cells are almost an inexhaustible source of material to work with as the cells are capable of proliferation. They can readily be grown in culture so place no limits upon the number of experiments or number of experimental repeats that can be performed. This is not the case for cultured primary motor neurons which are obtained in relatively small numbers from embryonic mice and which have a limited usable lifespan in culture. Relative to other ALS models maintenance and use of NSC34 cells is inexpensive.
- NSC34 cells share many features of motor neurons as discussed above. Because NSC34 cells are monoclonal, experiments performed on NSC34 cells are experiments performed on isolated motor neuronal cells without contamination from other cell types. In whole spinal cord preparations from SOD1 transgenic mice, for example, motor neurons are heavily outmassed by glia, connective and vascular tissue.
- The monoclonal nature of the NSC34 cell lines used in this study should, at least in theory, make for a homogeneous experimental substrate increasing the chances of reproducible results between experiments (see Chapter 4).
- NSC34 cells are motor neuronal cells that can be grown in culture for relatively long periods of time. They may readily be transfected with mutated genes known to cause ALS in humans to create either stable or transient transfectants. This allows investigation of the effects of ALS-causing genes on motor neuronal cells.

Disadvantages

- NSC34 cells are of murine and not human origin.
- NSC34 are proliferative unlike fully-differentiated, post-mitotic motor neurons. This constitutes a significant difference in biology between the two.
- NSC34 cells grown in culture display both a proliferative and a partially differentiated phenotype. Over time their proliferation makes it possible that their genetic make-up may change and that their neuroblastoma-like characteristics may begin to outweigh their motor-neuronal characteristics.
- Interesting work by Cleveland et al. in murine transgenic chimeras demonstrated that astrocytes and glia surrounding motor neurons may play an important role in disease pathogenesis (Clement et al., 2003). NSC34 cells are a monoculture of motor neuronal cells. For this reason, and because they lack both functional and physical connections with muscle, spinal interneurons and surrounding glia, NSC34 cells cannot inform about the influence of many potentially important intercellular interactions.
- Although NSC34 cells share many features of motor neurons, application of glutamate does not produce vacuolization of dendrites, indicating that NSC34 cells lack functional glutamate receptors (Cashman et al., 1992). As such, NSC34 cells are not a good model in which to study the effects of excitotoxicity.

2.3.3 Preparation of stable NSC34 cell transfectants

Non-transgenic (NTG) NSC34 cells were stably transfected with wild-type human SOD1 (WT) and with three mutant forms of human SOD1: H48Q, I113T and G93A (Fig. 2.3). These transfections had been previously performed by Dr. Adrian Higginbottom and Dr. Sian Barber in our laboratory using the pIRES vector system (Clonetech, California, USA). NSC34 cells transfected with empty vector and with WT SOD1 along with non-transgenic cells (NTG) cells were used as controls. Stably transfected cell lines were then maintained in culture along with NTG NSC34 cells. Selection of transfected cells (pIRES, WT, H48Q, I113T and G93A) was maintained using G418 Geneticin G418-sulphate (Gibco, Paisley, Scotland, UK) at 250 μg/ml. All cells were grown in 5% CO_2 in an incubator with a humidified atmosphere at 37˚C (Incusafe™, Sanyo, Japan).

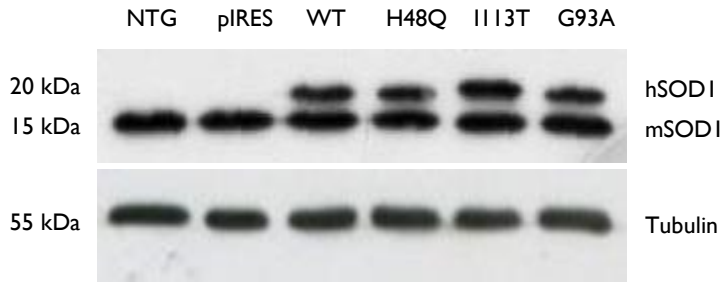

Figure 2.3: *Representative Western blots showing levels of endogenous mouse SOD1 (mSOD1) and transfected human SOD1 (hSOD1) in whole cell preparations of various NSC34 cell lines grown under basal conditions. NTG = non-transgenic NSC34 cells, pIRES = vector-only stably transfected NSC34 cells, WT = NSC34 cells stably expressing WT human SOD1, H48Q = NSC34 cells stably expressing H48Q human SOD1, I113T = NSC34 cells stably expressing I113T human SOD1 and G93A = NSC34 cells stably expressing G93A human SOD1. Protein loading of 20 µg per lane, SOD1 and tubulin (loading control) blots exposed for 1.5 min.*

2.4 G93A SOD1 transgenic mice

Two lines of human SOD1 transgenic mice (G93A SOD1 and WT SOD1), bred on a C57BL6 background, were initially purchased from The Jackson Laboratory (Bar Harbor, ME). The G93A SOD1 transgenic mice overexpress G93A mutant human SOD1 at levels approximately 10-fold higher than that of endogenous murine SOD1 (Gurney et al., 1994). The WT SOD1 overexpressing mice overexpress a full length WT human SOD1 at levels approximately 7 times greater than those of endogenous murine SOD1 (Dal Canto and Gurney, 1994) (Fig 2.4).

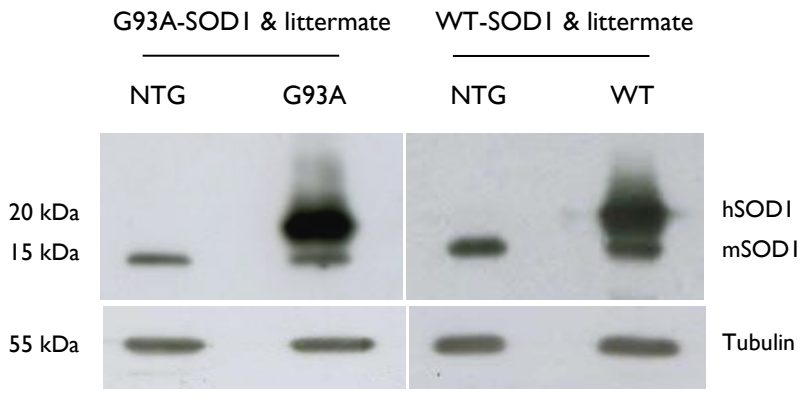

Figure 2.4: *Representative Western blots showing levels of endogenous mouse SOD1 (mSOD1) and transfected human SOD1 (hSOD1) in spinal cord preparations from G93A and WT transgenic mice and their respective non-transgenic littermates. Lanes: NTG = non-transgenic littermate, G93A = G93A mutant human SOD1 overexpressing mice and WT = WT human SOD1 overexpressing mice. Protein loads were 20 µg protein per lane and both SOD1 and tubulin (loading control) blots were exposed for 1.5 min.*

2.4.1 Generation and phenotype of G93A SOD1 transgenic mice

The G93A SOD1 transgenic mice used in this study were generated from fertilized eggs that were the result of crosses of C57BL6 x SJL F_1 hybrid mice (Gurney et al., 1994). A complete SOD1 transgene comprising an amplified fragment of DNA from a G93A SOD-1 familial ALS patient containing exon 4 of the SOD1 gene was generated. The transgene, in the presence of an overexpressing promoter sequence, was injected into the fertilized eggs obtained from the F_1 hybrid mice. Screening for the highest expression of human SOD1 in the transgenic mice generated was carried out using antigen-capture immunoassay in isolated red blood cells. The mouse with highest human SOD1 expression was selected to establish the transgenic line by breeding with C57BL6 mice. This generated G93A-SOD1 overexpressing mice and non-transgenic littermates with each cross. It is not possible accurately to identify transgenic from non-transgenic pups by phenotype but polymerase chain reaction (PCR) amplification of DNA from ear clippings taken from mice of 14 days of age allows differentiation of the transgenic pups from their non-transgenic littermates well before the onset of disease.

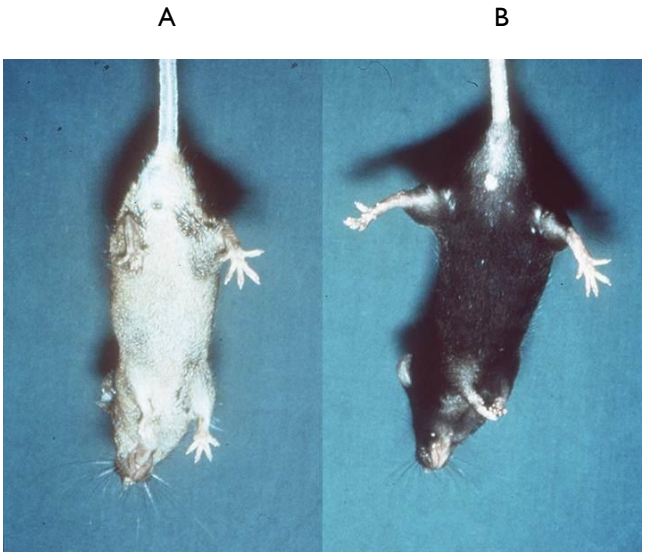

Figure 2.5: *A) G93A SOD1 transgenic mouse and B) its non-transgenic littermate being held by the tail. The G93A SOD1 transgenic mouse shows a decreased leg-splay reaction when compared to its non-transgenic littermate.*

G93A SOD1 mice are born with a normal motor phenotype and develop normally into adulthood. Disease is clearly evident by ~90 days of age by which stage mice are unable to walk normally and when picked up by the tail display an impaired leg-splay reflex (Fig. 2.5). More subtle motor deficits can, however, be elicited as early as 60 days by formal testing of motor performance, for example by using a rotarod apparatus (Mead et al., 2011) and this is more properly considered disease onset. G93A mice exhibit evidence of progressive motor weakness which first affects the hindlimbs. The mice become progressively less able to walk, eat, drink and groom themselves. Affected mice are frequently tremulous and commonly show muscle twitches as is the case in ALS patients in whom muscle

fasciculation is indicative of muscle denervation secondary to motor neuronal loss. Examination of the spinal cord of G93A mice confirms a progressive loss of motor neurons (Dal Canto and Gurney, 1994).

Left to their own devices the G93A mice used in this work typically die at ~140 days of age. On ethical grounds G93A transgenic mice not already used for experiments are euthanized when their condition becomes sufficiently severe that they cannot maintain an adequate intake of food or fluid or groom themselves. In our facility this point is defined by an animal's inability to get back on its feet after 5 seconds when placed on its side. This typically occurs at around 140 days of age. The usual lifespan of the non-transgenic littermates of G93A mice is around 810 days.

2.4.2 Advantages and disadvantages of G93A SOD1 transgenic mice as a model of human ALS

Advantages

- G93A SOD1 transgenic mice are born normal, undergo normal motor development then in adulthood develop relentlessly progressive motor weakness that leaves them unable to move, eat, drink or groom themselves. Premature death follows. In all of these respects G93A mice very accurately model the sequence of events occurring in patients with ALS. What is more, the underlying cause of disease is their expression of a human mutant SOD1 transgene known to cause ALS in humans.
- Despite overexpression of the mutant SOD1 transgene in every tissue of the G93A mouse model, just as is the case in human familial ALS, motor neurons are preferentially affected and their loss is responsible for the death of the animal (Gurney et al., 1994).
- Identification of pre-symptomatic G93A mice is possible by PCR of DNA obtained from ear clippings, enabling access to CNS tissue from animals at a stage when the earliest pathological events are occurring. This allows investigation of key cellular pathways contributing to disease onset and progression.
- G93A mice allow the study of motor neurons in the company of neighbouring neuronal and non-neuronal cells. This can be in the form of whole spinal cord homogenates or, even more physiologically, by the study of explanted organotypic slices in which motor neurons remain in situ.
- Crossing G93A SOD1 transgenic mice with other ALS-related transgenic mice has contributed to the understanding of disease pathogenesis in ALS. For example, by crossing the legs at odd angles (LOA) mice with SOD1 transgenic mice the effects of mutant SOD1 on axonal transport within neurons were demonstrated (Kieran et al., 2005).
- The G93A SOD1 transgenic model is a relatively economical whole-animal platform upon which to study the effects of potential therapeutic drugs for ALS. The accelerated disease course in the high overexpressor model shortens experimental time courses allowing faster throughput of therapeutic targets and reduced animal maintenance costs. There are important related disadvantages and will be discussed next.

Disadvantages

- Mutant SOD1 transgenic mouse models are a model of SOD1 familial ALS which represents only ~2% of all ALS in patients. This raises questions about how readily extrapolable findings in this model are to other, commoner, forms of ALS.
- The most commonly used G93A SOD1 transgenic mice (including those used in this work) overexpress the mutant human transgene many-fold, whereas patients with SOD1 fALS manifest disease as a result of only one copy of the mutant SOD1 gene. Given that G93A mutant SOD1 retains its superoxide dismutase function this introduces an important potential confounder.
- The organization of the motor system is significantly different in mice and in particular does not share the human arrangement of upper and lower motor neurons. As symptoms and signs attributable to the loss of upper motor neurons are often a prominent feature of ALS in humans the absence of this system in the G93A SOD1 transgenic mouse model is a weakness.
- Despite being a theoretically suitable model in which to test therapeutic drug candidates, the vast majority of drugs shown to have positive effects in these mice have failed to demonstrate similar effects in human trials (Choudry and Cudkowicz, 2005; Desnuelle et al., 2001; Drory and Gross, 2002; Klivenyi et al., 1999).
- The maintenance costs of transgenic mice colonies are significant when compared with those of cellular models of ALS.

2.4.3 Maintenance of SOD1 transgenic mice colonies

Colonies of both G93A SOD1 and WT SOD1 transgenic SOD1 mice and their respective non-transgenic littermates are maintained by the Field Laboratories of the University of Sheffield. Transgenic mice are identified by genotyping genomic DNA obtained from ear clips of 14 day old pups using PCR. Quantitative-PCR is then employed to confirm the copy-number of the WT or G93A SOD1 transgene to ensure that individual animals have not lost transgene copy-number.

CHEMICALS AND WORKING SOLUTIONS

All chemicals were purchased from Sigma, Poole, UK and all tissue culture plasticware was purchased from Greiner Bio-One Cellstar (Frickenhausen, Germany) unless otherwise stated. The constituents and method of preparation of working solutions are provided in the Working Solutions section (page 120).

2.5 HEK293 cells

2.5.1 HEK293 cell culture

HEK293 cells were grown in 5% CO_2 in an incubator with a humidified atmosphere at 37˚C (Incusafe™, Sanyo, Japan). The culture medium was DMEM supplemented with 10% fetal calf serum (FCS) (Biosera, East Sussex, UK) and 1% Penicillin-Streptomycin cocktail (see Section 2.20). When cells reached 80-95% confluency they were passaged. The medium was poured off and the cells released into suspension by incubating the flask at 37˚C for 5 min in 4 ml of EDTA-Trypsin solution (Section 2.20). Suspended cells were then added to 12 ml pre-warmed fresh DMEM supplemented with 10% FCS and 1% Penicillin-Streptomycin cocktail and 1/12th of the diluted cells were seeded back into a new T-75 culture flask containing 14 ml of fresh culture medium. The HEK293 cells were split twice a week and experiments were performed on cells between passages 7 and 12.

2.5.2 HEK293 cell harvest

For the purposes of Western blotting, HEK293 cells were harvested at 80-90% confluency. Culture medium was poured off and the cells were released into suspension by incubating them in 4 ml EDTA-Trypsin solution for 5 min at 37˚C. Suspended cells were pelleted down by centrifugation (Sigma 1-14K, DJB Labcare, UK) at 400 g for 5 min. The pellet was washed twice with sterile phosphate buffered saline (PBS) and spun down by centrifugation at 400 g for 5 min on each occasion. The PBS was then carefully poured off and the pellets transferred onto ice. The cell pellets were then resuspended in 75 µl per T-75 of ice-cold Buffer A (see Section 2.21) and were homogenized with 30 passes of a Kontes™ mini-homogenizer (Anachem, Bedfordshire, UK). The resultant homogenate was centrifuged at 3000 g for 6 min at 4˚C. The post-nuclear S1 supernatant was retained on ice. The remaining pellet was resuspended in 75 µl of Buffer A and homogenized again as above. The second homogenate was once again centrifuged at 3000 g for 6 min at 4˚C. The second, S2, supernatant obtained was pooled with the first S1 fraction. This combined S1 and S2 supernatant contained the cytosol and all cellular organelles apart from the nuclei. It was sonicated on ice at 6 µm for 10 short pulses using a probe sonicator (Soniprep 150, Sanyo, Japan) and was then centrifuged once more at 3000 g for 6 minutes at 4˚C. The final supernatant was aliquotted and stored at -20˚C.

2.6 Human fibroblasts

2.6.1 Human fibroblast culture

Monolayers of primary fibroblast cells were maintained in T-75 flasks with 20 ml of Ham's F-10 Media (Gibco, Paisley, Scotland, UK) supplemented with 10% FCS (Biosera, East Sussex, UK), 1% Penicillin-Streptomycin cocktail, 0.25% Holo-transferrin and 2.5 ng of epidermal growth factor per 500 ml of

Ham's media. Cells were maintained in 5% CO_2 in an incubator with a humidified atmosphere at 37˚C (Incusafe™, Sanyo, Japan).

Fibroblast cell lines generated from skin biopsies donated by three I113T SOD1-ALS patients, 3 TDP43-ALS patients and 4 control subjects, were used for experiments. Details are shown in Table 2.1 (see page 93). Control and patient fibroblasts were age- and sex-matched as closely as possible prior to being paired for experimental work (Table 2.2).

Pair number	Control (Age/Sex)	Patient (Age/Sex)
Pair 1	Control 11 (58/M)	Patient 28 (SOD1) (62/M)
Pair 2	Control 4 (55/M)	Dutch Patient (SOD1) (61/M)
Pair 3	Control 1 (45/M)	Patient 91 (SOD1) (62/M)
Pair 4	Control 8 (42/F)	Patient 48 (TDP-43) (43/F)
Pair 5	Control 11 (58/M)	Patient 51 (TDP-43) (66/M)
Pair 6	Control 4 (55/M)	Patient 55 (TDP-43) (60/M)

Table 2.2: *Table showing the pairs of control and patient fibroblasts used for experiments.*

When cultures reached 70-80% confluency, the medium was drawn off and the cells were washed with PBS (BioWhitaker, Lonza, Belgium) prior to being released into suspension by incubating the flask at 37˚C for 15 min in 4 ml of EDTA-Trypsin solution. The suspended cells were then diluted in 15ml complete fibroblast medium and 1/4th-1/6th of the diluted cells were seeded back into a new T-75 culture flask. Fibroblast cell lines were not used for experiments beyond passage 12 to ensure that when experiments were performed cells were in the proliferative phase of their growth curve and had not reached replicative senescence (Hutter et al., 2004).

2.6.2 Human fibroblast harvest

For the purposes of SDS PAGE preparatory to Western blotting, human fibroblasts were harvested at 60-70% confluency. Medium was poured off and cells were released into suspension by incubating them in 4 ml EDTA-Trypsin solution for 5 min at 37˚C. Suspended cells were pelleted down by centrifugation (Sigma 1-14K, DJB Labcare, UK) at 400 g for 5 min. The pellet was washed twice with sterile PBS and spun down each time by centrifugation at 400 g for 5 min. The PBS was then carefully poured off and the pellets placed on ice. The cell pellets were then resuspended in 75 µl per T-75 of ice-cold Buffer A (see Section 2.21) and were homogenized with 30 passes of a Kontes™ mini-homogenizer (Anachem, Bedfordshire, UK). The resultant homogenate was centrifuged at 3000 g for 6 min at 4˚C. The post-nuclear (S1) supernatant was retained on ice. The remaining pellet was resuspended in a further 75 µl of Buffer A and homogenized a second time as above. The resultant homogenate was once again centrifuged at 3000 g for 6 min at 4˚C. The second (S2) supernatant was

pooled with the first S1 fraction. This combined supernatant contained the cytosol and cellular organelles apart from the nuclei. It was sonicated on ice at 6 µm using 10 short pulses from a probe sonicator (Soniprep 150, Sanyo, Japan) and was then centrifuged one final time at 3000 g for 6 min at 4˚C. The final supernatant was aliquotted out and stored at -20˚C.

2.7 NSC34 motor neuronal cells

2.7.1 NSC34 cell culture

NSC34 cells were grown in 5% CO_2 in an incubator with a humidified atmosphere at 37˚C (Incusafe™, Sanyo, Japan). The culture medium was Dulbecco's Modified Eagle Medium (DMEM) supplemented with 10% FCS (Biosera, East Sussex, UK) and 1% Penicillin-Streptomycin cocktail. Six cell lines – non-transgenic (NTG), vector-only (pIRES), wild-type human SOD1 expressing cells (WT) and cells expressing one of three forms of mutant human SOD1 (H48Q, I113T and G93A) were cultured for experimental work. Selection of transfected cells (pIRES, WT, H48Q, I113T and G93A) was maintained using Geneticin® G418-sulphate (G418, Gibco, Paisley, Scotland, UK) at 250 µg/ml.

NSC34 cells were passaged twice a week by splitting. The splitting ratio ranged from 1 in 5 to 1 in 8 for mutant SOD1-expressing cells, and for the remaining cells from 1 in 8 to 1 in 10. Flasks were passaged at 60-75% confluency. The medium was drawn off and the cells were released into suspension by gently knocking them off in 10 ml fresh medium using a gentle jet of medium from the pipette to release more stubbornly adherent cells where needed. Knocked-off cells were carefully triturated before a proportion of cells (see above) were seeded back into a fresh T-75 culture flask containing 12 ml of fresh culture medium. Each of the six cell lines was allowed to grow for a minimum of 3 days before performing any experiment or splitting in order to allow them to develop their more motor neuronal phenotype (Cashman et al., 1992). Cells were not used for experiments beyond passage 40.

2.7.2 NSC34 cell harvest

For the purposes of Western blotting, 60-70% confluent flasks of NSC34 cells were harvested. The medium was drawn off and the cells were released into suspension by knocking them off in 10 ml fresh medium at room temperature. Suspended cells were pelleted down by centrifugation (Sigma 1-14K, DJB Labcare, UK) at 400 g for 5 min. The pellet was washed twice with sterile PBS and spun down by centrifugation at 400 g for 5 min. The PBS was then carefully poured off and the pellets transferred onto ice. The cell pellets were then resuspended in ice-cold Buffer A (75 µl per T-75) and homogenized with 30 passes of a Kontes™ mini-homogenizer (Anachem, Bedfordshire, UK). The resultant homogenate was centrifuged at 3000 g for 6 min at 4˚C. The post-nuclear S1 supernatant was retained on ice. The remaining pellet was resuspended in 75 µl of Buffer A and homogenized again as above. The second homogenate was centrifuged at 3000 g for 6 min at 4˚C. The second (S2) supernatant obtained was then pooled with the first S1 fraction. The combined supernatant contained

the cytosol and cell organelles apart from the nuclei. It was sonicated on ice at 6 µm for 10 short pulses using a probe sonicator (Soniprep 150, Sanyo, Japan) and was centrifuged one final time at 3000 g for 6 min at 4˚C. The final supernatant was aliquotted out and stored at -20˚C.

2.8 Freezing down of cultured cells

NSC34 motor neuronal cells, human fibroblasts and HEK293 cells were frozen down using the same basic method with small cell-line specific modifications described below. T-75 flasks of 60% confluent cells were frozen down as single vials. The medium was drawn off and the cells were released into suspension. In the case of NSC34 cells this was done by knocking them off into fresh medium. In the case of HEK293 cells and human fibroblasts, cells were released into suspension by incubating them in 4 ml EDTA-Trypsin solution for 5-10 min at 37˚C. Suspended cells were harvested by centrifugation at 400 g for 5 min. The cell pellet was then resuspended in 0.5-1.0 ml of sterile-filtered 10 % Dimethyl Sulphoxide (DMSO) made up in sterile FCS and transferred to a sterile 1 ml Nalgene cryovial (Nalge Nunc International, Rochester, USA). The cryovials were then placed in a Nalgene freezer box containing isopropanol in a -80˚C freezer allowing regulated freezing of cells at the rate of -1˚C/min. Once frozen, the vials were transferred to liquid nitrogen dewars where they were stored at -196˚C.

2.9 Resuscitation of cultured cells

Frozen NSC34 and HEK293 cells stored in sterile 1 ml sealed Nalgene cryovials were quickly defrosted under hot tap water before being seeded in T-75 culture flasks containing DMEM supplemented with 10% FCS and 1% Penicillin-Streptomycin cocktail (see Section 2.20) pre-warmed to 37˚C. Frozen human fibroblast cells were resuscitated in a similar way before seeding into flasks containing pre-warmed complete fibroblast culture medium. For all cell lines, the culture medium was changed the following day and the cells were allowed to grow on.

2.10 Mycoplasma testing of cultured cells

Regular testing for Mycoplasma infection was carried out in all cultured cell lines. Cell lines were initially tested for mycoplasma infection two passages after resuscitation and thereafter were tested once every 6 weeks. All mycoplasma testing was carried out by our senior laboratory research technician, Mrs Kim Crewe, who tested samples using a Lonza MycoAlert Mycoplasma detection kit (Lonza, Basel, Switzerland) according to the manufacturer's protocol.

EXPERIMENTAL DESIGN AND METHODS – CULTURED CELLS

2.11 Work-up of antibodies in HEK293 cells

In order to work-up antibodies to be used in human fibroblasts, whole cell preparations of HEK293 cells grown under basal culture conditions were made. HEK293 cells were plated in T-75 tissue culture

flasks (Section 2.5.1) and were grown to 80-90% confluency. The medium was drawn off, the cells were harvested and whole cell preparations made as described in Section 2.5.2. These preparations were Western blotted (see Section 2.18) for Prx 2, Prx 3, $PrxSO_{2/3}$, total 2-cys Prxs, sestrin 2, tubulin and actin. Antibody concentrations and incubation conditions were optimized for each protein species. The concentrations and incubation conditions settled on for use in the human fibroblasts are given in Table 2.3 (see page 118).

2.12 Work-up of oxidative stress experiments in HEK293 cells

2.12.1 HEK293 cells: Oxidative stress experiment work-up

Two T-75 culture flasks were seeded with HEK293 cells which were allowed to grow in parallel until they reached 80-90% confluency. To induce overoxidation of peroxiredoxins, the HEK293 cells in one flask were stressed by exposure to hydrogen peroxide (H_2O_2) 600 μM for 6 hours (STR). The other flask was used as a non-stressed control (NS). The medium was drawn off from both flasks and replaced by complete growth medium containing 600 μM H_2O_2 in the STR flask. Cells in the NS flask received only a media change. Both flasks were then incubated for 6 hours at 37˚C before being harvested and whole cell preparations made (Section 2.5.2) for Western blotting. Western blotting (see Section 2.18) of the samples was then performed for overoxidized Prxs, total 2-cys Prxs and tubulin (used as a loading control), in duplicate for each of two independent experiments. Protein loads were 20 μg per lane.

2.12.2 HEK293 cells: Stress-recovery experiment work-up

HEK293 cells were plated in ten Petri dishes (10 cm) and grown up in parallel to reach 80-90% confluency. The medium was removed from all ten. In five, designated the stressed cells (STR), it was replaced by medium containing 600 μM H_2O_2. The remaining five dishes of non-stressed (NS) control cells received a media change only. Cells were then placed in the 37˚C incubator for an hour. After one hour the medium containing H_2O_2 was removed from the STR dishes and replaced with DMEM supplemented with 10% FCS and 1% Penicillin-Streptomycin cocktail. The NS dishes also received a second media change. All 10 Petri dishes were then replaced in the 37˚C incubator. One petri dish each of NS and STR cells were harvested after 1, 3, 5, 7 and 9 hours as described in Section 2.5.2 in preparation for Western blotting (Section 2.18). Two independent experiments were performed and the samples Western blotted in duplicate for overoxidized Prxs, sestrin 2, tubulin and actin. Protein loads were 20 μg per lane.

2.13 Human fibroblasts – basal culture preparations

In order to determine whether there was a difference in the levels of the 2-cys Prxs or their regenerators in patient fibroblasts compared to controls grown under basal culture conditions, whole cell preparations were made from control and patient fibroblasts grown up in parallel. Experiments were carried out on 3 pairs of human fibroblasts (3 pairs of I113T SOD1-ALS fibroblasts age- and sex-matched with fibroblasts from healthy controls – Pairs 1-3 in Table 2.2). For each experiment one T-

175 flask each of patient and control cells were seeded and allowed to reach 80% confluency prior to harvest. Control and patient flasks were harvested in parallel as described in Section 2.6.2 and whole cell preparations made for Western blotting. Three independent experiments were performed in each of the three pairs of fibroblasts. Samples from each experiment were Western blotted (see Section 2.18) in triplicate for Prx 2, Prx 3, $PrxSO_{2/3}$, total 2-cys Prxs, sulfiredoxin 1 and sestrin 2. Tubulin and actin were used as loading controls as appropriate. Protein loads were 20 μg per lane except for the sulfiredoxin 1 blots for which 40 μg of protein was loaded per lane.

2.14 Stressing human fibroblasts with hydrogen peroxide

Initially, oxidative stress experiments conducted on human fibroblasts were performed using 300 μM H_2O_2 for 15 min. This concentration of H_2O_2 was selected based on the antibody work-up experiments conducted in HEK293 cells and on the literature (Moon et al., 2005; Woo et al., 2003). Western blotting from these experiments showed no differences in the levels of overoxidized Prxs between stressed patient and control cells (see Chapter 3, Section 3.3). We suspected that exposure to 300 μM H_2O_2 for 15 min may have overoxidized the 2-cys Prxs present in the cells to saturation. A stress titration experiment was therefore performed (see Section 2.14.1).

2.14.1 Human fibroblasts: Stress-titration experiment

In order to establish at what concentration of H_2O_2 the 2-cys Prxs became overoxidized to saturation and what concentration would constitute a non-saturating oxidative stress, patient fibroblasts were exposed to various concentrations of H_2O_2 for 15 min. Cells were then harvested and whole cell preparations made for Western blotting for $PrxSO_{2/3}$. Patient fibroblasts were seeded into twelve T-175 culture flasks and were grown until they reached 80% confluency. The medium was discarded and replaced by the same volume of fresh medium containing the desired concentration of H_2O_2. To induce overoxidation of 2-cys Prxs, each of eleven flasks was exposed for 15 min to one of the following concentrations of H_2O_2: 10 μM, 20 μM, 30 μM, 40 μM, 50 μM, 60 μM, 70 μM, 80 μM, 100 μM, 200 μM and 300 μM. The remaining, twelfth, flask received only a medium change, serving as a non-stressed control. After 15 min the H_2O_2-containing medium was removed and replaced by fresh medium. The non-stressed control flask also received a medium change. The cells were then harvested as described in Section 2.6.2 and whole cell preparations made. Two independent experiments were performed and the samples Western blotted (see Section 2.18) in duplicate for $PrxSO_{2/3}$ as well as for tubulin. Protein loads were 20 μg per lane. As a result of these experiments (see Chapter 3, Sections 3.4 and 3.5) exposure of fibroblasts to 30 μM H_2O_2 for 15 min was established as an oxidative stress that would not overoxidize 2-cys Prxs to saturation.

2.14.2 Human fibroblasts: Oxidative stress experiments

Oxidative stress experiments were carried out in 3 pairs of human fibroblasts as shown in Table 2.2 (Pairs 1-3 of I113T SOD1-ALS fibroblasts *vs* fibroblasts from age- and sex-matched healthy controls).

For each pair, healthy control and patient fibroblasts were seeded into two T-175 culture flasks each and grown up in parallel until they reached 80% confluency. To induce overoxidation of 2-cys Prxs, the fibroblasts in one healthy control and one patient flask were exposed to 300 μM H_2O_2 for 15 min, a saturating oxidative stress. These were the stressed (STR) cells. The other two flasks, one each of healthy control fibroblasts and patient fibroblasts, were not exposed to H_2O_2 but instead had their medium changed. These were the non-stressed control flasks (NS). After 15 min all four flasks underwent a second medium change and the cells were harvested as described in Section 2.6.2. This experiment was then repeated in exactly the same way but using 30 μM H_2O_2, a non-saturating oxidative stress. Three independent experiments were performed in each case and the whole cell preparations generated from each experiment were then Western blotted (see Section 2.18) in triplicate for overoxidized Prxs, total 2-cys Prxs and tubulin. Protein loads were 20 μg per lane.

2.14.3 Human fibroblasts: Stress-recovery experiments

Fibroblast set-up

Stress-recovery experiments were carried out in Pairs 1-3 of I113T SOD1-ALS fibroblasts and controls and a second set of experiments carried out in Pairs 4-6 of TDP43-ALS fibroblasts and controls as shown in Table 2.2. One pair of fibroblasts (patient and matched healthy control) was used in each experiment and a total of 3 separate experiments were carried out in each set. For each experiment healthy control and patient fibroblasts were seeded into two T-175 culture flasks each (4 flasks per pair) and the cells grown up in parallel until they reached 80-90% confluency.

Stress-recovery experiments

The culture medium was removed from each of the 4 flasks per pair then the cells released into suspension by incubating them in 4 ml per flask of EDTA-Trypsin solution for 5 min at 37°C. The resuspended cells were centrifuged at 400 g for 5 min at room temperature (Sigma 1-14K, DJB Labcare, UK) and each of the cell pellets separately resuspended in 10 ml of complete fibroblast medium. Both flasks-worth of healthy control fibroblasts were pooled together and then seeded into sixteen T-75 culture flasks. The same was done for both flasks-worth of patient fibroblasts. Care was taken to seed the cells in equal divisions. The 32 T-75 flasks generated for each stress-recovery experiment were then grown up in parallel until they reached 70% confluency.

In 15 of the 16 flasks of both healthy control and patient fibroblasts 2-cys Prxs were overoxidized to saturation with H_2O_2 (STR) while in the remaining two flasks, one each of healthy control fibroblasts and patient fibroblasts were not exposed to H_2O_2 (NS). The H_2O_2 was then washed out and the cells allowed to recover with samples taken at various time-points.

In order to achieve this, the culture medium was first removed from the 30 flasks to be stressed and replaced with the same volume of medium containing 300 μM H_2O_2. After 15 min in the incubator the H_2O_2-containing medium in each of the 30 stressed flasks was poured off and replaced by fibroblast

culture medium. The remaining two flasks – one each of healthy control and patient cells were not exposed to H_2O_2 (NS) but had their culture medium changed in parallel with the STR flasks. All 32 flasks were then replaced in the incubator. One flask each of stressed patient and healthy control fibroblasts (STR) was harvested as described previously (Section 2.6.2) at the following experimental time points (hours after H_2O_2 washout): 0, 0.5, 1.0, 1.5, 2.0, 2.5, 3.0, 3.5, 4.0, 5.0, 6.0, 8.0, 9.0, 12.0 and 26.0. The two unstressed (NS) flasks (one each of healthy control and patient cells) were harvested immediately after the first medium change at 0 hours.

Three independent experiments were performed in each of the 3 pairs of fibroblasts for each set of experiments. Samples from each experiment were Western blotted (see Section 2.18) in triplicate. Preparations from SOD1 *vs* control fibroblast pairs were Western blotted for overoxidized Prxs, sulfiredoxin 1, sestrin 2, activator protein-1, total 2-cys Prxs along with tubulin or actin which were used as loading controls. Preparations from TDP43 *vs* control fibroblast pairs were Western blotted for overoxidized Prxs and tubulin. Protein loads were 20 μg per lane except for sulfiredoxin 1 blots where 40 μg of protein was loaded per lane.

Pre-treatment with Cycloheximide

To determine whether recovery of overoxidized Prxs was dependent upon new protein synthesis, stress-recovery experiments in I113T SOD1 fibroblasts (Pairs 1-3, Table 2.2) were repeated after pre-treatment of the cells with Cycloheximide (CHX) a known blocker of protein translation (Obrig et al., 1971).

The experiments were set-up in essentially the same manner as the originals (see Section 2.14.3) but with an additional complete set of 32 flasks of fibroblasts (16 patient, 16 control) grown in parallel. One set of 32 flasks was pre-treated with Cycloheximide before the experiment was started, the other set was not. The medium was removed from cells in the set of 32 T-75 flasks to be CHX-treated and replaced with medium containing CHX (0.5 μg/ml) (Kim et al., 2010). The cells were placed back in the incubator for 1 hour. After CHX treatment, the medium was changed and the cells used for a stress-recovery experiment as already described. The second set of fibroblasts that were not pre-treated with CHX were used as controls for this experiment. One experiment was performed in each of the three pairs of fibroblasts, whole cell preparations were made and Western blotted (see Section 2.18) in duplicate for overoxidized Prxs and tubulin. Protein loads were 20 μg per lane.

2.14.4 Human fibroblasts: Two-hit stress-recovery experiments

Fibroblast set-up

Two-hit stress-recovery experiments were carried out in Pairs 1-3 of control and I113T SOD1-ALS patient fibroblasts as shown in Table 2.2. The aim of the experiment was to determine the response of healthy control and SOD1-ALS patient fibroblasts to sequential oxidative challenge by exposing them

twice to a non-saturating oxidative stress (30 μM H_2O_2 for 15 min). The second stress was applied only after overoxidized Prxs could no longer be detected, 16 hours after washout of the first H_2O_2.

Each pair of healthy control and patient fibroblasts were first seeded into three T-175 culture flasks per cell line and the cells grown up in parallel until they reached 80-90% confluency. Cells from each of the three T-175 flasks per cell line were then released separately into suspension by incubating them in 4 ml of EDTA-Trypsin solution for 5 min at 37˚C. The resuspended cells were centrifuged at 400 g for 5 min at room temperature and each cell pellet resuspended in 10 ml of complete fibroblast medium. The three flasks-worth of cells per cell line were then pooled together and seeded into 16 T-75 culture flasks per line. Care was taken to seed the cells in equal divisions. The 32 T-75 flasks generated for each stress-recovery experiment were then grown up in parallel until they reached 70% confluency.

Two-hit stress-recovery experiments

In this experiment, 14 of the 16 flasks of healthy control and patient fibroblasts were exposed to a non-saturating oxidative stress of 30 μM H_2O_2 for 15 min (STR). The medium from each of the 14 flasks was removed and replaced by medium containing H_2O_2 at 30 μM. The remaining four flasks – two flasks each of healthy control and patient cells received only a media change (NS). All flasks were then placed in the 37˚C incubator for 15 min. The H_2O_2-containing medium was then poured off the 28 STR flasks and replaced with fresh media before the cells were replaced in the 37˚C incubator and allowed to recover. The four NS flasks received a second media change. One flask each of STR patient and healthy control fibroblasts was then harvested (see Section 2.6.2) at the following experimental time points: t = 0, 2, 5, 8, 10, 12 and 16 hours after H_2O_2 -washout. One flask each of NS healthy control and patient cells were harvested at 0 hours to serve as a basal control for the first exposure.

After the two t = 16 hr time point flasks had been harvested, 7 of the remaining 8 flasks each of healthy control and patient fibroblasts were exposed to a second, identical, non-saturating oxidative challenge. These 7 flasks were exposed for a second time to 30 μM H_2O_2 for 15 min. The remaining two flasks – one each of healthy control and patient cells were not stressed (NS) and received only a media change (their third since the beginning of the experiment). All flasks were then replaced in the 37˚C incubator for 15 min. The H_2O_2-containing media was then poured off the STR flasks and replaced with fresh media and the cells replaced in the 37˚C incubator to recover. The two remaining NS flasks, one each of healthy control and patient cells received a media change. One flask each of stressed patient and healthy control fibroblasts (STR) were then harvested as described in Section 2.13 at t_2 = 0, 2, 5, 8, 12, 24 and 30 hours after the second H_2O_2 washout. The two flasks containing the remaining unstressed (NS) healthy control and patient cells were harvested immediately after their fourth media change (t_2 = 0 hours) to serve as basal controls for the second exposure.

Three independent experiments were performed in each of the 3 pairs of fibroblasts. Whole cell preparations from each experiment were Western blotted (see Section 2.18) in triplicate for overoxidized Prxs and tubulin. Protein loads were 20 μg per lane.

2.15 NSC34 cells – basal culture preparations

Whole cell preparations of the 6 NSC34 cell lines grown under basal culture conditions were investigated to determine whether the presence of mutant human SOD1 altered levels of the 2-cys Prxs and their related proteins. For each experiment, one T-75 flask was cultured per each cell line. All cell lines were grown in parallel until they reached 70% confluency. The 6 flasks were then harvested and whole cell preparations made for Western blotting (Sections 2.2.6 and 2.18 respectively). Three independent experiments were performed. All cells were between passages 11 and 15. Samples were Western blotted in triplicate for Prx 2, Prx 3, $PrxSO_{2/3}$, sulfiredoxin 1, sestrin 2 and Thioredoxin-interacting protein (Txnip) for each independent experiment.

2.15.1Trouble-shooting inter-experiment variability in $PrxSO_{2/3}$ levels within NSC34 cell lines

In an effort to resolve the persistently variable levels of $PrxSO_{2/3}$ and Srx 1 observed experiment to experiment within individual NCS34 cell lines grown under basal culture conditions (see Chapter 4) these experiments were repeated in three more preparations per cell line after a few weeks' delay when the cell lines were at higher passages and better established in culture.

Additional precautions were taken with the cells to be used for the repeat experiments which were between passages 30 and 35 at the time of harvest. The cells were screened for mycoplasma infection every 4 passages to ensure that this did not lie behind the inter-experimental variability. The expression level of human SOD1, the stably-transfected transgene present in the WT, H48Q, I113T and G93A transfected lines, was measured by Western blotting every 4 passages to make sure that expression of the transgene was not changing. Particular care was taken to make sure that cell culture, cell-splitting and cell harvest was consistent both between cell lines and between experiments. Experiments were performed on preparations made after exactly 3 days in culture and around the same time of the day to reduce any effect of circadian rhythms (O'Neill and Reddy, 2011). The NSC34 cells were harvested and whole cell preparations made for Western blotting for $PrxSO_{2/3}$ as before. Triplicate blots of each experiment were made. For all Western blots of NSC34 cells grown under basal conditions, protein loads were 20 μg per lane, increased to 40 μg per lane for sulfiredoxin 1 blots. Tubulin and actin were used as loading controls as appropriate.

2.16 Stressing NSC34 cells with hydrogen peroxide

2.16.1 General principles

All 6 NSC34 cell lines (NTG, vector-only pIRES, WT, H48Q, I113T and G93A) were grown in parallel in T-75 culture flasks for Western blotting. Given the difficulties experienced in obtaining a consistent read-out from NSC34 cells grown under basal culture conditions, cell lines to be used in any given

experiment were harvested at the same time. As previously, care was taken to maintain consistency of handling between cell lines during cell culture and harvest. Prior to immunoblotting for proteins of interest, each of the preparations was first immunoblotted for SOD1 to confirm comparable expression of the human transgene where relevant. Non-transgenic (NTG), vector-only (pIRES) and WT-SOD1 (WT) cell lines were considered controls (Fig 2.3). When comparing expression levels of proteins of interest, the chief comparison of interest was considered to be that between cells expressing the various species of mutant SOD1 and those expressing WT SOD1.

2.16.2 NSC34 cells: Oxidative stress experiments

In order to determine whether exposure to H_2O_2 had different effects on the oxidation state of the typical 2-cys Prxs in NSC34 cells stably transfected with different forms of human SOD1, two control cell lines (NTG, pIRES), a wild-type SOD1 expressing cell line (WT), and a G93A mutant SOD1 expressing cell line (G93A) were investigated. Two T-75 culture flasks per cell line were seeded and grown up in parallel until they reached 60-75% confluency. To induce overoxidation of 2-cys peroxiredoxins, the NSC34 cells in one set of flasks (one flask each of NTG, pIRES, WT and G93A) were exposed to 300 μM H_2O_2 for 15 min (STR). The other flask of each cell line was used as a non-stressed control (NS). The medium was first drawn off from both flasks of each cell line and replaced by complete growth medium containing 300 μM H_2O_2 in the STR flasks while cells in the NS flask received a media change only. Both flasks from each cell line were then incubated for 15 min at 37˚C before harvest (Section 2.7.2) and preparation of whole cell lysates for Western blotting (Section 2.18). Three independent experiments were carried out and the samples obtained were immunoblotted in triplicate for overoxidized 2-cys Prxs and tubulin (loading control). Protein loads were 20 μg per lane.

EXPERIMENTAL DESIGN AND METHODS - SOD1 TRANSGENIC MICE

2.17 G93A SOD1 transgenic mice experiments

In order to establish whether levels of overoxidized 2-cys peroxiredoxins and their regenerators were different in G93A SOD1 transgenic mice compared to their non-transgenic littermates, whole spinal cord and brain homogenates were prepared (see Sections 2.17.2, 2.17.3 & 2.17.5) and blotted for $PrxSO_{2/3}$, Prx 2, Prx 3, sulfiredoxin 1 and sestrin 2. Tubulin and actin were used as loading controls as appropriate. Pairs comprising a G93A mouse and a NTG littermate of the same sex were sacrificed at 60 days of age, 90 days of age and 120 days of age. These ages were selected to represent onset, symptomatic and late-stage G93A mice (Ferraiuolo et al., 2007; Gurney et al., 1994). WT SOD1 overexpressing mice were to be examined subsequently were a difference in the amount of $PrxSO_{2/3}$ between G93A and NTG homogenates identified.

2.17.1 Sacrifice of mice with sucrose perfusion

Littermate pairs of NTG and G93A mice were sacrificed together with sucrose perfusion at 60, 90 and 120 days of age as needed. The brain and spinal cord were dissected out and whole brain and whole spinal cord homogenates prepared. Terminal anaesthesia and sucrose perfusion was performed by Dr. Richard Mead on my behalf. I performed the remainder of the tissue dissection and extraction. For each experiment, samples from three pairs of sex-matched G93A transgenic and NTG littermate mice of 60, 90 and 120 days of age were used i.e., a total of six mice of each age per experiment.

The mice were killed by terminal anaesthesia using sodium pentobarbital (JM Loveridge Ltd., UK). Mice were injected intravenously with 50 mg/kg sodium pentobarbital. The tail of each anaesthetized mouse was pinched and the absence of any reaction ensured before proceeding further. The thorax was then opened using sharp scissors until the heart was accessible. The heart was perfused with 30% (w/v) sucrose in 1 M PBS by piercing the left ventricle with a 25 g (orange) needle (Medisupplies, Dorset, UK) attached to a 30 ml syringe. The right atrium was then opened using small scissors and 20-25 ml of the same PBS/sucrose solution injected.

2.17.2 Harvest of mouse brain for Western blotting

Mouse brains were extracted by first cutting away the skin over the skull until bone was clearly visible. A small cut, using small sharp scissors, was made through the posterior skull in order to open up the occipital bone as far as the origin of the sagittal suture. The skull was then carefully removed with round-tipped tweezers piece by piece, being careful not to damage the underlying brain. When the brain was totally accessible, it was removed from the cranial cavity using curved tweezers. Dissected brains were placed in labelled, sterile eppendorfs (Eppendorf, Hamburg, Germany) and immediately snap-frozen in liquid nitrogen. Frozen mouse brains were stored at -80˚C until required.

2.17.3 Harvest of mouse spinal cord for Western blotting

After removal of the brain, each mouse was laid on its front and the skin removed from its back using tweezers and fine forceps to expose the spinal column from cervical to lumbar spine. Snips were then made with a pair of small, sharp scissors just behind the head and above the pelvic bones to expose the ends of the spinal cord as it lay within the spinal column. The tip of a 10 ml syringe containing ice-cold PBS solution was inserted firmly but gently into the bottom end of the bony spinal canal. PBS was then injected until the spinal cord emerged at the cervical end of the spinal column. The squirted-out cord was carefully placed in a sterile, labelled 1ml cryovial (Nalgene Nunc International, Rochester, USA) then immediately snap-frozen in liquid nitrogen. Frozen spinal cords were stored at -80˚C until required.

2.17.4 Harvest of mouse brain and spinal cord from previously banked samples

Brain and spinal cord from unallocated G93A mice, WT mice and their respective NTG littermates were routinely dissected out and banked as they became available by members of the Academic

Neurology Unit for general use. Central nervous system tissue was subdivided into cerebellum, brain stem, upper spinal cord, lower spinal cord, posterior cortex and anterior cortex and was extracted from mice of varying ages. Samples were snap-frozen in liquid nitrogen prior to being stored in 1 ml cryovials (Nalgene Nunc International, Rochester, USA) at -80˚C. For my experiments I pooled the subdivided portions of each individual animal's brain, using the pooled brain tissue as a whole brain sample. Similarly, I pooled the upper and lower spinal cord portions obtained from each individual animal and used the pooled cord tissue as whole spinal cord for my experiments. The exact method of dissection employed for this material is unknown and is likely to have differed according to the member of staff who performed the dissection. The post-mortem delay before freezing is also unknown for these mice. The likely variability in post-mortem delay and possibly also dissection method between individual mice was less than ideal. At the time I used these samples, mice of appropriate ages were not available in the colony. Previously banked material was therefore used in the knowledge of its limitations and for preliminary investigations into levels of overoxidized Prxs in mouse CNS tissue pending availability of animals of the appropriate ages from the colony for sacrifice according to the methods described in Sections 2.17.2 and 2.17.3.

2.17.5 Preparation of whole cell lysates from mouse CNS tissue

Whole cell lysates from snap-frozen murine CNS tissue were prepared for Western blotting. Snap-frozen mouse brain and mouse cord were prepared in the same way. Samples were removed from the -80˚C freezer, immediately weighed, and were then allowed to soften by placing at -20˚C for an hour. Softened tissue was then chopped into small pieces using a sterile scalpel blade (Swann Morton, Sheffield, UK) and transferred to a 7 ml Dounce™ (Wheaton, Millville, USA) tissue grinder. Ten volumes (volume equal to 10 times the weight of the tissue to be homogenized) of ice-cold 0.25 M Sucrose/Buffer A (see Section 2.21) was added to the tissue pieces. The tissue was homogenized in two phases, first by 15 passes of the loose-fitting pestle and then by 15 passes of the tight-fitting pestle. The resulting homogenate was centrifuged at 600 g for 5 min at 4˚C (Sigma 1-14K, DJB Labcare, UK) and the post-nuclear supernatant was retained. This supernatant was then sonicated on ice using a probe sonicator (Soniprep 150, Sanyo, Japan) to deliver 10 brief pulses at 6 µm before aliquotting and snap freezing in liquid nitrogen. The aliquotted samples were stored at -20˚C until needed.

2.17.6 N-Ethylmaleimide (NEM)-perfused mouse CNS tissue

Thiol-blocking reagents such as N-ethylmaleimide (NEM) block the oxidation of thiol groups by covalently binding free cysteine residues (Cox et al., 2009). In order to analyze the relative abundance of the dimerized form of each of the 2-cys Prxs (the physiologically oxidized form – see Fig. 1.3 in Section 1.13.1 of Chapter 1) relative to the reduced, monomeric form of the same 2-cys Prx (Kumar et al., 2009) in murine CNS tissue by Western blotting, anaesthetized mice were perfused with NEM before brain and spinal cord harvest as described below.

Sacrifice and harvesting of NEM-perfused mouse CNS tissue

Three pairs of G93A-SOD1 mice and their NTG littermates (Pair 1 = 100 days of age, Pair 2 = 105 days, Pair 3 = 107 days) were sacrificed using the modified protocol below and whole brain and spinal cord harvested and used for experiments. CNS tissues were carefully extracted as already described after perfusion of the anaesthetized mice with NEM-perfusion solution (Section 2.24). All procedures involving NEM were carried out in a fume hood and additional protective eye wear and gas masks were worn. As previously the terminal anaesthesia and perfusion of the mice was performed by Dr. Richard Mead on my behalf and I carried out the remainder of the dissection and tissue extraction. This was done exactly as in Section 2.17.1 above until the perfusion step was reached. The anaesthetized mice were first placed in a fume hood before the thorax was opened until the heart was totally accessible. The left ventricle and right atrium of the heart were perfused as before but this time using NEM-perfusion solution rather than sucrose-perfusion solution (see Section 2.24). The brain and spinal cord were harvested from the mice exactly as described in Sections 2.17.2 and 2.17.3 but the procedures were carried out in a fume hood wearing a protective mask and eye-wear.

Preparation of whole cell lysates from NEM-perfused mouse CNS tissue

Whole cell lysates of NEM-perfused, snap-frozen NTG and G93A mutant SOD1-overexpressing mouse CNS samples were prepared exactly as in Section 2.17.5 until the homogenization step was reached. Once the defrosting tissue had been added to the Dounce tissue homogenization tube the set-up was transferred to a fume hood and ten volumes (volume equal 10 times the weight of tissue) of NEM homogenisation buffer (see Section 2.24) was added to the tissue pieces. The tissue was homogenized in two phases, first by 15 passes of the loose-fitting pestle and then by 15 passes of the tight-fitting pestle. The resulting homogenate was centrifuged at 600 g for 5 min at 4˚C (Sigma 1-14K, DJB Labcare, UK) and the post-nuclear supernatant was retained.

CHAPS 25 % (w/v) (3-[(3-cholamidopropyl) dimethylammonio]-2-hydroxy-1-propanesulfonate) solution, 600 µl, (Section 2.24) was then added to the supernatant and the sample vortexed for 10 s to aid solubilization. The samples were left at room temperature (within the fume hood) for 20-30 min for solubilization to occur and were vortexed for 10 s every 5 min. The samples were then aliquotted and stored at -20˚C until needed.

QUANTIFICATION OF PROTEINS OF INTEREST

2.18 Western blotting

2.18.1 Protein estimation, sample preparation and protein loading for Western blotting

Preparatory to Western blotting the protein concentration of cell lysates obtained from cell culture and from homogenization of murine CNS tissue was estimated using a Bradford Assay as per the

manufacturer's instructions (Pierce, Rockford, USA) (Bradford, 1976; Stoscheck, 1990). In general, 10-40 µg of protein was loaded per lane for Western blotting, the precise protein load varying with the protein of interest and nature of the sample (exact protein loads are provided in the accounts of individual experiments). However, in the case of mouse brain or spinal cord homogenates blotted for $PrxSO_{2/3}$, higher loads such as 80, 100 or even 120 µg of protein per lane were used.

In most cases prior to electrophoresis, samples were denatured in 1x Laemmli sample buffer (LSB, see Section 2.22), containing 5 % (v/v) β-mercaptoethanol, by boiling at 100˚C for 5 min in a heated block (Fisher Scientific, Loughborough, UK) (Kurien and Scofield, 2006). In the case of NEM-perfused mouse CNS tissues, samples were prepared in 1x non-reducing sample buffer containing no β-mercaptoethanol (Section 2.22) and were heated in a heat block (Fisher Scientific, Loughborough, UK) at 70˚C for 2-3 minutes. Following denaturation, samples were placed on ice for 1-2 min before being centrifuged gently (~600 g for 30 s) (ThermoFisher, Surrey, UK) to avoid loss of sample.

2.18.2 Sodium dodecyl sulphate polyacrylamide gel electrophoresis (SDS PAGE)

Protein electrophoresis was carried out in a Biorad (Hercules, California, USA) Mini-PROTEAN™ system which was assembled as per the manufacturer's instructions. Briefly, two gels at a time were poured using the gel-casting rig. The gel-casting plates were first inserted into plate-clamps and clamped together. One pair of clamped plates was then fixed onto each side of the gel-casting rig, using the spring clip on the rig. Care was taken to fix the plates tightly to prevent leaking. Fifteen percent polyacrylamide gels were used for protein separation unless otherwise stated whilst 5% polyacrylamide was used for the stacking gels.

In order to prepare 15 ml of 15 % polyacrylamide gel solution, enough for 2 resolving gels of 1.5 mm thickness, 3.8 ml water, 7.5 ml 30 % acrylamine-bis acrylamide solution (Protogel™ (37:5:1) solution, National Diagnostics, Geneflow, Staffordshire, UK), 3.8 ml of 4X resolving gel buffer pH 8.8 (see Section 2.22) and 150 µl 10 % SDS were added together. Just before the gels were poured 150 µl of 10 % ammonium persulfate (APS) and 10 µl of N,N,N',N'-tetramethylethylenediamine (TEMED) were added to the gel solution which was carefully mixed by inversion without introducing air bubbles. Once the gels were poured, approximately 200 µl of water-saturated butanol was overlaid on top of each resolving gel to prevent uneven oxidation (Kurien and Scofield, 2006). Once the gel had set, (approximately 25 min), the water-saturated butanol was discarded and the top of the gel was washed twice with 200 µl of deionized water. In order to make enough stacking gel for 2 gels, 8 ml of 5% stacking gel solution was prepared by adding 4.5 ml water, 1.3 ml 30 % acrylamine-bis acrylamide solution, 2 ml of 4X stacking gel buffer, pH 6.8, (Section 2.22) and 80 µl of 10 % SDS. Just before the stacking gel was required, 80 µl of 10 % APS and 8 µl of TEMED were added to the stacking gel solution which was carefully mixed by inversion. The stacking gel solution was then carefully pipetted over the top of the already set resolving gel and the relevant comb inserted. Gels were left for 20 min to set. Gels not required immediately were wrapped in tissue roll (Wypall, Kimberly-Clark, Kent, UK)

soaked in deionized water and covered in cling film (Caterwrap). The wrapped gels were then stored at 4˚C until required.

Samples for SDS PAGE were then carefully loaded into the wells using gel-loading tips (Anachem, Bedfordshire, UK). On most occasions 5 µl of biotinylated molecular weight standards and 2 µl of prestained All Blue™ (Biorad, California, USA) molecular weight standards were also loaded (one per lane) onto the gel in addition to the samples. Samples were initially electrophoresed at 70 V (constant voltage) for 45 min to allow stacking of proteins at the stacking gel/resolving gel interface. The voltage was then increased to 150 V for 1 to 1.5 hours to resolve the proteins. On most occasions the run was stopped when the dye front approached the bottom of the gel.

2.18.3 Transfer of protein from gel to polyvinylidene fluoride (PVDF) membrane

Resolved proteins were electro-blotted from the gels onto Immobilon™ PVDF membrane (Millipore, Massachusetts, USA) (LeGendre, 1990) using the Biorad Mini Trans-blot™ electrophoretic transfer cell system (Hercules, California, USA). The PVDF membrane was cut to size, soaked in 100 % methanol for a few minutes then allowed to equilibrate in transfer buffer (Section 2.23). For each gel, two Teflon pads and 4 filter papers (3MM grade, Whatman chromatography paper, Brentford, UK) were used. These were also soaked in transfer buffer. The gel was removed from the Mini-PROTEAN™ system and the stacking gel carefully excised. The position of the prestained All blue molecular weight standards was marked on the membrane using scissors. Care was taken not to touch the surface of the membrane. The blotting assembly was prepared by sandwiching the gel and PVDF membrane between 2 pre-soaked Whatman filter papers on either side. Care was taken to avoid air bubbles especially between gel and PVDF membrane. One Teflon pad was placed on either side of the sandwich. The whole arrangement was placed in a transfer cassette with the PVDF membrane positioned towards the positive (+ve) electrode (white surface). The cassette was then placed in the transfer tank filled with ice-cold transfer buffer. Transfer was either carried out overnight (30 V for 6 hours) or at 100 V over 2 hours at 4˚C using an ice pack to keep the transfer buffer cold.

2.18.4 Immunoblotting

In order to quantify the relative amount of each of the proteins of interest present in the sample immunoblotting was performed (Kurien and Scofield, 2006). The electro-blotted PVDF membranes were recovered from the blotting cassette and their orientation marked by snipping off the bottom left corner using scissors. Where membranes were to be probed with more than one antibody (e.g. the protein of interest and a loading control) and the two proteins had sufficiently different molecular masses for the two bands to run with adequate separation, scissors were used to cut the membranes horizontally into two portions. The prestained All Blue™ molecular weight marker bands on the membrane were used to judge where the cut should be made so as to ensure that each portion of membrane contained one band. One of two loading controls was used for all blotting experiments. Where possible, β-tubulin (MW ~55 kDa) was used. Where the protein of interest had a molecular

mass too close to that of tubulin, for example sestrin 2 (MW ~58 kDa), actin (MW ~37 kDa) was used in its place.

The following blocking and incubation steps were carried out in a 30 ml universal tube (DJB Labcare, Buckinghamshire, UK) into which the PVDF membrane was carefully placed with the protein-containing side facing inwards. The membrane was handled with fine forceps and care was taken not to touch this surface. Each membrane was first blocked by incubating in phosphate buffered saline Tween-20 (PBST, see Section 2.23) containing 5% (w/v) dried skimmed milk at room temperature for 1 hour on a rocker (R100B Rotatest orbital shaker, Denley Instruments Ltd., Colchester, UK). It was then incubated with primary antibody diluted in blocking buffer for an hour at room temperature, unless stated otherwise, with gentle rotation (Stuart Roller mixer, Bibby Sterlin Ltd., Staffordshire, UK). The details and dilutions of each primary antibody used are provided in Table 2.3, page 118. This was followed by three 5 min washes in PBST. The PVDF membrane was then incubated with the relevant species of horse-radish peroxidase (HRP)-conjugated secondary antibody diluted in blocking buffer for an hour with gentle shaking at room temperature. Details and dilutions of the secondary antibodies used are provided in Table 2.4 (page 119). If biotinylated molecular weight markers were loaded on the original gel, avidin/HRP (ExtrAvidin Peroxidase™) was added to the secondary antibody at a dilution of 1:2000 to enable their visualization. Five 5 min washes with PBST were finally done to remove any non-specifically bound secondary antibody before detection using chemiluminescence.

2.18.5 Detection of bands using chemiluminescence

The blotted proteins were detected using an EZ-ECL™ HRP chemiluminescence detection kit (Biological Industries, Haemek, Israel) as per the manufacturer's instructions. Briefly, equal volumes of solution A and solution B were mixed and equilibrated for 5 min on a roller (Stuart Roller mixer, Bibby Sterlin Ltd., Staffordshire, UK). The PVDF membrane was recovered from its PBST wash and was incubated for 5 min in the mixture. Care was taken to remove excess chemiluminescence reagent before placing the membrane in a lead-coated X-ray/photo film development cassette. Chemiluminescence was detected using Hyperfilm™ photo film (Amersham, Chalfont St Giles, UK), taking care to avoid bubbles between film and membrane. Where the original membrane had been cut in half to allow different proteins to be probed, the complete PVDF membrane was reconstituted at this stage prior to exposure of the film. The exposed film was then placed directly in developer (Ilford Multigrade™, Harman Tech Ltd, Cheshire, UK) until bands of the required intensity appeared. The film was then given a short wash (5-10 s) in water to remove excess developing reagent before being placed in the fixative (Ilford Hypam™, Harman Tech Ltd, Cheshire, UK). Fixation was allowed to continue until the film became transparent. Finally, the film was washed in copious amounts of water prior to drying at room temperature.

Primary Antibody	Antigen	Species raised in	Source	Dilution
Anti hSOD-1	Human SOD1	Sheep	Calbiochem	1:2500
Anti Prx 2	Peroxiredoxin 2	Rabbit	ABfrontier (Seoul, Korea)	1:2500
Anti Prx 3	Peroxiredoxin 3	Rabbit	ABfrontier (Seoul, Korea)	1:2000
Anti Prx-$SO_{2/3}$	Overoxidized typical 2-cys Peroxiredoxins	Rabbit	ABfrontier (Seoul, Korea)	1:2500
Anti 2-cys Prxs	Prxs 1-4	Mouse	Abcam (Cambridge, UK)	1:2000
Anti Srx	Sulfiredoxin	Rabbit	Abcam (Cambridge, UK)	1:2000
Anti mSrx	Mouse Sulfiredoxin	Rabbit	Donation*	1:2000
Anti Sesn2	Human Sestrin 2	Rabbit	Protein Tech Group Inc (Illinois, USA)	1:1000
Anti Txnip	Thioredoxin interacting protein	Mouse	MBL (Naka-ku, Japan)	1:2000
Anti Phospho-C-jun (ser63)	Phosphorylated C-jun (A proxy for activated AP-1)	Rabbit	Cell signalling (Massachusetts, USA)	1:2000
Anti β-Tubulin III	Tubulin	Rabbit	Sigma (Poole, UK)	1:20000
Anti N-terminal Actin	Actin	Rabbit	Sigma (Poole, UK)	1:8000

Table 2.3: *Table showing primary antibodies used for immunoblotting. *This antibody was a kind gift from Dr. Tong-Shin Chang, Laboratory of Molecular and Cellular Biochemistry, Seoul, Korea. All primary antibodies were incubated in blocking buffer for one hour at room temperature.*

Secondary Antibody	Raised against	Raised in	Source	Dilution
HRP-tagged anti-mouse	Mouse Immunoglobulins	Rabbit	DAKO (Glostrup, Denmark)	1:5000
HRP tagged anti-rabbit	Rabbit Immunoglobulins	Goat	DAKO (Glostrup, Denmark)	1:5000
HRP tagged anti-sheep	Sheep Immunoglobulins	Donkey	Sigma (Poole, UK)	1:5000

Table 2.4 *Secondary antibodies used for immunoblotting. All secondary antibodies were incubated in blocking buffer with the PVDF membrane for one hour at room temperature.*

2.18.6 Quantification by densitometry

Bands of interests on Western blots were quantified using densitometry. All densitometry analyses were carried out on the G-box (Syngene, Cambridge, UK). For each analysis blots featuring protein bands of mid-grey intensity were chosen, as far as was possible. The size of the area to be measured was determined by the largest protein band on a blot and remained constant through the analyses of all the bands on that particular blot. For blots featuring multiple proteins bands of interest in one lane, for example, blots for $PrxSO_{2/3}$ and total 2–cys Prxs that featured multiple Prx bands, the area to be measured was drawn around all the relevant protein bands appearing in a lane, as shown in Fig 2.5. Before calculating the relative expression changes of protein of interest between control and patient samples, variability in protein loading was corrected for using the intensity of the relevant loading control bands.

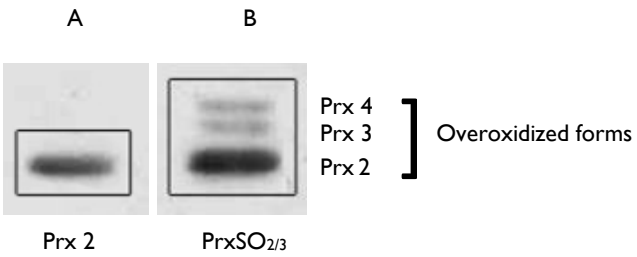

Figure 2.5: *Representative Western blot showing the G-box quantification window for A) a single protein band, applicable to most of the proteins investigated in this study, and B) blots that resulted in multiple protein bands of interest for example samples blotted for $PrxSO_{2/3}$ or the typical 2-cys Prxs in which the antibody detects bands for Prxs 2, 3 and 4. A) Protein band is Prx 2 B) Protein bands generated by an antibody to $PrxSO_{2/3}$ that detected 3 bands representing overoxidized Prx 2, Prx 3 and Prx 4.*

2.19 Statistics

All data were analyzed using Graphpad Prism Version 6 (Graphpad software, California, USA) and appropriate statistical tests were performed for each experiment. Details are provided for each experiment in the relevant results chapters.

All solutions were prepared in deionized water (Millipore, Massachusetts, USA) and all chemicals were purchased from Sigma (Poole, UK) unless otherwise stated.

2.20 Cell culture

1. *NSC34 and HEK293 cell culture medium:* Each 500 ml of Dulbecco's Modified Eagle Medium (DMEM) (BioWhitaker, Lonza, Belgium) with 2 mM L-Glutamine and 4.5 g/l Glucose but without Sodium pyruvate, was supplemented with 10 % Fetal Calf Serum (FCS) (Biosera, East Sussex, UK) and Penicillin-Streptomycin cocktail (see below).

2. *Human fibroblast culture medium:* Each 500 ml bottle of Ham's F-10 Media (Gibco, Paisley, Scotland, UK) was supplemented with 10 % FCS, Penicillin-Streptomycin cocktail (see below), 0.25 % Holo-transferrin and 2.5 ng of epidermal growth factor.

3. *Penicillin-Streptomycin cocktail:* Contains 10 000 units/ml of Penicillin (Penicillin G sodium base) and 10 000 µg/ml of Streptomycin (streptomycin sulphate) in 0.85 % saline.

4. *Phosphate buffered saline (PBS) (pH 7.2) (BioWhitaker, Lonza, Belgium):* 800 ml of deionized water containing 135 mM NaCl, 3.2 mM Na_2HPO_4, 0.5 mM KH_2PO_4 and 1.3 mM KCl was prepared. The pH was adjusted to pH 7.2 using 1M HCl solution. The buffer was made up to 1 litre using deionized water and stored at room temperature.

2.21 Cell & mouse CNS tissue harvest

1. *1x Laemmli sample buffer (LSB):* 62.5 mM Tris-HCl (pH 6.8), 2 % (w/v) SDS, 10 % Glycerol, 5 % (v/v) Beta mercaptoethanol and 0.001 % (w/v) Bromophenol blue (Laemmli, 1970). LSB (50 ml) was prepared and stored at room temperature.

2. *1x Non-reducing sample buffer:* 62.5 mM Tris-HCl (pH 6.8), 2 % (w/v) SDS, 10 % Glycerol and 0.001 % (w/v) Bromophenol blue (Laemmli, 1970).

3. *Buffer A:* 20 mM HEPES (pH 7.4), 10 mM KCl, 1.5 mM $MgCl_2$, 1 mM Dithiothreitol (DTT), 250 mM sucrose. One protease inhibitor cocktail (PIC) tablet (Complete™ Mini EDTA-free protease inhibitor cocktail (PIC) tablets, Roche, Mannheim, Germany) was added to 10 ml of Buffer A before aliquotting and storing at -20˚C.

4. *0.25M Sucrose/Buffer A:* 50 mM triethanolamine (TEA) , 25 mM KCl, 5 mM $MgCl_2$, 0.5 mM Dithiothreitol (DTT), 0.5 mM phenylmethanesulfonyl fluoride (PMSF), 250 mM sucrose and 1 PIC tablet per 10 ml of solution. The solution was stored at 4˚C

5. *Phenylmethanesulfonyl fluoride (PMSF) stock solution:* 100 mM PMSF solution was prepared in 10 ml of 100 % ethanol (Fisher Scientific, Loughborough, UK) and stored at 4˚C for up to 1 month.

2.22 Sodium dodecyl sulphate polyacrylamide gel electrophoresis (SDS PAGE)

1. *10 % (w/v) Sodium dodecyl sulphate (SDS):* 10 g of SDS was weighed out and dissolved in deionized water made up to 100 ml. The solution was stored at room temperature.

2. *4x Resolving gel buffer (pH 8.8):* 1.5 M Tris base and 0.4 % (w/v) SDS. Tris base 90.85 g and 2 g SDS were dissolved in 450 ml of deionized water. The pH was then adjusted using 1M HCl and the solution made up to 500 ml using deionized water. The solution was stored at room temperature.

3. *4x Stacking gel buffer (pH 6.8):* 0.5 M Tris base and 0.4 % (w/v) SDS. Tris base 30.28 g and 2 g SDS were dissolved in 450 ml of deionized water. The pH was then adjusted using 1M HCl and the solution was made up to 500 ml using deionized water. The solution was stored at room temperature.

4. *10 % (w/v) Ammonium persulphate (APS) (Electran, BDH laboratory supplies, Poole, UK).* APS1 g was weighed out and dissolved in 10 ml of deionized water. APS 10 % solution was stored at 4˚C for up to 3 weeks.

5. *15 % Resolving gel (~15 ml for 2 gels):* The following were added together: 3.8 ml deionized water, 7.5 ml 30 % Acrylamine-bis acrylamide solution (Protogel™ (37:5:1) solution, National Diagnostics, Geneflow, Staffordshire, UK), 3.8 ml 4x resolving gel buffer (pH 8.8) and 150 µl 10 % SDS. Just prior to pouring the gel 150 µl 10 % APS and 10 µl of TEMED were added and the solution gently mixed by inversion. The gel solution was used immediately.

6. *5 % Stacking gel (~10 ml for 2 gels):* The following were added together: 4.5 ml deionized water, 1.3 ml 30 % Acrylamine-bis acrylamide solution (Protogel™ (37:5:1) solution, National Diagnostics, Geneflow, Staffordshire, UK), 2 ml 4x stacking gel buffer (pH 6.8) and 80 µl of 10 % SDS. Just prior to pouring the gel, 80 µl of10 % APS and 8 µl of TEMED were added and the solution mixed gently by inversion. The gel solution was used immediately.

7. *1x Electrophoresis running buffer:* 25 mM Tris, 250 mM Glycine and 0.1 % (w/v) SDS, pH 8.3. Tris base 30.3 g along with 144 g Glycine and 100 g SDS were dissolved in 1 litre of deionized water. The solution was stored at room temperature.

2.23 Western Blotting

1. *1x Transfer buffer:* 25 mM Tris, 250 mM Glycine and 10 % (w/v) Methanol (Fisher Scientific, Loughborough, UK), pH 8.4. Tris base 30.3 g along with 144 g Glycine and 100 ml of 100 % Methanol were mixed with 900 ml of distilled water to make 1 litre of solution. The solution was stored at 4˚C.

2. *Washing solution (PBS-Tween-20, PBST):* PBS with 0.25 % (w/v) Polyoxyethylene-Sorbitan Monolaurate (Tween-20). Tween-20, 2.5 g (w/v), was dissolved in 1 litre of PBS. The solution was stored at room temperature.

3. *Blocking solution:* PBST containing 5 % w/v dried skimmed milk (casein block) (Kurien and Scofield, 2006). Blocking solution was freshly prepared just prior to use.

2.24 N-Ethylmaleimide (NEM) solutions

All solutions containing NEM were prepared inside a fume hood. When large volumes were being prepared additional eye protection and a breathing mask were worn.

1. *NEM base buffer:* 40 mM HEPES (4-(2-hydroxyethyl)-1-piperazineethanesulfonic acid), 50 mM NaCl and 1 mM EGTA (ethylene glycol tetra-acetic acid), pH 7.2. HEPES 4.76 g along with 1.46 g of NaCl and 190.23 g of EGTA were dissolved in 500 ml of distilled water. The solution was stored at 4˚C.

2. *NEM perfusion buffer:* NEM base buffer containing 100 mM NEM. The perfusion solution was prepared fresh each time it was required. Excess NEM buffer was stored securely at 4˚C until disposed of via the University's hazardous chemical waste disposal scheme. The perfusion solution was collected by specialised contractors who liaised with the laboratory technical team.

3. *NEM homogenization buffer:* NEM perfusion buffer containing 10 µg/ml of catalase and 1 PIC tablet per 10 ml of solution, pH 7.2.

4. *NEM-CHAPS solution: NEM ba*se buffer containing 25 % (w/v) CHAPS (3-[(3-cholamidopropyl) dimethylammonio]-2-hydroxy-1-propanesulfonate). The solution was prepared fresh each time it was required.

REFERENCES

Aguirre, T., Van Den Bosch, L., Goetschalckx, K., Tilkin, P., Mathijs, G., Cassiman, J.J., and Robberecht, W. (1998). Increased sensitivity of fibroblasts from amyotrophic lateral sclerosis patients to oxidative stress. Ann Neurol *43*, 452-457.

Bradford, M.M. (1976). A rapid and sensitive method for the quantitation of microgram quantities of protein utilizing the principle of protein-dye binding. Analytical Biochemistry *72*, 248-254.

Cashman, N.R., Durham, H.D., Blusztajn, J.K., Oda, K., Tabira, T., Shaw, I.T., Dahrouge, S., and Antel, J.P. (1992). Neuroblastoma x spinal cord (NSC) hybrid cell lines resemble developing motor neurons. Dev Dyn *194*, 209-221.

Choudry, R.B., and Cudkowicz, M.E. (2005). Clinical trials in amyotrophic lateral sclerosis: the tenuous past and the promising future. J Clin Pharmacol *45*, 1334-1344.

Clement, A.M., Nguyen, M.D., Roberts, E.A., Garcia, M.L., Boillee, S., Rule, M., McMahon, A.P., Doucette, W., Siwek, D., Ferrante, R.J., *et al.* (2003). Wild-type nonneuronal cells extend survival of SOD1 mutant motor neurons in ALS mice. Science *302*, 113-117.

Cox, A.G., Peskin, A.V., Paton, L.N., Winterbourn, C.C., and Hampton, M.B. (2009). Redox potential and peroxide reactivity of human peroxiredoxin 3. Biochemistry *48*, 6495-6501.

Dal Canto, M.C., and Gurney, M.E. (1994). Development of central nervous system pathology in a murine transgenic model of human amyotrophic lateral sclerosis. Am J Pathol *145*, 1271-1279.

Desnuelle, C., Dib, M., Garrel, C., and Favier, A. (2001). A double-blind, placebo-controlled randomized clinical trial of alpha-tocopherol (vitamin E) in the treatment of amyotrophic lateral sclerosis. ALS riluzole-tocopherol Study Group. Amyotroph Lateral Scler Other Motor Neuron Disord *2*, 9-18.

Dimos, J.T., Rodolfa, K.T., Niakan, K.K., Weisenthal, L.M., Mitsumoto, H., Chung, W., Croft, G.F., Saphier, G., Leibel, R., Goland, R., *et al.* (2008). Induced pluripotent stem cells generated from patients with ALS can be differentiated into motor neurons. Science *321*, 1218-1221.

Drory, V.E., and Gross, D. (2002). No effect of creatine on respiratory distress in amyotrophic lateral sclerosis. Amyotroph Lateral Scler Other Motor Neuron Disord *3*, 43-46.

Durham, H.D., Dahrouge, S., and Cashman, N.R. (1993). Evaluation of the spinal cord neuron X neuroblastoma hybrid cell line NSC-34 as a model for neurotoxicity testing. Neurotoxicology *14*, 387-395.

Ferraiuolo, L., Heath, P.R., Holden, H., Kasher, P., Kirby, J., and Shaw, P.J. (2007). Microarray analysis of the cellular pathways involved in the adaptation to and progression of motor neuron injury in the SOD1 G93A mouse model of familial ALS. J Neurosci *27*, 9201-9219.

Graham, F.L., Smiley, J., Russell, W.C., and Nairn, R. (1977). Characteristics of a human cell line transformed by DNA from human adenovirus type 5. J Gen Virol *36*, 59-74.

Gurney, M.E., Pu, H., Chiu, A.Y., Dal Canto, M.C., Polchow, C.Y., Alexander, D.D., Caliendo, J., Hentati, A., Kwon, Y.W., Deng, H.X., *et al.* (1994). Motor neuron degeneration in mice that express a human Cu,Zn superoxide dismutase mutation. Science *264*, 1772-1775.

Hayflick, L., and Moorhead, P.S. (1961). The serial cultivation of human diploid cell strains. Exp Cell Res *25*, 585-621.

Hein, N.D., Rainier, S.R., Richardson, R.J., and Fink, J.K. (2010). Motor neuron disease due to neuropathy target esterase mutation: enzyme analysis of fibroblasts from human subjects yields insights into pathogenesis. Toxicology letters *199*, 1-5.

Hutter, E., Renner, K., Pfister, G., Stockl, P., Jansen-Durr, P., and Gnaiger, E. (2004). Senescence-associated changes in respiration and oxidative phosphorylation in primary human fibroblasts. The Biochemical Journal *380*, 919-928.

Ito, E., Oka, K., Etcheberrigaray, R., Nelson, T.J., McPhie, D.L., Tofel-Grehl, B., Gibson, G.E., and Alkon, D.L. (1994). Internal Ca2+ mobilization is altered in fibroblasts from patients with Alzheimer disease. Proceedings of the National Academy of Sciences of the United States of America *91*, 534-538.

Kieran, D., Hafezparast, M., Bohnert, S., Dick, J.R., Martin, J., Schiavo, G., Fisher, E.M., and Greensmith, L. (2005). A mutation in dynein rescues axonal transport defects and extends the life span of ALS mice. J Cell Biol *169*, 561-567.

Kim, H., Jung, Y., Shin, B.S., Song, H., Bae, S.H., Rhee, S.G., and Jeong, W. (2010). Redox regulation of lipopolysaccharide-mediated sulfiredoxin induction, which depends on both AP-1 and Nrf2. The Journal of Biological Chemistry *285*, 34419-34428.

Klivenyi, P., Ferrante, R.J., Matthews, R.T., Bogdanov, M.B., Klein, A.M., Andreassen, O.A., Mueller, G., Wermer, M., Kaddurah-Daouk, R., and Beal, M.F. (1999). Neuroprotective effects of creatine in a transgenic animal model of amyotrophic lateral sclerosis. Nat Med *5*, 347-350.

Kumar, V., Kitaeff, N., Hampton, M.B., Cannell, M.B., and Winterbourn, C.C. (2009). Reversible oxidation of mitochondrial peroxiredoxin 3 in mouse heart subjected to ischemia and reperfusion. FEBS Lett *583*, 997-1000.

Kurien, B.T., and Scofield, R.H. (2006). Western blotting. Methods *38*, 283-293.

Laemmli, U.K. (1970). Cleavage of structural proteins during the assembly of the head of bacteriophage T4. Nature *227*, 680-685.

LeGendre, N. (1990). Immobilon-P transfer membrane: applications and utility in protein biochemical analysis. Biotechniques *9*, 788-805.

Mead, R.J., Bennett, E.J., Kennerley, A.J., Sharp, P., Sunyach, C., Kasher, P., Berwick, J., Pettmann, B., Battaglia, G., Azzouz, M*., et al.* (2011). Optimised and rapid pre-clinical screening in the SOD1(G93A) transgenic mouse model of amyotrophic lateral sclerosis (ALS). PLoS One *6*, e23244.

Mendonsa, G., Dobrowolska, J., Lin, A., Vijairania, P., Jong, Y.J., and Baenziger, N.L. (2009). Molecular profiling reveals diversity of stress signal transduction cascades in highly penetrant Alzheimer's disease human skin fibroblasts. PLoS One *4*, e4655.

Moon, J.C., Hah, Y.S., Kim, W.Y., Jung, B.G., Jang, H.H., Lee, J.R., Kim, S.Y., Lee, Y.M., Jeon, M.G., Kim, C.W*., et al.* (2005). Oxidative stress-dependent structural and functional switching of a human 2-Cys peroxiredoxin isotype II that enhances HeLa cell resistance to H2O2-induced cell death. J Biol Chem *280*, 28775-28784.

O'Neill, J.S., and Reddy, A.B. (2011). Circadian clocks in human red blood cells. Nature *469*, 498-503.

Obrig, T.G., Culp, W.J., McKeehan, W.L., and Hardesty, B. (1971). The mechanism by which cycloheximide and related glutarimide antibiotics inhibit peptide synthesis on reticulocyte ribosomes. The Journal of Biological Chemistry *246*, 174-181.

Robberecht, W. (2000). Oxidative stress in amyotrophic lateral sclerosis. Journal of Neurology *247 Suppl 1*, 11-6.

Shiraha, H., Gupta, K., Drabik, K., and Wells, A. (2000). Aging fibroblasts present reduced epidermal growth factor (EGF) responsiveness due to preferential loss of EGF receptors. The Journal of Biological Chemistry *275*, 19343-19351.

Stoscheck, C.M. (1990). Quantitation of protein. Methods in Enzymology *182*, 50-68.

Villegas, J., and McPhaul, M. (2005). Establishment and culture of human skin fibroblasts. Curr Protoc Mol Biol *Chapter 28*, Unit 28 23.

West, M.D., Pereira-Smith, O.M., and Smith, J.R. (1989). Replicative senescence of human skin fibroblasts correlates with a loss of regulation and overexpression of collagenase activity. Exp Cell Res *184*, 138-147.

Woo, H.A., Chae, H.Z., Hwang, S.C., Yang, K.S., Kang, S.W., Kim, K., and Rhee, S.G. (2003). Reversing the inactivation of peroxiredoxins caused by cysteine sulfinic acid formation. Science *300*, 653-656.

3. RESULTS – HUMAN FIBROBLASTS

INTRODUCTION

This section presents results obtained in human fibroblasts from fALS patients and healthy control volunteers. HEK293 cells (see Chapter 2, Section 2.1) were used to establish preliminary working protocols and this work is also presented here. After optimization of the Western blotting protocols for detecting 2-cys Prxs (reduced and overoxidized forms) and the regenerators of overoxidized 2-cys Prxs, fibroblast cell lines derived from familial ALS patients and healthy control volunteers were investigated. The characteristics, merits and limitations of the use of patient fibroblasts as a model of ALS have already been discussed in Chapter 2, Section 2.2.

Fibroblasts were obtained from patients suffering from fALS caused by mutations in SOD1 and TDP43 and from age- and sex-matched healthy control individuals. Three mutant SOD1 and three mutant TDP43 patient fibroblast lines were each paired with age- and sex-matched control fibroblast lines. Experiments were conducted in cells grown under basal culture conditions and under conditions of oxidative stress by exposing the cells to various concentrations of hydrogen peroxide (H_2O_2) (Moon et al., 2005; Woo et al., 2003a). Alterations in the levels of the typical 2-cys Prxs (reduced and overoxidized) and their regenerators were then investigated in patient and control fibroblasts at a protein level using Western blotting. Stress-recovery experiments were then carried out in which the 2-cys Prxs were overoxidized to saturation by exposure to H_2O_2 and then allowed to recover. Levels of overoxidized typical 2-cys Prxs and their regenerators were then measured at various time points over the next 24 hours. Finally, the response of SOD1 fALS and control fibroblasts to two sequential non-saturating oxidative challenges was investigated.

WORK IN HEK293 CELLS

3.1 Work-up experiments in HEK293 cells

3.1.1 Antibody work-up

HEK293 cells were used to work-up experimental protocols and to optimize Western blotting antibody concentrations and incubation times. Whole cell preparations from HEK293 cells grown under basal culture conditions were made and blotted with antibodies that recognized 1) β-tubulin (to be used as a loading control – Fig. 3.1); 2) individual typical 2-cys Prxs (Prx 2, Prx 3 and Prx 4) and with an antibody that recognized all four typical 2-cys Prxs (Fig. 3.2); 3) sulfiredoxin 1 (Srx 1) and sestrin 2 (Sesn 2),

putative regenerators of overoxidized 2-cys Prxs (Fig. 3.3); and 4) actin - used as a loading control for the sestrin blots (also Fig. 3.3).

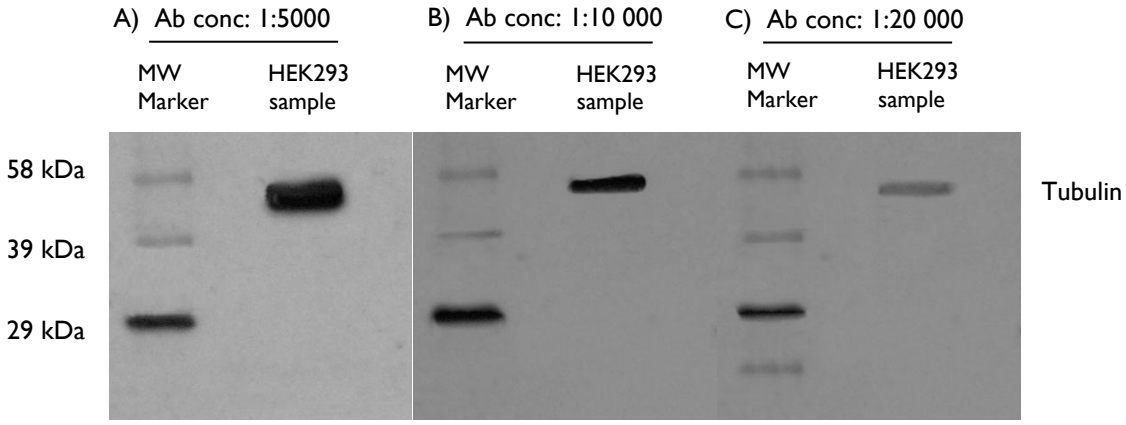

Figure 3.1: *Representative Western blots showing the work-up of the β-tubulin antibody. A whole-cell preparation of HEK293 cells, grown under basal culture conditions, was Western blotted for β-tubulin. The antibody was used at progressively more dilute concentrations until a concentration was identified that resulted in a mid-grey band after an exposure of 1 minute. A) β-tubulin band obtained using the antibody at the recommended concentration of 1:5000 with an exposure of 1 min. B) Antibody used at a concentration of 1:10 000 with an exposure of 1 min and C) β-tubulin antibody used at a concentration of 1:20 000 that resulted in an optimal mid-grey tubulin band with an exposure of 1 min (Blot C). Protein loads were 20 µg per lane in all blots.*

Western blotting of 20 µg of a HEK293 whole cell preparation with an antibody to β-tubulin using the manufacturer's recommended concentration and incubation time resulted in an oversaturated β-tubulin band after even a 1 min exposure (Fig. 3.1 – A). Keeping the protein load per lane constant, the concentration of the antibody used was worked down to 1:20 000 which resulted in a mid-grey, unsaturated, Western blot band (Fig. 3.1 – C) with a one minute exposure. This concentration of the β-tubulin antibody was then used throughout my work.

The manufacturer's recommended antibody concentrations and incubation times were used (see Chapter 2, Section 2.18.4 & Table 2.3) the first time HEK293 whole cell preparations were Western blotted with antibodies to Prx 2, Prx 3, total typical 2-cys Prxs, Sesn 2, Srx 1 and actin. These blots produced mid-grey, unsaturated protein bands after reasonable exposures with the recommended antibody concentration and a protein load of 20 µg per lane. No further work-up of these antibodies was therefore required.

An Abcam antibody that recognized all four typical 2-cys Prxs, whether reduced or oxidized (total typical 2-cys Prxs) was used as a control in various of my experiments. In order to establish which protein band represented which 2 cys Prx when this antibody was used, a whole cell preparation of HEK293 cells was blotted with the Abcam total typical 2-cys Prx antibody as well as with antibodies to three of the four individual typical 2-cys Prxs, Prx 2, Prx 3 and Prx 4 (Fig. 3.2). The PVDF membrane was reconstituted prior to visualization of the protein bands.

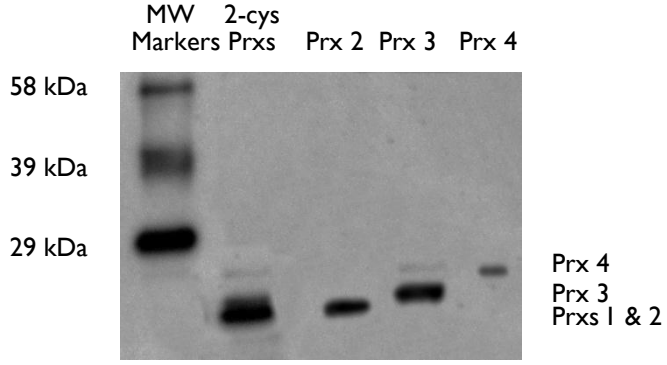

Figure 3.2: *Western blot of a whole cell preparation of HEK293 cells showing from left to right 1) Biotinylated molecular weight (MW) markers, 2) the bands resulting from Western blotting a whole cell lysate of HEK293 cells grown under basal culture conditions with an antibody that recognizes all four typical 2-cys Prxs; 3) the same lysate blotted for Prx 2; 4) Prx 3; and 5) Prx 4. The multiple bands observed with the antibody to total typical 2-cys Prxs represent (from bottom to top) levels of Prx 1 & Prx 2, Prx 3 and Prx 4. With the Abcam total typical 2-cys antibody, the bands for Prx 1 and Prx 2 overlap. Some cross-reactivity is seen with the Prx 3 antibody which recognizes primarily Prx 3 (the darker bottom band) but also to lesser extent Prx 4 (the very faint upper band). The blot was exposed for 2 min after the PVDF membrane was reconstituted.*

From this experiment and the product datasheet it was evident that the bottom band seen when the Abcam total typical 2-cys Prx antibody was used corresponded to a combination of Prx 1 (MW = 22 kDa) and 2 (MW = 22 kDa), the middle band corresponded to Prx 3 (MW = 26 kDa) and the top, faint, band Prx 4 (MW = 28kDa). When used as a control, however, the densitometry reading of all 3 bands generated by this antibody was measured collectively (Chapter 2, Section 2.18.6).

It was not possible to use β-tubulin as a loading control for sestrin 2 as the two proteins have very similar molecular weights. β-Tubulin has a molecular weight of ~55 kDa whilst sestrin 2 has a molecular weight of ~58 kDa and therefore insufficient clearance is achieved between the two bands (Fig. 3.3) for the PVDF membrane to be cut between them so that they can be separately exposed to their respective primary and secondary antibodies. Actin, on the other hand, has a molecular weight of ~ 37 kDa allowing the PVDF membrane to be easily cut between sestrin 2 and actin bands allowing each portion separately incubated with its respective antibody. This can be seen from the illustrative blot overleaf (Fig. 3.3).

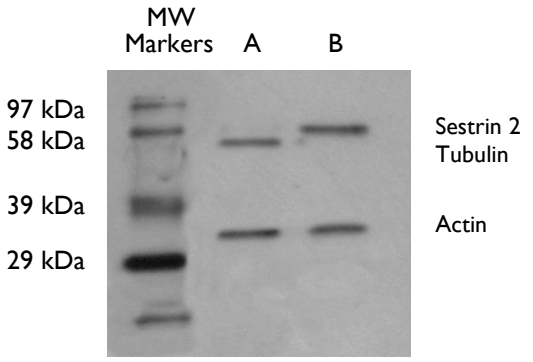

Figure 3.3: *Representative Western blot of a whole cell preparation of HEK293 cells grown under basal culture conditions blotted for sestrin 2 (Sesn 2), actin and tubulin. The PVDF membrane was divided vertically between lanes A and B prior to incubation with the following primary antibodies: Lane A was blotted for tubulin and actin and Lane B was blotted for sestrin 2 and actin. After incubation with appropriate secondary antibodies the PVDF membrane was reconstituted. Exposure = 1.5 min.*

The same whole cell preparations of HEK293 cells grown under basal conditions were then blotted with an antibody that recognized only overoxidized forms of all four typical 2-cys Prxs ($PrxSO_2$ and $PrxSO_3$ collectively written as $PrxSO_{2/3}$) in addition to the Abcam total typical 2-cys Prx antibody previously described (see Fig. 3.2 on the previous page). No overoxidized typical 2-cys Prx ($PrxSO_{2/3}$) bands were detected (Fig. 3.4, Lane A) despite plentiful Prxs clearly being present (Fig. 3.4 Lane B). In order further to work up this antibody HEK293 cells were exposed to H_2O_2 prior to whole cell preparations being made and blotted with the same antibodies (Section 3.1.2).

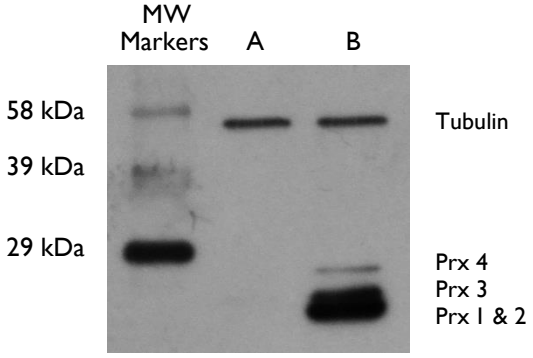

Figure 3.4: *Representative Western blot showing the bands produced by Western blotting of a whole cell preparation of HEK293 cells with Lane A) an antibody to overoxidized Prxs ($PrxSO_{2/3}$) that recognizes only overoxidized forms of all four 2-cys Prxs and Lane B) an antibody that recognizes reduced forms of all four 2-cys Prxs (total 2-cys Prxs). No overoxidized Prxs were detected in HEK293 cells grown under basal conditions. Tubulin was used as a loading control. Protein loads were 20 µg and the blot was exposed for 2 min.*

3.1.2 Work-up of the anti-Prx$SO_{2/3}$ antibody & oxidative stress experiments

HEK293 cells were exposed to H_2O_2, 600 µM, for 6 hours to bring about the overoxidization of typical 2-cys Prxs present in the cells (Chapter 2, Section 2.12). This concentration of H_2O_2 and duration of exposure was chosen based on the literature (Moon et al., 2005; Rhee and Woo, 2011) and my previous work on HEK293 cells (Sundara Rajan, 2008). Samples were then Western blotted for Prx$SO_{2/3}$ and total 2-cys Prxs with tubulin used as the loading control (Fig. 3.5). Manufacturer recommended antibody concentration and incubation time was used for antibodies to overoxidized Prxs (Prx$SO_{2/3}$) (see Table 2.3 in Chapter 2, Section 2.18.4).

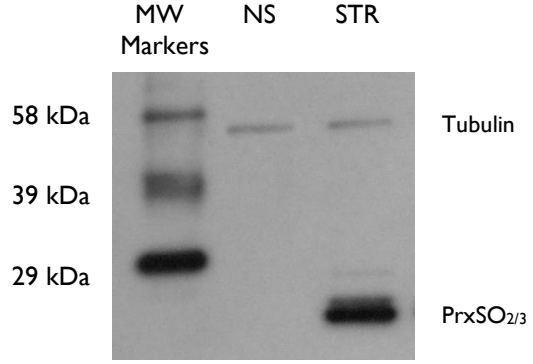

Figure 3.5: *Detection of overoxidized Prxs in HEK293 cells exposed to 600 µM H_2O_2 for 6 hours. Representative Western blots showing levels of Prx$SO_{2/3}$ in a work-up oxidative stress experiment performed in HEK293 cells. Lanes NS – indicate non-stressed HEK293 cells grown under basal conditions while STR – indicates samples exposed to H_2O_2. In keeping with previous results, no Prx$SO_{2/3}$ bands were detected in HEK293 cells not previously exposed to H_2O_2. Protein loads were 20 µg per lane. The blots were cut horizontally, with aid of pre-stained molecular weight markers, to be incubated with respective antibodies and were reconstituted before being exposed for 2 min in both cases.*

These preliminary oxidative stress experiments in HEK293 cells indicated that overoxidized forms of typical 2-cys Prxs were generated by exposure to H_2O_2 as described in the literature and that Prx$SO_{2/3}$ could be readily detected by Western blotting using the Abfrontier anti-Prx$SO_{2/3}$ antibody.

3.1.3 Work-up of the stress-recovery experiments

With the detection of Prx$SO_{2/3}$ demonstrated to be feasible in HEK293 cells treated with H_2O_2, a stress-recovery experiment was worked up to determine whether Prx$SO_{2/3}$ generated after H_2O_2-treatment would gradually disappear with time and over what period. HEK293 cells were exposed to H_2O_2, 600 µM, for 1 hour and were allowed to recover over a period of 9 hours. A one hour H_2O_2 exposure was used in this instance as it was evident that overoxidation of Prxs could be achieved in less than 30 min and that antibody for detecting Prx$SO_{2/3}$ was optimized for the experiment (Moon et al., 2005; Woo et al., 2003b). Samples were then harvested at various experimental time points as described in Chapter 2, Section 2.12.2 and were Western blotted for Prx$SO_{2/3}$ (Fig. 3.6 A and B).

A)

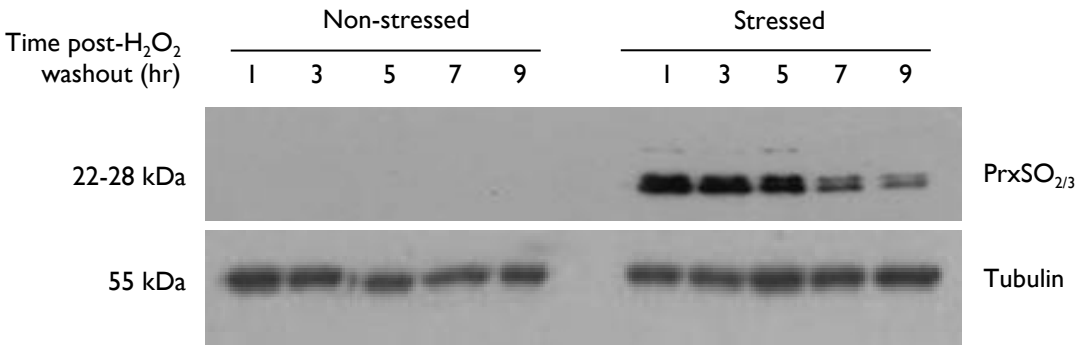

Figure 3.6: A) *Stress-recovery experiment in HEK293 cells. $PrxSO_{2/3}$ was detected immediately after H_2O_2 washout in the stressed cells but not the non-stressed cells and gradually disappeared thereafter over several hours. The stressed cells were exposed to 600 µM H_2O_2 for 1 hr to overoxidize 2-cys Prxs and were allowed to recover after H_2O_2 wash-out over 9 hours. Two independent experiments were performed and the samples were harvested at the time points indicated. Western blotting for $PrxSO_{2/3}$ was performed in duplicate with tubulin used as loading control. Protein loads were 20 µg per lane. Both $PrxSO_{2/3}$ and tubulin blots were exposed for 2 min.*

B)

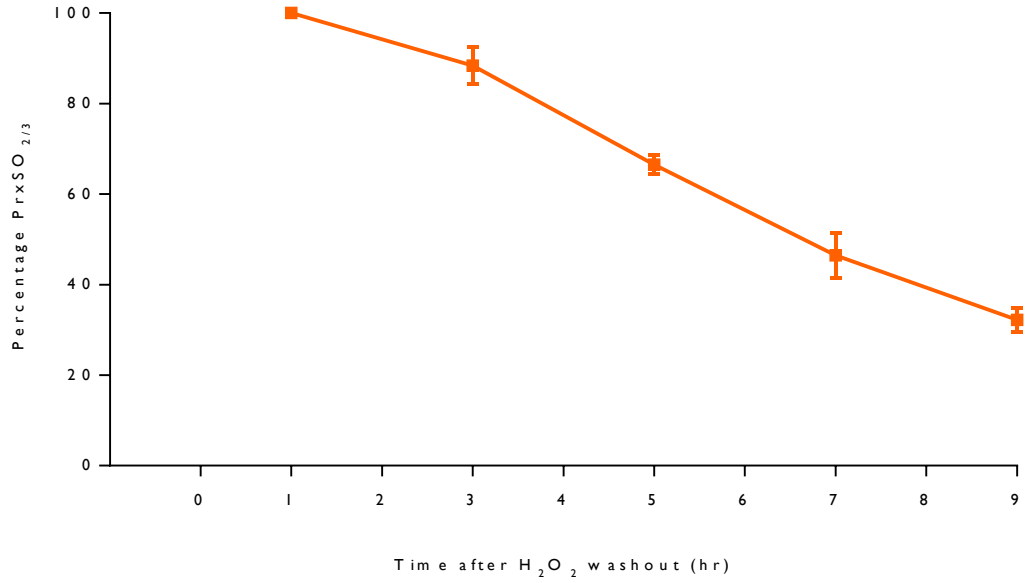

Figure 3.6: B) *Quantification of the stress-recovery experiment in HEK293 cells. Graph showing the disappearance of $PrxSO_{2/3}$ in HEK293 cells subjected to H_2O_2 exposure. Nine hours after H_2O_2 washout, the stressed samples still contained detectable $PrxSO_{2/3}$. No $PrxSO_{2/3}$ was detected in the non-stressed samples at any time points (Fig. 3.6 A). $PrxSO_{2/3}$ densitometry values for each time point were first normalized to those of their respective tubulin bands to correct for protein loading and the corrected values were then expressed as a percentage of the corrected $PrxSO_{2/3}$ at the first experimental time point immediately post-H_2O_2 washout (experiment time point = 1). Data include two independent experiments each Western blotted in duplicate. Error bars represent standard error of the mean (SEM).*

Western blotting of samples from the stress-recovery experiment in HEK293 cells showed the gradual disappearance of $PrxSO_{2/3}$ over the 9-hour recovery period after H_2O_2-washout. However, even at 9 hours post-H_2O_2 washout, $PrxSO_{2/3}$ was still readily detectable at 37% of the level measured immediately after washout. These data indicated that in HEK293 cells at least, complete disappearance of $PrxSO_{2/3}$ after exposure of the cells to 600 μM H_2O_2 for 1 hour would require a longer recovery time post-washout and/or a lesser H_2O_2 exposure in the first place if disappearance of $PrxSO_{2/3}$ was to be followed to completion.

The gradual disappearance of $PrxSO_{2/3}$ after H_2O_2-washout was likely to be a consequence of the actions of one or both of two putative regenerators of $PrxSO_{2/3}$ – sulfiredoxin 1 (Srx 1) and sestrin 2 (Sesn 2) (see Chapter 1, Section 1.14). As I wanted to investigate changes in levels of the $PrxSO_{2/3}$ regenerators after oxidative stress in human ALS and control fibroblasts I performed Western blotting for Sesn 2 on the samples from the stress-recovery work-up experiment carried out in HEK293 cells (Fig. 3.7 A and B). At the time of these work-up experiments, I did not have access to an Srx 1 antibody, although one was subsequently obtained.

A)

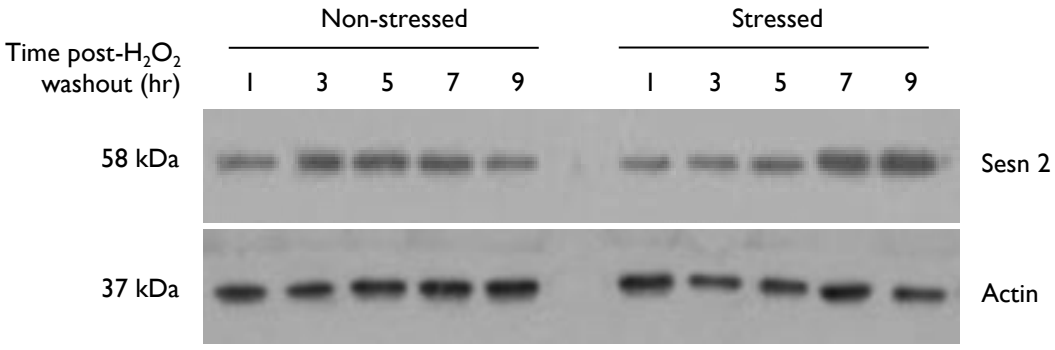

Figure 3.7: A) *Induction of Sesn 2 observed in the stress-recovery work-up experiment in HEK293 cells. Representative Western blots showing the induction of Sesn 2 at ~7 hours post-H_2O_2 washout. HEK293 cells were stressed with 600 μM H_2O_2 for 1 hr to overoxidize the 2-cys Prxs and were allowed to recover back after H_2O_2 wash-out over a 9 hour recovery period as before. Samples were harvested at the time points indicated. Two independent experiments were carried out and Western blotting for Sesn 2 performed in duplicate. Actin was used as loading control. Protein loads were 20 μg per lane. Both Sesn 2 and actin blots were exposed for 2 min.*

B)

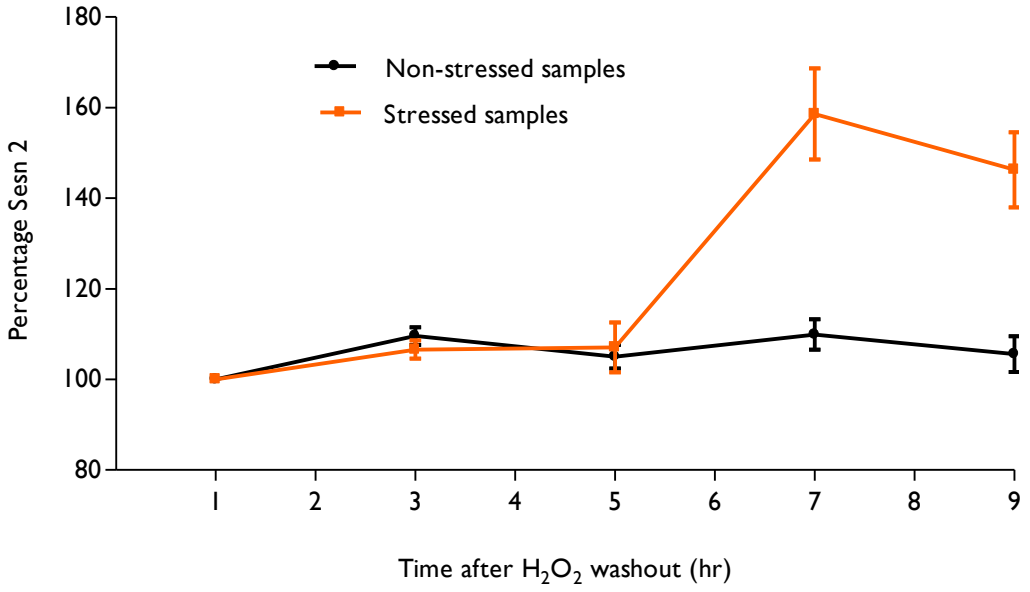

Figure 3.7: B) *Graph showing induction of Sesn 2 in HEK293 cells subjected to H_2O_2 exposure in the stress-recovery work-up experiments. Levels of Sesn 2 increased in the stressed samples ~7 hours after H_2O_2 washout and remained elevated at 9 hours post-H_2O_2 washout. No induction was observed in the non-stressed samples at any time-point. The stress-recovery experiments were performed twice and samples from each independent experiment were Western blotted in duplicate. Sesn 2 densitometry values were first normalized to their respective actin densitometry values in order to correct for protein loading. Corrected Sesn 2 values were then expressed as a percentage of those measured immediately after H_2O_2-washout at the first experimental time point (experiment time point = 1). Error bars represent standard error of the mean (SEM).*

The sestrin 2 blotting of the stress-recovery work-up experiment showed induction seven hours after H_2O_2 washout with elevated levels still evident at the end of the experiment at 9 hours. No sestrin 2 induction was seen in the unstressed cells as expected.

WORK IN MUTANT SOD1-ASSOCIATED ALS FIBROBLASTS

Having established working protocols and optimized Western blotting conditions in HEK293 cells, work was begun in ALS patient fibroblasts. Three fibroblast cell lines, each generated from skin biopsies donated by an individual with familial ALS due to the I113T mutation of SOD1, were used for the experiments. Each ALS fibroblast line was paired, with another matched as closely as was possible by age and sex, with a fibroblast cell line generated from a skin biopsy donated by a healthy control individual (see Pairs 1-3, Table 2.2, Chapter 2, Section 2.6). Levels of 2-cys Prxs, both reduced and overoxidized, the regenerators of overoxidized 2-cys Prxs and related proteins were investigated in whole cell lysates from cells grown under basal culture conditions; after saturating and non-saturating oxidative stress and in stress-recovery experiments.

3.2 Patient and control fibroblasts grown under basal culture conditions

3.2.1 Levels of total (reduced and overoxidized) Prx 2 and Prx 3

Levels of total Prx 2, total Prx 3 and $PrxSO_{2/3}$ were measured by Western blotting of whole cell lysates prepared from the three pairs of age- and sex-matched I113T SOD1-ALS patient and healthy control fibroblasts grown under basal culture conditions (Chapter 2, Section 2.13). Three independent experiments were carried out in each of the three pairs of fibroblasts and Western blotting for each protein of interest was performed in triplicate for each independent experiment (Fig. 3.8 A). The intensities of the resultant bands were quantified using the G-box Gel Doc system (Syngene, Cambridge, UK) as discussed in Chapter 2, Section 2.18.6 (Fig. 3.8 B and C).

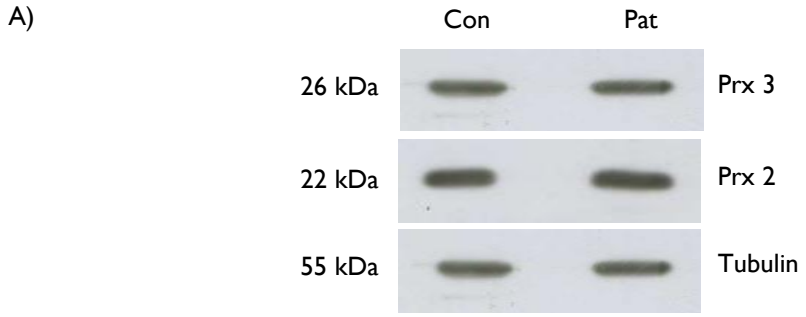

Figure 3.8: A) *No difference in the level of either total Prx 2 or total Prx 3 was observed between I113T SOD1-ALS patient (Pat) and control (Con) fibroblasts grown under basal culture conditions. Representative Western blots. Three independent preparations were made from the three pairs of SOD1-ALS patient and control fibroblasts grown under basal culture conditions. Each experiment was blotted in triplicate for total Prx 2 and total Prx 3 as well as for tubulin, used as a loading control. Protein loads were 20 µg per lane. Prx 2 and Prx 3 blots were exposed for 2 min, tubulin blots for 1 min.*

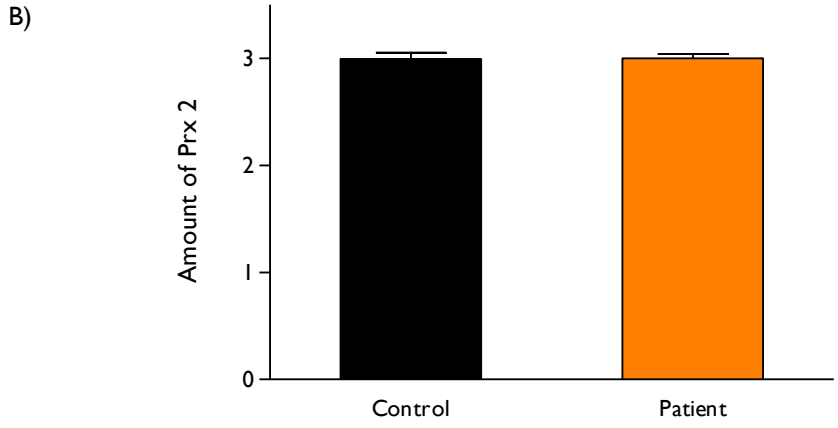

Figure 3.8: B) *Quantification of Western blotting for total Prx2 of whole cell preparations of I113T SOD1 and control fibroblasts grown under basal conditions. Graph showing basal levels of total Prx 2 in control and patient fibroblasts normalized to tubulin. Data include three replicate blots from each of three independent experiments in each of the three pairs of fibroblasts. Error bars represent standard error of the mean (SEM). A Student's t-test showed there was no statistically significant difference in Prx 2 levels between control and patient fibroblasts (p-value: 0.8978).*

C)

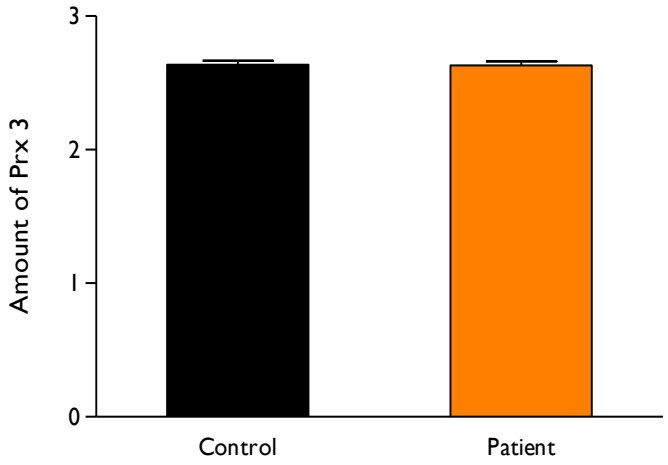

Figure 3.8: C) *Quantification of Western blotting for total Prx 3 of whole cell preparations of I113T SOD1 and control fibroblasts grown under basal conditions. Graph showing basal levels of total Prx 3 in control and patient fibroblasts normalized to tubulin. Data include three replicate blots from each of three independent experiments in each of the three pairs of fibroblasts. Error bars represent standard error of the mean (SEM). A Student's t-test showed that there was no statistically significant difference in Prx 3 levels between control and patient fibroblasts (p-value: 0.8677).*

In summary, whole cell preparations made from all three pairs of I113T SOD1-ALS patient and matched healthy control fibroblasts grown under basal culture conditions showed no difference in total Prx 2 or Prx 3 levels.

3.2.2 Levels of overoxidized 2-cys Prxs

Levels of overoxidized 2-cys Prxs ($PrxSO_{2/3}$) were then measured in whole cell preparations of the three pairs of I113T SOD1 patient and healthy control fibroblasts, again grown under basal culture conditions. Three independent whole cell preparations in each of the three pairs of patient and control fibroblasts were Western blotted in triplicate for $PrxSO_{2/3}$ (Fig. 3.9 A – C).

A)

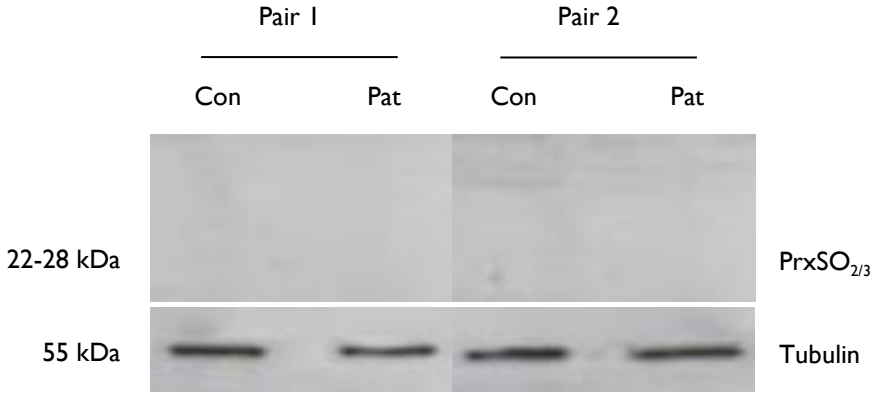

B)

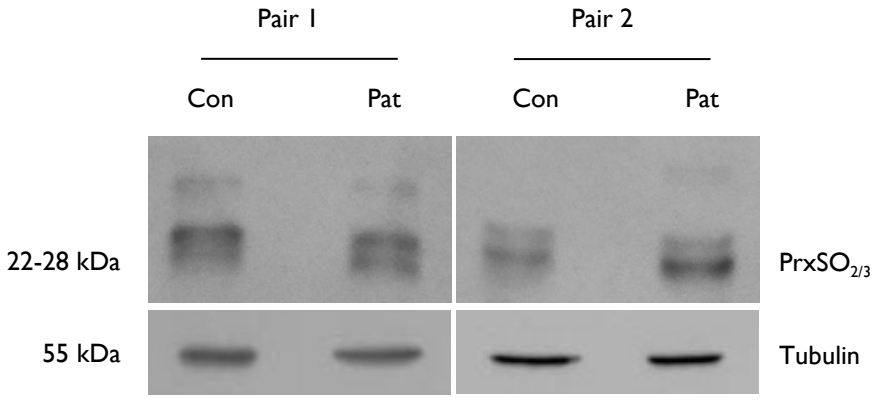

Figure 3.9: *Minimal overoxidized Prxs were detectable in whole cell preparations of I113T patient and healthy fibroblasts grown under basal culture conditions.* ***A)*** *Representative Western blots from two of the three fibroblast pairs showing no detectable $PrxSO_{2/3}$ with a 20 µg protein load per lane and 5 min exposure. Tubulin (loading control) blots were exposed for 1 min.* ***B)*** *Representative blots of the same preparations from two of the three fibroblast pairs again blotted for $PrxSO_{2/3}$ but with a higher (40 µg protein per lane) protein load. On this occasion very faint ill-defined bands were detected at the position expected for $PrxSO_{2/3}$. $PrxSO_{2/3}$ blots were exposed for 5 min while tubulin (loading control) blots were exposed for 1 min.*

C)

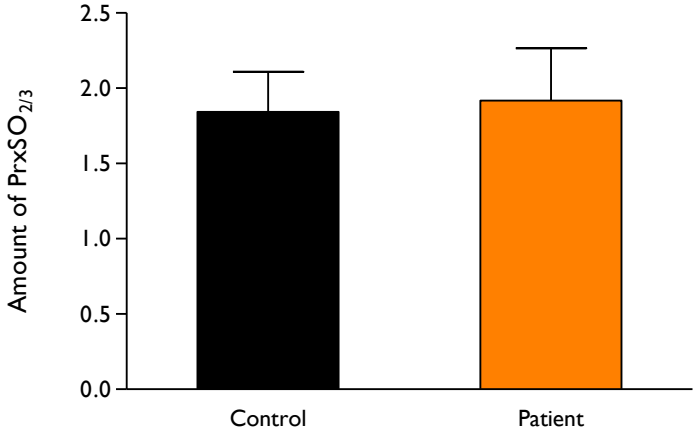

Figure 3.9: C) *Quantification of Western blots for $PrxSO_{2/3}$ in whole cell preparations of I113T SOD1-ALS patient and healthy control fibroblasts grown under basal conditions. $PrxSO_{2/3}$ values were first normalized to tubulin to correct for protein loading. Data include three replicate blots from three independent experiments in each of the three pairs. Error bars represent standard error of the mean (SEM). Barely any $PrxSO_{2/3}$ was detected in patient or control fibroblasts. A Student's t-test showed no statistically significant difference between the very small quantity of $PrxSO_{2/3}$ present in I113T SOD1-ALS patient and control fibroblasts grown under basal conditions (p-value: 0.7839).*

When whole cell preparations of the three pairs of I113T SOD1-ALS patient and control fibroblasts grown under basal culture conditions were Western blotted for $PrxSO_{2/3}$ with the usual protein load of 20 µg per lane, no overoxidized peroxiredoxins could be detected in either. In an effort to visualize $PrxSO_{2/3}$ bands, the samples were blotted again with an increased protein load of 40 µg per lane. With this increased load faint, poorly defined bands were detected at the expected molecular weights, the density and size of which were variable from preparation to preparation within each pair and across three pairs of fibroblasts. Statistical analyses of densitometry values of these faint $PrxSO_{2/3}$ bands across all the experiments showed no significant differences between control and patient fibroblasts under basal conditions. In conclusion, very little $PrxSO_{2/3}$ was present in I113T SOD1-ALS patient fibroblasts or control fibroblasts grown under basal culture conditions.

3.2.3 Levels of $PrxSO_{2/3}$ regenerators

Two regenerators of overoxidized Prxs had been identified by other groups at the time these experiments were carried out – Sulfiredoxin 1 (Srx 1) and Sestrin 2 (Sesn 2). The mechanism by which these regenerators were thought to reduce overoxidized 2-cys Prxs has already been discussed in Chapter 1, Section 1.14. I wanted to know whether levels of either Srx 1 or Sesn 2 were altered in patient fibroblasts compared to healthy control fibroblasts grown under basal culture conditions (Fig. 3.10).

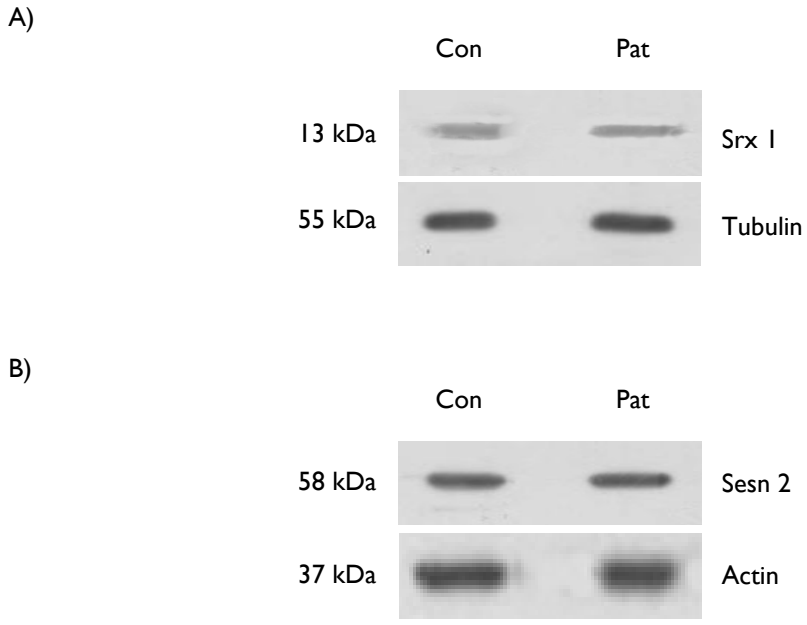

Figure 3.10: *No difference in the levels of either Srx 1 or Sesn 2 was observed between I113T SOD1-ALS patient fibroblasts and healthy control fibroblasts grown under basal culture conditions. Three independent whole cell preparations were made from each of three pairs of I113T SOD1-ALS patient and healthy control fibroblasts grown under basal culture conditions. Representative Western blots showing levels of* ***A)*** *Srx 1 and* ***B)*** *Sesn 2. Each experiment was blotted in triplicate for Srx 1 and Sesn 2. Protein loads were 40 µg per lane for Srx 1 blots and 20 µg per lane for Sesn 2 blots. Srx 1 and Sesn 2 blots were exposed for 1.5 min while tubulin and actin blots were exposed for 1 min.*

The three whole cell preparations already made from each of the three pairs of I113T SOD1-ALS patient and healthy control fibroblasts grown under basal culture conditions were therefore Western blotted for Srx 1 and Sesn 2 along with β-tubulin and actin to be used as their respective loading controls. Each independent experiment was Western blotted in triplicate and the intensities of the $PrxSO_{2/3}$, β-tubulin and actin bands quantified using the G-box as previously (Fig. 3.10 A-D).

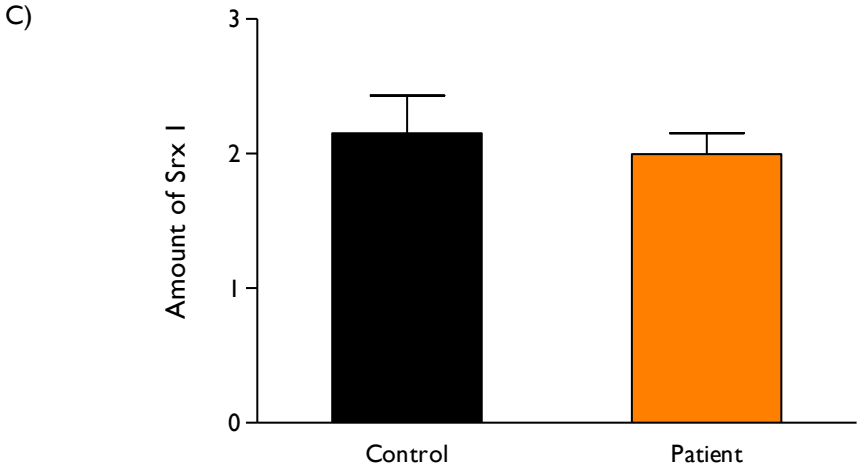

Figure 3.10: C) *Quantification of Western blots for Srx 1 in whole cell preparations of I113T SOD1-ALS patient and healthy control fibroblasts grown under basal conditions. Srx 1 band densitometry values were normalized to those of their respective tubulin bands to correct for protein loading. Data include three replicate blots from three independent experiments in each of the three pairs. Error bars represent standard error of the mean (SEM). A Student's t-test showed no statistically significant difference between the quantity of Srx 1 present in I113T SOD1-ALS patient and control fibroblasts (p-value: 0.6445).*

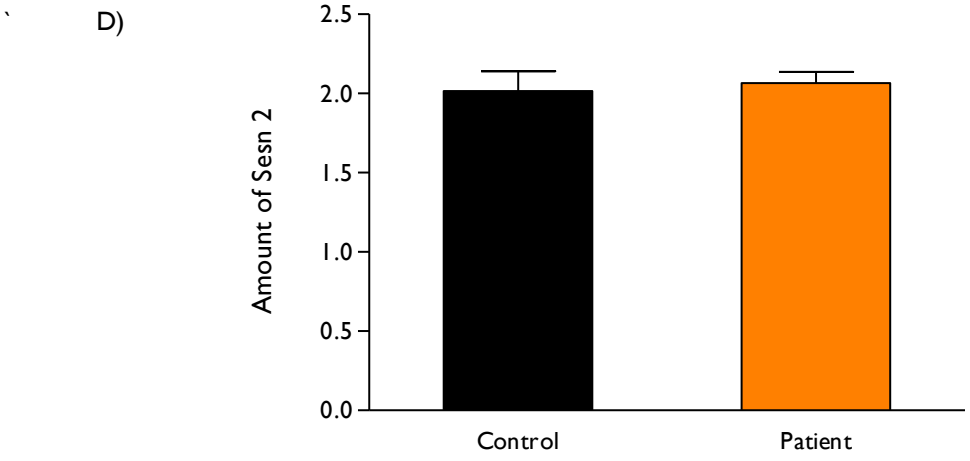

Figure 3.10: D) *Quantification of Sesn 2 Western blots in whole cell preparations of I113T SOD1-ALS patient and healthy control fibroblasts grown under basal conditions. Sesn 2 band densitometry values were normalized to those of their respective actin bands to correct for protein loading. Data include three replicate blots from three independent experiments in each of the three pairs. Error bars represent standard error of the mean (SEM). A Student's t-test showed no statistically significant difference between the quantity of Sesn 2 present in I113T SOD1-ALS patient and control fibroblasts (p-value: 0.8237).*

This work indicated that there was no difference in the levels of either of the putative $PrxSO_{2/3}$ regenerators Srx 1 and Sesn 2 in I113T SOD1-ALS patient and control fibroblasts grown under basal culture conditions.

3.3 Response of patient and control fibroblasts to H_2O_2 exposure

3.3.1 Levels of $PrxSO_{2/3}$ in patient and control fibroblasts after H_2O_2 exposure

Having identified minimal $PrxSO_{2/3}$ in I113T SOD1-ALS patient or control fibroblasts grown under basal culture conditions and no difference in basal levels of Srx 1 or Sesn 2 between the two, the focus of my next set of experiments was to determine whether 2-cys Prxs in patient fibroblasts overoxidize more readily than control cells when exposed to H_2O_2. Based on the work-up experiments carried out in HEK293 cells (Section 3.1.2), and the literature it was decided to stress the cells with a 15 min exposure to 300 μM H_2O_2. The three pairs of healthy control and I113T patient fibroblasts were subjected to 300 μM H_2O_2 exposure for 15 min, the H_2O_2 washed out and whole cell preparations made (see Chapter 2, Section 2.14.2 for the experiment). The resultant samples were then Western blotted for $PrxSO_{2/3}$. Three independent experiments were performed in each of the three pairs and three replicate blots made per experiment. As previously $PrxSO_{2/3}$ and tubulin bands were quantified using the G-box (Fig. 3.11 A and B).

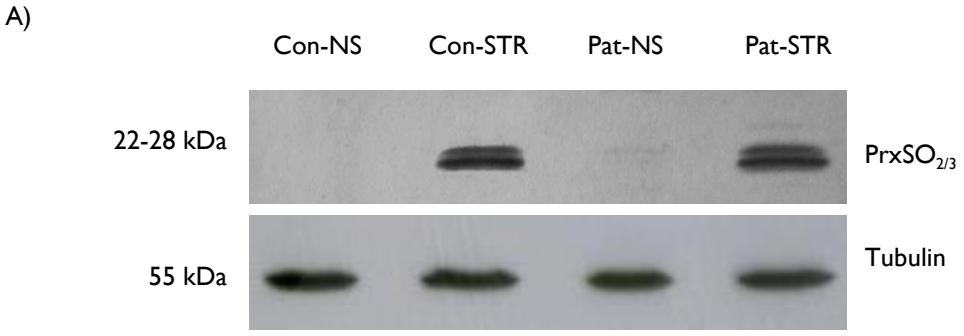

Figure 3.11: A) *Both control (Con-STR) and patient (Pat-STR) fibroblasts showed similar levels of $PrxSO_{2/3}$ when exposed to 300 μM H_2O_2 for 15 min. Control (Con-NS) and patient (Pat-NS) fibroblasts not exposed to H_2O_2 served as non-stressed controls. Minimal $PrxSO_{2/3}$ was detected in these cells. Representative Western blots showing levels of $PrxSO_{2/3}$ in stressed (STR) and non-stressed (NS) control and I113T SOD1-ALS patient fibroblasts. One set of control and patient fibroblasts were exposed to 300 μM H_2O_2 for 15 min while the other was maintained under basal conditions undergoing parallel medium changes. After 15 min the H_2O_2 was removed and whole cell lysates prepared from all four flasks. Three independent experiments were performed in each of the three fibroblast pairs and samples blotted in triplicate for $PrxSO_{2/3}$. Protein loads were 40 μg per lane. $PrxSO_{2/3}$ blots were exposed for 3 min, tubulin blots were exposed for 1 min.*

B)

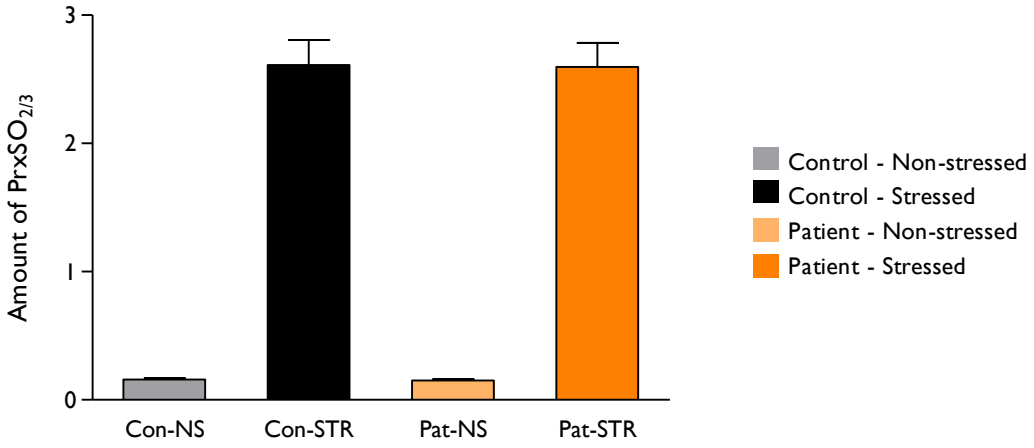

Figure 3.11: B) *Quantification of $PrxSO_{2/3}$, in whole cell preparations of healthy control (Con) and I113T SOD1-ALS patient (Pat) fibroblasts subjected to 300 μM H_2O_2 for 15 min (STR) and harvested immediately after washout or subjected only to parallel medium changes with no H_2O_2 (NS). The densitometry value of each $PrxSO_{2/3}$ band was normalized to that of its respective tubulin band to correct for protein loading. Error bars represent standard error of the mean (SEM) from three replicate blots in three independent experiments in each of the three fibroblast pairs. A Student's t-test showed no statistically significant difference in the amount of $PrxSO_{2/3}$ present in patient and control fibroblasts after H_2O_2 treatment (p-value: 0.8616).*

In conclusion, Western blotting for $PrxSO_{2/3}$ of whole cell preparations of patient and control fibroblasts made after subjecting them to 300 μM H_2O_2 for 15 min revealed no statistically significant difference in the amount of $PrxSO_{2/3}$ between them. This was consistent across all three independent experiments in all three fibroblast pairs. Consistent with the findings of similar experiments carried out in the same fibroblasts grown under basal culture conditions, minimal $PrxSO_{2/3}$ was detected in non-stressed (NS) cells (both patient and control).

3.3.2 Levels of total 2-cys Prxs in patient and control fibroblasts after H_2O_2 exposure

To confirm whether there had been any change in total 2-cys peroxiredoxins in response to treatment with H_2O_2, samples from the oxidative stress experiments described in Section 3.3.1 above were blotted with an antibody to total 2-cys Prxs (Prxs 1, 2, 3 and 4). Samples from each of the three independent experiments carried out in each of three fibroblast pairs was Western blotted twice to determine the levels of total typical 2-cys Prxs (Fig. 3.12 A and B). Band intensities and size were quantified using the G-box as previously.

A)

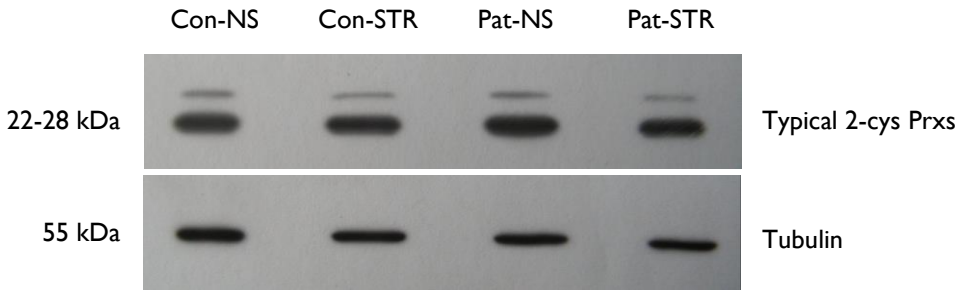

Figure 3.12: A) *Levels of total 2-cys Prxs were the same in whole cell preparations made from both patient and control fibroblasts treated with 300 μM H_2O_2 for 15 min (STR) as in those from patient and control cells not treated with H_2O_2 (NS). Representative Western blots showing levels of total 2-cys Prxs in control (Con) and I113T SOD1-ALS patient (Pat) fibroblasts treated (STR) and untreated (NS) with 300 μM H_2O_2 for 15 min. One set of control and patient fibroblasts were exposed to 300 μM H_2O_2 for 15 min while the other was not, undergoing parallel medium changes only. Three independent experiments were performed in each of the three fibroblast pairs and samples were blotted in duplicate for total 2-cys Prxs. Protein loads were 20 μg per lane. Total 2-cys Prxs blots were exposed for 2 min while tubulin blots were exposed for 1 min.*

B)

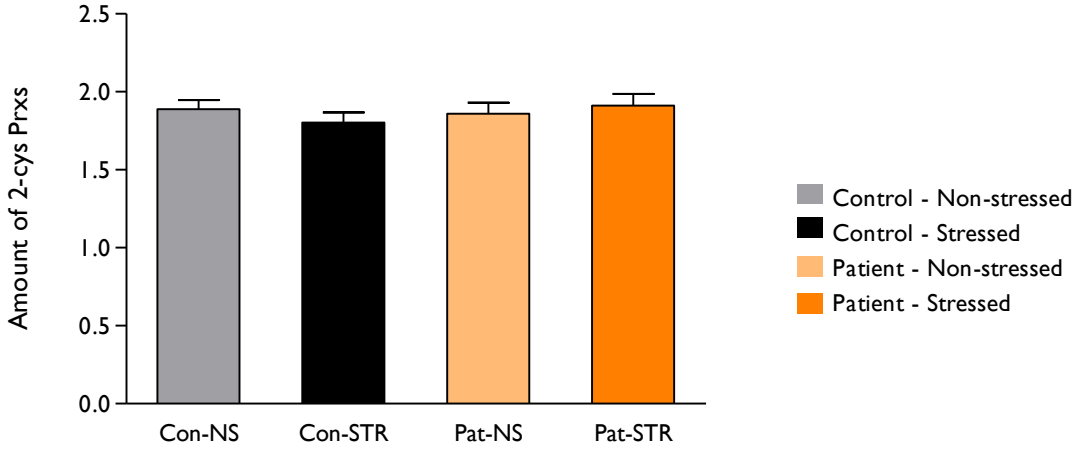

Figure 3.12: B) *Quantification of total typical 2-cys Prxs in whole cell preparations of healthy control (Con) and I113T SOD1-ALS patient (Pat) fibroblasts subjected to 300 μM H_2O_2 for 15 min (STR) or subjected only to parallel medium changes with no H_2O_2 (NS). The densitometry value of each total typical 2-cys Prxs band was normalized to that of its respective tubulin band to correct for protein loading. Error bars represent standard error of the mean (SEM) from two replicate blots in three independent experiments in each of the three fibroblast pairs. A Student's t-test showed no statistically significant difference in the amount of total typical 2-cys Prxs present in either patient or control fibroblasts before and after H_2O_2 treatment (p-value: 0.8797 for control cells, p-value: 0.8943 for patient cells).*

It was evident that levels of total typical 2-cys Prxs were the same in whole cell preparations from both I113T SOD1-ALS patient and healthy control fibroblasts whether they had been treated with 300μM H_2O_2 for 15 min or not. These results suggest that there had been no induction of 2-cys Prxs in response to H_2O_2 treatment by the time the H_2O_2 had been washed out after 15 minutes exposure although this clearly does not preclude a later induction. Statistical analysis of the densitometry values (as before after correction for protein loading) of total typical 2-cys Prxs showed no significant difference in levels between either patient NS and STR fibroblasts or control NS and STR fibroblasts. This was true of all experiments performed in all of the three pairs.

3.4 Stress-titration experiment in fibroblasts

The experiments conducted with exposures to 300 μM H_2O_2 for 15 min (Section 3.3) showed no change in $PrxSO_{2/3}$ levels in either control or patient fibroblasts. There was also no change in levels of total typical 2-cys Prxs after the same stress. I was concerned to verify that the lack of a difference between the overoxidation of typical 2-cys Prxs in patient and control fibroblasts after exposure to 300 μM H_2O_2 for 15 min wasn't simply due to overoxidation of typical 2-cys Prxs to saturation. In order to establish what concentration of H_2O_2 would constitute a non-saturating oxidative stress (as measured by Prx overoxidation) when applied for 15 min, an H_2O_2 stress-titration experiment was performed. This experiment was carried out in one of the three I113T SOD1-ALS patient fibroblast lines (see Chapter 2, Section 2.14.1). Individual flasks of these fibroblasts were each exposed to a different concentration of H_2O_2 (from 10 to 300 μM) for 15 min, before the H_2O_2-containing media was removed, the cells harvested (see Section 2.14.1) and whole cell lysates prepared from each. The resultant samples were then Western blotted for $PrxSO_{2/3}$ (Fig. 3.13 A & B) and the $PrxSO_{2/3}$ bands quantified as before. Levels of $PrxSO_{2/3}$, corrected for protein loading, were then plotted against [H_2O_2] to generate a $PrxSO_{2/3}$ dose-response curve (Fig. 3.13 C).

As expected, Western blotting for $PrxSO_{2/3}$ of samples from the stress-titration experiment showed a gradual increase in levels of $PrxSO_{2/3}$ with increasing in H_2O_2 concentration. This increase was more or less linear between 20 and 40 μM H_2O_2 then $PrxSO_{2/3}$ levels approached saturation above 100 μM H_2O_2. Based on the results of this experiment, a concentration of 30 μM H_2O_2 was chosen as an appropriate non-saturating oxidative stress for the next set of oxidative stress experiments in the I113T SOD1-ALS patient and healthy fibroblast pairs.

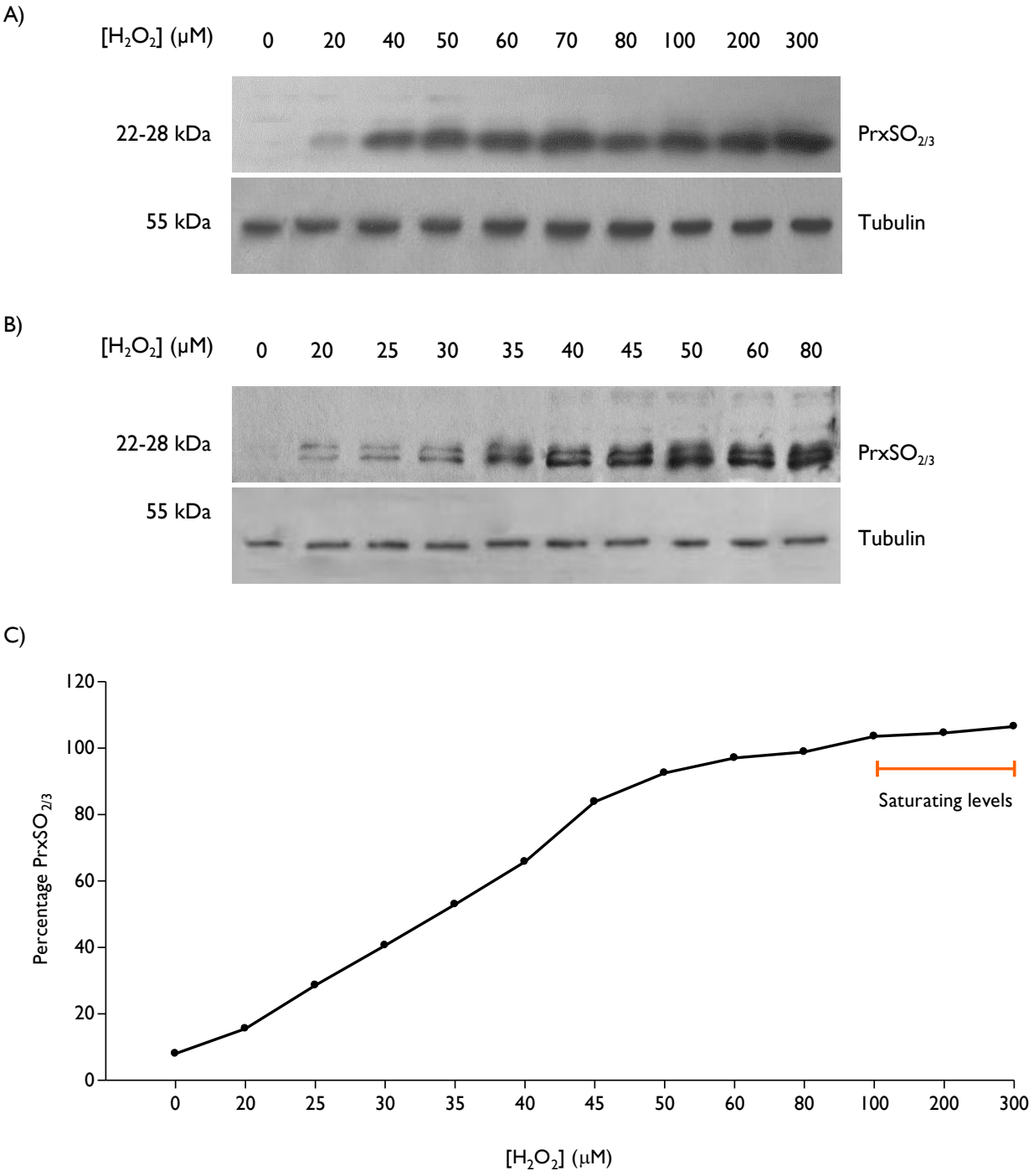

Figure 3.13: *Stress-titration experiment showing increasing levels of $PrxSO_{2/3}$ in I113T SOD1-ALS patient fibroblasts when subjected to increasing H_2O_2 concentrations (see labels above each blot for concentrations) for 15 min. Representative Western blots of the stress-titration experiment performed on an I113T SOD1-ALS patient fibroblast cell line to determine an appropriate non-saturating oxidative stress.* ***A)*** *Concentrations between 0 and 300 μM H_2O_2 and* ***B)*** *Concentrations between 0 and 80 μM H_2O_2. Protein loads were 20 μg per lane. The $PrxSO_{2/3}$ blots were exposed for 3 min, the tubulin blots for 1 min.* ***C)*** *H_2O_2 dose-response curve of $PrxSO_{2/3}$ levels in whole cell preparations of I113T SOD1-ALS patient fibroblasts exposed to increasing concentrations of H_2O_2 for 15 min. For each concentration of H_2O_2 the densitometry value of the $PrxSO_{2/3}$ band was normalized to that of its respective tubulin band to correct for protein loading. This value was then plotted against $[H_2O_2]$.*

3.5 Response of fibroblasts to a non-saturating oxidative stress

Having determined what constituted a non-saturating oxidative stress (as measured by $PrxSO_{2/3}$ levels) for human fibroblasts, the three pairs of I113T SOD1-ALS patient and control fibroblasts were exposed to 30 μM H_2O_2 for 15 min. The experiment performed was otherwise identical to that done using 300 μM H_2O_2 (Section 3.3) with parallel sets of stressed and non-stressed patient and control cells. My intention was to determine whether exposure to what I knew was a non-saturating concentration of H_2O_2 might cause greater overoxidation of typical 2-cys Prxs in patient fibroblasts than control cells. Three independent experiments were performed in each of the three fibroblast pairs and levels of $PrxSO_{2/3}$ were analyzed using Western blotting. Western blotting was performed in triplicate for each of the three independent experiments conducted in the three fibroblast pairs) (Fig. 3.14 A). Band size and intensity were quantified on the G-box as previously described (Chapter 2, Section 2.18.6) (Fig. 3.14 B).

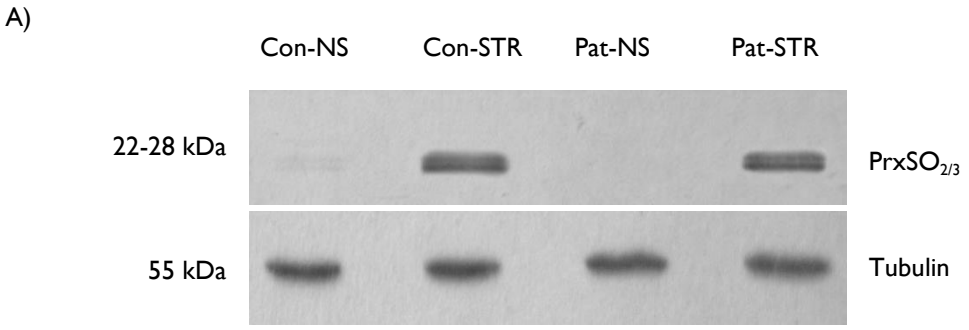

Figure 3.14: A) *Both control and patient fibroblasts showed similar levels of $PrxSO_{2/3}$ when subjected to a non-saturating H_2O_2-mediated oxidative stress (STR) of 30 μM H_2O_2 for 15 min. Representative Western blots showing levels of $PrxSO_{2/3}$ in stressed (STR) and non-stressed (NS) control (Con) and I113T SOD1-ALS patient (Pat) fibroblasts. One set of control and patient fibroblasts were exposed to a non-saturating H_2O_2-mediated stress of 30 μM H_2O_2 for 15 min while the other was not, undergoing parallel medium changes only. After 15 min H_2O_2-containing medium was removed from the STR flasks, NS flasks received a simple medium change and whole cell lysates were prepared from all. Three independent experiments were performed in the three fibroblast pairs and samples from each experiment were blotted in triplicate for $PrxSO_{2/3}$. Protein loads were 40 μg per lane. $PrxSO_{2/3}$ blots were exposed for 3 min and tubulin blots for 1 min.*

$PrxSO_{2/3}$ bands were readily detected in both patient and control fibroblasts after exposure to 30 μM H_2O_2 for 15 min, an oxidative stress that should not overoxidize typical 2-cys Prxs present in the fibroblasts to saturation. Consistent with previous experiments, only minimal $PrxSO_{2/3}$ was detected in the non-stressed patient and control cells. As was the case with the saturating oxidative stress experiment, however, there was still no difference in the amount of overoxidized typical 2-cys Prxs formed in response to treatment with 30 μM H_2O_2 for 15 min between I113T SOD1-ALS fibroblasts and healthy control cells. This absence of a difference in the amount of $PrxSO_{2/3}$ formed between patient and control fibroblasts was consistent in all experiments across all three fibroblast pairs.

B)

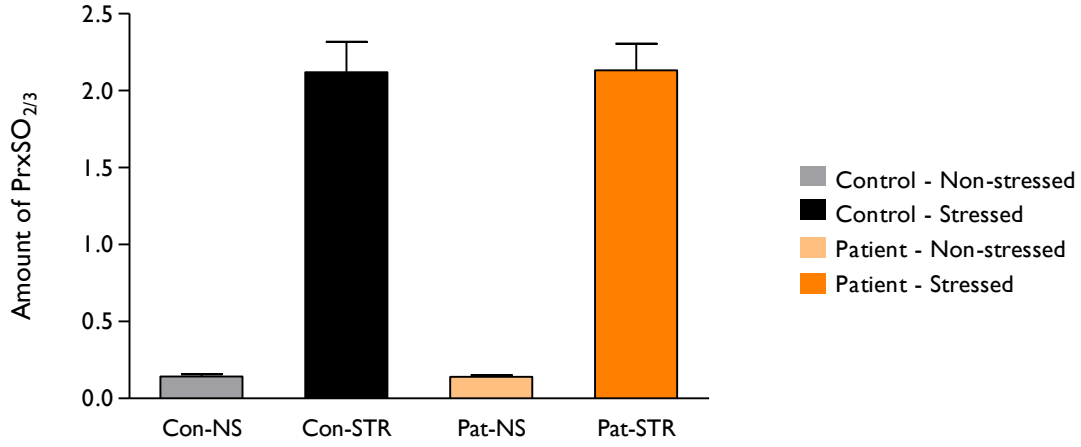

Figure 3.14: B) *Quantification of $PrxSO_{2/3}$ in whole cell preparations of healthy control (Con) and I113T SOD1-ALS patient (Pat) fibroblasts subjected to 30 µM H_2O_2 for 15 min (STR) or to parallel medium changes only with no H_2O_2 (NS). The densitometry values of the $PrxSO_{2/3}$ bands were normalized to those of their respective tubulin band to correct for protein loading. Error bars represent standard error of the mean (SEM) from three replicate blots in three independent experiments in each of the three fibroblast pairs. A Student's t-test showed no statistically significant difference in the amount of $PrxSO_{2/3}$ present between patient and control fibroblasts after H_2O_2 treatment (p-value: 0.9424).*

3.5.1 Levels of total 2-cys peroxiredoxins in a non-saturating oxidative stress experiment

Western blotting for total typical 2-cys Prxs in the whole cell preparations obtained from the non-saturating oxidative stress experiment described in Section 3.5 above was then carried out in order to establish whether or not there was any change in overall typical 2-cys Prx levels after treatment with 30 µM H_2O_2 for 15 min (Fig. 3.15 A overleaf). Each independent experiment in each of the three fibroblast pairs was Western blotted in duplicate to determine the levels of typical 2-cys Prxs. The bands were quantified using the G-box as before (Fig. 3.15 B overleaf).

From the Western blots for total typical 2-cys Prxs of these non-saturating oxidative stress experiments, conducted using an exposure to 30 µM H_2O_2 for 15 min, it was evident that levels of total typical 2-cys Prxs did not change after H_2O_2 treatment in patient or control cells. No induction of total typical 2-cys Prxs was observed immediately after treatment for 15 min with 30 µM H_2O_2 in either patient or control cells. Statistical analysis of the densitometry data showed no significant difference in the levels of typical 2-cys Prxs between the NS and STR conditions in either patient or control fibroblasts across all preparations in all of the three fibroblast pairs.

A)

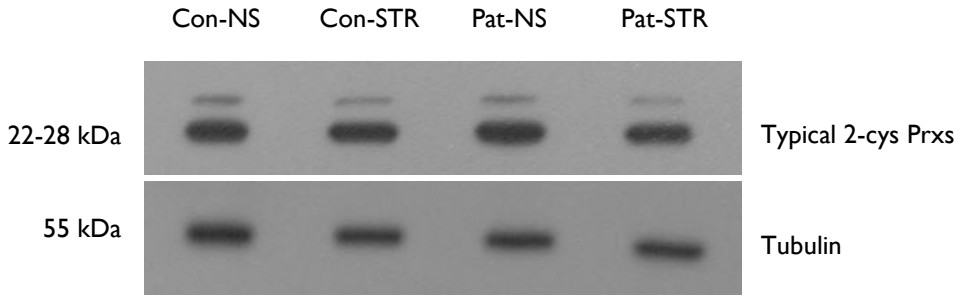

Figure 3.15: A) *Levels of total 2-cys Prxs were the same in whole cell preparations of non-stressed (NS) and stressed (STR) patient fibroblasts exposed to a non-saturating concentration of H_2O_2 for 15 min. Representative Western blots showing levels of total 2-cys Prxs in control (Con) and I113T SOD1-ALS patient (Pat) fibroblasts exposed to 30 μM H_2O_2 for 15 min (STR) or not (NS). One set of control and patient fibroblasts were exposed to 30 μM H_2O_2 for 15 min while the other set underwent parallel medium changes but had no H_2O_2 exposure. Three independent experiments were performed in each of the three fibroblast pairs. Whole cell lysates were Western blotted in duplicate for total typical 2-cys Prxs. Protein loads were 20 μg per lane. Total typical 2-cys Prxs blots were exposed for 2 min while tubulin blots were exposed for 1 min.*

B)

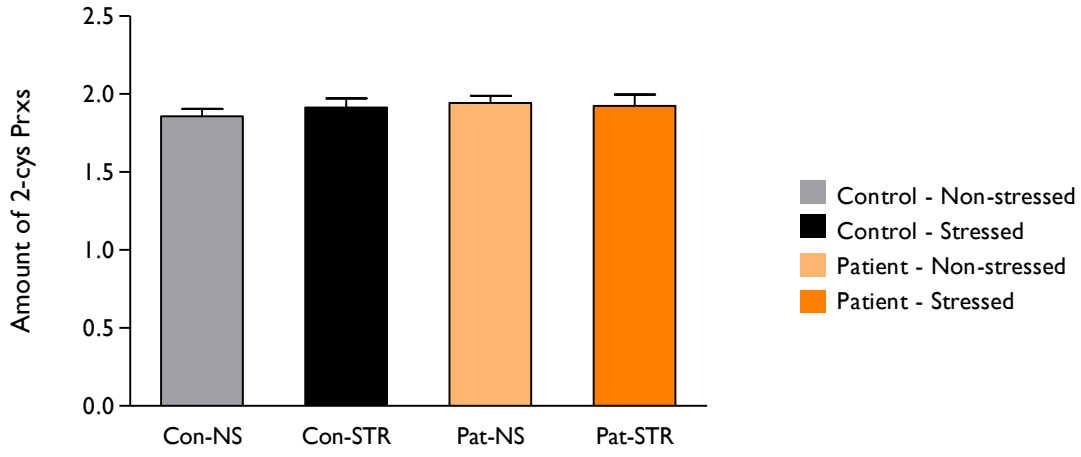

Figure 3.15: B) *Quantification of the levels of total typical 2-cys Prxs in control and I113T SOD1-ALS patient fibroblasts after they were subjected to a non-saturating oxidative stress of 30 μM H_2O_2 for 15 min. Densitometry values of the total typical 2-cys Prxs bands were normalized to their respective tubulin bands to correct for protein loading. Error bars represent the standard error of the mean (SEM) from two replicate blots in three independent experiments in each of the three fibroblast pairs. A Student's t-test showed no significant difference in the levels of typical 2-cys Prxs between non-stressed (NS) and stressed (STR) in whole cell preparations of both control and patient cells (p-value: 0.7788 for control cells, p-value: 0.8692 for patient cells).*

In summary, oxidative stress experiments conducted in the three pairs of I113T SOD1-ALS patient and healthy control fibroblasts at two different H_2O_2 concentrations (non-saturating – 30 μM and saturating – 300 μM) showed no difference in the levels of $PrxSO_{2/3}$ generated in patient and control fibroblasts. It was therefore evident, in the three pairs of fibroblast cell lines tested, that typical 2-cys Prxs were not overoxidized to a greater extent in I113T SOD1-ALS patient cells than in their matched control fibroblasts. Furthermore these results indicate that this absence of difference cannot be attributed to overoxidation of the typical 2-cys Prxs to saturation in patient and control cells.

3.6 Stress-recovery experiments

3.6.1 Recovery from overoxidation of typical 2-cys Prxs

Having determined that both patient and control fibroblasts appear to overoxidize their typical 2-cys Prxs to the same extent after exposure to both saturating and non-saturating concentrations of H_2O_2, I went on to examine the recovery of overoxidized typical 2-cys Prxs in the same cells after exposure to H_2O_2. My original hypothesis was that the typical 2-cys Prxs might exist in a more oxidized state in ALS than in health. This did not appear to be the case in our SOD1 ALS fibroblast model. Even if patient fibroblasts did not overoxidize their typical 2-cys Prxs to a greater extent than control fibroblasts after an oxidative stress, I wondered whether their typical 2-cys Prxs might recover less well from overoxidation, effectively spending more time in an overoxidized state than those of control cells.

In order to investigate this, the same three pairs of age- and sex-matched I113T SOD1-ALS patient and control fibroblasts were again subjected to a saturating oxidative stress (300 μM H_2O_2 for 15 min) as described in Chapter 2, Section 2.14.3. Levels of overoxidized typical 2-cys Prxs were measured by Western blotting of whole cell preparations made from cells harvested at various time-points after H_2O_2 washout over the subsequent 26 hours (Fig. 3.16 A). Three independent experiments were carried out in the three pairs of I113T SOD1-ALS patient and control fibroblasts. As before, protein bands on the resultant Western blots were quantified on the G-box (Fig. 3.16 B).

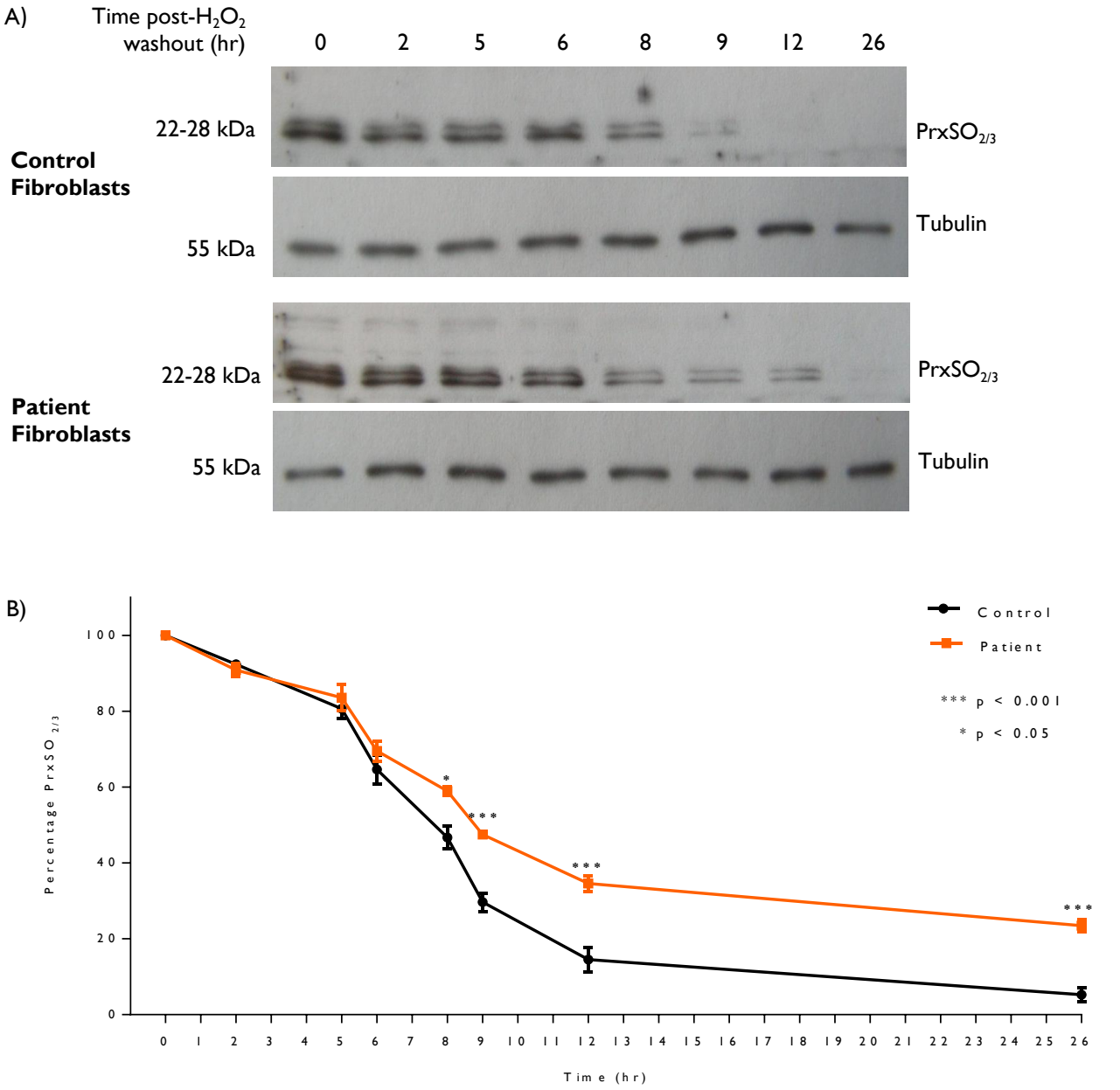

Figure 3.16: A) *Stress-recovery experiment. The disappearance of $PrxSO_{2/3}$ was delayed in patient fibroblasts compared to control cells. At 12 hours after H_2O_2-washout no $PrxSO_{2/3}$ was visible in control cells but $PrxSO_{2/3}$ bands were clearly detectable in patient cells with faint bands visible 26 hours post-washout. Representative Western blots showing the disappearance of $PrxSO_{2/3}$ in I113T SOD1-ALS patient and control fibroblasts after oxidative challenge as described in Section 3.6.1. Protein loads were 20 µg per lane. $PrxSO_{2/3}$ blots were exposed for 2 min and tubulin blots for 1 min.* ***B)*** *Graph showing the delay in disappearance of $PrxSO_{2/3}$ in I113T SOD1-ALS patient fibroblasts. Twenty-six hours after H_2O_2-washout, control fibroblasts have almost undetectable levels of $PrxSO_{2/3}$ whereas ~27 % of the $PrxSO_{2/3}$ generated by the original H_2O_2 exposure remained in patient cells. Data include 3 independent experiments carried out in each of the 3 fibroblast pairs blotted in triplicate. $PrxSO_{2/3}$ bands were first normalized to their respective tubulin bands to correct for protein loading and were then expressed as a percentage of the corrected $PrxSO_{2/3}$ values at t = 0. The dataset was analyzed using two-way ANOVA. At t = 8 * denotes a p-value of 0.0211, while at t = 9, t = 12 and t = 26 *** denotes p-values of 0.00043, 0.00031 and 0.00022 respectively. Error bars represent standard error of the mean (SEM).*

Western blotting for $PrxSO_{2/3}$ in the stress-recovery experiment showed a gradual disappearance of $PrxSO_{2/3}$ in both I113T SOD1-ALS patient and control fibroblasts over the 26 hour recovery period. The disappearance of $PrxSO_{2/3}$ was delayed in patient cells by several hours when compared to control cells and although control fibroblasts eventually cleared almost all of their $PrxSO_{2/3}$ this was not the case in the patient fibroblasts. The delay in the disappearance of $PrxSO_{2/3}$ from the patient samples was consistent across all three fibroblast pairs. At the end of the experiment, control fibroblasts contained levels of $PrxSO_{2/3}$ <5 % of those present immediately after H_2O_2 washout whereas at 26 hours, patient cells still contained ~27 % of the $PrxSO_{2/3}$ present immediately after washout. Analysis of the dataset using 2-way ANOVA showed that there was a statistically significant difference in the amount of $PrxSO_{2/3}$ present in patient and control cells at t = 8, t = 9, t = 12 and t = 26 hr after H_2O_2-washout.

3.6.2 Levels of total 2-cys Prxs during recovery from oxidative stress

The preparations made from the stress-recovery experiments described in Section 3.6.1 were next Western blotted for total typical 2-cys Prxs. This was to establish what was happening to typical 2-cys Prx levels overall at the same time as overoxidized 2-cys Prxs were gradually decreasing as the fibroblasts recovered from exposure to H_2O_2. Each of three independent preparations from the three pairs of I113T SOD1-ALS patient and control fibroblasts were Western blotted in duplicate for total typical 2-cys Prxs and for tubulin (Fig. 3.17 A overleaf). Protein bands were quantified using the G-box as previously (Fig. 3.17 B overleaf).

Western blotting of samples from the stress-recovery experiments for total typical 2-cys Prxs showed no statistically significant difference in levels between I113T SOD1-ALS patient and healthy control fibroblasts at any time point. Furthermore, levels of typical 2-cys Prxs increased (by 63%) between 6 and 8 hours post-H_2O_2 washout in both patient and control cells. This confirms that the gradual disappearance of $PrxSO_{2/3}$ from fibroblasts as they recovery from exposure to H_2O_2 demonstrated in Fig. 3.16 is not due to a parallel fall in total levels of typical 2-cys Prxs. This will be further considered in Chapter 6.

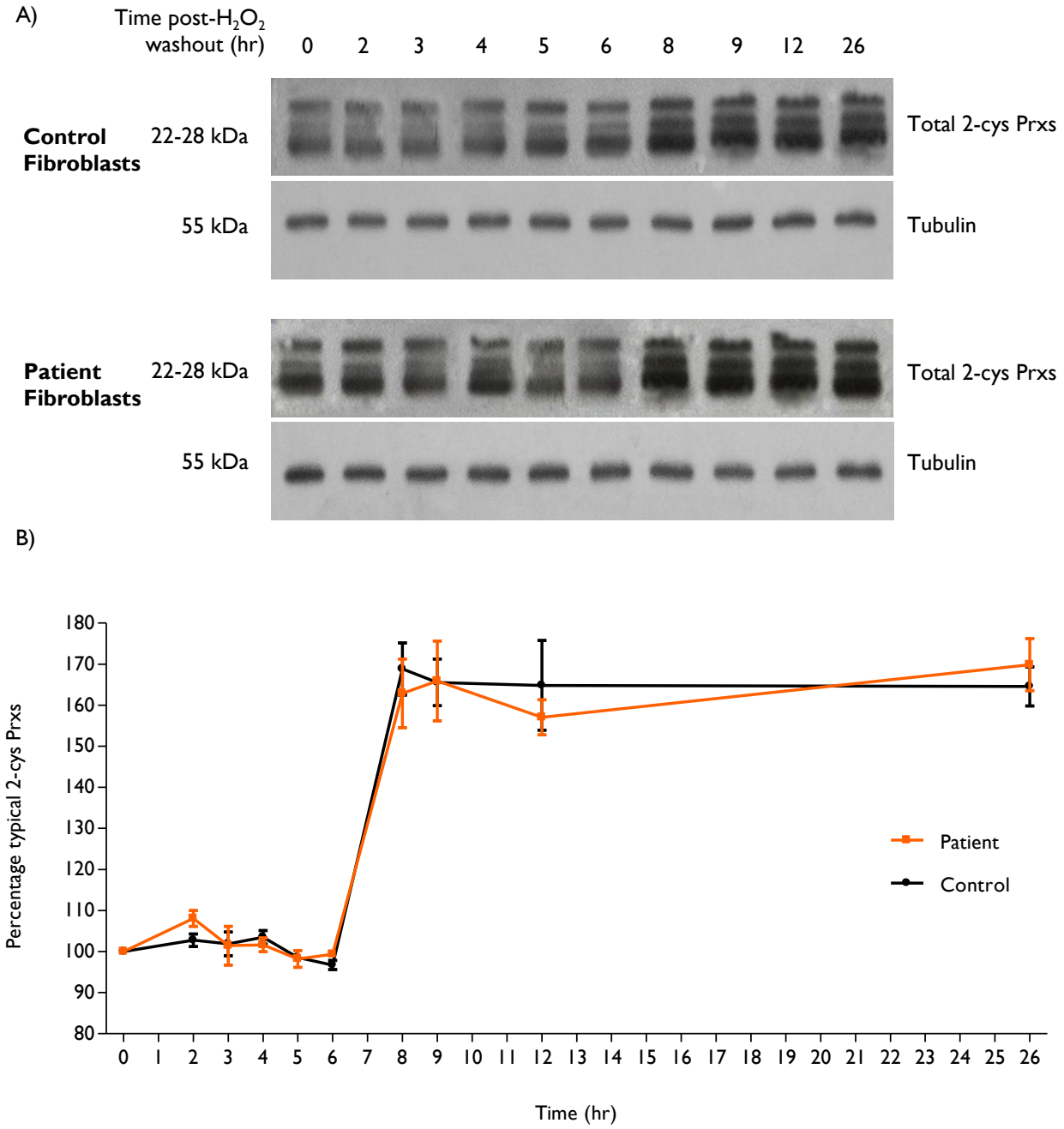

Figure 3.17: A) *Representative Western blots showing induction of total typical 2-cys Prxs in patient and control fibroblasts 6-8 hours after oxidative stress. The cells were stressed with 300 µM H_2O_2 for 15 min to overoxidize the 2-cys Prxs to saturation, H_2O_2 was washed out and the cells allowed to recover. Pairs of patient and control flasks were harvested at the time points indicated. Whole cell lysates were then Western blotted twice for total typical 2-cys Prxs and for tubulin. Protein loads were 20 µg per lane. Prx blots were exposed for 2 min, tubulin blots for 1 min.* ***B)*** *Quantification of total typical 2-cys Prx induction. Data include duplicate Western blots of three independent experiments in three pairs of fibroblasts. Densitometry values of the total typical 2-cys Prx bands were first normalized to those of their respective tubulin bands to correct for protein loading. These values were then expressed as a percentage of the corrected total typical 2-cys Prx value immediately after H_2O_2-washout at t = 0 hr. Statistical analysis using two-way ANOVA showed no statistically significant differences in the levels of total typical 2-cys Prxs at any time point or in the amount of induction of typical 2-cys Prxs between I113T SOD1-ALS patient and control fibroblasts. Error bars represent standard error of the mean (SEM).*

3.6.3 Levels of Prx regenerators during recovery from oxidative stress

In an effort to determine the cause of the delayed disappearance of $PrxSO_{2/3}$ in the I113T SOD1-ALS patient fibroblasts after an oxidative insult, levels of the two putative $PrxSO_{2/3}$ regenerators, sulfiredoxin 1 (Srx 1) and sestrin 2 (Sesn 2), were measured by Western blotting of the samples generated in the stress-recovery experiment (Fig. 3.18 and Fig. 3.19).

Western blotting for sulfiredoxin 1

Western blotting for Srx 1 in the stress-recovery experiment samples showed that after treatment with 300 μM of H_2O_2 both patient and control cells mounted an induction of Srx 1 after some hours. This induction was delayed and reduced in the patient cells when compared with healthy control cells (Fig. 3.18 A). Quantification of Srx 1 levels showed that the onset of Srx 1 induction occurred significantly later in the patient fibroblasts than in the control fibroblasts and that this induction was significantly less in the patient fibroblasts than in the control cells (Fig. 3.18 B).

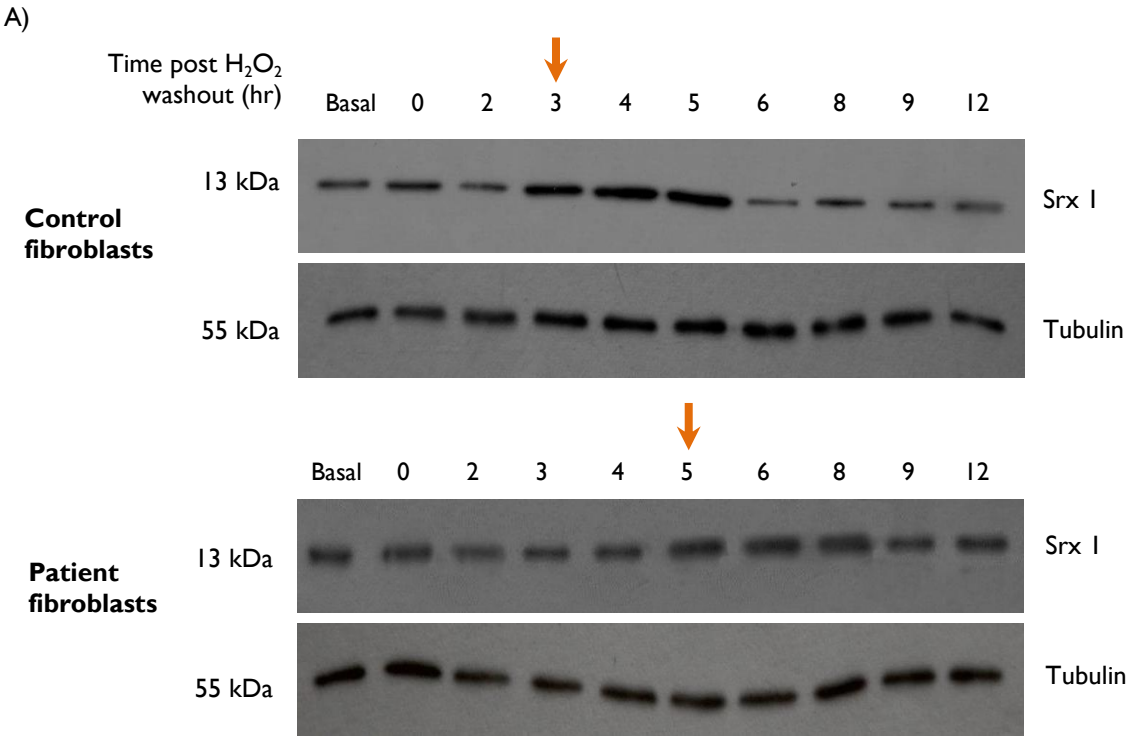

Figure 3.18: A) *Induction of Srx 1 was both delayed (orange arrows) and reduced in I113T SOD1-ALS patient fibroblasts compared to healthy control fibroblasts after exposure to 300 μM H_2O_2 for 15 min. Representative Western blots showing levels of Srx 1 induction in I113T SOD1-ALS patient fibroblasts and control fibroblasts in a stress-recovery experiment. Three independent experiments were carried out in each of three fibroblast pairs. The cells were stressed with 300 μM H_2O_2 for 15 min to overoxidize the typical 2-cys Prxs to saturation. Hydrogen peroxide was washed out and the cells were allowed to recover over the next 26 hours. Pairs of patient and control flasks were harvested at the time points indicated previously, whole cell preparations were made and the samples up to 12 hours post H_2O_2-washout were Western blotted for Srx 1 and tubulin. Protein loads were 40 μg per lane. Srx 1 blots were exposed for 3 min, tubulin blots for 1 min.*

B)

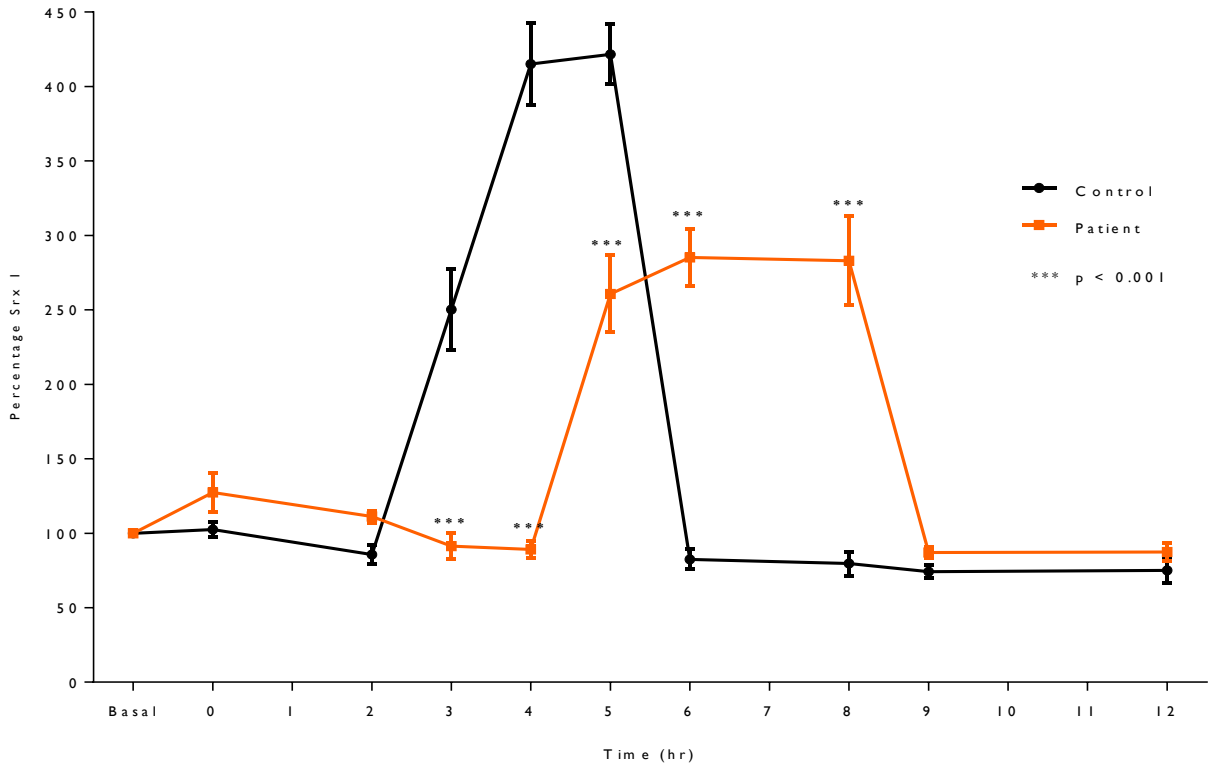

Figure 3.18: B) *Graph showing reduced and delayed induction of Srx 1 in I113T SOD1-ALS patent fibroblasts compared to healthy control fibroblasts after oxidative challenge. Control fibroblasts mounted a Srx 1 induction three hours after H_2O_2-washout while the Srx 1 induction in patient fibroblast occurred approximately 2 hours later. Data from 3 independent experiments each in three fibroblast pairs with each experiment Western blotted in duplicate. Densitometry values for Srx 1 bands were first normalized to those of their respective tubulin bands to correct for protein loading. Corrected Srx 1 values were then expressed as a percentage of corrected basal values. Two-way ANOVA was used to analyze the dataset. At t = 3, t = 4, t= 5, t = 6 and t = 8 hours *** denotes p-values of 0.00075, 0.00022, 0.00053, 0.00037 and 0.00019 respectively. Error bars represent standard error of the mean (SEM).*

In summary, Western blotting of patient and control fibroblasts had earlier shown no difference in basal levels of the Prx regenerator Srx 1 (Section 3.2.3) nor any difference in levels immediately after washout of a hydrogen peroxide challenge (Section 3.6.3). Western blotting for Srx 1 in the stress-recovery experiments, however, revealed that there was an induction in Srx 1 after H_2O_2 treatment in both patient and control fibroblasts some hours after washout. The induction of Srx 1 in patient cells, however, was delayed by approximately two hours. Control fibroblasts began to show increased levels of Srx 1 between 2 and 3 hours post-washout with the induction reaching a peak at 5 hours, whereas patient fibroblasts first showed an increase in Srx 1 levels between 4 and 5 hours post-washout with maximum Srx 1 levels reached at 6 hours post-washout. The increase in Srx 1 levels achieved by patient fibroblasts moreover

was less than that achieved by control cells. Statistical analysis showed that both the delayed induction of Srx 1 and the levels of induced Srx 1 observed in the patient cells were both significantly different to those in the control fibroblasts. The maximum induced levels of Srx 1 achieved in the I113T SOD1-ALS patient fibroblasts at (t = 8) were 42% less than those achieved in the healthy control fibroblasts (t = 5) and this difference was statistically significant (*p-value* 0.0012). It is also interesting to note that in both patient and control cell lines Srx 1 induction occurred well before the disappearance of $PrxSO_{2/3}$ (Fig. 3.16).

Western blotting for sestrin 2

The levels of sestrin 2 were then measured in the same samples (up to 12 hours post-H_2O_2-washout) from the stress-recovery experiments, again by Western blotting (Fig. 3.19 A). Duplicate Western blots for Sesn 2 and for actin, to serve as a loading control (see Section 3.1.1), were performed in each of the three independent experiments done in each of the three pairs of I113T SOD1-ALS patient and control fibroblasts. Quantification of the resultant bands was done using the G-box as before (Fig. 3.19 B).

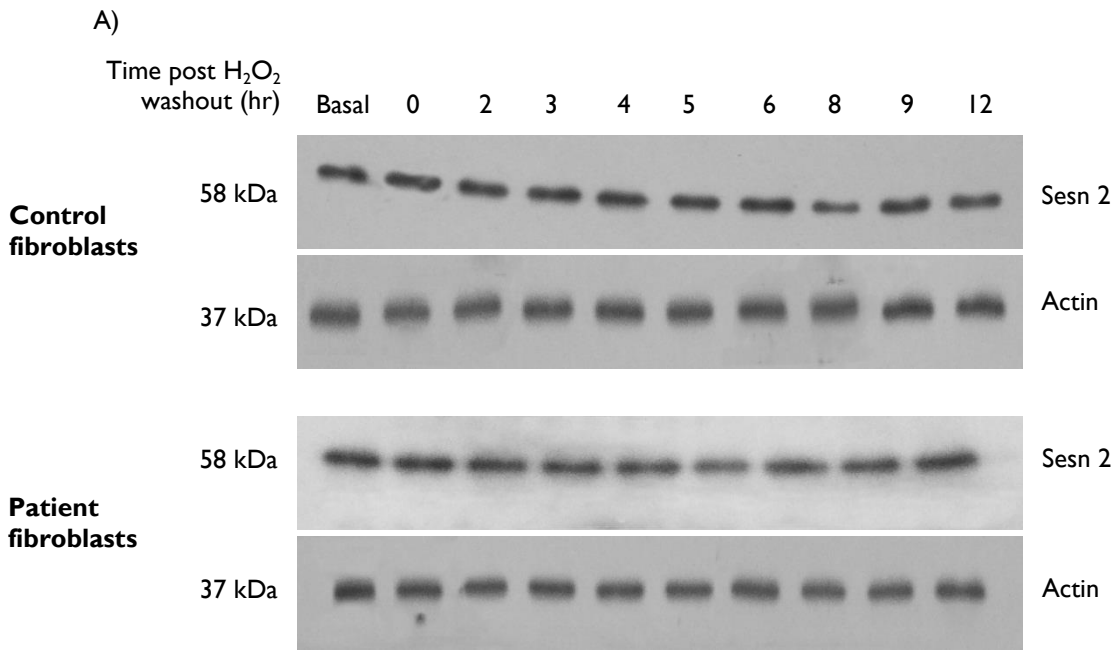

Figure 3.19: A) *Levels of Sesn 2 in I113T SOD1-ALS patient and control fibroblasts did not change after exposure to 300 μM H_2O_2 for 15 min, washout and 12 hours recovery. Representative Western blots showing levels of Sesn 2 in I113T SOD1-ALS patient fibroblasts and control fibroblasts in a stress-recovery experiment. Three independent experiments were carried out in each of three fibroblast pairs. The cells were stressed with 300 μM H_2O_2 for 15 min to overoxidize the 2-cys Prxs to saturation, H_2O_2 was washed out and the cells were allowed to recover for 26 hours. A pair of patient and control flasks was harvested at the time points indicated in Fig. 3.16 and whole cell preparations were made. Time points up to 12 hours post-washout were then blotted for Sesn 2 and actin. No difference was evident in levels of Sesn 2 in either patient or control fibroblasts at any time point. Protein loads were 20 μg per lane. Sesn 2 blots were exposed for 2 min, actin blots for 1 min.*

B)

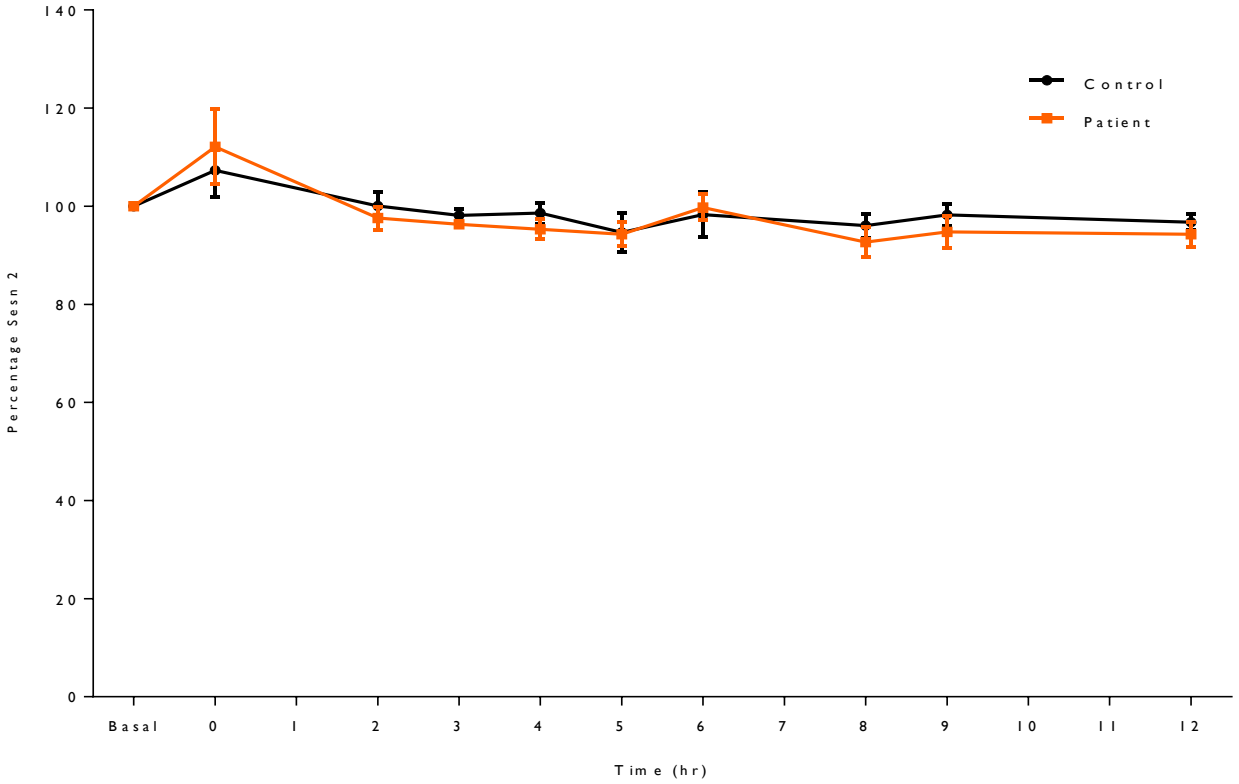

Figure 3.19: B) *There was no change in the level of Sesn 2 in either I113T SOD1-ALS patient or healthy control fibroblasts at any time point after H_2O_2-washout in the stress-recovery experiments. Data include 3 independent experiments in each of three fibroblast pairs, Western blotted twice per experiment. Densitometry values for Sesn 2 bands were first normalized to those of their respective actin bands to correct for protein loading. Corrected Sesn 2 values were then expressed as a percentage of corrected basal Sesn 2 values (experiment time point = basal). Two-way ANOVA was applied to the data and it indicated that there was no significant difference in Sesn 2 levels at any time point between patient and controls. Error bars represent standard error of the mean (SEM).*

In conclusion, Western blotting for Sesn 2 of samples generated by the stress-recovery experiments did not show 1) any change in Sesn 2 at any time-point after H_2O_2-washout in either patient or control fibroblasts; or 2) any difference in levels of Sesn 2 between patient and control fibroblasts at any time point after H_2O_2-washout. In short, levels of Sesn 2 remained the same in both control and patient samples and the same as basal throughout. Although there was an apparent increase in Sesn 2 levels in the patient fibroblasts immediately after H_2O_2-washout (experimental time point t = 0), this increase was only seen in one fibroblast pair and overall the Sesn 2 level in the patient fibroblasts at this time-point was not statistically different to that observed in control cells.

3.6.4 Levels of activator protein-1 (a Srx 1 transcription factor) in the stress-recovery experiments

With the consistent delay in the onset of Srx 1 induction and the reduced levels of Srx 1 induced in patient cells after H_2O_2 exposure, it seemed likely that this apparently defective response to oxidative challenge in I113T SOD1-ALS fibroblasts might at least partially underlie the delay in disappearance of overoxidized typical 2-cys Prxs from these cells. As no change in the levels of the other putative regenerator Sesn 2 were observed in the stress-recovery experiments and the more recent literature provided strong evidence that Sesn 2 two might not in fact act to reduce $PrxSO_{2/3}$ back to a reduced, active form (Rhee et al., 2009), I next decided to focus my efforts on the investigation of the molecular pathways responsible for the induction of Srx 1.

A)

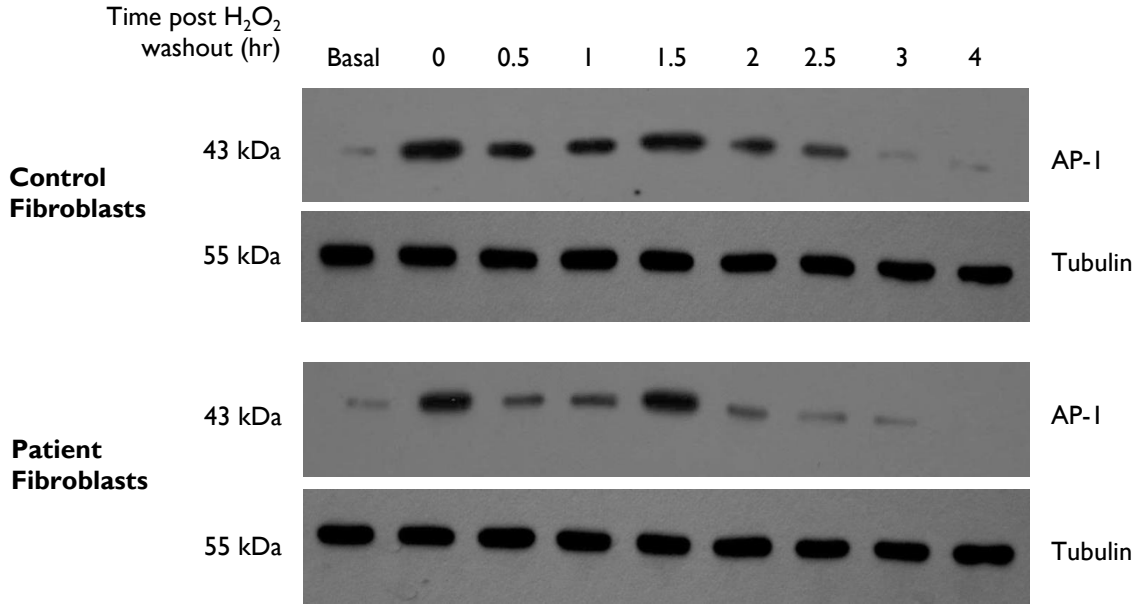

Figure 3.20: A) *Lower levels of phosphorylated c-jun, standing in for activated AP-1, were observed in I113T SOD1-ALS patient fibroblasts than in healthy control fibroblasts in the 4 hours after H_2O_2-washout. Representative Western blots showing the biphasic induction of AP-1 in I113T SOD1-ALS patient and control fibroblasts after 15 min treatment with 300 μM H_2O_2 then washout and recovery over 26 hours. Whole cell preparations obtained at the time-points indicated were then blotted for phosphorylated c-jun. Three independent experiments were carried out in each of the three fibroblast pairs with pairs of patient and control flasks harvested at the time points indicated. Levels of activated AP-1 increased rapidly in both control and patient fibroblasts at t = 0 and 1.5 hours after H_2O_2-washout. This induction appeared to be less pronounced in the patient fibroblasts. Protein loads were 20 µg per lane. AP-1 blots were exposed for 2 min and tubulin blots for 1 min.*

As has been discussed in Chapter 1, Section 1.14.1, one of the two known transcription factors believed to regulate Srx 1 levels is activator protein-1 (AP-1). The pathway by which AP-1 is generated in response to an oxidative stress and goes on to induce Srx 1 transcription is summarized in Fig. 1.6 also to be found in Chapter 1. Using an antibody to the phosphorylated form of c-jun that acts as a proxy for the activated

form of the transcription factor AP-1 (Lan et al., 2012), the whole cell lysates generated from new stress-recovery experiments that included more point points (see Chapter 2, Section 2.14.3) were Western blotted to determine whether levels of phosphorylated c-jun (and by extension activated AP-1) were different in patient and control fibroblasts as they recovered from exposure to H_2O_2 (Fig. 3.20 A). Western blotting for phosphorylated c-jun/AP-1 was carried out in duplicate in the three independent experiments performed in each of the three fibroblast pairs. Quantification of intensities of the bands was done on G-box as previously (Fig. 3.20 B).

B)

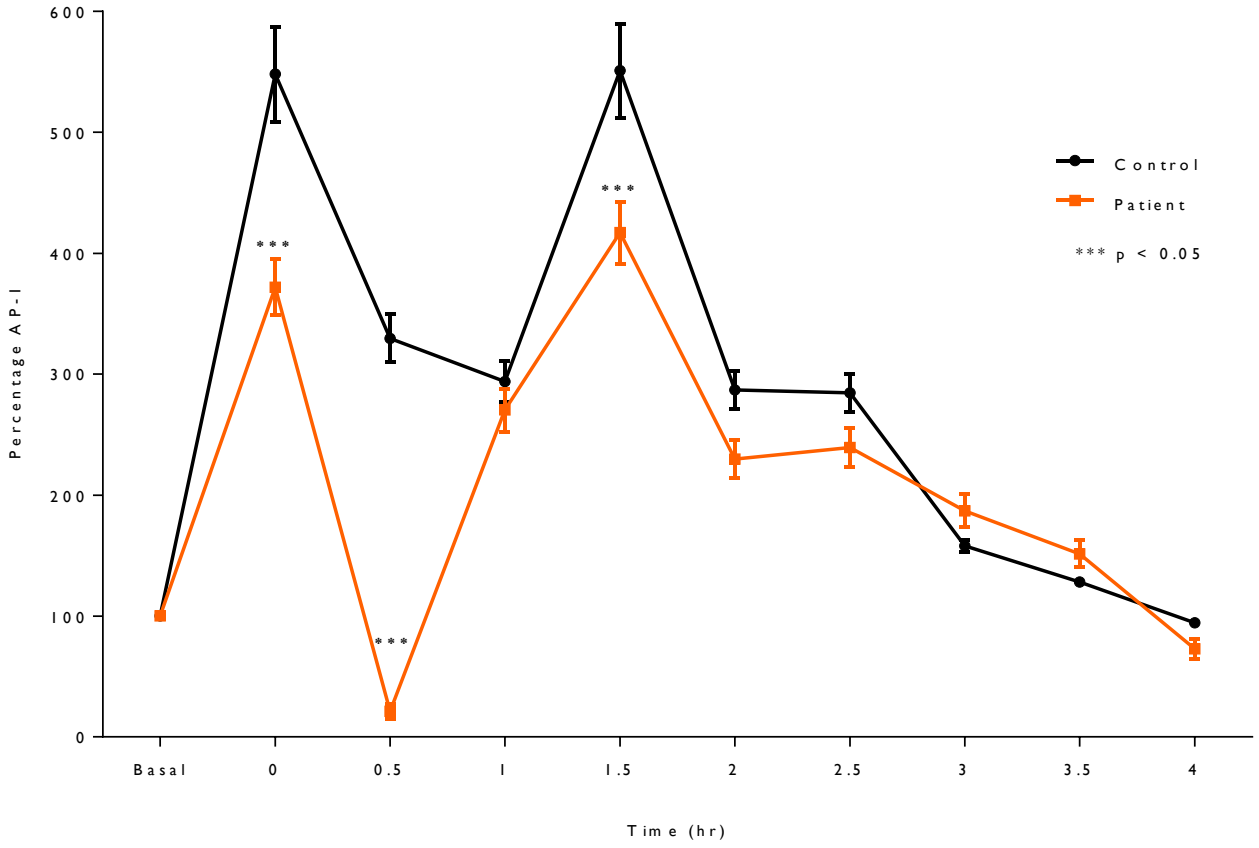

Figure 3.20 B): *Graph showing the biphasic induction of activated AP-1 in both I113T SOD1-ALS patient and control fibroblasts in the first 4 hours after oxidative challenge. Both increases in AP-1 were lower in the patient fibroblasts than the controls. Data include duplicate blots of 3 independent experiments, in three independent pairs of fibroblasts. Densitometry values for AP-1bands were first normalized to those of their respective tubulin bands to correct for protein loading. Corrected AP-1 levels were then expressed as a percentage of corrected basal AP-1 levels (experiment time point = basal). Two-way ANOVA was used analyze the dataset and showed that there was a statistically significant difference between AP-1 levels at the peak of both inductions and also during the trough in AP-1 levels between them. At t = 0, t = 0.5 and t = 1.5 hours *** denotes p-values of 0.0151, 0.0045 and 0.0109 respectively. Error bars represent standard error of the mean (SEM).*

Western blotting for phosphorylated c-jun/activated AP-1 showed a biphasic induction in the levels of AP-1 which peaked at 0 and at 1.5 hours after H_2O_2-washout in both I113T SOD1-ALS patient and control fibroblasts. Unlike the post-H_2O_2 induction of Srx 1 which was delayed in patient cells, the biphasic activation of AP-1 occurred synchronously in patient and control fibroblasts. The maximum AP-1 level reached in each induction peak, however, was lower in patient fibroblasts than in controls, as was the trough in levels between the two peaks. Quantification of the data and subsequent statistical analysis confirmed that the differences in AP-1 activation at t = 0, t = 0.5 and t = 1.5 hours after H_2O_2-washout between patient and control fibroblasts were statistically significant (*p-value*s: 0.0151, 0.0045 and 0.0109 respectively). The peak levels of activated AP-1 (at t = 1.5) in patients were less by 24 % in comparison to that of the control cells and this difference was statistically significant (*p-value*: 0.0109). Both peaks in AP-1 activation occurred prior to the induction of Srx 1 (at 2-3 hours post-washout in control cells and at 4-5 hours post-washout in patient cells).

3.7 Effect of cycloheximide (CHX) on stress-recovery experiments

To verify whether the recovery of overoxidized Prxs was dependent upon the synthesis of new protein, the stress-recovery experiments were repeated in two sets of patient and control fibroblasts. One set was pre-treated with the translational blocking agent cycloheximide (CHX) prior to the stress-recovery experiment; the other set was not pre-treated undergoing only parallel medium changes. After CHX pre-treatment of one set of cells, both CHX and control sets were exposed to a saturating oxidative stress (300 µM H_2O_2 for 15 min) as previously described in Chapter 2, Section 2.14.3 and were allowed to recover over 26 hours as before. Levels of overoxidized Prxs and Srx 1 were analyzed by Western blotting in whole cell preparations made at t = 0, t = 2, t = 5, t = 6, t = 8, t = 9, t = 12 and t = 26 hours after H_2O_2 washout. One experiment was performed in each of two pairs of I113T SOD1-ALS patient and control fibroblasts and the samples generated blotted in duplicate for $PrxSO_{2/3}$ (Fig. 3.21 A) and Srx 1 (Fig. 3.22 A). The resultant Western blots were quantified using the G-box as before and $PrxSO_{2/3}$ and Srx 1 levels, corrected for protein loading, were plotted against time (Fig. 3.21 B and Fig. 3.22 B respectively).

3.7.1 Western blotting for $PrxSO_{2/3}$ in stress-recovery experiments after CHX pre-treatment

A)

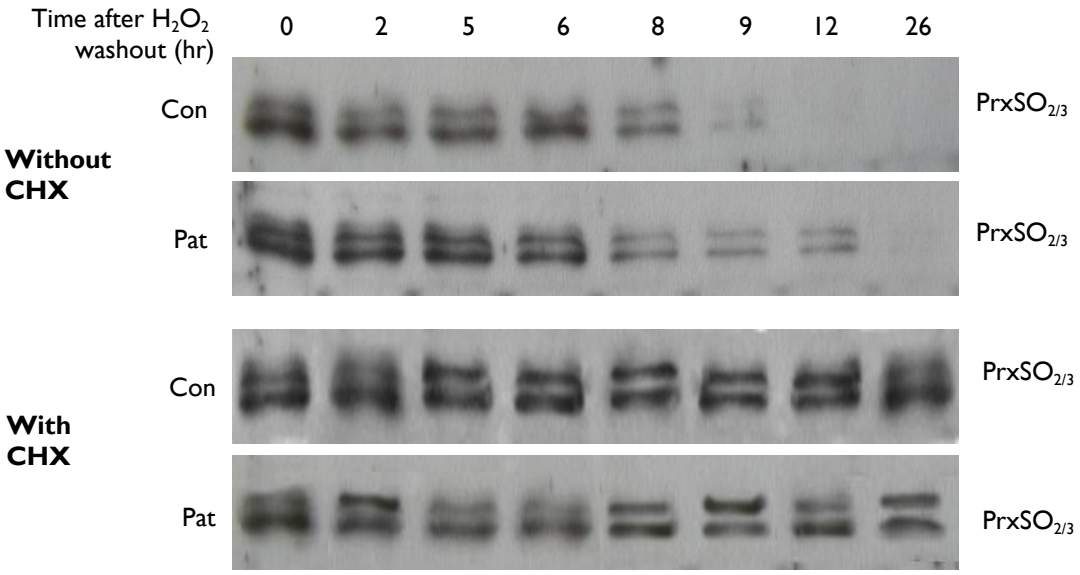

Fig. 3.21: A) *Pre-treatment with CHX abolished the disappearance of $PrxSO_{2/3}$ in I113T SOD1-ALS patient (Pat) and control (Con) fibroblasts after treatment for 15 min with 300 μM H_2O_2 (bottom two panels). Without CHX pre-treatment, $PrxSO_{2/3}$ gradually disappeared, doing so more slowly in the patient cells than the control cells, consistent with previous experiments (top two panels). One experiment was performed in two sets each of two pairs of control and patient fibroblasts and samples Western blotted in duplicate for $PrxSO_{2/3}$ and tubulin. For each experiment, one set of cells was pre-treated with CHX for 1 hour before exposure to 300 μM H_2O_2 for 15 min to overoxidize the 2-cys Prxs to saturation. The other set of cells underwent parallel medium changes only, serving as non-stressed controls. After H_2O_2 washout both sets of cells were then allowed to recover for 26 hours. Cells were harvested at the time points indicated. Protein loads were 20 μg per lane. $PrxSO_{2/3}$ blots were exposed for 2 min, tubulin blots for 1 min (not shown).*

Pre-treatment of patient and control fibroblasts with a blocker of protein translation prior to exposure to a saturating concentration of H_2O_2 had a marked effect on the subsequent disappearance of overoxidized typical 2-cys Prxs in the hours after washout. Western blotting for $PrxSO_{2/3}$ showed an initial reduction in $PrxSO_{2/3}$ levels between t = 0 and t = 12 hours after H_2O_2-washout of 28% but no further reduction in $PrxSO_{2/3}$ was then seen. $PrxSO_{2/3}$ levels were all-but identical in patient and control cells throughout the 26 hour recovery period. In contrast, fibroblasts that were not pre-treated with CHX prior to H_2O_2 exposure demonstrated a much faster and much more complete disappearance of $PrxSO_{2/3}$ consistent with earlier stress-recovery experiments (Fig. 3.16). The previously identified delay in $PrxSO_{2/3}$ disappearance in patient fibroblasts was also reiterated.

B)

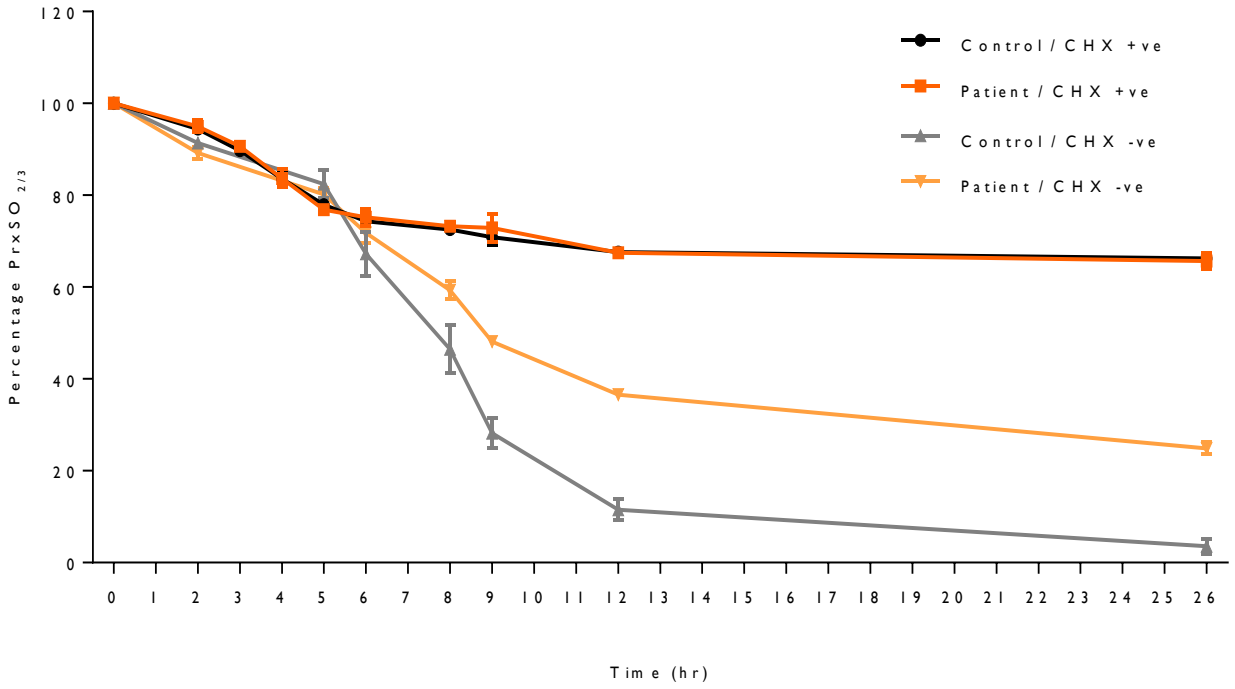

Figure 3.21: B) *Graph showing the quantified levels of $PrxSO_{2/3}$ in I113T SOD1-ALS patient and control fibroblasts in the 26 hours after H_2O_2 washout of in stress-recovery experiments conducted with and without CHX pre-treatment as described in Fig. 3.21 A. Data include two duplicate Western blots of one experiment carried out in two pairs of patient and control fibroblasts. Densitometry values of $PrxSO_{2/3}$ bands were first normalized to those of their respective tubulin bands to correct for protein loading and were then expressed as a percentage of the corrected $PrxSO_{2/3}$ values at t = 0, immediately after H_2O_2-washout. In the fibroblasts pre-treated with CHX there was a fall in $PrxSO_{2/3}$ of 28% in both patient and control cells between t = 0 and 12 hr after washout. Two-way ANOVA showed no significant difference in the levels of $PrxSO_{2/3}$ between patient and control cells pre-treated with CHX at any time point. In the set of cells not treated with CHX prior to H_2O_2 exposure, levels of $PrxSO_{2/3}$ fell much more significantly and did so more quickly in control cells than in patient cells reiterating the results of previous stress-recovery experiments (Fig. 3.16). Error bars represent standard error of the mean (SEM).*

3.7.2 Western blotting for Srx 1 in stress-recovery experiments after CHX pre-treatment

The effects of blocking *de novo* protein synthesis on Srx 1 levels in the recovery period after exposure to a saturating oxidative stress were then studied. Whole cell preparations made from samples obtained from each of the CHX stress-recovery experiments carried out as described in the previous section were Western blotted in duplicate for Srx 1 (Fig. 3.22 A) and tubulin (blots not shown). Quantification of the proteins bands was done using the G-box as before and the values, corrected for protein loading, were plotted against time (Fig. 3.22 B).

A)

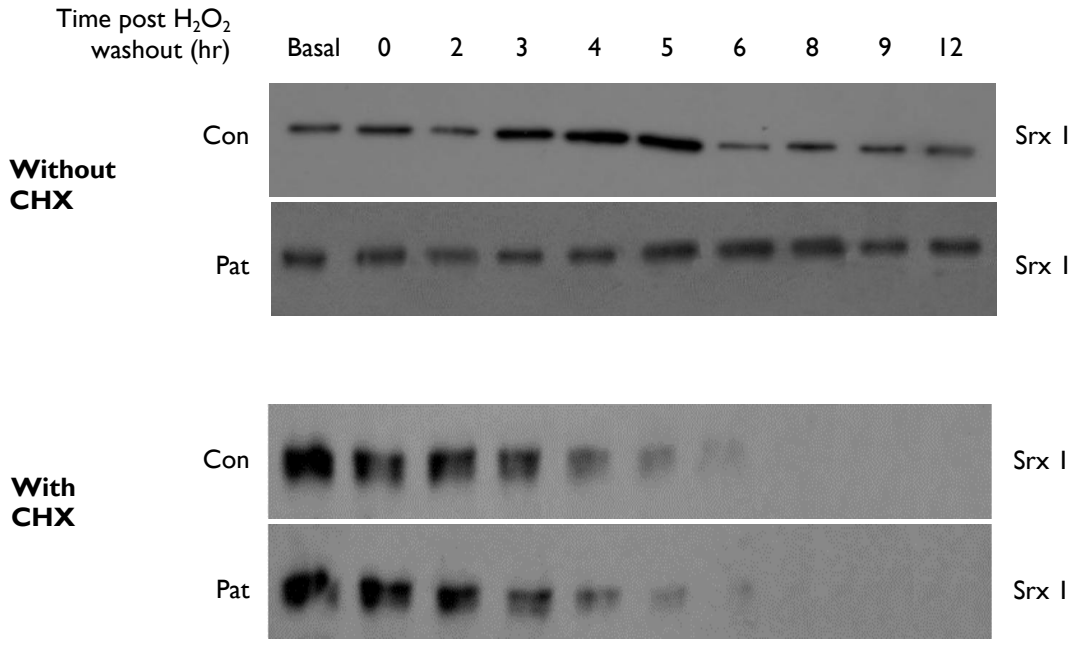

Figure 3.22: A) *Pre-treatment with CHX abolished the induction of Srx 1 in both I113T SOD1-ALS patient and control fibroblasts in response to treatment for 15 min with 300 μM H_2O_2. Srx 1 levels instead gradually fell in the 12 hours after H_2O_2 wash-out. In the control set of cells, which were not pre-treated with CHX, the delayed and reduced induction of Srx 1 observed previously in patient cells when compared to control cells was reiterated. Representative Western blots showing a failure of Srx 1induction in I113T SOD1-ALS patient and control fibroblasts in response to an oxidative stress. One experiment was performed in each of two fibroblast pairs. One set of cells was pre-treated with CHX for 1 hour before exposure to 300 μM H_2O_2 for 15 min to overoxidize the 2-cys Prxs to saturation. After H_2O_2 wash-out, cells were allowed to recover over 26 hours with pairs of patient and control flasks harvested at the time-points indicated. A second, control, set of cells was not pre-treated with CHX but otherwise underwent an identical treatment. Protein loads were 40 μg per lane. Srx 1 blots were exposed for 2 min, tubulin blots for 1 min.*

Pre-treatment of both patient and control fibroblasts with a translational blocker, cycloheximide, abolished the induction of Srx 1 that occurs in response to a saturating oxidative challenge in the absence of CHX. After CHX pre-treatment there was a gradual decrease in Srx 1 levels over the 12 hours following H_2O_2-washout that was identical in patient and control cells.

B)

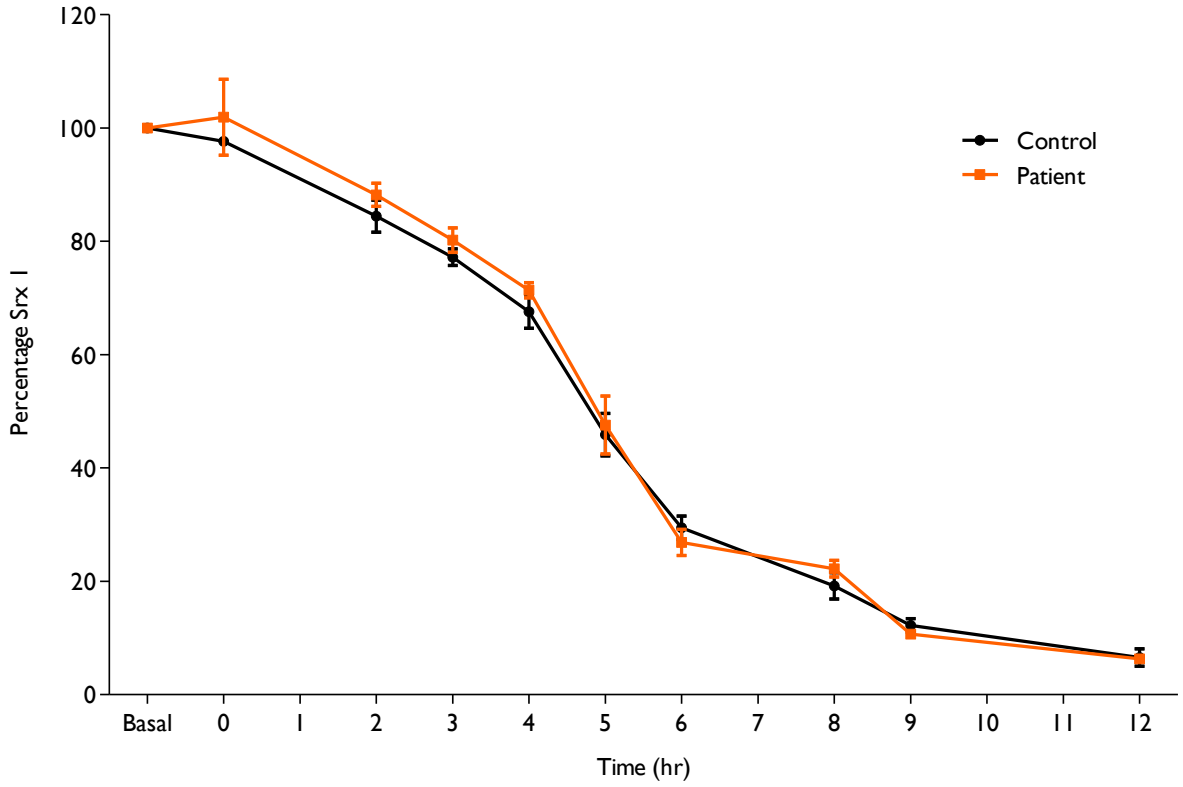

Figure 3.22: B) *Graph showing an absence of Srx 1 induction and the gradual disappearance of Srx 1 in both I113T SOD1-ALS patient and control fibroblasts in the stress-recovery experiments when pre-treated with CHX. Experiments were carried out as described in Fig. 3.21 A with samples Western blotted for $PrxSO_{2/3}$ and tubulin. Densitometry values for the Srx 1 bands were first normalized to those of their respective tubulin bands to correct for protein loading. Corrected Srx 1 values were then expressed as a percentage of corrected basal Srx 1 values (experiment time point = basal). Two-way ANOVA was performed and no statistically significant difference in Srx 1 levels were observed between the control and patient cells. Error bars represent standard error of the mean (SEM).*

In conclusion, the stress-recovery experiments conducted in human fibroblasts with and without CHX pre-treatment confirmed that recovery of overoxidized typical 2-cys Prxs was a process dependent upon new protein synthesis. The induction of the $PrxSO_{2/3}$ regenerator Srx 1 in response to an oxidative challenge was, moreover, abolished by CHX pre-treatment. The significance of these findings is discussed in Chapter 6, Section 6.5.

3.8 Two-hit stress-recovery experiments

In order to determine whether recurrent exposures to a non-saturating oxidative stress cause greater overoxidation of typical 2-cys Prxs in I113T SOD1-ALS patient fibroblasts than in healthy control cells, I next investigated the effects of sequential non-saturating H_2O_2 exposures on the three pairs of control and I113T SOD1-ALS fibroblasts. Two-hit stress-recovery experiments were carried out in which each pair of control and patient fibroblasts was subjected to two sequential exposure to 30 µM H_2O_2 for 15 minutes prior to washout and recovery (Chapter 2, Section 2.14.4). The two exposures were separated by 16 hours by which time no residual $PrxSO_{2/3}$ was detectable after the first oxidative challenge. The two-hit stress-recovery experiments were conducted twice on each of the three fibroblast pairs and the levels of $PrxSO_{2/3}$ determined by Western blotting (Fig. 3.23 A). Western blotting was performed in triplicate for each independent experiment and levels of $PrxSO_{2/3}$ were quantified on the G-box (Fig 3.23 B).

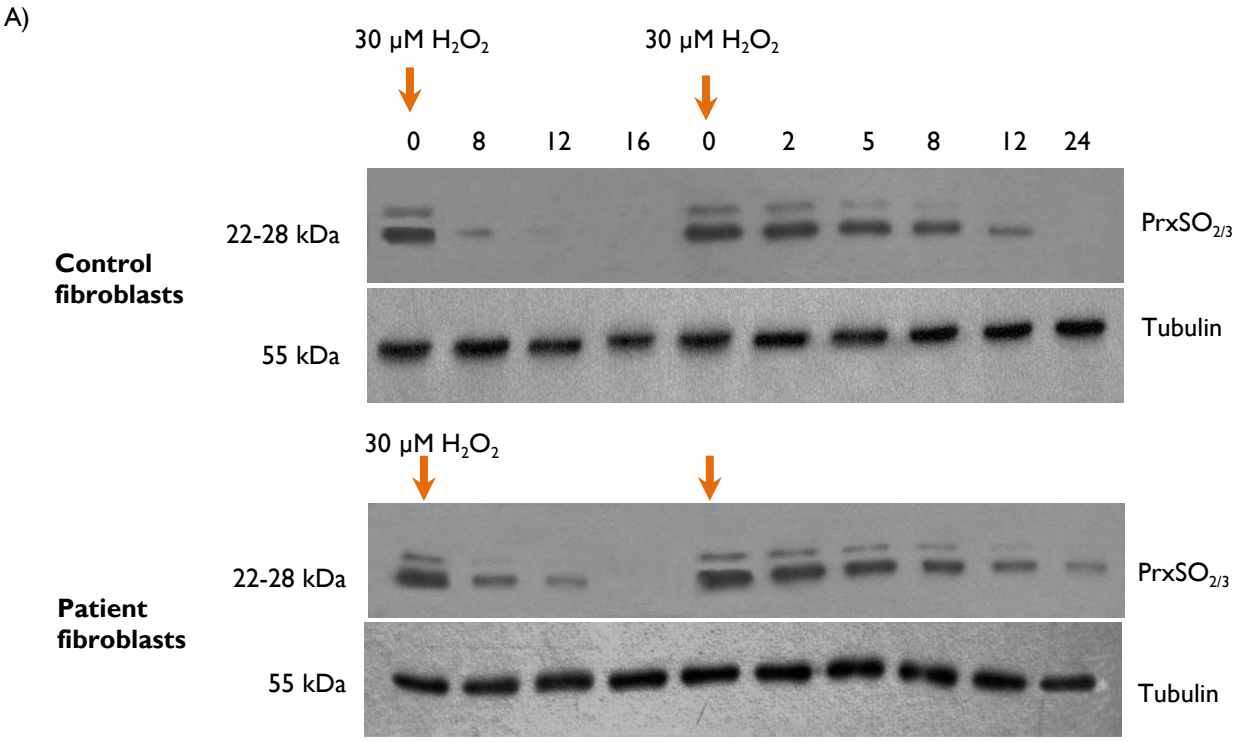

Figure 3.23: A) *Two hit stress-recovery experiment showing an exaggerated delay in the disappearance of $PrxSO_{2/3}$ in patient fibroblasts when compared to healthy control fibroblasts after a second non-saturating exposure to H_2O_2. Representative Western blot showing the disappearance of $PrxSO_{2/3}$ in I113T SOD1-ALS patient and control fibroblasts after two sequential 15 min exposures to 30 µM H_2O_2 16 hours apart. The two-hit stress-recovery experiment was conducted twice in each of the three pairs of control and I113T patient fibroblasts. Cells were first exposed to 30 µM H_2O_2 for 15 minutes (orange arrow), the H_2O_2 was washed out and the cells allowed to recover over the following 16 hours. Control and patient fibroblasts were then exposed for a second time to 30 µM H_2O_2 16 hours after the washout of the first stress (orange arrow). Samples were harvested at the time-points after H_2O_2 washout indicated after each H_2O_2 exposure. Protein loads were 20 µg per lane. $PrxSO_{2/3}$ blots were exposed for 2 min, tubulin blots for 1 min.*

B)

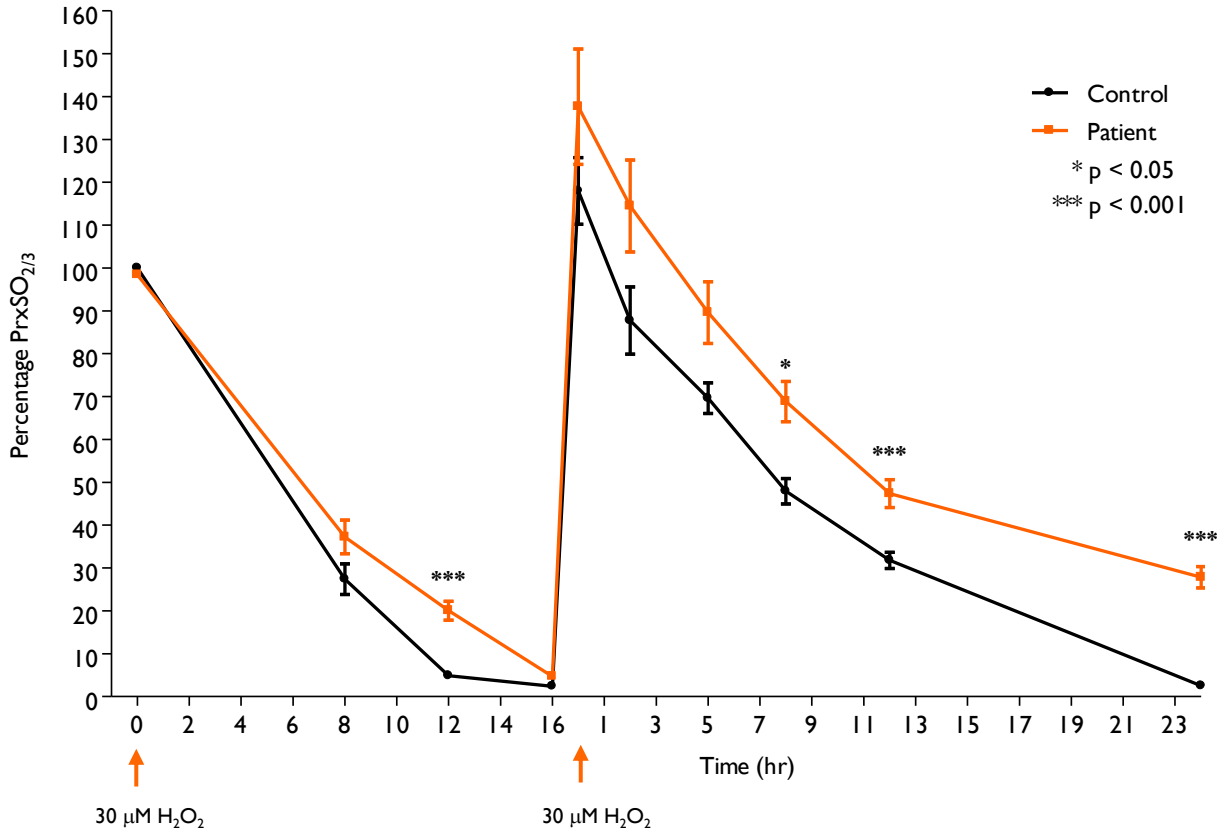

Figure 3.23: B) *Graph showing the exaggerated delay in the disappearance of $PrxSO_{2/3}$ from I113T SOD1-ALS patient fibroblasts compared to that in control cells after a second, non-saturating, exposure to 30 μM H_2O_2 in the two-hit stress-recovery experiments. The disappearance of $PrxSO_{2/3}$ takes longer after the second H_2O_2 exposure in both control and patient cells but this prolongation is much greater in the patient fibroblasts. Indeed, at 48 hours when the experiment was concluded levels of $PrxSO_{2/3}$ in control cells had fallen to almost zero but levels in the patient cells were still 29 % of those immediately after washout of the second H_2O_2 treatment. Data include 3 replicate blots in two independent experiments in the three fibroblast pairs. Densitometry values of the $PrxSO_{2/3}$ bands were first normalized to those of their respective tubulin bands to correct for protein loading and were then expressed as a percentage of the corrected $PrxSO_{2/3}$ value immediately after washout of the first stress (experimental time-point t = 0 after the first stress). Two-way ANOVA was performed to analyze the data set. From left, at t=12 *** denotes a p-value of 0.00034, at t=8 *denotes a p-value of 0.0143 while at t=12 and t=24 *** denote p-values of 0.00033 and 0.00017 respectively. Error bars represent standard error of the mean (SEM) from triplicate blots in two independent experiments in three fibroblast pairs.*

The two-hit stress-recovery experiments showed that even when challenged the first time with 30 μM H_2O_2, an oxidative challenge that does not overoxidized the typical 2-cys Prxs present in the cells to saturation, the disappearance of $PrxSO_{2/3}$ was slower in I113T SOD1-ALS patient fibroblasts than in those from healthy controls. This is evident from the representative Western blot in Fig. 3.23 A as well as from

the graph of the quantified data (Fig. 3.23 B). At 12 hours after H_2O_2-washout, $PrxSO_{2/3}$ levels were 6% of those immediately after washout in control cells but 23% in patient cells. This difference was statistically significant (*p-value* = 0.0011). By 16 hours after the first exposure to 30 μM H_2O_2, however, the $PrxSO_{2/3}$ in both patient and control cells had almost completely disappeared. This is in contrast to the time taken for $PrxSO_{2/3}$ to disappear after fibroblasts were challenged with 300 μM H_2O_2, a saturating oxidative stress, where $PrxSO_{2/3}$ had almost disappeared by 26 hours after H_2O_2-washout whilst at 26 hours after washout patient cells still contained at $PrxSO_{2/3}$ at 29% of the amount measured immediately after H_2O_2-washout (Fig. 3.16). It appears from the comparison between these two stress-recovery experiments that the greater the concentration of H_2O_2 applied, the longer it takes for $PrxSO_{2/3}$ to disappear from the cells.

As previously (Section 3.5), there was no difference in the amount of $PrxSO_{2/3}$ measured immediately after H_2O_2-washout after the first exposure to 30 μM H_2O_2 (*p-value* = 0.6447). Although it appeared that after the second exposure to 30 μM H_2O_2 levels of $PrxSO_{2/3}$ appeared to be higher in patient fibroblasts than in control cells this difference also was not statistically significant (*p-value* = 0.0783). By 8 hours after H_2O_2-washout, however, there was a statistically significant increase in the level of $PrxSO_{2/3}$ present in patient cells compared to control cells and this difference became more evident as further recovery time elapsed. When the time course of recovery is considered it is clear that both patient and control cells took longer for their $PrxSO_{2/3}$ to disappear after the second exposure than after the first, despite the fact that the two exposures were identical (15 min exposure to 30 μM H_2O_2). Further time-points would be needed to establish exactly when $PrxSO_{2/3}$ disappeared altogether. It is, though, evident from the quantification graph that the difference in the time taken for $PrxSO_{2/3}$ to disappear after the first and second exposures was greater in the patient cells than in the control cells, that is the delay in $PrxSO_{2/3}$ disappearance in patient cells is exacerbated after a second oxidative challenge.

WORK IN MUTANT TDP43-ASSOCIATED ALS FIBROBLASTS

Having identified delayed disappearance of overoxidized typical 2-cys Prxs after oxidative challenge in fibroblasts from I113T SOD1-ALS patients, my next set of experiments was designed to determine whether this effect might also be identified in fibroblasts from patients suffering from other forms of familial ALS. Three fibroblast cell lines generated from skin biopsies donated by patients with familial ALS due to mutations in TAR DNA binding protein (TDP43) were investigated. Each patient had a different disease-causing mutation (A321V, G287S, and M337V). The TDP43 patient fibroblasts were paired up with fibroblasts donated by healthy controls, age- and sex-matched as closely as was possible (see Chapter 2, Table 2.2).

3.9 Patient and control fibroblasts grown under basal culture conditions

To establish whether mutant TDP43-ALS fibroblasts exhibited higher levels of overoxidized typical 2-cys Prxs than control fibroblasts when grown under basal culture conditions, three independent whole-cell preparations were made from each of the three pairs of TDP43-ALS patient (Pat) and control (Con) fibroblasts and levels of $PrxSO_{2/3}$ measured in triplicate by Western Blotting in each independent preparation (Fig. 3.24 A and B). As before, the $PrxSO_{2/3}$ bands were quantified using the G-box (Fig. 3.24 C).

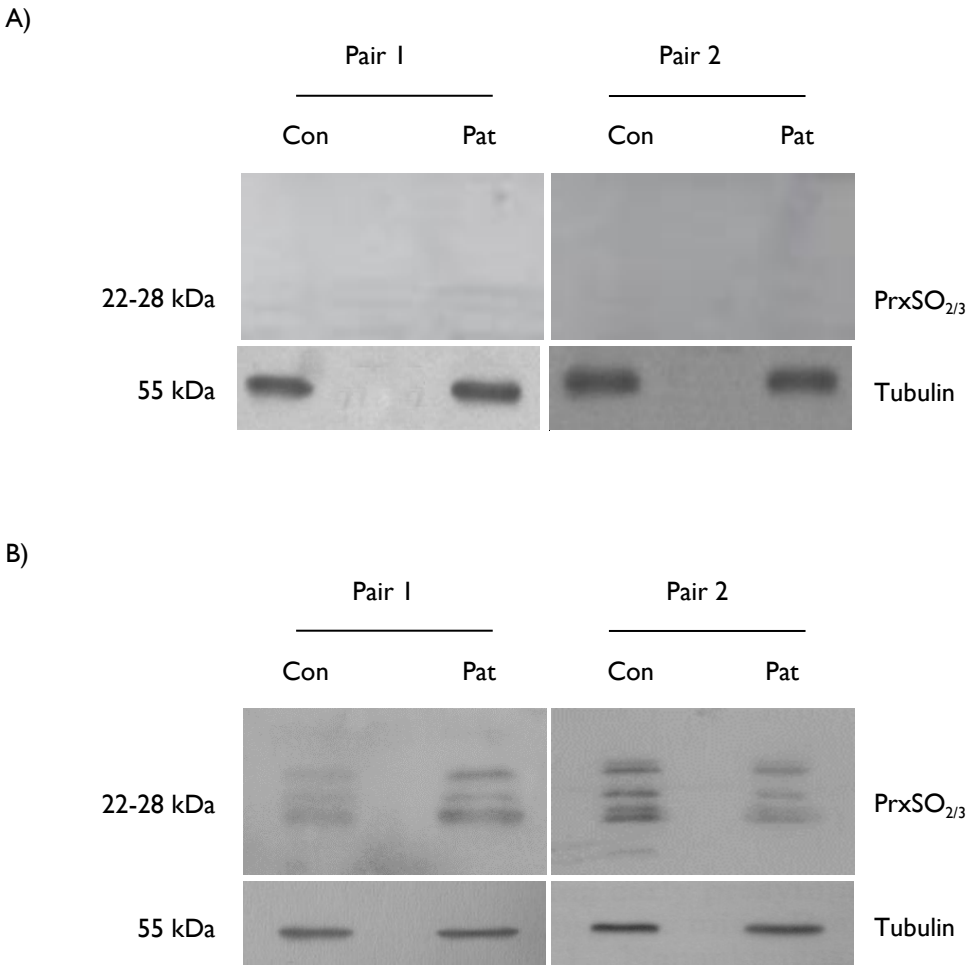

Figure 3.24: *Western blotting of TDP43-ALS patient and control fibroblasts for $PrxSO_{2/3}$ showed that very little was present in either cell line grown under basal culture conditions. Three independent whole-cell preparations were made from three pairs of TDP43-ALS patient (Pat) and control (Con) fibroblasts grown under basal culture conditions and blotted for $PrxSO_{2/3}$.* ***A)*** *Representative Western blots showing that with protein loads of 20 µg per lane $PrxSO_{2/3}$ could not be detected in whole cell preparations of either patient or control cells. $PrxSO_{2/3}$ blots were exposed for 5 min while tubulin blots were exposed for 1 min.* ***B)*** *In an effort to visualize $PrxSO_{2/3}$ bands, protein loads were increased to 40 µg per lane. Representative Western blots showing faint, ill-defined $PrxSO_{2/3}$ bands obtained by blotting more protein from the same samples as in A). Each experiment was blotted in triplicate as in A). $PrxSO_{2/3}$ blots were exposed for 5 min while tubulin blots were exposed for 1 min.*

C)

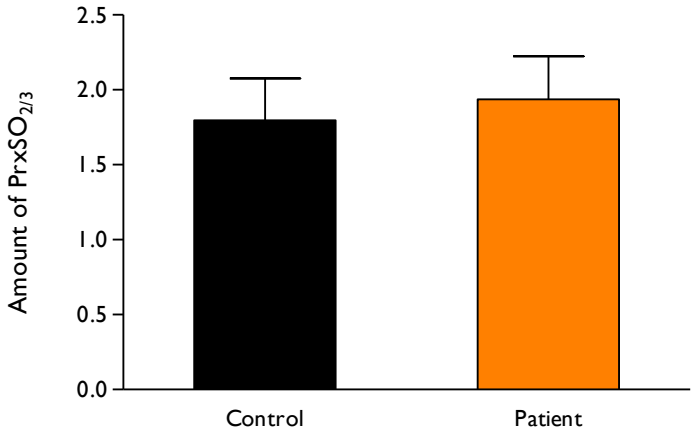

Figure 3.24: C) *Quantification of levels of $PrxSO_{2/3}$ in mutant TDP43-ALS patient and control fibroblasts grown under basal culture conditions normalized to the loading control tubulin. Error bars represent standard error of the mean (SEM). Data include three replicate blots in each of three independent experiments carried out in each of the three fibroblast pairs. A Student's t-test showed no statistical significant difference between the amount of $PrxSO_{2/3}$ in patient and controls fibroblasts (p-value: 0.7289).*

As was the case in I113T SOD1-ALS patient fibroblasts, no $PrxSO_{2/3}$ bands were detected after Western blotting using the usual protein load per lane of 20 µg in whole cell preparations of mutant TDP43-ALS patient and control fibroblasts grown under basal culture conditions. When the protein load was increased to 40 µg per lane faint and rather ill-defined $PrxSO_{2/3}$ bands were detected. The density of these bands was variable both between experiments and within fibroblast type. Quantification of the bands showed no statistically significant difference in $PrxSO_{2/3}$ levels overall between patient and control cells grown under basal conditions.

3.10 Response of TDP43-ALS fibroblasts to oxidative stress

Having confirmed that there was hardly any $PrxSO_{2/3}$ present in either TDP43-ALS patient fibroblasts or in healthy control fibroblasts growing under basal culture conditions, the levels of $PrxSO_{2/3}$ in the cells both immediately after oxidative challenge with H_2O_2 and in the hours following H_2O_2-washout were examined in a series of stress-recovery experiments.

3.10.1 Stress-recovery experiments

Levels of overoxidized Prxs were investigated by first subjecting the fibroblast pairs to a saturating H_2O_2 exposure of 300 µM H_2O_2 for 15 min as described in Chapter 2, Section 2.14. After washout of the H_2O_2, fibroblasts were then allowed to recover over a 26 hour period with pairs of patient and control flasks harvested at various time-points. Two independent experiments were performed in each of the three fibroblast pairs and Western blotting for $PrxSO_{2/3}$ was carried out in duplicate.

Pair 1: Control 08 and Patient 48 (A321V mutant TDP43-ALS patient)

Western blotting for $PrxSO_{2/3}$ of the stress-recovery experiments carried out in this pair of fibroblasts showed a delayed disappearance of $PrxSO_{2/3}$ from the patient cells when compared to control cells. This delay was similar to that observed in the I113T SOD1-ALS patient fibroblasts and was seen in both of the independent experiments performed in this pair (Fig. 3.25 A and B).

A)

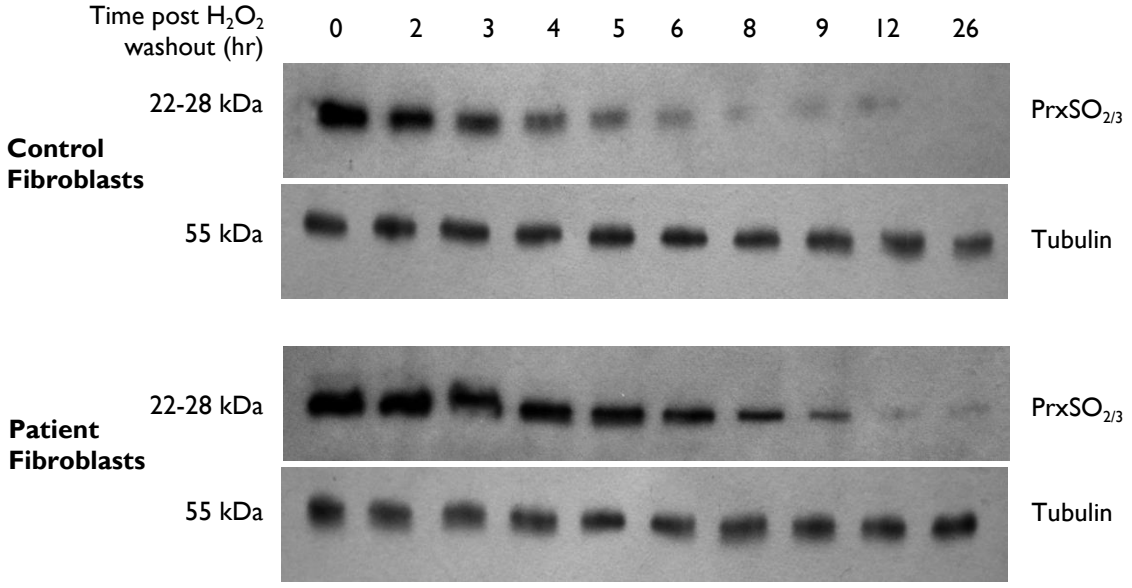

Figure 3.25: A) *The disappearance of $PrxSO_{2/3}$ after exposure of the cells to 300 μM H_2O_2 for 15 min and washout was delayed in Pair 1, which featured A321V mutant TDP43-ALS patient fibroblasts. Representative Western blots from Pair 1 showing the gradual disappearance of $PrxSO_{2/3}$ in control and A321V TDP43-ALS patient fibroblasts in a stress-recovery experiment. Two independent experiments were carried out. The cells were stressed with 300 μM H_2O_2 for 15 min to overoxidize the 2-cys Prxs to saturation and were then allowed to recover over 26 hours after H_2O_2 wash-out. Pairs of patient and control flasks were harvested at the time-points indicated and whole cell preparations made. Protein loads were 20 μg per lane. $PrxSO_{2/3}$ blots were exposed for 2 min and tubulin blots for 1 min.*

B)

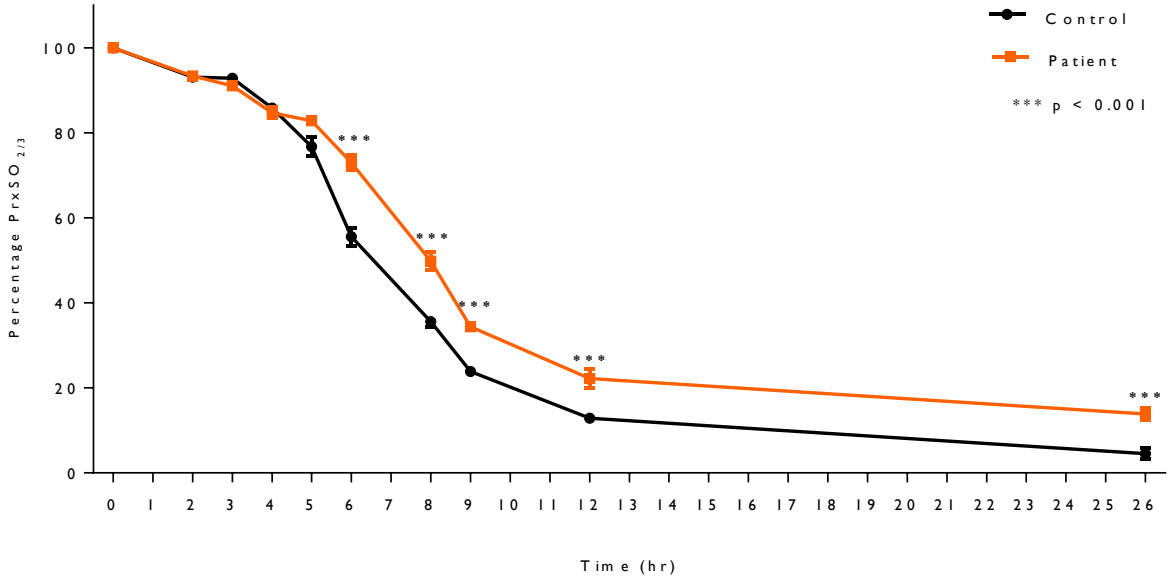

Figure 3.25: B) *Graph showing the delay in the disappearance of $PrxSO_{2/3}$ from the A321V mutant TDP43-ALS patient fibroblasts when compared to that in control fibroblasts in the stress-recovery experiment. Twenty-six hours after H_2O_2-washout control fibroblasts have almost undetectable levels of $PrxSO_{2/3}$ whereas $PrxSO_{2/3}$ remains present at levels 19 % of those measured immediately after H_2O_2-washout in patient cells. Data include duplicate Western blots in two independent experiments in this pair of fibroblasts. Densitometry values of $PrxSO_{2/3}$ bands were first normalized to those of their respective tubulin bands in order to correct for protein loading and were then expressed as a percentage of the normalized $PrxSO_{2/3}$ value obtained immediately after H_2O_2-washout (experimental time-point t = 0 hr). Two-way ANOVA was used to analyze the dataset. At t = 6, t = 8 t = 9, t = 12 and t = 26 ***denotes p-values of 0.00075, 0.00066, 0.00051, 0.00037 and 0.00028 respectively. Error bars represent standard error of the mean (SEM).*

Pair 2: Control 11 and Patient 51 (M337V mutant TDP43-ALS patient)

Two independent stress-recovery experiments were performed in this mutant TDP43-ALS patient and control fibroblast pair. Each experiment was Western blotted twice for $PrxSO_{2/3}$. Unlike Pair 1, however, Western blotting for $PrxSO_{2/3}$ in Pair 2 showed no difference in the rate at which $PrxSO_{2/3}$ levels decreased between M337V mutant TDP43-ALS patient fibroblasts and control cells (Fig. 3.26 A and B).

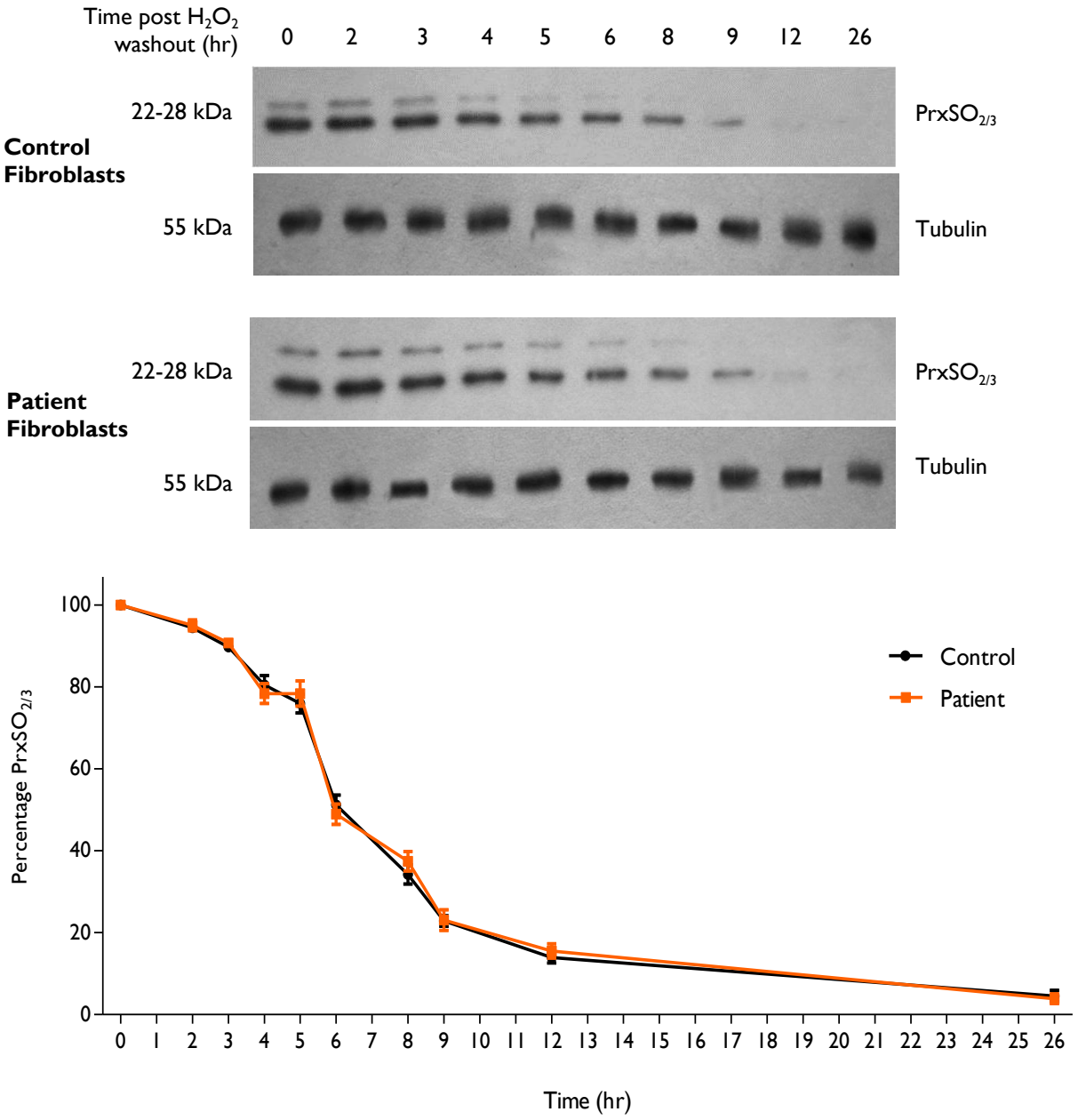

Figure 3.26: A) *The disappearance of $PrxSO_{2/3}$ was identical in M337V mutant TDP43-ALS patient and control fibroblasts. Representative Western blots from Pair 2 showing the disappearance of $PrxSO_{2/3}$ in patient and control fibroblasts in a stress-recovery experiment. Cells were treated with 300 µM H_2O_2 for 15 min to overoxidize the 2-cys Prxs to saturation, H_2O_2 was washed out and the cells allowed to recover over 26 hours. Pairs of TDP43 patient and control flasks were harvested at the time-points indicated, whole cell preparations made and Western blotted for $PrxSO_{2/3}$ and tubulin. Protein loads were 20 µg per lane. $PrxSO_{2/3}$ blots were exposed for 2 min, tubulin blots for 1 min.* ***B)*** *Quantification of the disappearance of $PrxSO_{2/3}$ in the M3371V mutant TDP43-ALS patient and control fibroblasts. At 26 hours after H_2O_2-washout $PrxSO_{2/3}$ in both control and patient fibroblasts had almost disappeared. Data include duplicate blots in two independent experiments in this pair. Densitometry values of $PrxSO_{2/3}$ bands were normalized to those of their respective tubulin bands to correct for protein loading and then expressed as a percentage of the corrected $PrxSO_{2/3}$ value obtained immediately after H_2O_2-washout. Two-way ANOVA was used to analyze the dataset and no statistically significant difference between $PrxSO_{2/3}$ levels in control and patient fibroblasts was identified at any time-point. Error bars represent standard error of the mean (SEM).*

Pair 3: Control 04 and Patient 58 (G287S mutant TDP43-ALS patient)

Two independent stress-recovery experiments were performed in this mutant TDP43-ALS patient and control fibroblast pair. Each experiment was Western blotted twice for $PrxSO_{2/3}$. In this pair, $PrxSO_{2/3}$ in the G287S mutant TDP43 patient fibroblasts appeared to disappear slightly earlier than that present in the control fibroblasts (Fig. 3.27 A), however, this difference was not statistically significant (Fig. 3.27 B).

A)

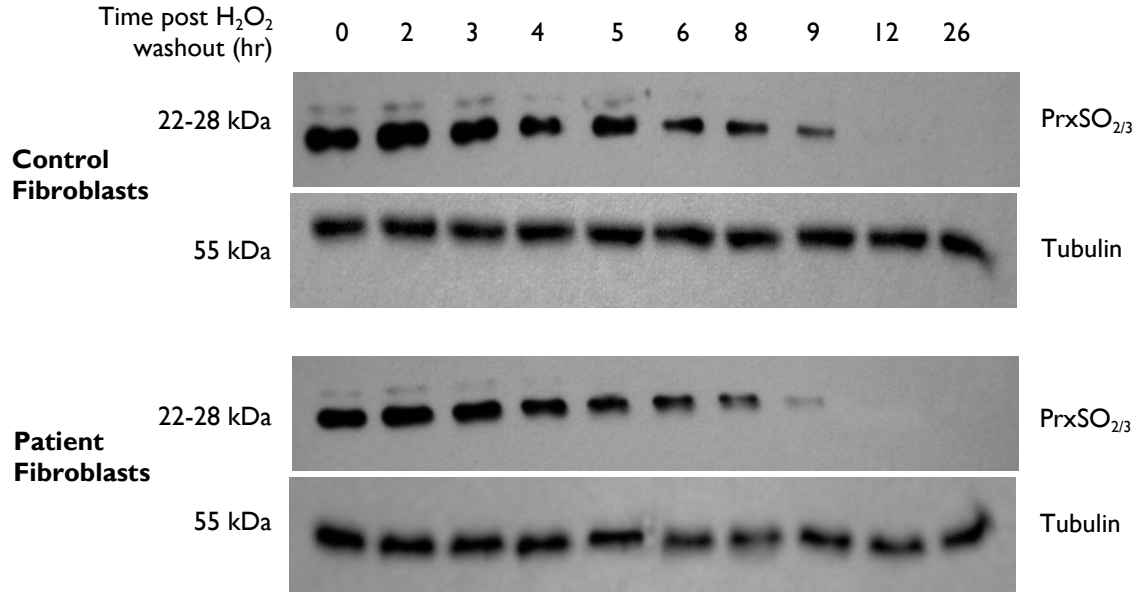

Figure 3.27: A) *The disappearance of $PrxSO_{2/3}$ from G287S mutant TDP43-ALS patient and control fibroblasts after a saturating oxidative challenge. Representative Western blots from Pair 3 showing the gradual disappearance of $PrxSO_{2/3}$ in G287S TDP43-ALS patient and control fibroblasts in a stress-recovery experiment. Two independent experiments were carried out in Pair 3. The cells were first stressed with 300 µM H_2O_2 for 15 min to overoxidize the 2-cys Prxs to saturation, H_2O_2 was washed out and the cells were allowed to recover over 26 hours. Pairs of patient and control flasks were harvested at the time-points indicated, whole cell preparations made and the lysates Western blotted twice for $PrxSO_{2/3}$ and tubulin. Protein loads were 20 µg per lane. $PrxSO_{2/3}$ blots were exposed for 2 min and tubulin blots for 1 min.*

B)

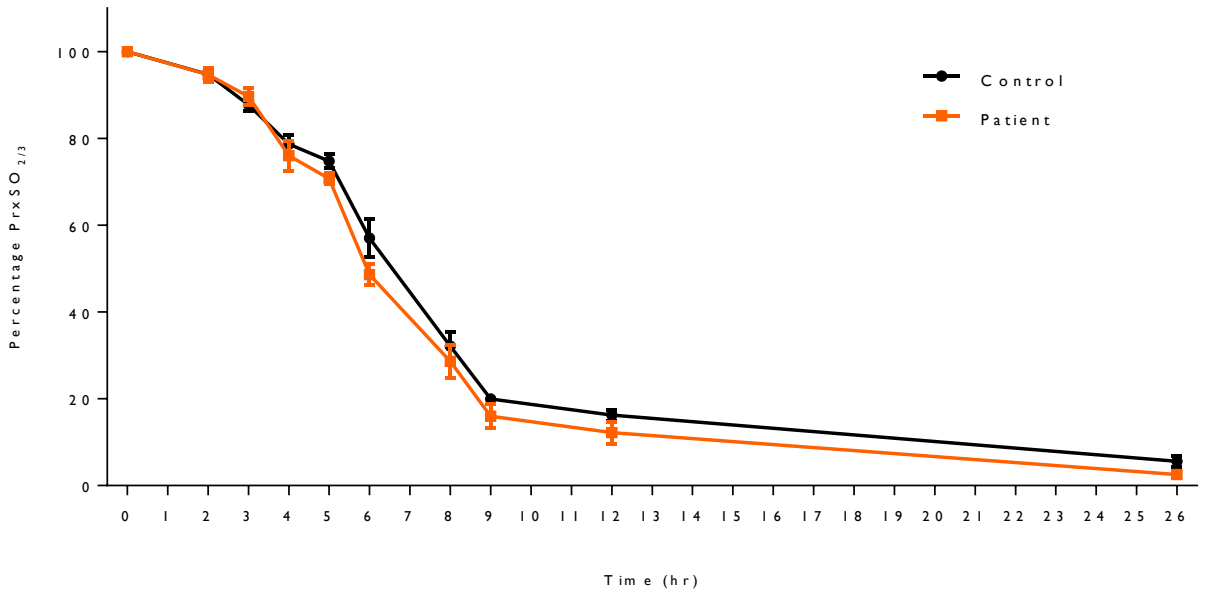

Figure 3.27 B): *Graph showing the disappearance of $PrxSO_{2/3}$ in the G287S mutant TDP43-ALS patient and control fibroblast pair in the stress-recovery experiment. At the experimental end-point (26 hours after H_2O_2-washout) $PrxSO_{2/3}$ levels in both patient and control fibroblasts had almost returned back to basal. Data include duplicate Western blots in each of two independent experiments in this pair of fibroblasts. Densitometry values of the $PrxSO_{2/3}$ bands were first normalized to those of their respective tubulin bands in order to correct for protein loading and were then expressed as a percentage of corrected $PrxSO_{2/3}$ values immediately after H_2O_2-washout (experimental time-point t = 0 hr). Two-way ANOVA was used to analyze the data and no significant differences were observed between $PrxSO_{2/3}$ levels in patient and control fibroblasts at any time-point. Error bars represent standard error of the mean (SEM).*

Levels of overoxidized Prxs immediately after H_2O_2-washout

To establish that there were no differences in the levels of $PrxSO_{2/3}$ between control and mutant TDP43-ALS patient fibroblasts measured immediately after H_2O_2-washout (e.g., the start of the recovery period), the data obtained at t = 0 from the two independent stress-recovery experiments performed in each of the three TDP43 patient and control fibroblast pairs described in Section 3.10.1 were separately re-analyzed (Fig. 3.28).

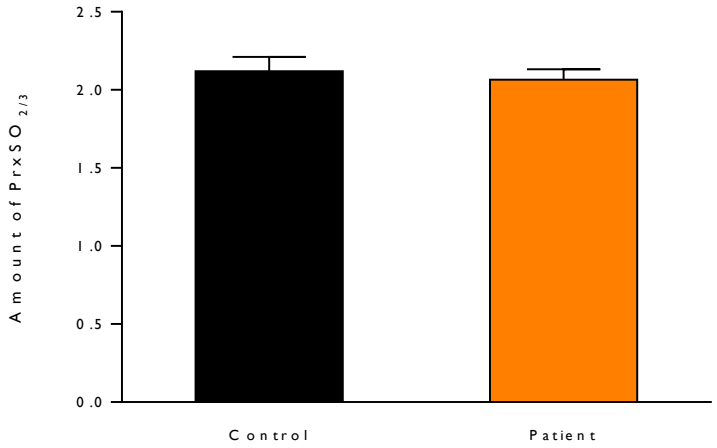

Figure 3.28: *Graph showing the levels of $PrxSO_{2/3}$ in whole cell preparations of mutant TDP43-ALS patient fibroblasts and healthy control fibroblasts measured immediately after H_2O_2-washout (experimental time point t = 0 hours) in the stress-recovery experiment described in Section 3.10.1. Densitometry values for $PrxSO_{2/3}$ bands were normalized to those of their respective tubulin bands to correct for protein loading. Data include three replicate blots in from two independent experiments in each of the three pairs. A Student's t-test showed no statistically significant difference between the levels of $PrxSO_{2/3}$ between patient and control fibroblasts (p-value: 0.7897) immediately after H_2O_2-washout.*

Statistical analysis confirmed that levels of $PrxSO_{2/3}$ were similar in both control and TDP43 patient fibroblasts immediately post-H_2O_2 exposure and washout. This indicates that as was the case for the I113T fibroblasts there were no baseline differences in the levels of $PrxSO_{2/3}$ generated in response to a 15 min exposure to 300 μM H_2O_2 between control and patient fibroblasts at the beginning of the recovery period in the stress-recovery experiment.

Levels of overoxidized Prxs in control fibroblasts in the stress-recovery experiments

Given that a delay in the disappearance of $PrxSO_{2/3}$ was only observed in Pair 1 of the mutant TDP43-ALS patient and control fibroblasts (Fig. 3.25 B) but not in Pairs 2 or 3 (Fig. 3.26 B and 3.27 B respectively), I wanted to establish whether this inconsistency was due to inherent differences between the patient fibroblasts (which did have three different mutations to one copy of their TDP43 gene) or a difference in the response of the Pair 1 control fibroblasts. The levels of $PrxSO_{2/3}$ observed in the stress-recovery experiments performed in each of the control fibroblasts (Control 04, Control 08 and Control 11), were thus re-analyzed and compared to each other rather than to their respective mutant TDP43 fibroblast partners (Fig. 3.29).

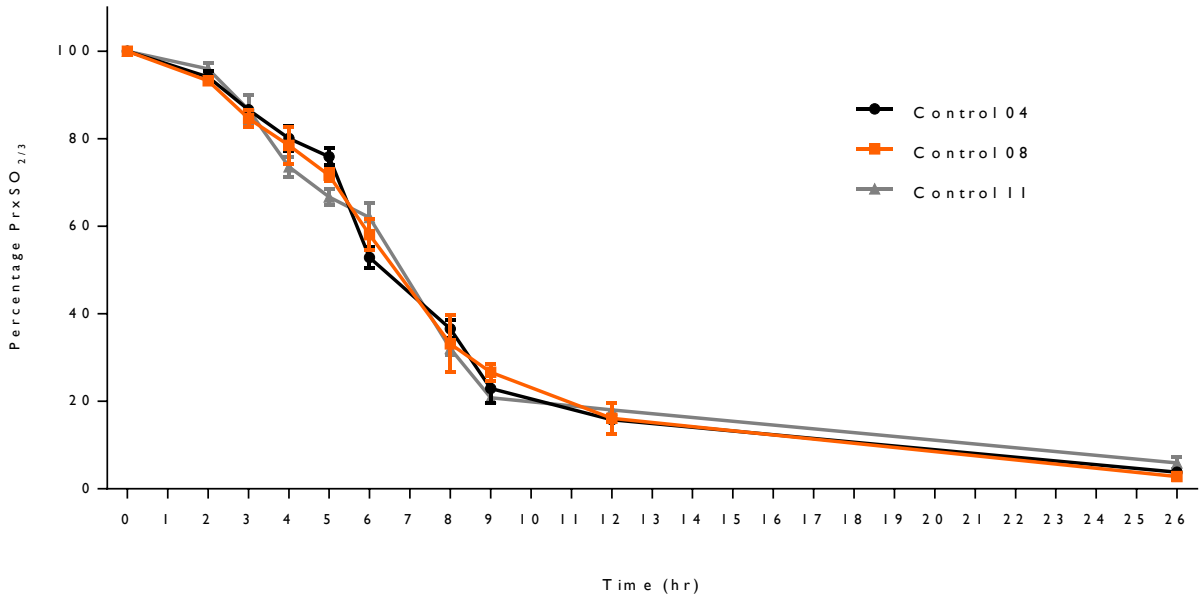

Figure 3.29: *Graph showing the disappearance of $PrxSO_{2/3}$ in the three control fibroblast lines (Control 04, Control 08 and Control 11) in the stress-recovery experiments. At the experimental end-point (26 hours after H_2O_2-washout) levels of $PrxSO_{2/3}$ in all the control fibroblasts had returned almost to basal. Data include two independent experiments in each control fibroblast Western blotted for $PrxSO_{2/3}$ and tubulin twice. Densitometry values of the $PrxSO_{2/3}$ bands were first normalized to those of their respective tubulin bands in order to correct for protein loading and were then expressed as a percentage of corrected $PrxSO_{2/3}$ values immediately after H_2O_2-washout (experimental time-point t = 0 hr). Two-way ANOVA was used to analyze the data and no statistically significant difference was observed in $PrxSO_{2/3}$ levels between the three control fibroblast lines at any time-point. Error bars represent standard error of the mean (SEM).*

The stress-recovery experiments were conducted in fibroblasts from three different TDP43-ALS patients each paired with fibroblasts from age- and sex-matched healthy control individuals. In one of the three pairs, Pair 1 (featuring A321V TDP43-ALS fibroblasts), there was a statistically significant delay in the disappearance of $PrxSO_{2/3}$ from the patient cells after H_2O_2 treatment when compared to the control cells. From 6 hours after H_2O_2 washout there was less $PrxSO_{2/3}$ present in control cells than in patient cells. This statistically significant difference was maintained to the end of the experiment (t = 26 hours after H_2O_2 washout) by which time levels of $PrxSO_{2/3}$ had fallen almost to basal in control cells but remained at 19 % of those immediately after H_2O_2-washout in patient cells. This difference between patient and control fibroblasts was observed in both independent experiments carried out in Pair 1. The delay in disappearance of $PrxSO_{2/3}$ from the A321V TDP43 fibroblasts in this pair was consistent with the results of the stress-recovery experiments performed in the I113T SOD1-ALS fibroblasts (Section 3.6.1).

In both of the other TDP43 pairs, however, which included M337V mutant TDP43-ALS fibroblasts (Pair 2) and G287S mutant TDP43 ALS fibroblasts (Pair 3), no statistically significant difference between $PrxSO_{2/3}$ levels in patient and control fibroblasts was detected at any measured time-point in their recovery after H_2O_2-exposure (Fig 3.26 B and 3.27 B).

I also wanted to be sure that there was no overall difference in the levels of $PrxSO_{2/3}$ between mutant TDP43 and control fibroblasts immediately after H_2O_2-exposure. A separate analysis of $PrxSO_{2/3}$ levels immediately post-H_2O_2 exposure and washout obtained as part of the three stress-recovery experiments, was therefore carried out as presented above. These data (Fig. 3.28) confirmed that there were no differences in $PrxSO_{2/3}$ levels between TDP43 patient and control fibroblasts at t = 0.

Finally, given the inconsistency in the results of the stress-recovery experiments from Pair 1 and the other two TDP43 fibroblast pairs, I wondered whether the difference lay with the behaviour of the patient cells or the control cells. A separate analysis of $PrxSO_{2/3}$ levels in each of the control cell lines during the stress-recovery experiments was therefore carried out as described in Section 3.10.1. These data confirmed that all the three control cell lines showed similar levels of $PrxSO_{2/3}$ at all experimental time points during the recovery period after exposure to H_2O_2 (Fig. 3.29). It was therefore likely that the difference in $PrxSO_{2/3}$ clearance between Pair 1 and Pairs 2 and 3 lay with the patient cells. Possible reasons for this inconsistency between TDP43 pairs will be considered in the Discussion (Chapter 6).

REFERENCES

Lan, R., Geng, H., Polichnowski, A.J., Singha, P.K., Saikumar, P., McEwen, D.G., Griffin, K.A., Koesters, R., Weinberg, J.M., Bidani, A.K., *et al.* (2012). PTEN loss defines a TGF-beta-induced tubule phenotype of failed differentiation and JNK signaling during renal fibrosis. American Journal of Physiology Renal physiology *302*, F1210-1223.

Moon, J.C., Hah, Y.S., Kim, W.Y., Jung, B.G., Jang, H.H., Lee, J.R., Kim, S.Y., Lee, Y.M., Jeon, M.G., Kim, C.W., *et al.* (2005). Oxidative stress-dependent structural and functional switching of a human 2-Cys peroxiredoxin isotype II that enhances HeLa cell resistance to H2O2-induced cell death. J Biol Chem *280*, 28775-28784.

Rhee, S.G., and Woo, H.A. (2011). Multiple functions of peroxiredoxins: peroxidases, sensors and regulators of the intracellular messenger HO, and protein chaperones. Antioxid Redox Signal *15*, 781-794.

Rhee, S.G., Woo, H.A., Bae, S.H., and Park, S. (2009). Sestrin 2 Is Not a Reductase for Cysteine Sulfinic Acid of Peroxiredoxins. Antioxid Redox Signal.

Sundara Rajan, S. (2008). Generation of novel cellular model for analysis of the pathobiology of Motor Neurone Disease. Master of Science Thesis, Academic Unit of Neurology (University of Sheffield).

Woo, H.A., Chae, H.Z., Hwang, S.C., Yang, K.S., Kang, S.W., Kim, K., and Rhee, S.G. (2003a). Reversing the inactivation of peroxiredoxins caused by cysteine sulfinic acid formation. Science *300*, 653-656.

Woo, H.A., Kang, S.W., Kim, H.K., Yang, K.S., Chae, H.Z., and Rhee, S.G. (2003b). Reversible oxidation of the active site cysteine of peroxiredoxins to cysteine sulfinic acid. Immunoblot detection with antibodies specific for the hyperoxidized cysteine-containing sequence. J Biol Chem *278*, 47361-47364.

4. RESULTS – NSC34 CELLS

INTRODUCTION

Work in I113T SOD1-ALS patient fibroblasts demonstrated deficient clearance of overoxidized Prxs ($PrxSO_{2/3}$) after exposure to an externally-applied oxidative stress, a deficit which became even more marked after exposure to the same oxidative stress for a second time. This deficient clearance of $PrxSO_{2/3}$ was accompanied by a delayed and reduced induction of the $PrxSO_{2/3}$ regenerator Srx 1 and reduced activation of AP-1, a Srx 1 transcription factor. The fibroblasts in which this work was done contain only one copy of the ALS-causing gene and are derived from patients suffering from ALS. They are, however, derived from skin cells and are both morphologically and biochemically far distant from motor neurons – the cells affected in ALS. It was therefore important to establish whether expression levels of the 2-cys Prxs and their related proteins and the extent of their overoxidation differed in the disease state in a cell type with more of the characteristics of motor neurons. In the first instance I elected to use NSC34 cells, a motor neuronal cell model well-established in our laboratory, for my experiments. The generation of NSC34 cells, their characteristics and the rationale for their use as a cell model of ALS has already been discussed in Chapter 2, Section 2.3.

I used a panel of six NSC34 cells in my experiments. These included non-transgenic NSC34 cells (NTG), vector-only transfected NSC34 cells (pIRES), NSC34 cells stably transfected with wild-type human SOD1 (WT) and NSC34 cells stably transfected with three forms of mutant human SOD1 (H48Q, I113T and G93A). Previous work in this model of SOD1-related fALS by members of my department has shown levels of several of the typical 2-cys Prxs to be altered at both a mRNA and protein level in NSC34 cells expressing G93A mutant SOD1 (discussed in Section 1.16.1) (Kirby et al., 2005; Wood-Allum et al., 2006).

To determine whether there is any alteration in the Prx redox system in NSC34 cells expressing mutant SOD1 species known to cause ALS in patients, levels of involved proteins were measured in three of these disease-state cell lines and compared with those measured in control cells that were untransfected (NTG), transfected with empty transfection vector (pIRES) and, most relevantly, transfected with normal human SOD1 (WT). Levels of two of the main neuronal typical 2-cys Prxs (Prxs 2 and 3), overoxidized Prxs ($PrxSO_{2/3}$), two putative regenerators of $PrxSO_{2/3}$ (Srx 1 and Sesn 2) and Txnip, a protein that helps regulate the oxidation state of the Prxs, were investigated under basal culture conditions. Levels of $PrxSO_{2/3}$ were also measured under conditions of oxidative stress after exposure to hydrogen peroxide (H_2O_2). Western blotting was used to assess the protein expression levels in each experiment.

Levels of total typical 2-cys Prxs and overoxidized typical 2-cys Prxs and those of proteins related to the peroxiredoxin redox pathway were first investigated in whole cell preparations from NSC34 cell lines prepared under basal culture conditions. This was to determine whether the presence of mutant human SOD1 causes alterations in the levels of Prxs or their related proteins. Three independent preparations from NSC34 cells (passages between 11 and 15), comprising non-transgenic NSC34 cells (NTG), cells expressing vector only (pIRES), wild-type human SOD1 (WT) and three forms of mutant human SOD1 (H48Q, I113T and G93A), were harvested as described in Section 2.15.

4.1 Levels of endogenous and transfected human SOD1

Confirmation of the expression of endogenous murine SOD1 and transfected mutant human SOD1 was first sought by Western blotting of whole cell lysates from each of the six NSC34 cell lines to be investigated. An antibody that recognized both endogenous murine SOD1 and transfected human SOD1 was used. Western blotting with this antibody (Chapter 2, Table 2.3) was performed to establish whether human SOD1 was expressed at comparable levels in each of the WT, H48Q, I113T and G93A-expressing NSC34 cell lines, in addition to levels of endogenous murine SOD1 in all six cell lines, before I began my investigations of their expression of the peroxiredoxins and related proteins (Fig. 4.1 A, B, C and D).

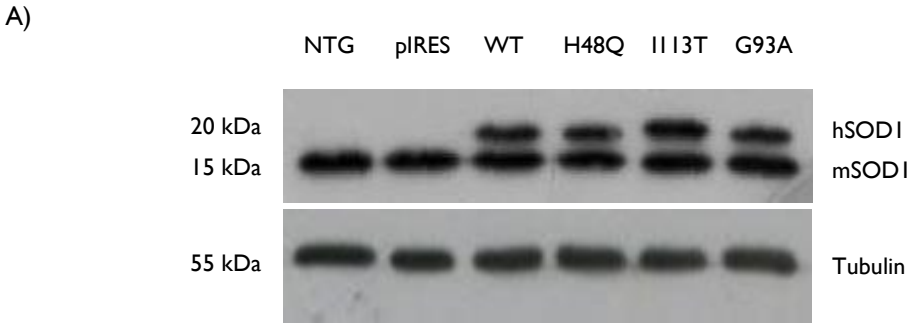

Figure 4.1: A) *Levels of transfected human SOD1 (hSOD1) were similar in the four NSC34 cell lines stably transfected with various species of human SOD1, as were levels of endogenous murine SOD1 (mSOD1) in all six NSC34 cell lines. Representative Western blots showing levels of mSOD1 and transfected hSOD1. Three independent experiments were carried out in the six NSC34 cell lines grown under basal culture conditions. Cells were grown up in parallel, harvested and whole cell lysates prepared. Western blotting for mSOD1 and hSOD1 was performed in duplicate in each independent experiment. Lanes comprised NTG = non-transgenic NSC34 cells, pIRES = vector-only NSC34 cells, WT = NSC34 cells stably expressing WT human SOD1, H48Q = NSC34 cells stably expressing H48Q mutant human SOD1, I113T = NSC34 cells stably expressing I113T mutant human SOD1 and G93A = NSC34 cells stably expressing G93A mutant human SOD1. Protein loads were 20 µg per lane. Both SOD1 and tubulin (loading control) blots were exposed for 1.5 min.*

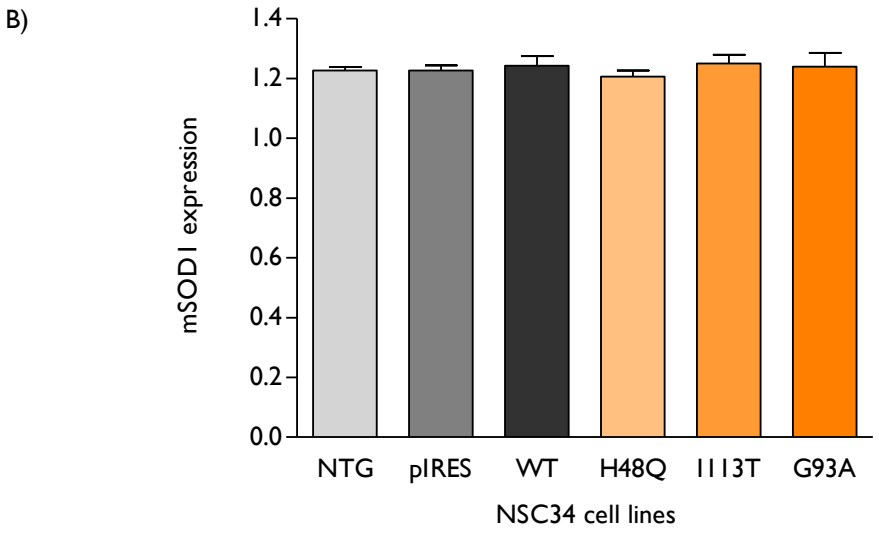

Figure 4.1: B) *Quantification of endogenous mouse SOD1 (mSOD1) in NSC34 cell lines grown under basal culture conditions. Three independent experiments were performed and each experiment was blotted in duplicate for SOD1. Densitometry was performed as described in Chapter 2, Section 2.18.6 on the G-Box. Densitometry values of mSOD1 bands were normalized to those of their respective tubulin bands to correct for protein loading. A Student's t-test showed no statistically significant difference in the levels of mSOD1 between NTG cells and cells transfected with vector only (p-value: 0.8074) and between NTG cells and those stably expressing all four species of human SOD1: WT (p-value: 0.9044), H48Q (p-value: 0.7308), I113T (p-value: 0.8771) and G93A (p-value: 0.9452).*

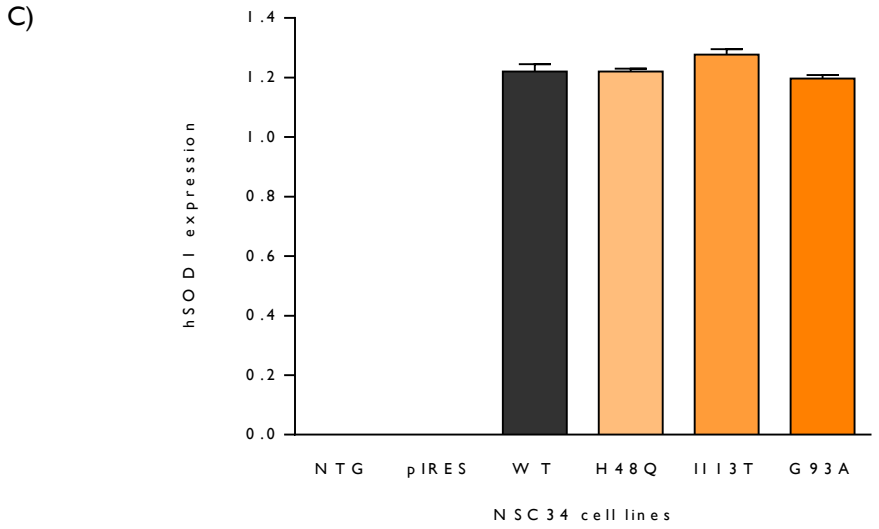

Figure 4.1: C) *Quantification of the level of transfected hSOD1 in NSC34 cell lines grown under basal culture conditions. Three independent experiments were performed and each experiment was Western blotted twice for SOD1. As before hSOD1 bands were normalized to those of their respective tubulin bands to correct for protein loading. Error bars represent the standard error of the mean (SEM). A Student's t-test showed no statistically significant difference in the levels of hSOD1 between WT SOD1-expressing cells and any of the mutant SOD1 expressing cells: H48Q (p-value: 0.9101), I113T (p-value: 0.8252) and G93A (p-value: 0.6302).*

D)

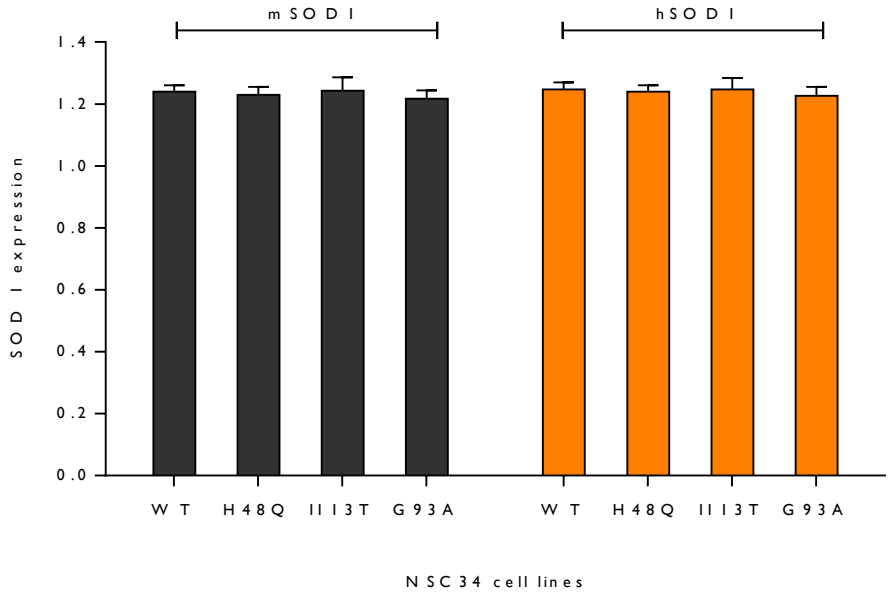

Figure 4.1: D) *Comparison of mSOD1 and hSOD1 expression in each of the WT SOD1, H48Q SOD1, 1113T SOD1 and G93A SOD1-expressing NSC34 cell lines grown under basal culture conditions. Three independent experiments were performed and each experiment was Western blotted in duplicate for SOD1. Endogenous SOD1and hSOD1 bands were normalized to their respective tubulin bands to correct for protein loading. Error bars represent the standard error of the mean (SEM). A Student's t-test showed no statistically significant difference between levels of mSOD1 and hSOD1 in any of the human SOD1 transfected cell lines: WT (p-value: 0.8601), H48Q (p-value: 0.7571), 1113T (p-value: 0.8522) and G93A (p-value: 0.7342).*

Levels of endogenous murine SOD1 (mSOD1) appeared similar across all cell lines in all three independent preparations and statistical analysis confirmed no significant differences in the levels of mSOD1 present in whole cell lysates from all six NSC34 cell lines grown under basal culture conditions. More importantly, the levels of each of the four species of transfected human SOD1 (WT, H48Q, 1113T and G93A) in whole cell preparations of their respective cell lines were also observed to be comparable. Although the level of hSOD1 in the 1113T-expressing NSC34 cells appeared to be slightly higher than that of the other two species of mutant hSOD1, this difference was not statistically significant. Comparison of the expression levels of mSOD1 and hSOD1 in the four NSC34 cell lines expressing both SOD1 species showed no statistically significant difference between the two in any of the four cell lines (Fig. 4.1 D).

Thus, blotting of the NSC34 cells for SOD1 confirmed expression of the human transgene at similar levels in WT, H48Q, 1113T and G93A SOD1-expressing cell lines grown under basal culture conditions. The blotting also verified that the transgene was not significantly overexpressed in comparison to levels of endogenous murine SOD1 in any of the cell lines.

4.2 Levels of total Prx 2 and Prx 3

I next investigated levels of total Prx 2 and Prx 3 in whole cell preparations made from each of the six NSC34 cell lines grown under basal culture conditions. Western blotting for Prx 2 (Fig. 4.2 A and B) and Prx 3 (Fig. 4.3 A and B) was performed in triplicate in each of three independent experiments. Prx 2 and Prx 3 expression levels were then quantified using the G-box as described in Chapter 2, Section 2.18.6.

A)

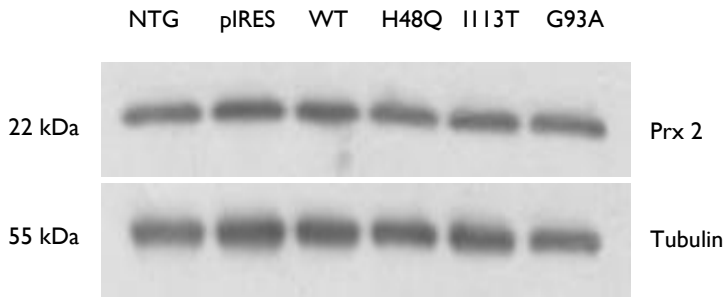

Figure 4.2: A) *Levels of Prx 2 were observed to be similar in whole cell preparations of all six NSC34 cell lines grown under basal culture conditions. Representative Western blots for Prx 2 and tubulin. Three independent preparations were performed and Western blotted in triplicate for Prx 2. Lanes comprise NTG = non-transgenic NSC34 cells, pIRES = vector-only NSC34 cells, WT = NSC34 cells stably expressing WT human SOD1, H48Q = NSC34 cells stably expressing H48Q mutant human SOD1, I113T = NSC34 cells stably expressing mutant I113T human SOD1 and G93A = NSC34 cells stably expressing G93A mutant human SOD1. Protein loads were 20 µg per lane. Both Prx 2 and tubulin blots were exposed for 1.5 min.*

B)

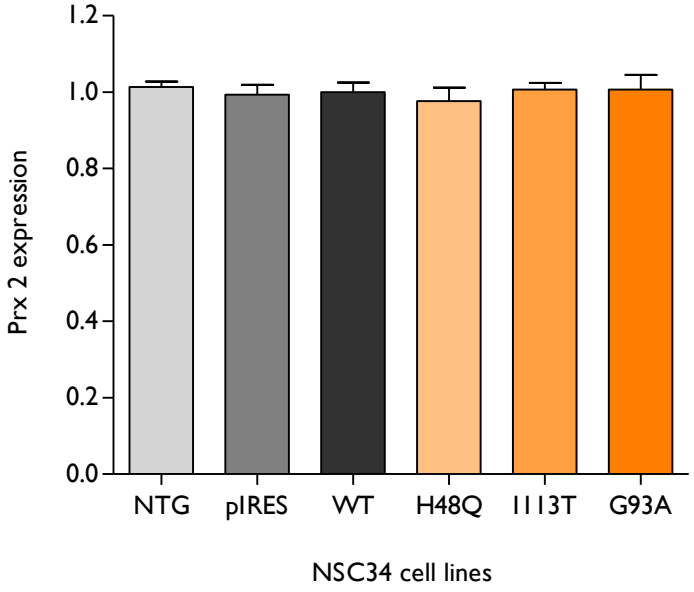

Figure 4.2: B) *Quantification of Western blots for Prx 2 in whole cell preparations of all six NSC34 cell lines grown under basal conditions. Data include values from three independent experiments blotted in triplicate for Prx 2. Densitometry values of Prx 2 bands were normalized to those of their respective tubulin bands to correct for protein loading. Error bars represent the standard error of the mean (SEM). A Student's t-test showed no statistically significant difference in Prx 2 levels between NTG and pIRES cells (p-value: 0.8415), NTG and WT cells (p-value: 0.7699) or between WT and mutant SOD1 expressing cells: H48Q (p-value: 0.5799), I113T (p-value: 0.8782) and G93A (p-value: 0.6989).*

A)

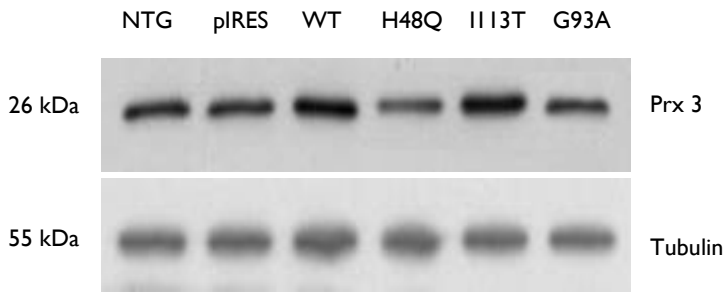

Figure 4.3: A) *Levels of Prx 3 in whole cell preparations of the six NSC34 cell lines grown under basal culture conditions. Representatives of triplicate Western blots performed in each of three independent preparations. Prx 3 levels appeared to be slightly lower in H48Q-expressing NSC34 cell lines in all three independent preparations. Lanes comprise NTG = non-transgenic NSC34 cells, pIRES = vector-only NSC34 cells, WT = NSC34 cells stably expressing WT human SOD1, H48Q = NSC34 cells stably expressing H48Q mutant human SOD1, I113T = NSC34 cells stably expressing mutant I113T human SOD1 and G93A = NSC34 cells stably expressing G93A mutant human SOD1. Protein loads were 20 µg per lane and both Prx 3 and tubulin blots were exposed for 2 min.*

B)

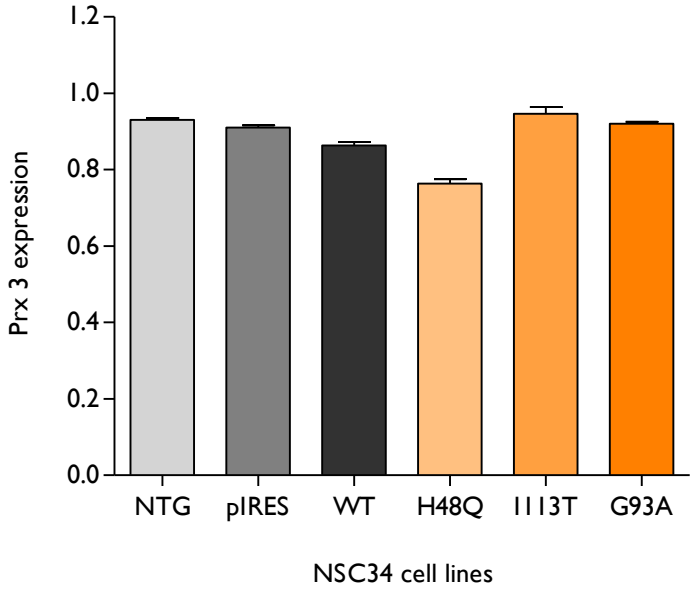

Figure 4.3: B) *Quantification of Western blots for Prx 3 levels in whole cell preparations of NSC34 cell lines grown under basal conditions. Each of three independent experiments was blotted three times for Prx 3. Levels of Prx 3 in the H48Q-expressing NSC34 cell line appeared to be lower than those in WT cells in all experiments. This difference, however, was not statistically significant. As before, densitometry values from Prx 3 bands were normalized to those of their respective tubulin bands to correct for protein loading. Error bars represent the standard error of the mean (SEM). A Student's t-test showed no statistically significant difference in Prx 3 levels between NTG and vector-only NSC34 cells (pIRES) (p-value: 0.8639), between NTG and WT cells (p-value: 0.7244) or between WT cells and any of the three mutant SOD1-expressing cell lines tested: H48Q (p-value: 0.1247), I113T (p-value: 0.6699) and G93A (p-value: 0.7451).*

Western blotting for Prx 2 in whole cell preparations of NSC34 cells grown under basal culture conditions showed similar Prx 2 levels across each of the six cell lines in all three independent experiments. Statistical analysis of the densitometry values of the Prx 2 bands corrected for protein loading showed no statistically significant difference in Prx 2 levels between WT SOD1-expressing NSC34 cells and NSC34 cells expressing any species of mutant human SOD1 tested (H48Q, I113T and G93A).

Western blotting for Prx 3 in the same preparation of the six NSC34 cell lines showed similar levels of Prx 3 between the three control cell lines (NTG, pIRES, WT) and those expressing I113T and G93A mutant SOD1 across the three independent experiments. The H48Q mutant SOD1-expressing cell line, however, appeared to have lower levels of Prx 3 in all three independent experiments. Quantification of Prx 3 levels showed that the H48Q cells consistently had Prx 3 levels ~11 % lower than WT cells. This difference was not, however, statistically significant (*p-value*: 0.1247).

In conclusion, Western blotting for Prx 2 and Prx 3, the main neuronal typical 2-cys Prxs, in whole cell preparations of NSC34 cells grown under basal culture conditions showed the levels of both proteins to be the same in control cells and in cells expressing the three species of mutant human SOD1 tested.

4.3 Levels of overoxidized Prxs ($PrxSO_{2/3}$)

I next measured the levels of overoxidized typical 2-cys Prxs ($PrxSO_{2/3}$) in the same three independent whole cell preparations made from the six NSC34 cell lines grown under basal culture conditions. This was to determine whether the presence of mutant human SOD1 was itself sufficient to cause overoxidation of typical 2-cys Prxs. All three preparations were made from cells between passages 11 and 15. Western blotting for $PrxSO_{2/3}$ was performed in triplicate in each of the three preparations (Fig. 4.4 A overleaf) and the $PrxSO_{2/3}$ bands quantified as previously on the G-box (Fig. 4.4 B overleaf).

Western blotting for $PrxSO_{2/3}$ in the three independent whole cell preparations of the six NSC34 cell lines grown under basal culture conditions showed readily detectable levels of overoxidized Prxs present in all the cell lines including the control cell lines (NTG, pIRES and WT). Furthermore, levels of $PrxSO_{2/3}$ within each cell line varied from one preparation to the other as observed from the representative Western blots shown in Fig. 4.4 A. Unsurprisingly, no statistically significant difference in $PrxSO_{2/3}$ level was found between WT SOD1-expressing NSC34 cells and those expressing any of the three species of mutant human SOD1when levels of $PrxSO_{2/3}$ were quantified by densitometry and the three experiments analysed together (Fig. 4.4 B).

A)

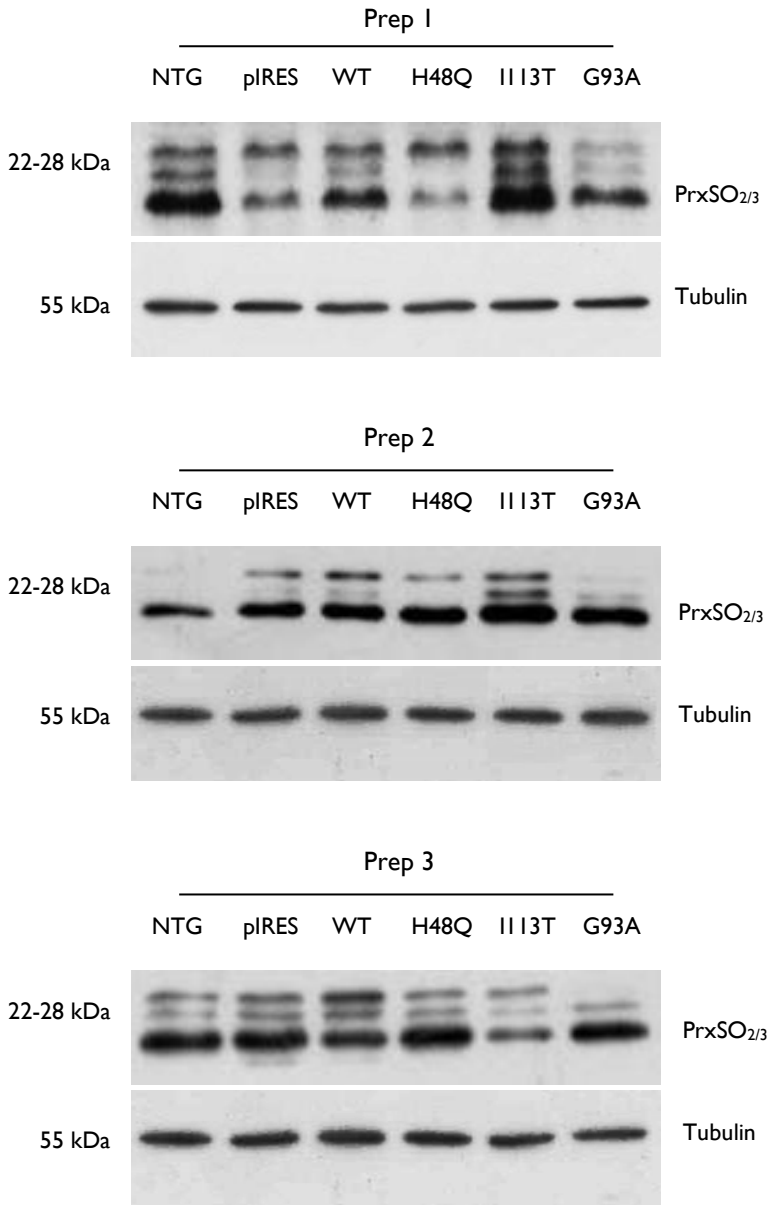

Figure 4.4: A) *Representative Western blots for $PrxSO_{2/3}$ performed in three independent whole cell preparations of the six NSC34 cell lines grown under basal culture conditions. $PrxSO_{2/3}$ bands were readily detected in all cell lines. These levels were consistent within each cell line between replicate blots in each of the three preparations but were not consistent within each cell line between preparations. In some preparations control cell lines appeared to have higher levels of $PrxSO_{2/3}$ than those expressing the various species of mutant SOD1. Lanes comprise NTG = non-transgenic NSC34 cells, pIRES = vector-only NSC34 cells, WT = NSC34 cells stably expressing WT human SOD1, H48Q = NSC34 cells stably expressing H48Q mutant human SOD1, I113T = NSC34 cells stably expressing mutant I113T human SOD1 and G93A = NSC34 cells stably expressing G93A mutant human SOD1. Protein loads were 20 µg per lane. $PrxSO_{2/3}$ and tubulin blots were exposed for 2 min.*

B)

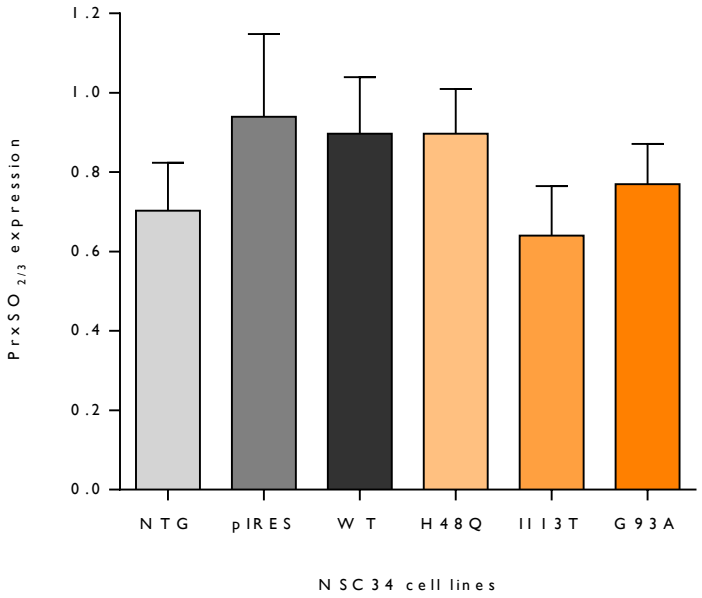

Figure 4.4: B) *Quantification of Western blots for $PrxSO_{2/3}$ in NSC34 cell lines from three independent experiments prepared between passage 11 and 15 from cells growing under basal culture conditions. Each independent experiment was blotted three times. As before, densitometry values from $PrxSO_{2/3}$ bands were normalized to those of their respective tubulin bands to correct for protein loading. Error bars represent the standard error of the mean (SEM). A Student's t-test showed no statistically significant difference in $PrxSO_{2/3}$ levels between NTG and vector-only cells (pIRES) (p-value: 0.2241), between NTG and WT cells (p-value: 0.3136) or between WT cells and any of the three mutant SOD1-expressing cells: H48Q (p-value: 0.7857), I113T (p-value: 0.1798) and G93A (p-value: 0.2011).*

4.4 Repeat experiments in cells of higher passages

The results of the experiments described in Section 4.3 above were unexpected and difficult to explain given the consistency of the levels of total Prx 2 and Prx 3 both between NSC34 cell lines and most importantly within each cell line from preparation to preparation in NSC34 cells growing under basal culture conditions. As levels of $PrxSO_{2/3}$ varied dramatically from one preparation to the next within the same NSC34 cell line and in several (but not all) instances $PrxSO_{2/3}$ levels were higher in control cells than in those transfected with mutant human SOD1 it was not possible to determine whether or not my underlying hypothesis was true or untrue in this cellular model of SOD1-related fALS. As detailed in the Methods (Chapter 2, Section 2.15.1) extensive troubleshooting was carried out in order to minimize the chance that variability in any aspect of the handling of the cells from the setting up and maintenance of the cultures to the harvesting and preparation of whole cell lysates might underlie my inconsistent results. Similar attention was paid to all aspects of the Western blotting. Despite these efforts, levels of $PrxSO_{2/3}$ remained inconsistent between independent preparations. Possible explanations for this are discussed in more detail in the Discussion (Chapter 6, Section 6.8). Having limited, as far as it was possible, any technical variability in the manner by which the whole cell lysates were obtained and Western blotted

without success, a further complete set of experiments was performed on a set of NSC34 cells that were longer established in culture (up to passage 36). Prior to beginning this repeat set of experiments, further Western blotting for SOD1 was carried out to ensure that in the cells to be investigated levels of mSOD1 and hSOD1 were still similar between cell lines. Two complete sets of whole cell lysates were made from the six NSC34 cell lines growing under basal culture conditions and were Western blotted in duplicate for SOD1 (Fig. 4.5 A, B and C).

A)

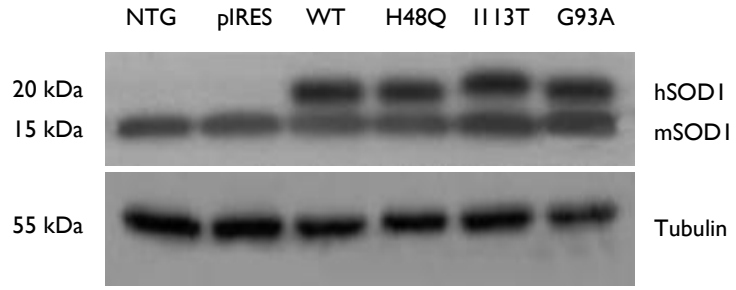

B)

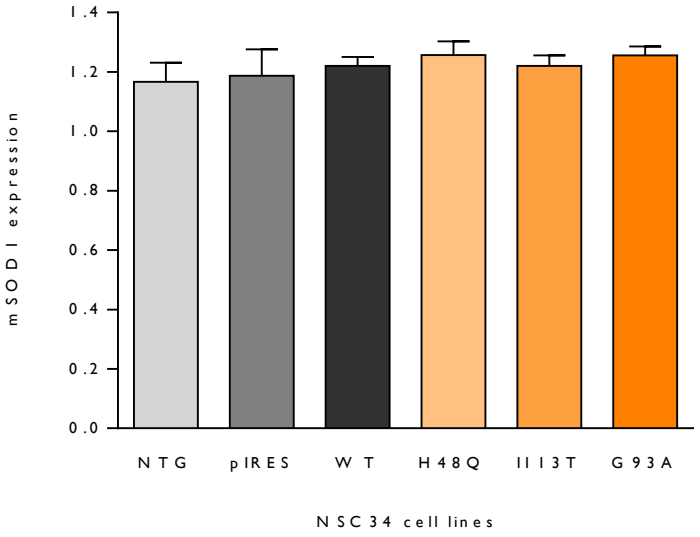

Figure 4.5: A) *Representative Western blot showing levels of mSOD1 and transfected hSOD1 in whole cell lysates from NSC34 cells at higher passages growing under basal culture conditions. Levels of mSOD1 appeared to be similar in all the NSC34 cell lines whilst levels of hSOD1 were comparable across those NSC34 cell lines expressing the various forms of hSOD1as was observed in cells of lower passages (Fig. 4.1). Lanes as previously. Protein loads were 20 µg per lane. SOD1 and tubulin blots were exposed for 1.5 min.* ***B)*** *Quantification of Western blots for levels of mSOD1 in NSC34 cell lines grown under basal culture conditions. Two sets of whole cell lysates were made and each Western blotted for SOD1 in duplicate. Densitometry values of mSOD1 bands were normalized to those of their respective tubulin bands to correct for protein loading. Error bars represent standard error of the mean (SEM). A Student's t-test showed no statistically significant difference in the levels of mSOD1 between NTG cells and those transfected with vector-only or with human SOD1: pIRES (p-value: 0.7574), WT (p-value: 0.8269), H48Q (p-value: 0.6828), I113T (p-value: 0.9391) and G93A (p-value: 0.8433).*

C)

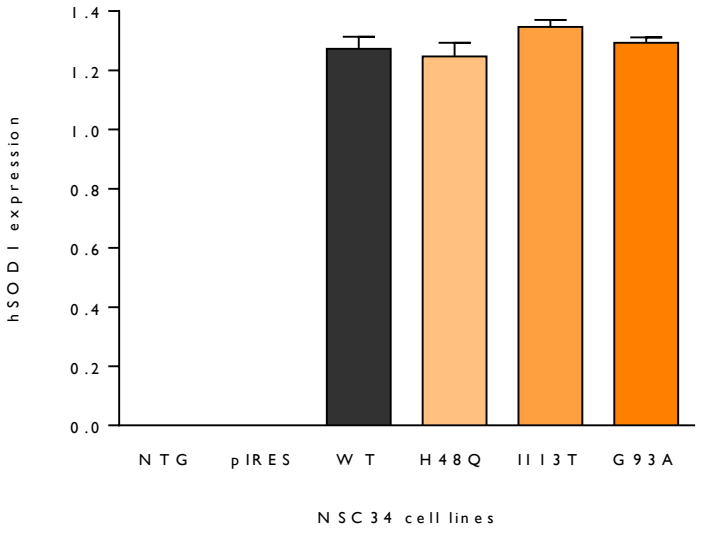

Figure 4.5 C): *Quantification of Western blots for transfected human SOD1 (hSOD1) in NSC34 cell lines of higher passages grown under basal culture conditions. Two sets of whole cell lysates were made and each Western blotted in duplicate for SOD1. Densitometry values of hSOD1 bands were normalized to those of their respective tubulin bands to correct for protein loading. Error bars represent standard error of the mean (SEM). A Student's t-test showed no statistically significant difference in the levels of hSOD1 in WT SOD1-expressing cells and any of the three different mutant SOD1-expressing cells: H48Q (p-value: 0.8575), I113T (p-value: 0.7922) and G93A (p-value: 0.8321).*

Western blotting for endogenous murine and transfected human SOD1 confirmed that there were no statistically significant differences in the levels of mSOD1 across all six NSC34 cell lines or in the levels of transfected hSOD1 between the four NSC34 cell lines engineered to express the various species of hSOD1 (WT, H48Q, I113T and G93A). As was observed in NSC34 cells of earlier passages (Fig. 4.1), the levels of hSOD1 in the I113T expressing NSC34 cells appeared to be slightly higher than those in the cell lines expressing the other two species of mutant hSOD1. Again, however, this difference was not statistically significant.

Having confirmed that mSOD1 and hSOD1 levels remained similar across the relevant NSC34 cell lines growing under basal culture conditions at these later passages and that the cell lines were not infected with mycoplasma (Chapter 2, Section 2.10), three further independent whole cell preparations were made from the six NSC34 cell lines. These preparations were denoted Prep 4, Prep 5 and Prep 6. The cells were between passages 30 and 35. Each independent preparation was then Western blotted in triplicate for $PrxSO_{2/3}$ (Fig. 4.6 A & B).

A)

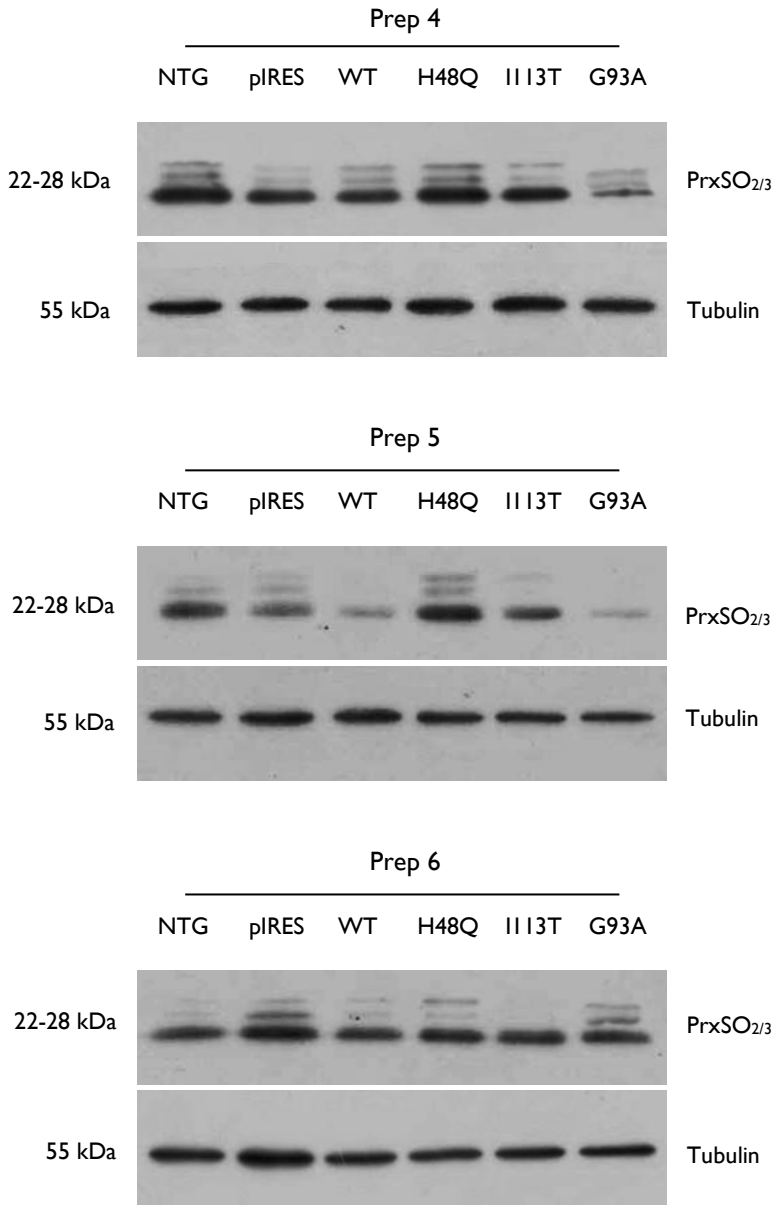

Figure 4.6: A) *Repeat Western blots for $PrxSO_{2/3}$ in three further independent whole cell preparations made from NSC34 cells at passages 30-35 growing under basal culture conditions. As was the case in the earlier set of experiments in cells less well established in culture (Fig. 4.4) $PrxSO_{2/3}$ bands were readily detectable in all cell lines. $PrxSO_{2/3}$ levels did not vary between replicate blots of the same preparation within cell lines but as before, levels varied significantly within cell lines between preparations. Levels of $PrxSO_{2/3}$ were frequently (but not consistently) higher in control cells than in those transfected to express mutant human SOD1. Lanes as previously. Three replicate blots were performed in each of the three independent experiments. Protein loads were 20 µg per lane. $PrxSO_{2/3}$ and tubulin blots were exposed for 2 min.*

B)

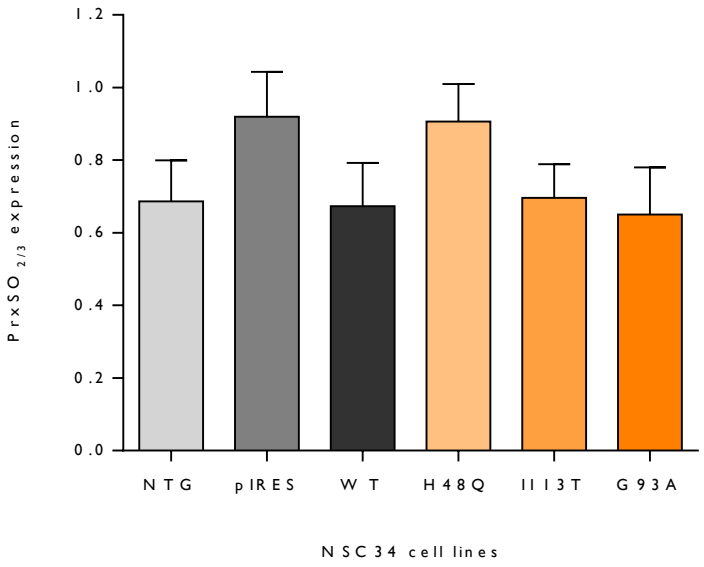

Figure 4.6: B) *Quantification of Western blots for $PrxSO_{2/3}$ in NSC34 cell lines between passage 30 and 35 growing under basal culture conditions. Each of three independent experiments was blotted in triplicate for $PrxSO_{2/3}$. Densitometry values of $PrxSO_{2/3}$ bands were normalized to those of their respective tubulin bands to correct for protein loading. Error bars represent standard error of the mean (SEM). A Student's t-test showed no statistically significant difference in the levels of $PrxSO_{2/3}$ between NTG NSC34 cells and vector-only NSC34 cells (pIRES) (p-value: 0.5376), between NTG NSC34 cells (NTG) and WT-SOD1 expressing cells (WT) (p-value: 0.8791) and between WT SOD1-expressing cells and the three different mutant SOD1-expressing cells: H48Q (p-value: 0.3317), I113T (p-value: 0.7618) and G93A (p-value: 0.8595).*

Western blotting for $PrxSO_{2/3}$ in Preps 4, 5, and 6 which were carried out in NSC34 cell lines that were longer established in culture than were the cells used for the first set of similar experiments (Section 4.3) once again showed that NSC34 cells growing under basal culture conditions (control cell lines included) contained abundant levels of overoxidized Prxs. These bands, moreover, were readily detected using protein loads of only 20 μg of protein per lane and relatively short exposures (~2 min). Similar to the results obtained previously, $PrxSO_{2/3}$ levels within each cell line varied markedly preparation to preparation despite all efforts to ensure that handling of cells was consistent between cell lines and preparations. As before, quantification of $PrxSO_{2/3}$ bands from this new set of Western blots unsurprisingly confirmed no significant differences in the levels of $PrxSO_{2/3}$ between NSC34 cells expressing any of the three mutant human SOD1 species tested and control NSC34 cells.

To conclude, despite extensive troubleshooting and having taken care to ensure consistency in the culture, harvest and Western blotting of the NSC34 cells within and between experiments, Western blotting for $PrxSO_{2/3}$ in NSC34 cell lines of both early and late passages grown under basal culture conditions showed often high levels of overoxidized Prxs that varied preparation to preparation within all cell lines including the control cells. These findings were both unexpected given the minimal levels of $PrxSO_{2/3}$ detected in patient and control human fibroblasts growing under basal conditions (Sections 3.2.2 and 3.9) and unwelcome as it made it difficult to establish a consistent baseline for $PrxSO_{2/3}$ levels in any one NSC34 cell line. Potential reasons for the variability observed are considered in the Discussion (Chapter 6, Section 6.8).

4.5 Levels of Prx-related proteins

The levels of various proteins involved in the regeneration cycles and regulation of the typical 2-cys Prxs were next investigated in the same whole cell lysates made from NSC34 cells growing under basal culture conditions. These included the putative $PrxSO_{2/3}$ regenerators sulfiredoxin 1 (Srx 1) and sestrin 2 (Sesn 2) (see Section 1.14) and the thioredoxin-inhibitor, thioredoxin-interacting protein (Txnip) (Section 1.15.3). As these proteins are believed to play a role in maintaining the typical 2-cys Prxs in their reduced state (but see Section 1.14.1 regarding sestrin 2) variations in their levels would be one possible explanation for the variability in levels of $PrxSO_{2/3}$ observed in the cells preparation to preparation. Western blotting for these three proteins was carried out in triplicate in the three independent whole cell preparations made from NSC34 cells grown under basal conditions and harvested between passages 11 and 15 (Figs. 4.7-4.9).

4.5.1 Levels of sulfiredoxin 1

Levels of Srx 1 were investigated first (Figs. 4.7 A & B overleaf). Sulfiredoxin 1 bands were detected in all NSC34 cell lines using a protein load of 40 μg per lane with exposures of 4 min. There was no consistent difference in levels of sulfiredoxin 1 between different NSC34 cell lines. As was the case with levels of $PrxSO_{2/3}$, levels of Srx 1 also varied within each cell line experiment to experiment. Quantification of the Western blots confirmed that the levels of Srx 1 in mutant SOD1-expressing cells and control NSC34 cell lines were not significantly different (Fig. 4.7 B). There did not appear to be any correlation between the variable Srx 1 levels in any one NSC34 cell line and the variable $PrxSO_{2/3}$ levels in the same cell line in any given whole cell preparation either, for example, low $PrxSO_{2/3}$ levels in NTG cells in Prep 1 were not accompanied by high Srx 1 levels in the same preparation of NTG cells.

A)

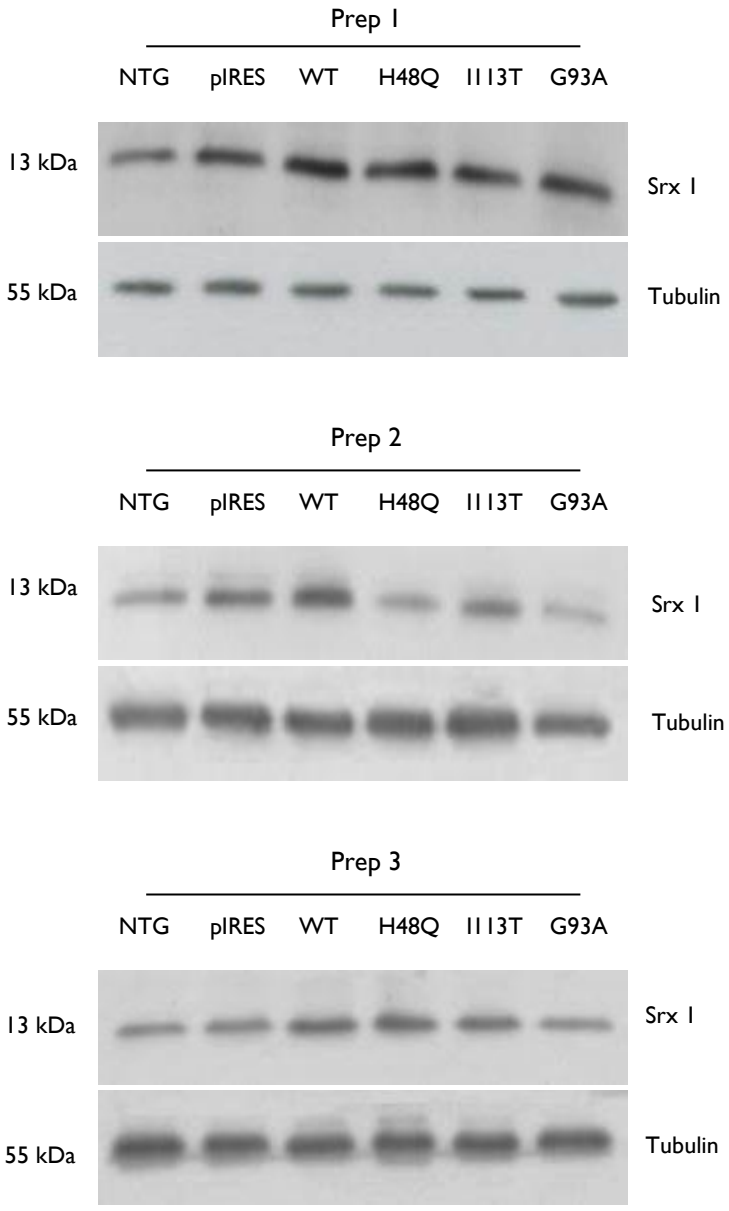

Figure 4.7: A) *Western blots for Srx 1 in NSC34 cells grown under basal culture conditions. Levels of Srx 1 varied considerably within each cell line from preparation to preparation and there was no consistent difference in Srx 1 levels between cell lines. Data include triplicate blots in each of the three independent preparations made from NSC34 cells between passage 11 and 15 growing under basal culture conditions. Lanes as previously. Protein loads were 40 µg per lane. Srx 1 blots were exposed for 4 min, tubulin blots for 1.5 min.*

B)

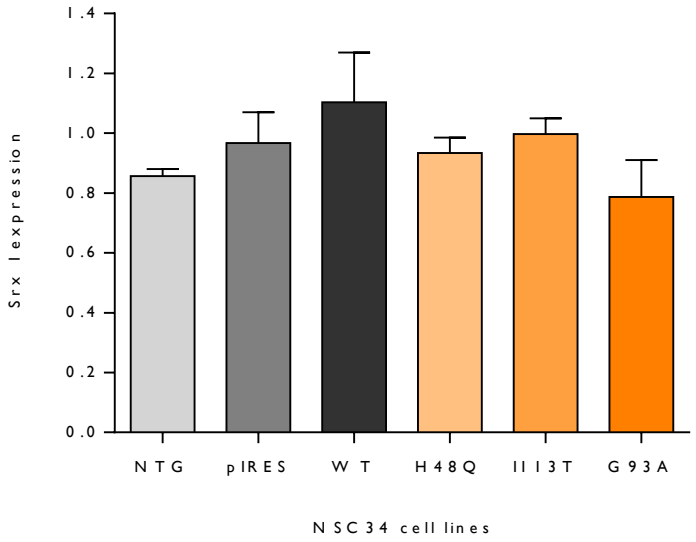

Figure 4.7: B) *Quantification of Western blots for Srx 1 in NSC34 cells grown under basal culture conditions. Data include triplicate Western blots of three independent whole cell preparations made from NSC34 cells between passage 11 and 15. Densitometry values of Srx 1 bands were normalized to those of their respective tubulin bands to correct for protein loading. Error bars represent standard error of the mean (SEM). A Student's t-test showed no statistically significant difference in levels of Srx 1 between NTG NSC34 cells and vector-only NSC34 cells (pIRES) (p-value: 0.5973), between NTG cells and WT-SOD1 expressing cells (WT) (p-value: 0.3712) and between WT SOD1-expressing cells and the three mutant SOD1-expressing cells: H48Q (p-value: 0.5478), I113T (p-value: 0.6719) and G93A (p-value: 0.2293).*

4.5.2 Levels of sestrin 2

Levels of sestrin 2, the other putative $PrxSO_{2/3}$ regenerator, were next measured in the same NSC34 whole cell preparations (Fig. 4.8 A & B overleaf). Sestrin 2 bands were detected in lysates from all NSC34 cell lines grown under basal culture conditions.

Western blotting for Sesn 2 in the whole cell preparations of NSC34 cells grown under basal culture conditions showed similar levels of Sesn 2 in all six cell lines tested with the exception of the I113T SOD1-expressing cells which consistently appeared to have somewhat lower levels of Sesn 2 than WT SOD1-expressing cells (Fig. 4.8 A). After quantification of the Sesn 2 bands using the G-box, correction for protein loading by normalization of these values to those of the appropriate actin bands (see Chapter 3, Section 3.1.1) and on application of a Student's t-test, however, this difference was not found to be statistically significant (Fig. 4.8 B).

A)

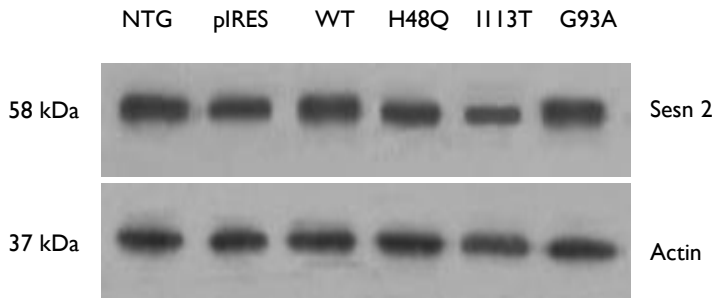

Figure 4.8: A) *Similar levels of Sesn 2 were observed across all NSC34 cell lines in each of the whole cell preparations under basal culture conditions with the exception of the I113T SOD1-expressing cell line which consistently appeared to have rather lower Sesn 2 levels. Representative Western blot showing levels of Sesn 2 in different NSC34 cell lines from three independent experiments prepared between passage 11 and 15. Lanes as previously. Protein loads were 20 µg per lane. Sesn 2 and actin (loading control) blots were both exposed for 2 min.*

B)

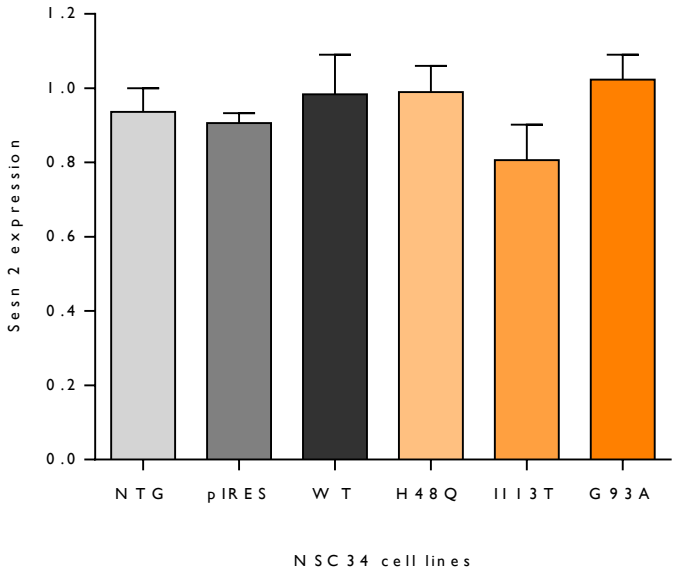

Figure 4.8: B) *Quantification of Western blots for Sesn 2 in whole cell preparations of NSC34 cell lines between passages 11 and 15 growing under basal culture conditions. Data include triplicate Western blots performed in each of three independent experiments. Levels of Sesn 2 appeared broadly similar in all cell lines with the exception of those in the I113T SOD1-expressing NSC34 cell line which appeared to be lower than those in WT SOD1-expressing cells. A Student's t-test, however, showed no statistically significant difference in levels of Sesn 2 between NTG NSC34 cells and vector-only NSC34 cells (pIRES) (p-value: 0.6321), between NTG NSC34 cells (NTG) and WT-SOD1 expressing cells (WT) (p-value: 0.6774) and between WT SOD1-expressing cells and any of the mutant SOD1 expressing cells including the I113T cells: H48Q (p-value: 0.8347), I113T (p-value: 0.2281) and G93A (p-value: 0.5784).*

4.5.3 Levels of thioredoxin-interacting protein (Txnip)

I next measured the levels of thioredoxin-interacting protein (Txnip) by Western blotting of the same three whole cell preparations of NSC34 cells grown under basal culture conditions (Fig. 4.9 A & B). Txnip is a protein that influences the oxidation state of the typical 2-cys Prxs by regulating the activity of thioredoxin which reduces physiologically oxidized Prxs (see Chapter 1, Section 1.15.3). When bound to Txnip, thioredoxin is unable to reduce physiologically oxidized typical 2-cys Prxs (Nishiyama et al., 1999).

A)

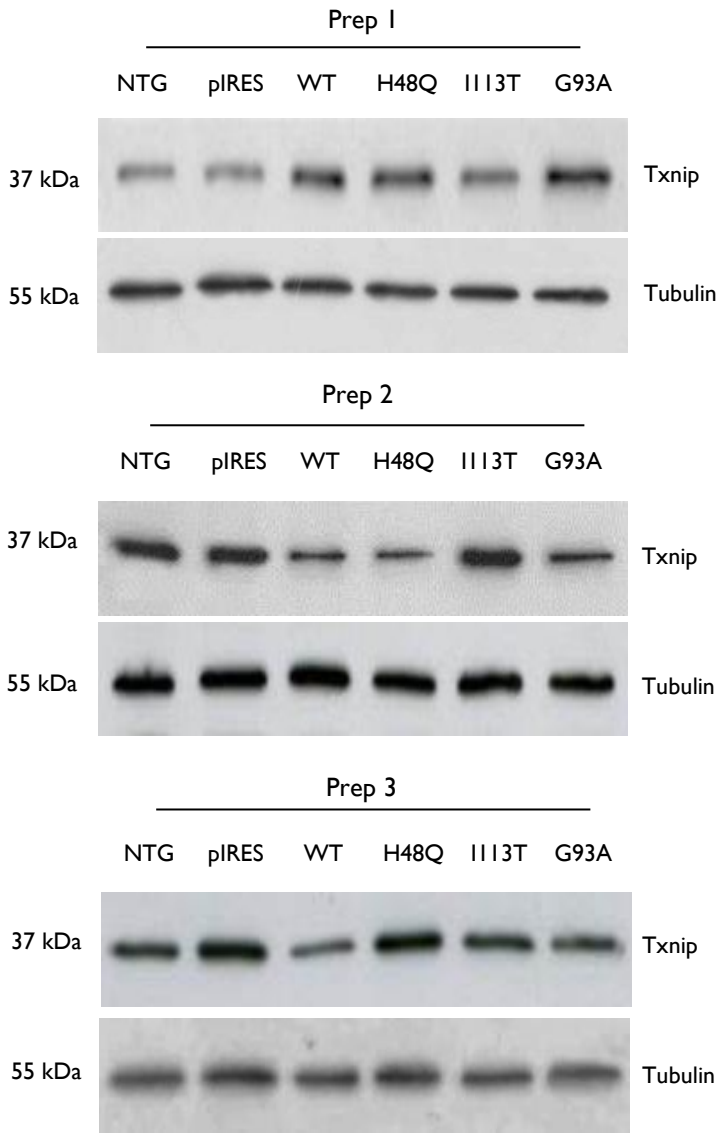

Figure 4.9: A) *Levels of Txnip varied within each NSC34 cell line from experiment to experiment. There was no consistent difference in Txnip levels between different NSC34 cell lines. Representative Western blots showing levels of Txnip in the six NSC34 cell lines in each of the three independent whole cell lysates prepared from NSC34 cells growing under basal culture conditions between passage 11 and 15. Lanes as previously. Protein loads were 40 µg per lane. Txnip blots were exposed for 3 min, tubulin blots for 1 min.*

B)

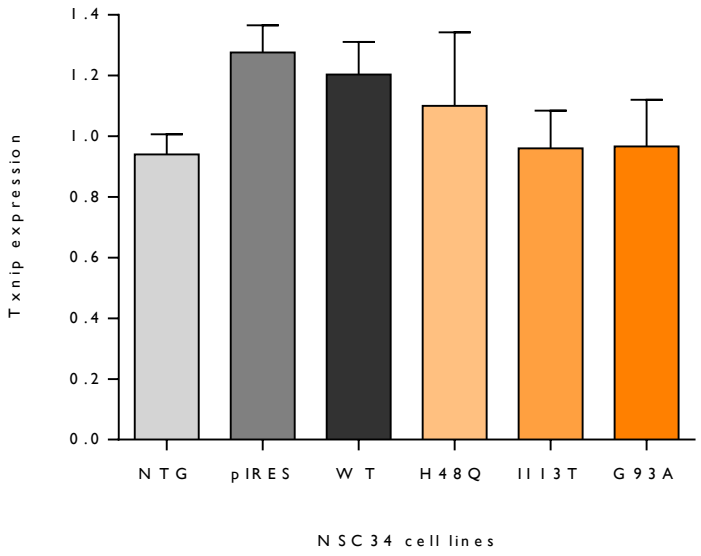

Figure 4.9: B) *Quantification of Western blots for Txnip in NSC34 cell lines between passages 11 and 15 grown under basal culture conditions. Data include triplicate blots in three independent experiments. Densitometry values of Txnip bands were normalized to those of their respective tubulin bands to correct for protein loading. Error bars represent standard error of the mean (SEM). A Student's t-test showed no statistically significant difference in levels of Txnip between NTG NSC34 cells and vector-only NSC34 cells (pIRES) (p-value: 0.2563), between NTG cells and WT-SOD1 expressing cells (p-value: 0.3108) and between WT SOD1-expressing cells and any of the three mutant SOD1-expressing cells: H48Q (p-value: 0.5075), I113T (p-value: 0.4694) and G93A (p-value: 0.5968).*

As was the case for $PxSO_{2/3}$ and Srx 1 levels in these basal NSC34 preparations, Western blotting for Txnip revealed marked variability within each NSC34 cell line experiment to experiment. This variability was a feature of both control lines and those expressing mutant human SOD1. There was no consistent difference in Txnip levels between the different NSC34 cell lines. This was confirmed by quantification of the band intensities by densitometry which showed no statistically significant difference in Txnip levels between control cell lines and mutant SOD1-expressing NSC34 cells.

In conclusion, experiments carried out to measure levels of Srx 1 and Txnip in whole cell preparations of the six NSC34 cell lines grown under basal culture conditions reiterated the experiment to experiment variability within and between NSC34 cell lines also seen when levels of $PrxSO_{2/3}$ were measured in this set of preparations and also in preparations 4-6 made from cells longer established in culture. Levels of Sesn 2, initially thought to be a regenerator of overoxidized typical 2-cys Prxs, did not change within or between cell lines experiment to experiment. Levels of total Prx 2 and Prx 3 moreover did not differ between the different NSC34 cell lines. Possible explanations for the inter-experimental variability of Srx 1 and Txnip as well as the differing behaviour of Sesn 2 are considered in the Discussion (Chapter 6).

4.6 Levels of $PrxSO_{2/3}$ after exposure to hydrogen peroxide

It proved impossible to establish consistent levels of $PrxSO_{2/3}$ in NSC34 cells growing under basal culture conditions. This consistently inconsistent variability extended to levels of the $PrxSO_{2/3}$ regenerator Srx 1 and the thioredoxin inhibitor Txnip. None of my attempts to ensure that the conduct of the experiments was consistent in all aspects altered this behaviour. In consequence, all that could be concluded from this work was that there was no consistent difference in $PrxSO_{2/3}$ level between NSC34 cell lines whether untransfected or transfected with vector only, WT SOD1 or any of the three species of mutant SOD1 investigated and that $PrxSO_{2/3}$ levels were variable in the absence of exogenous oxidative stress. Whilst it was clear that in the absence of consistent baseline $PrxSO_{2/3}$ levels interpretation of $PrxSO_{2/3}$ levels in NSC34 cells after oxidative stress would be difficult, I felt that it was nevertheless important to establish whether application of H_2O_2 might elicit a different response from the typical 2-cys Prxs present in control and mutant SOD1-expressing NSC34 cells. I therefore went on to conduct oxidative stress experiments in four of the six NSC34 cell lines by exposing them to H_2O_2 before harvest and the preparation of whole cell lysates for Western blotting for $PrxSO_{2/3}$. On the basis of the relevant literature (Moon et al., 2005; Woo et al., 2003) I decided to expose the NSC34 cells to H_2O_2 300 µM for 15 min followed by washout as described in Chapter 2, Section 2.16. Three independent experiments were performed on NTG, pIRES, WT and G93A NSC34 cell lines and were blotted in triplicate for $PrxSO_{2/3}$ and tubulin (Fig. 4.10 A-C).

A)

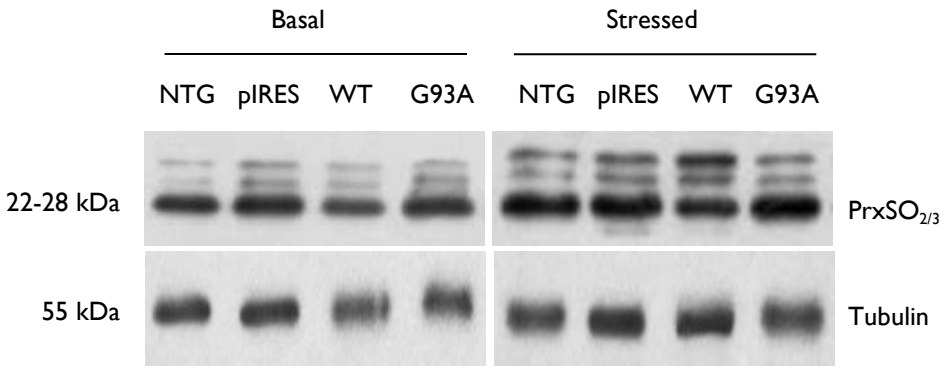

Figure 4.10: A) *Levels of $PrxSO_{2/3}$ in NSC34 cells grown under basal culture conditions (basal) and after a 15 min exposure to H_2O_2 300 µM H_2O_2 (stressed). Representative Western blots showing levels of $PrxSO_{2/3}$ in four NSC34 cell lines, stressed and unstressed. $PrxSO_{2/3}$ levels were observed to be elevated in all four lines after exposure to H_2O_2. Lanes comprise NTG = non-transgenic NSC34 cells, pIRES = NSC34 cells transfected with pIRES vector only, WT = NSC34 cells stably expressing WT human SOD1 and G93A = NSC34 cells stably expressing G93A human SOD1. Protein loads were 20 µg per lane. $PrxSO_{2/3}$ blots were exposed for 3 min, tubulin blots for 1 min.*

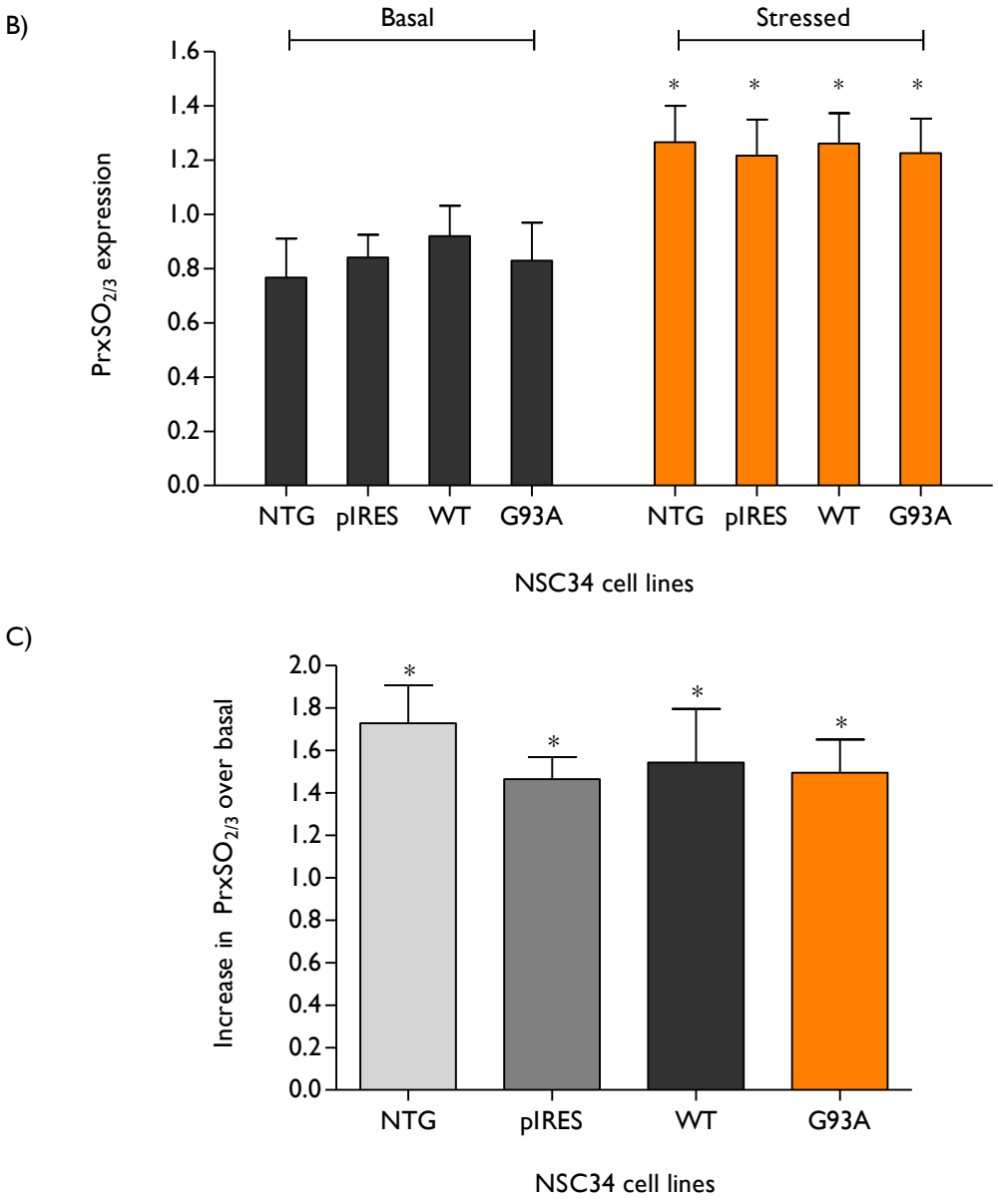

Figure 4.10: B) *Quantification of $PrxSO_{2/3}$ in NSC34 cell oxidative stress experiments. Data include at least duplicate blots in three independent experiments. Densitometry values of $PrxSO_{2/3}$ bands were first normalized to their tubulin bands to correct for protein loading. No more than one outlying $PrxSO_{2/3}$ value was excluded from the triplicate data for each cell line. All cell lines showed a statistically significant increase in $PrxSO_{2/3}$ after H_2O_2 exposure: Student t-test p-values NTG: 0.328, pIRES: 0.042, WT: 0.0482 and G93A: 0.0352. Error bars represent standard error of the mean (SEM).* ***C)*** *Graph showing no difference in the extent to which $PrxSO_{2/3}$ levels increased in WT and G93A SOD1-expressing cells after H_2O_2-treatment. Data include all values considered for Fig. 4.10 B. Densitometry values of $PrxSO_{2/3}$ bands were first normalized to those of their respective tubulin bands to correct for protein loading. The mean difference in $PrxSO_{2/3}$ level after H_2O_2 exposure was then calculated relative to corrected basal levels for each cell line. There was an increase in $PrxSO_{2/3}$ in all cell lines after H_2O_2 exposure. Error bars represent standard error of the mean (SEM). A Student's t-test showed that the amount by which $PrxSO_{2/3}$ levels increased after H_2O_2 exposure, although statistically significant in all of the cell lines, was no different between WT and G93A SOD1-expressing cell lines: (p-value: 0.9802).*

The NSC34 oxidative stress experiments were carried out in a different batch of resuscitated NSC34 cells than were the two previous sets of experiments carried out on NSC34 cells growing under basal culture conditions (Sections 4.3 and 4.4). As was observed in these previous experiments, there was still inconsistency in $PrxSO_{2/3}$ levels within each NSC34 cell line from preparation to preparation in those cells not exposed to H_2O_2 (data not shown).

After H_2O_2 exposure, $PrxSO_{2/3}$ levels were statistically significantly higher in all cell lines in comparison to $PrxSO_{2/3}$ levels in the same cell lines not exposed to H_2O_2. Although both WT SOD1-expressing and G93A SOD1-expressing NSC34 cells demonstrated increased levels of $PrxSO_{2/3}$ after H_2O_2-treatment the extent of the increase did not differ between them. The extent to which $PrxSO_{2/3}$ levels increased within individual cell lines after identical H_2O_2-treatment differed experiment to experiment (data not shown) in the same way as basal $PrxSO_{2/3}$ levels varied. This experiment to experiment variability of $PrxSO_{2/3}$ levels after exposure to H_2O_2 within each cell line made it difficult to determine whether the typical 2-cys Prxs present were overoxidized to saturation by 15 min exposure to 300 μM H_2O_2 or not. The persistent variability of $PrxSO_{2/3}$ levels within any one NSC34 cell line experiment to experiment both without and with H_2O_2 exposure made it unwise to draw firm conclusions about the biology of ALS from these data. Potential explanations for this inconsistent NSC34 cell behaviour are further considered in the Discussion.

4.6.1 Levels of typical 2-cys Prxs after exposure to hydrogen peroxide

To confirm that levels of total typical 2-cys Prxs remained similar in all NSC34 cell lines throughout the oxidative stress experiment, the whole cell lysates obtained from each of the three experiments were Western blotted using the Abcam antibody for total typical 2-cys Prxs (Chapter 3, Section 3.1.1). Western blotting was performed in duplicate for each independent experiment (Fig. 4.11 A & B).

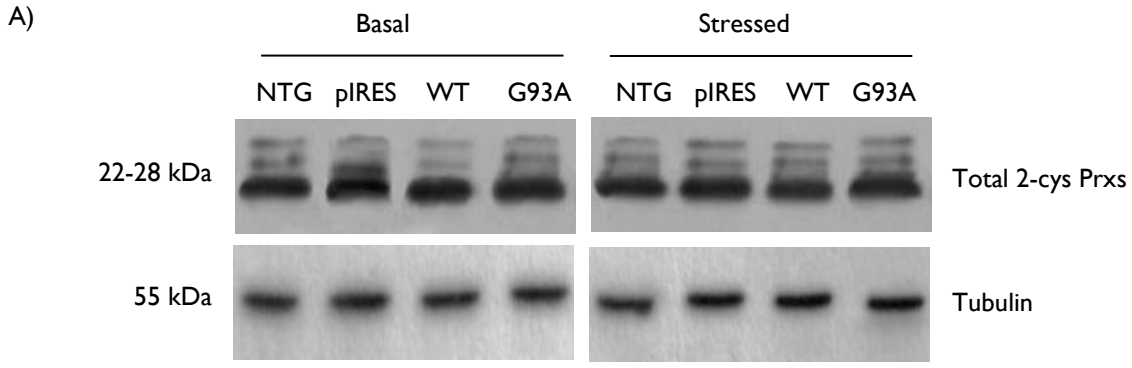

Figure 4.11: A) *Similar levels of total typical 2-cys Prxs were observed in NSC34 cells with (stressed) and without exposure to H_2O_2 (basal). Representative Western blots showing levels of typical 2-cys Prxs in four NSC34 cell lines from three independent preparations harvested after 15 min exposure to 300 μM H_2O_2 and after no exposure to H_2O_2. Lanes as previously. Protein loads were 20 μg per lane. Total typical 2-cys Prxs blots were exposed for 2 min, tubulin blots for 1 min.*

B)

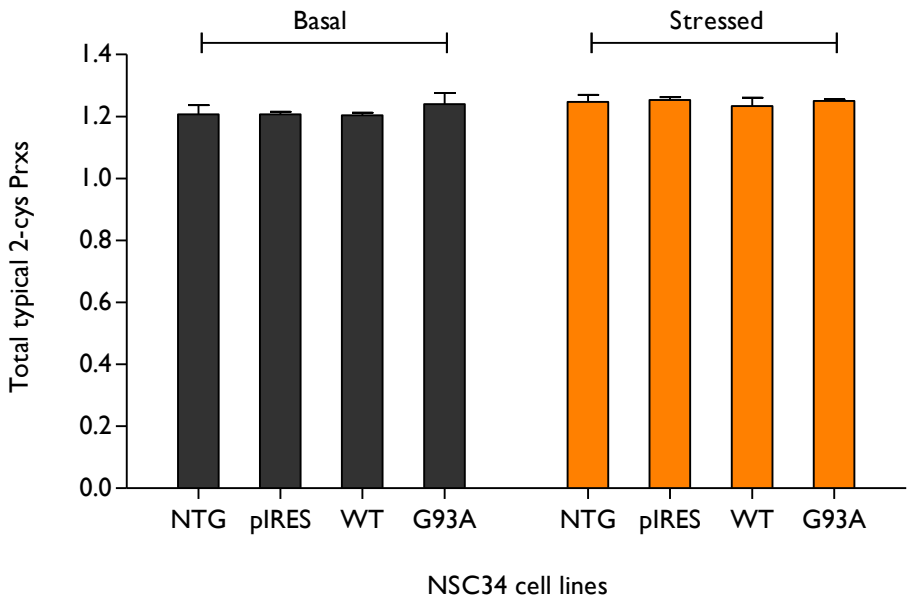

Figure 4.11: B) *Quantification of levels of total typical 2-cys Prxs from the Western blots in Fig. 4.11 A). Data include duplicate blots from three independent experiments. Densitometry values of total typical 2-cys Prx bands (see Chapter 2, Section 2.18.6) were normalized to those of their respective tubulin bands to correct for protein loading. Error bars represent standard error of the mean (SEM). Student's t-tests showed there were no statistically significant differences in the levels of total 2-cys Prxs within each cell line before and after H_2O_2 exposure: NTG (p-value: 0.7884), pIRES (p-value: 0.8731), WT (p-value: 0.8649) and G93A (p-value: 0.9127). There was also no statistically significant difference in total typical 2-cys Prx levels between WT SOD1 and G93A SOD1-expressing NSC34 cells either without H_2O_2 exposure (basal p-value: 0.8821) or after H_2O_2 exposure (stressed p-value: 0.8511).*

Western blotting for total typical 2-cys Prxs showed that levels did not change in any of the four NSC34 cell lines tested immediately after washout of a 15 min exposure to 300 μM H_2O_2 nor were there any statistically significant differences in levels of total typical 2-cys Prxs between cell lines with or without H_2O_2 exposure. This indicates that the increased $PrxSO_{2/3}$ levels measured after the NSC34 cells were treated with H_2O_2 was due to overoxidation of pre-existing typical 2-cys Prxs rather than to any increase in total typical 2-cys Prx levels. The absence of an increase in the levels of total typical 2-cys Prxs immediately after H_2O_2-washout does not preclude a later induction as was seen in the stress-recovery experiments carried out in the human fibroblasts (Chapter 3, Section 3.6.2). Stress-recovery experiments were not attempted in the NSC34 cells given the variability of $PrxSO_{2/3}$ levels in cells growing under basal culture conditions and after H_2O_2-treatment. Such experiments would have been difficult to interpret as establishing whether $PrxSO_{2/3}$ levels had returned to basal in any one NSC34 cell line would have been impossible.

To summarize, NSC34 cell lines grown under basal culture conditions showed variable levels of $PrxSO_{2/3}$, Srx 1 and Txnip between experiments and no convincing difference could be detected in their levels between WT and mutant SOD1-expressing NSC34 cells as a result. Similarly inconsistent variability in $PrxSO_{2/3}$ levels was recorded after exposure of a subset of the NSC34 cell lines to H_2O_2 although levels did convincingly increase after H_2O_2-treatment in the four NSC34 cell lines tested. There was no difference in the extent of this increase between WT SOD1- and G93A SOD1-expressing cells. Western blotting of the same oxidative stress experiment preparations for total typical 2-cys Prxs showed that variability in the levels of typical total 2-cys Prxs could not be held responsible for either the increase in $PrxSO_{2/3}$ levels measured immediately after H_2O_2-treatment, or for its unexpected variability.

Given the variability observed in $PrxSO_{2/3}$ levels between experiments even within NSC34 cell lines despite careful troubleshooting and systematic maintenance and harvest of cells, it was concluded that further work in the NSC34 cell model was unlikely to allow me convincingly to prove or disprove my primary hypothesis in motor neuronal cells. Work was therefore continued in central nervous system tissues obtained from the G93A transgenic mouse model of SOD1-related familial ALS (Chapter 5).

REFERENCES

Kirby, J., Halligan, E., Baptista, M.J., Allen, S., Heath, P.R., Holden, H., Barber, S.C., Loynes, C.A., Wood-Allum, C.A., Lunec, J., *et al.* (2005). Mutant SOD1 alters the motor neuronal transcriptome: implications for familial ALS. Brain *128*, 1686-1706.

Moon, J.C., Hah, Y.S., Kim, W.Y., Jung, B.G., Jang, H.H., Lee, J.R., Kim, S.Y., Lee, Y.M., Jeon, M.G., Kim, C.W., *et al.* (2005). Oxidative stress-dependent structural and functional switching of a human 2-Cys peroxiredoxin isotype II that enhances HeLa cell resistance to H2O2-induced cell death. J Biol Chem *280*, 28775-28784.

Nishiyama, A., Matsui, M., Iwata, S., Hirota, K., Masutani, H., Nakamura, H., Takagi, Y., Sono, H., Gon, Y., and Yodoi, J. (1999). Identification of thioredoxin-binding protein-2/vitamin D(3) up-regulated protein 1 as a negative regulator of thioredoxin function and expression. J Biol Chem *274*, 21645-21650.

Woo, H.A., Chae, H.Z., Hwang, S.C., Yang, K.S., Kang, S.W., Kim, K., and Rhee, S.G. (2003). Reversing the inactivation of peroxiredoxins caused by cysteine sulfinic acid formation. Science *300*, 653-656.

Wood-Allum, C.A., Barber, S.C., Kirby, J., Heath, P., Holden, H., Mead, R., Higginbottom, A., Allen, S., Beaujeux, T., Alexson, S.E., *et al.* (2006). Impairment of mitochondrial anti-oxidant defence in SOD1-related motor neuron injury and amelioration by ebselen. Brain *129*, 1693-1709.

5. RESULTS – G93A SOD1-TRANSGENIC MICE

INTRODUCTION

The unexplained variability of $PrxSO_{2/3}$ levels experiment to experiment in the NSC34 motor neuronal cell model of SOD1-related fALS, which remained unresolved despite extensive trouble-shooting, made it impossible to determine whether or not typical 2-cys Prxs were present in a more oxidized state in the presence of mutant SOD1 in this model of ALS. It was therefore still unclear whether my original hypothesis was true in any motor neuronal model of ALS. In an effort to resolve this question I elected to test the hypothesis in the G93A transgenic mouse model of SOD1-related fALS.

I had access to two lines of human SOD1 transgenic mice (G93A SOD1 and WT SOD1), bred on a C57BL6 background, colonies of which are maintained by the staff of the University of Sheffield Field Laboratories. The generation, phenotypic characterization and the strengths and weaknesses of using the G93A SOD1 transgenic mouse as a model of SOD1-related ALS have already been discussed in detail in Chapter 2, Section 2.4. In summary, however, the use of this model allowed me to investigate the oxidation state of the typical 2-cys Prxs in homogenates of brain and spinal cord from animals at various well-defined stages of their disease. These homogenates contained motor neurons, albeit in small numbers, undergoing degeneration due to their overexpression of a form of mutant SOD1 known to cause ALS in patients.

Pairs of G93A transgenic mice and their non-transgenic littermates were examined at three disease stages: earliest symptomatic at 60 days of age, mid-disease course at 90 days of age and late-stage disease at 120 days of age. Levels of the main neuronal typical 2-cys Prxs (Prx 2 and Prx 3), overoxidized typical 2-cys Prxs ($PrxSO_{2/3}$) and $PrxSO_{2/3}$ regenerators (Srx 1 and Sesn 2) were measured in whole brain and spinal cord homogenates from these mice by Western blotting.

Lastly, levels of physiologically-oxidized Prx 2 and Prx 3 were investigated in an additional three pairs of G93A and NTG littermate mice. This was to determine whether the overexpression of G93A SOD1 was sufficient to cause greater formation of the dimerized physiologically-oxidized forms of Prx 2 and Prx 3 (see Chapter 1, Section 1.13.1).

PREVIOUSLY-BANKED MURINE CNS TISSUE

Whilst waiting for mice of the required genotype and age to become available from our colony for sucrose-perfusion and harvest of CNS tissue for my work, preliminary experiments were performed on brain and spinal cord homogenates previously banked by members of the Department. This material consisted of mouse brain subdivided into cerebellum, anterior cortex, posterior cortex and brainstem and spinal cord divided into upper and lower spinal cord and frozen down for later use. Further details of the nature and limitations of this material are provided in the Methods (Chapter 2, Section 2.17.4).

For the purposes of this preliminary work all the portions of brain tissue stored from each individual animal were recombined to form a whole brain sample. The upper and lower spinal cord samples from the same animal were also recombined to generate a whole spinal cord sample. This material was identified from laboratory stocks for three pairs of 120 day-old G93A SOD1 transgenic (G93A) and their non-transgenic (NTG) littermates. In addition to the three NTG and G93A littermate pairs, whole brain and spinal cord tissue was identified for three 135 day-old wild-type (WT) human SOD1 transgenic mice. Unfortunately no non-transgenic littermates were available. Post-nuclear whole brain and spinal cord homogenates were prepared as described in Chapter 2, Section 2.17.4. After confirmation of the transgenic status of the samples by Western blotting for SOD1 (Section 5.1, below), levels of $PrxSO_{2/3}$ were measured in each of the samples by Western blotting (Section 5.2).

5.1 Confirmation of the transgenic status of the murine samples

Western blotting for SOD1 was first carried out in the post-nuclear whole tissue homogenates obtained from laboratory stocks. Samples from the NTG mice were expected to show a single band corresponding to endogenous murine SOD1 (mSOD1) (MW = 15 kDa) whilst samples from G93A SOD1 and WT SOD1 mice were expected to show two bands (Fig. 5.1 A & B), one corresponding to mSOD1 (MW = 15 kDa) and the other corresponding to the overexpressed human SOD1 (hSOD1) (MW = 20 kDa). Whilst this method is able to distinguish samples from NTG animals (one SOD1 band) from samples from transgenic animals (two SOD1 bands) it is not able to establish whether the hSOD1 band seen in samples from transgenic animals corresponds to WT or G93A SOD1.

A) Whole brain

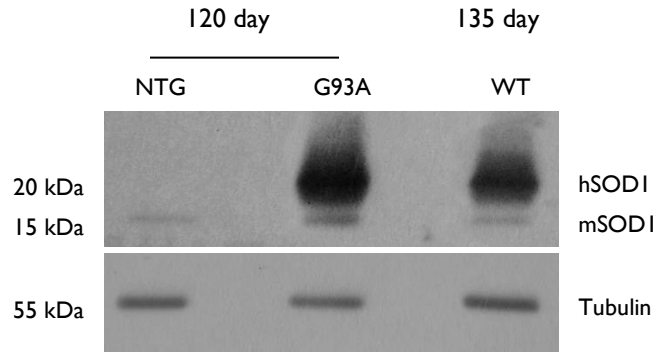

B) Whole spinal cord

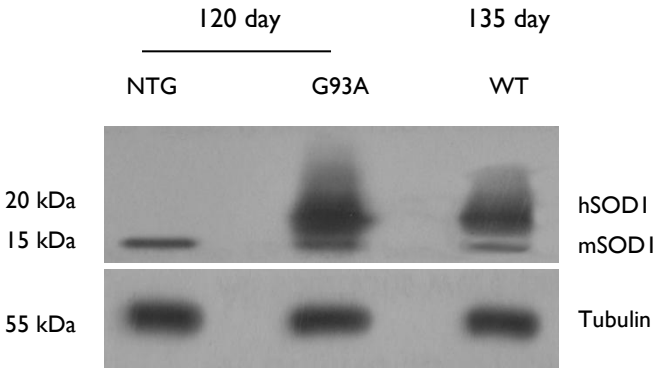

Figure 5.1: *Representative Western blots showing the levels of endogenous mouse SOD1 (mSOD1) and overexpressed human SOD1 (hSOD1) in* ***A)*** *whole brain and* ***B)*** *whole spinal cord post-nuclear homogenates from three pairs of 120 day-old G93A and NTG littermate mice and three 135 day-old WT mice. The samples from transgenic (WT or G93A) animals generated two SOD1 bands, one representing mSOD1 and the other higher band representing hSOD1. Samples from NTG animals had only one SOD1 band corresponding to mSOD1. Lanes comprise: G93A = 120 day-old G93A SOD1 transgenic mice; NTG = 120 day-old non-transgenic littermate mice; and WT = unrelated 135 day-old WT SOD1 mice. Protein loads were 20 µg per lane. SOD1 and tubulin (loading control) blots were exposed for 1.5 min.*

Western blotting for SOD1 of post-nuclear homogenates made from previously-banked whole brain (Fig. 5.1 A) and whole spinal cord (Fig. 5.1 B) samples confirmed the presence of endogenous murine SOD1in all samples and the presence of human SOD1 only within transgenic (G93A and WT) homogenates as expected. In the transgenic samples there was far more hSOD1 present than was there mSOD1. This effect was most marked in the G93A mice. This was expected as both the G93A and WT transgenic mouse lines maintained in our colony are significantly overexpressing (Chapter 2, Section 2.4).

5.2 Levels of overoxidized 2-cys Prxs ($PrxSO_{2/3}$)

Having confirming the expected expression of hSOD1 in the transgenic mice samples and its absence in the non-transgenic samples, levels of $PrxSO_{2/3}$ were measured in the same whole brain and whole spinal cord preparations. Western blotting was performed in duplicate in each of the post-nuclear homogenates of whole brain and whole spinal cord from each of the three pairs of G93A and NTG littermate mice and the three WT SOD1 mice (Fig. 5.2 A-D).

A) Whole brain

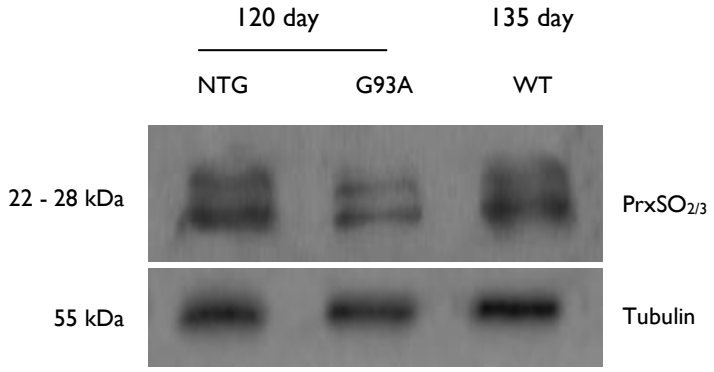

B) Whole spinal cord

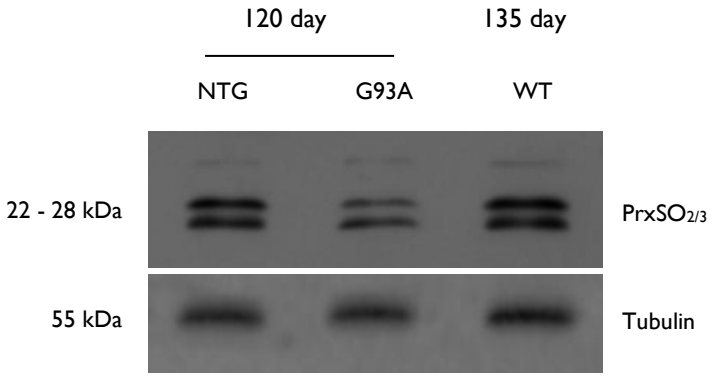

Figure 5.2: *Representative Western blots showing levels of $PrxSO_{2/3}$ in **A)** whole brain and **B)** whole spinal cord homogenates from three pairs of 120 day-old G93A mice and their NTG littermates as well as three 135 day-old WT mice. Western blotting for $PrxSO_{2/3}$ was performed in duplicate on each set of samples. Lanes comprise G93A = 120 day-old G93A SOD1 transgenic mice; NTG = 120 day-old non-transgenic littermates; and WT = unrelated 135 day-old WT SOD1 mice. Protein loads were 40 µg per lane. SOD1 and tubulin blots were both exposed for 2 min.*

C)

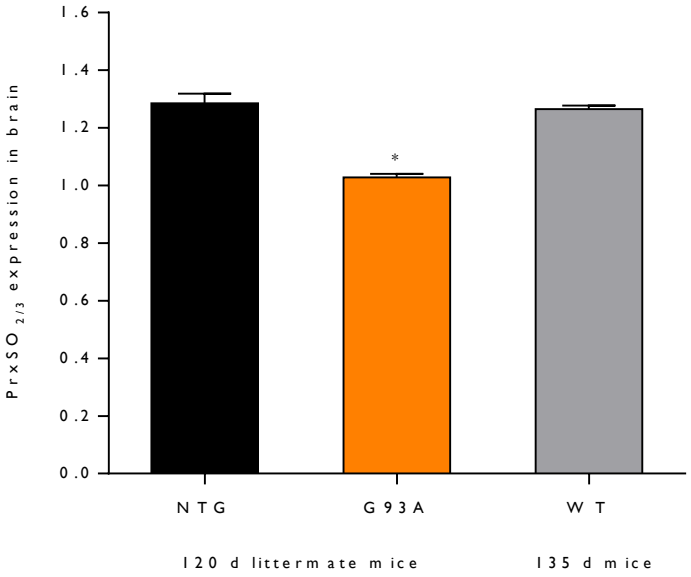

D)

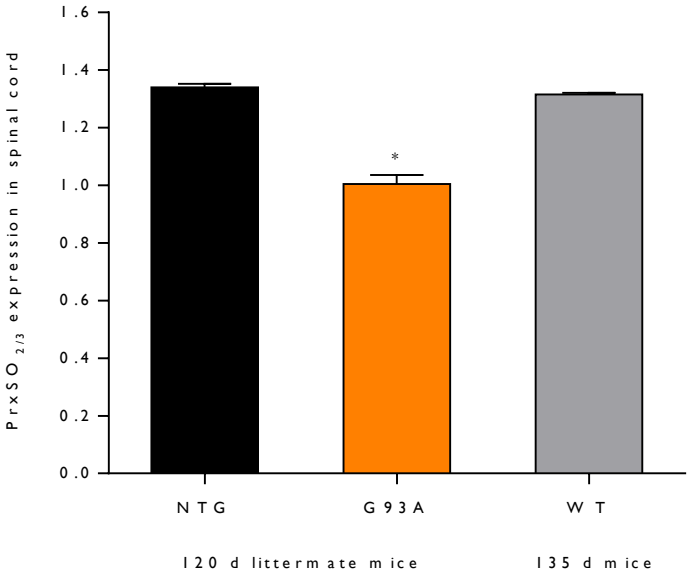

Figure 5.2: *Quantification of Western blotting for levels of $PrxSO_{2/3}$ in **C)** whole brain and **D)** whole spinal cord post-nuclear homogenates from120 day-old G93A mice and their NTG littermates as well as unrelated 135 day-old WT mice. Densitometry values from $PrxSO_{2/3}$ bands were normalized to those of their respective tubulin bands to correct for protein loading. Data include duplicate blots in each of the three pairs of G93A and NTG mice and the three WT mice. Error bars represent standard error of the mean (SEM). A Student's t-test showed a statistically significant difference in the level of $PrxSO_{2/3}$ between G93A SOD1 transgenic and NTG littermate mice in both brain (p-value: 0.0177) and spinal cord (p-value: 0.201) homogenates.*

Overoxidized typical 2-cys Prxs were readily detectable by Western blotting for $PrxSO_{2/3}$ in whole brain and whole spinal cord post-nuclear homogenates made from previously-banked murine CNS tissue from 120 day-old non-transgenic, 120 day-old G93A SOD1 and 135 day-old WT SOD1-overexpressing mice. The lack of availability of 135 day-old non-transgenic littermates with which to compare $PrxSO_{2/3}$ levels in the WT SOD1-overexpressing mice and the significant difference in the age of the WT SOD1 and G93A SOD1-overexpressing mice makes comparison between them unwise. Quantification of the levels of $PrxSO_{2/3}$ measured in post-nuclear whole tissue homogenates made from the previously-banked brain and spinal cord tissue of 120 day-old G93A and NTG littermate mice, however, indicated that there was less $PrxSO_{2/3}$ present in both whole brain and whole spinal cord of the mutant SOD1-expressing mice than in the NTG mice. Levels of $PrxSO_{2/3}$ in the G93A mice were 17.9 % lower in brain and 29.4 % lower in spinal cord in comparison to levels in non-transgenic littermate mice. This difference was statistically significant. On the surface this finding was unexpected and, if accepted as valid, would not support my original hypothesis. Given the lack of information about how the samples were banked, the absence of sucrose-perfusion and the unknown relative delay from death to freezing of the pre-banked CNS tissue from G93A *vs* NTG mice, however, interpretation of this albeit statistically significant difference was undertaken with caution (Chapter 6, Section 6.11). The results of work in cohorts of mice harvested by me at comparable ages using sucrose-perfusion and minimization of post-mortem delay were awaited before final conclusions were reached.

SUCROSE-PERFUSED MURINE CNS TISSUE

The unexpected results of the work-up experiments in the poorly-characterized previously-banked CNS tissue from G93A SOD1-overexpressing mice and their NTG littermates made it more important to measure levels of $PrxSO_{2/3}$ in optimally-prepared murine CNS tissue. Once animals were available from our colony, whole brain and spinal cord were extracted from three pairs each of 60, 90 and 120 day-old sex-matched G93A SOD1-overexpressing mice and their NTG littermates immediately after sucrose perfusion as described in Chapter 2, Section 2.17. Levels of total and overoxidized Prxs were then measured in post-nuclear whole-tissue homogenates of this tissue. If consistent differences in $PrxSO_{2/3}$ levels were identified between NTG and mutant SOD1-expressing murine CNS tissue, I planned to go on to measure $PrxSO_{2/3}$ in CNS tissue from WT SOD1-overexpressing mice.

5.3 Confirmation of the transgenic status of the G93A and NTG murine samples

The genotype and hence the transgenic status of the NTG and G93A mice sacrificed in these experiments was re-confirmed in the brain and spinal cord homogenates obtained from them by Western blotting for SOD1. As before, the antibody used recognized both endogenous murine SOD1 (mSOD1) and transgenic

human SOD1 (hSOD1). Samples obtained from NTG mice were expected to show a single band corresponding to mSOD1 (MW = 15 kDa) whilst samples from the G93A SOD1 mice were expected to show two bands, one representing mSOD1 (MW = 15 kDa) and the other, running at a slightly higher molecular weight, representing the transgenic overexpressed hSOD1 (MW = 20 kDa). Post-nuclear whole tissue homogenates, prepared from each of the three pairs of mice sacrificed at each time point, were Western blotted for SOD1 in duplicate (Fig. 5.3 A & B).

A) Whole brain

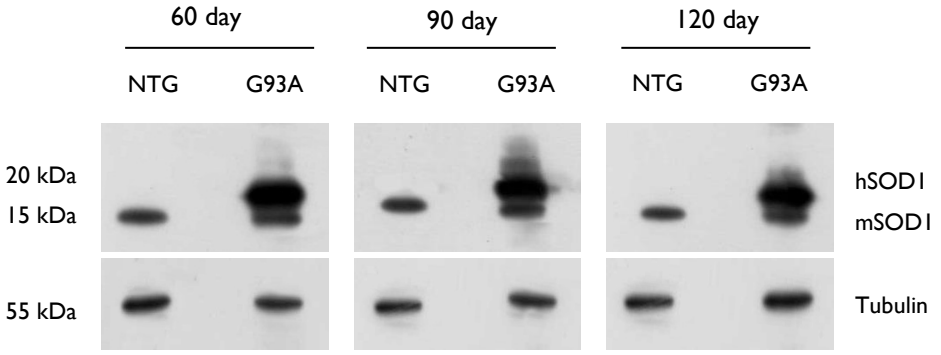

B) Whole spinal cord

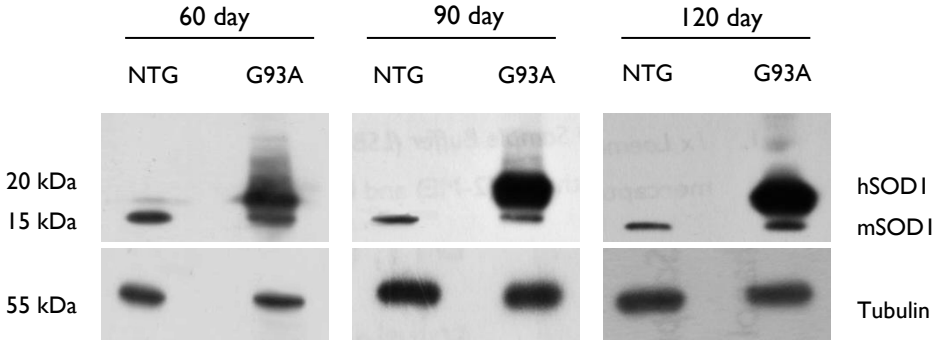

Figure 5.3: *Representative Western blots for SOD1 showing the levels of mSOD1 and overexpressed transgenic hSOD1 in* ***A)*** *whole brain and* ***B)*** *whole spinal cord post-nuclear homogenates from age- and sex-matched pairs of G93A and NTG littermate mice sacrificed at 60, 90 and 120 days of age. The genotypes of the mice were reconfirmed by the presence of hSOD1 in samples prepared from G93A SOD1 transgenic mice and its absence in samples prepared from their NTG littermates. Preparations were made from three independent pairs of G93A and NTG littermate mice at each of three different ages (60, 90 and 120 days-old) and were Western blotted in duplicate for SOD1. Lanes comprise G93A = brain or spinal cord homogenate from G93A SOD1 transgenic mice, NTG = brain or spinal cord homogenate from their NTG littermates. Protein loads were 20 µg per lane. SOD1 and tubulin blots were both exposed for 1 min.*

As expected, Western blotting for SOD1 in brain and spinal cord homogenates obtained from the G93A SOD1 transgenic mice sacrificed at all three ages confirmed the presence of transgenic human SOD1 in all samples in addition to endogenous murine SOD1. In contrast, all brain and spinal cord homogenates obtained from their NTG littermates revealed only one SOD1 band corresponding to endogenous murine

SOD1. The genotypes of the littermate mice pairs were thus confirmed as was the significant overexpression of the human transgene in this mouse model of G93A SOD1-related fALS.

5.4 Levels of total Prx 2 and Prx 3

After confirming the expected overexpression of hSOD1 in the G93A mice samples, the brain and spinal cord preparations were next Western blotted for total Prx 2 and Prx 3. I chose to measure the levels of these two typical 2-cys Prxs as they are the most abundant typical 2-cys Prx isoforms found within motor neurons (Goemaere and Knoops, 2012; Jin et al., 2005). Prx 1, as was discussed in Chapter 1, Section 1.13, is primarily expressed within glia and not within neurons. Levels of Prx 2 and Prx 3 were measured to determine whether either of their levels were different in whole brain or spinal cord from the G93A mice compared to their NTG littermates. Western blotting for each of the two Prxs was performed in triplicate in post-nuclear whole brain and spinal cord homogenates made from each of the three pairs of mice sacrificed at 60, 90 and 120 days of age (Fig 5.4 A-D, Fig 5.5 A-D). Protein expression levels were quantified using the G-box as previously described (Chapter 2, Section 2.18.6).

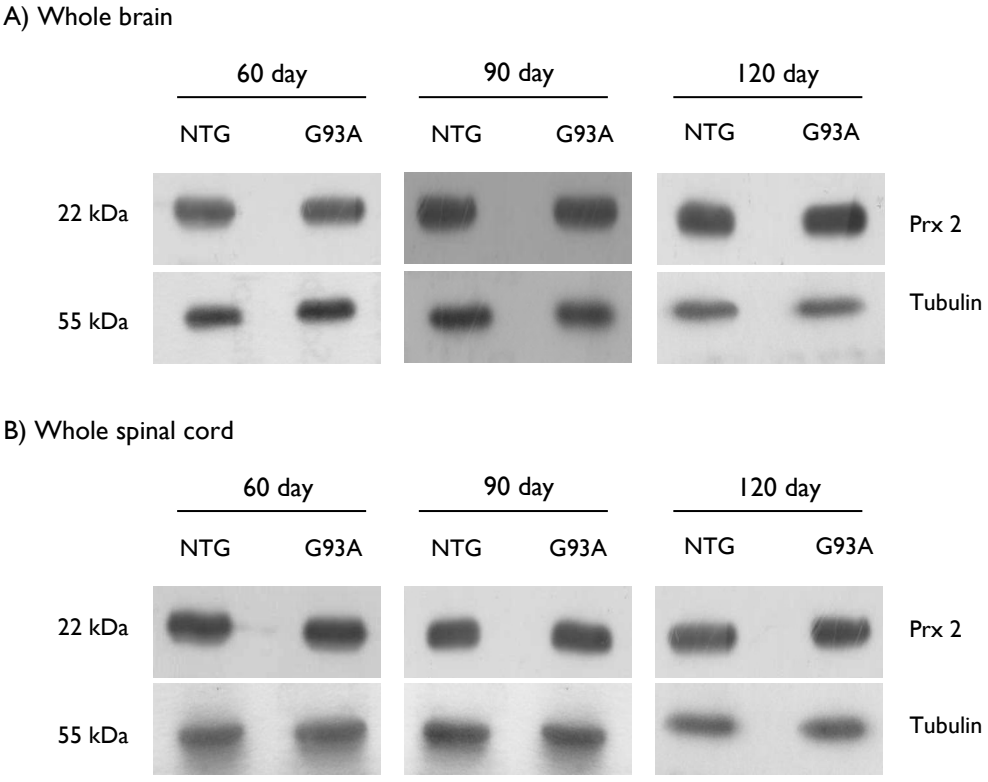

Figure 5.4: *Levels of Prx 2 were observed to be similar in* ***A)*** *whole brain and* ***B)*** *whole spinal cord homogenates in G93A SOD1 and NTG littermates at 60, 90 and 120 days of age. Representative Western blots showing levels of total Prx 2 in* ***A)*** *brain and in* ***B)*** *spinal cord homogenates from NTG and G93A transgenic mice. Three independent pairs each of G93A and NTG littermate mice of 60, 90 and 120 days of age were investigated. Western blotting for Prx 2 was performed in triplicate in each preparation. Lanes comprise G93A = CNS homogenates from G93A SOD1 transgenic mice, NTG = CNS homogenates from their NTG littermates. Protein loads were 20 µg per lane. Prx 2 and tubulin blots were both exposed for 1.5 min.*

C)

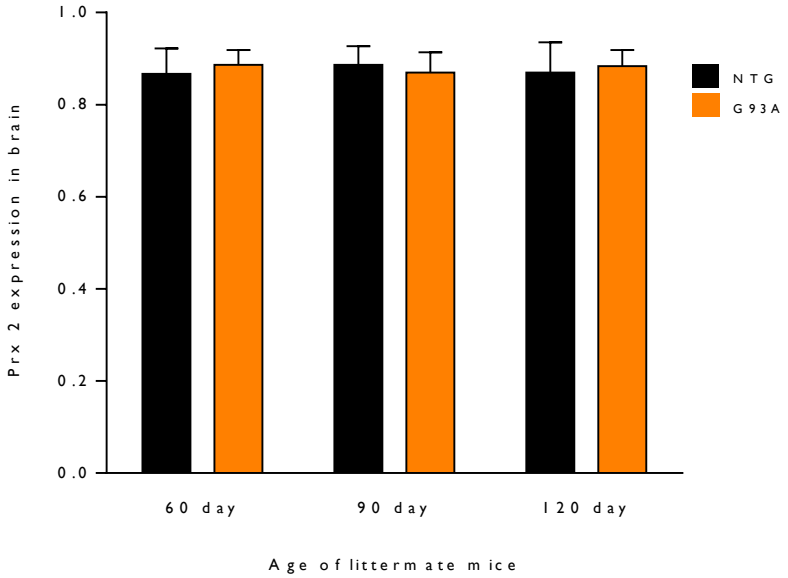

D)

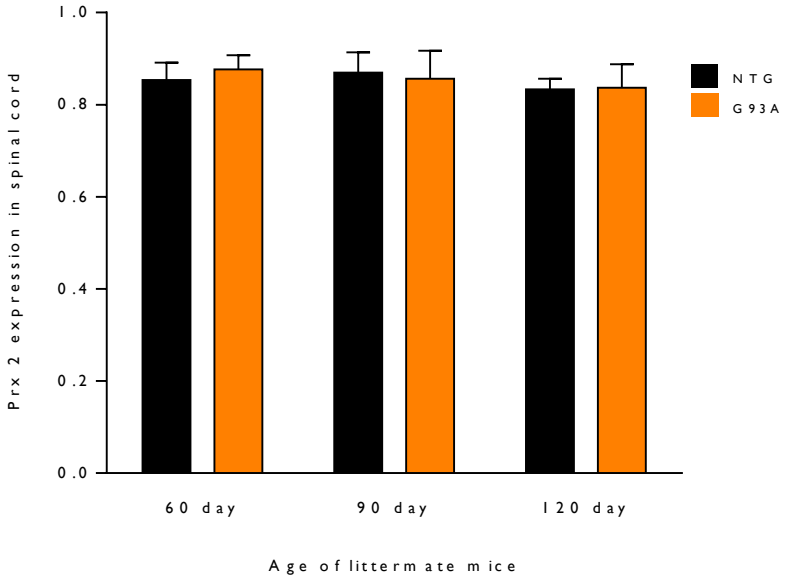

Figure 5.4: *Quantification of the levels of total Prx 2 in* ***C)*** *whole brain and* ***D)*** *whole spinal cord post-nuclear homogenates from G93A mice and their NTG littermates mice at 60, 90 and 120 days of age. Densitometry values of Prx 2 bands were first normalized to those of their respective tubulin bands to correct for protein loading. Data include triplicate blots in each of the three independent pairs of mice sacrificed at each time point. Error bars represent the standard error of the mean (SEM). A Student's t-test showed no statistically significant difference in the levels of Prx 2 between G93A and NTG mice in either brain homogenates: 60 day (p-value: 0.7487), 90 day (p-value: 0.6953) and 120 day (p-value: 0.7979) or in spinal cord homogenates: 60 day (p-value: 0.8220), 90 day (p-value: 0.7515) and 120 day (p-value: 0.6411).*

A) Whole brain

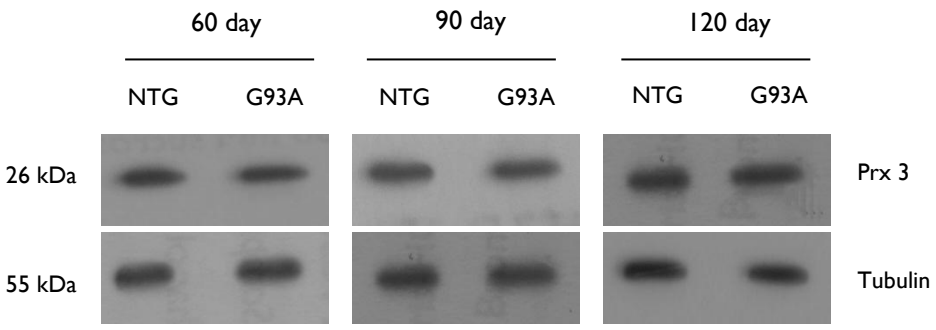

B) Whole spinal cord

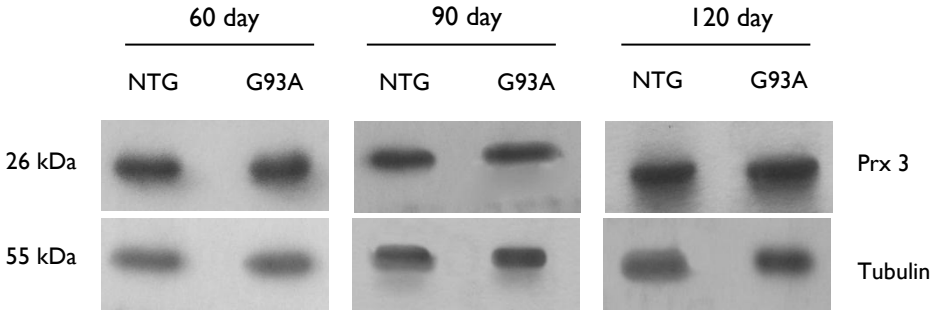

Figure 5.5: *Levels of Prx 3 were similar in brain and spinal cord post-nuclear whole tissue homogenates from G93A mice and their NTG littermates at the three ages measured. Representative Western blots showing levels of total Prx 3 in* ***A)*** *whole brain and* ***B)*** *whole spinal cord post-nuclear homogenates from G93A transgenic mice and their NTG littermates at 60, 90 and 120 days of age. Data include triplicate Western blots performed in three independent littermate pairs at each age. Lanes comprise NTG = CNS homogenates from non-transgenic littermate mice and G93A = CNS homogenates from G93A SOD1 transgenic mice. Protein loads were 20 µg per lane. Prx 3 and tubulin blots were both exposed for 1.5 min.*

Prx 2 and Prx 3 were readily detected by Western blotting in post-nuclear whole tissue homogenates made from brain and spinal cord from G93A SOD1 transgenic mice and their non-transgenic littermates sacrificed at symptom onset, mid-disease and late-stage disease. Levels of both total Prx 2 and total Prx 3 appeared to be the same in whole brain and in whole spinal cord from G93A transgenic mice and their NTG littermates at all three ages tested, and this was confirmed by quantification using densitometry and the application of a Student's t-test. This is further discussed in Chapter 6, Section 6.10.

C)

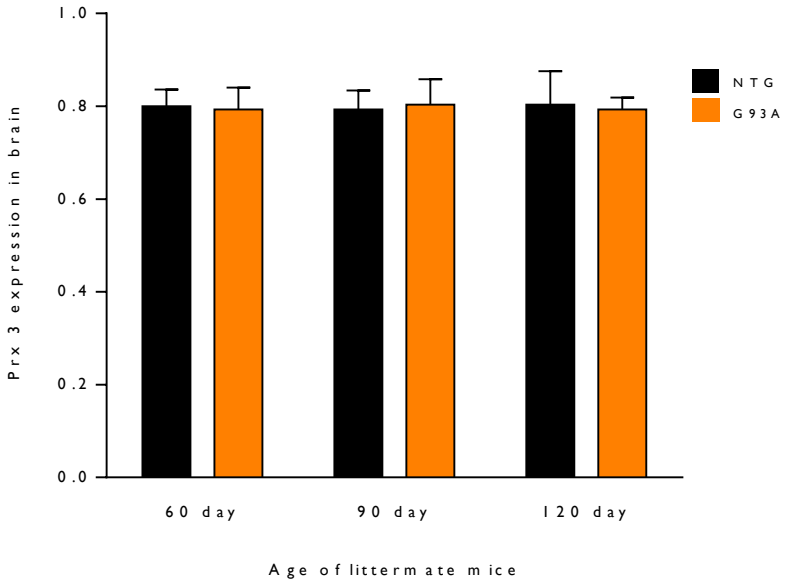

D)

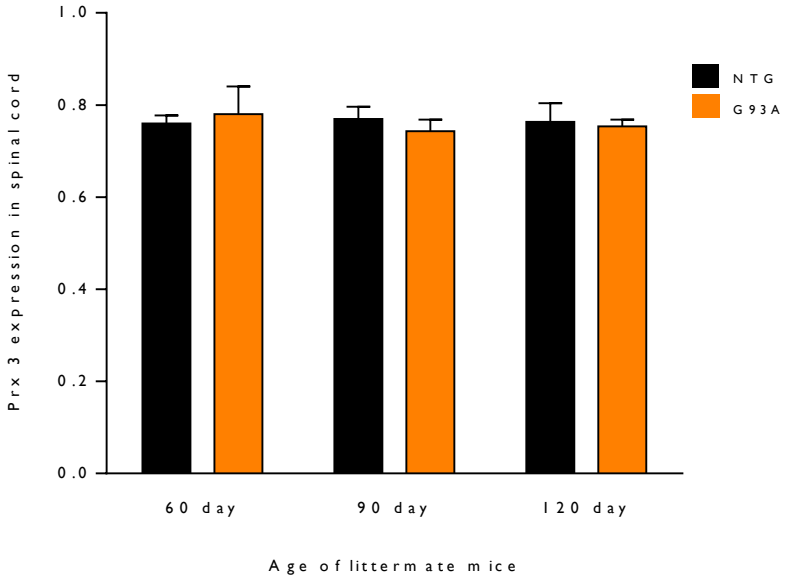

Figure 5.5: *Quantification of the levels of total Prx 3 in* ***C)*** *whole brain and in* ***D)*** *whole spinal cord post-nuclear homogenates from G93A mice and their NTG littermates at three different ages. Prx 3 bands were first normalized to those of their respective tubulin bands to correct for protein loading. Data include triplicate blots for Prx 3 in each of three independent pairs of mice sacrificed at each time point. Error bars represent standard error of the mean (SEM). A Student's t-test showed no statistically significant difference in the level of Prx 3 in G93A and NTG littermate mice in either brain homogenates: 60 day (p-value: 0.7546), 90 day (p-value: 08247) and 120 day (p-value: 0.7129) or in spinal cord homogenates: 60 day (p-value: 0.5534), 90 day (p-value: 0.6952) and 120 day (p-value: 0.6654) from mice of any of the three ages tested.*

5.5 Levels of overoxidized Prxs ($PrxSO_{2/3}$)

Having established that there was no difference in the levels of total Prx 2 or Prx 3 in whole brain or spinal cord homogenates from G93A mice and their NTG littermates, I next measured $PrxSO_{2/3}$ in the same panel of homogenates. $PrxSO_{2/3}$ bands had been readily detectable by Western blotting in brain and spinal cord homogenates made from previously-banked samples (Fig. 5.2). I wanted to determine whether the stable overexpression of mutant human SOD1 would result in increased levels of $PrxSO_{2/3}$ in optimally harvested and banked CNS homogenates from G93A mice compared to their NTG littermates, as I had originally hypothesized. Whole brain (Fig. 5.6 A- E) and whole spinal cord (Fig. 5.7 A-E) post-nuclear homogenates from three independent pairs of mice sacrificed at 60, 90 and 120 days old were Western blotted for $PrxSO_{2/3}$ in triplicate.

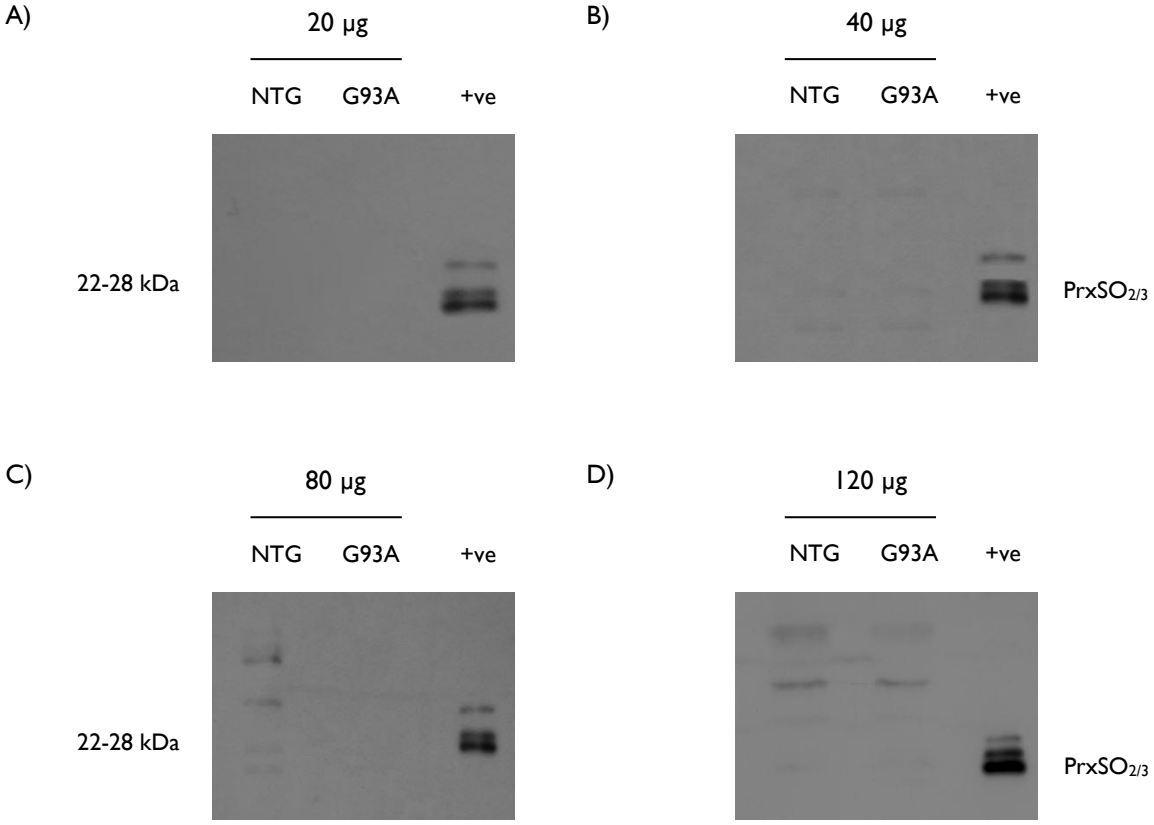

Figure 5.6: *Representative Western blots for $PrxSO_{2/3}$ in post-nuclear homogenates of whole brain from one pair of 120 day-old G93A and littermate NTG transgenic mice. No $PrxSO_{2/3}$ bands were detected despite increasing protein loads.* ***A)*** *20 µg per lane* ***B)*** *40 µg per lane* ***C)*** *80 µg per lane and* ***D)*** *120 µg per lane. +ve = whole cell lysate, 20 µg, from NTG NSC34 cells used as a positive control. All blots were exposed for 15 min to improve the chances of detecting $PrxSO_{2/3}$ bands.*

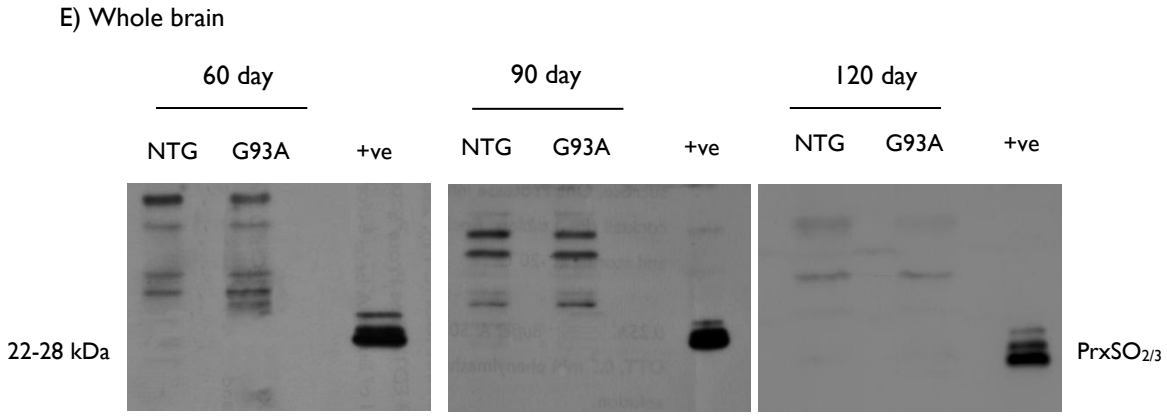

Figure 5.6: E) *Despite protein loads of 120 µg per lane, $PrxSO_{2/3}$ bands were not detected in post-nuclear homogenates of whole brain from G93A SOD1 transgenic mice or their NTG littermates at any of the three ages tested. Three independent littermate pairs of each age were Western blotted for $PrxSO_{2/3}$ in triplicate. +ve = whole cell lysate, 20 µg, from NTG NSC34 cells used as a positive control. All blots were exposed for 15 min.*

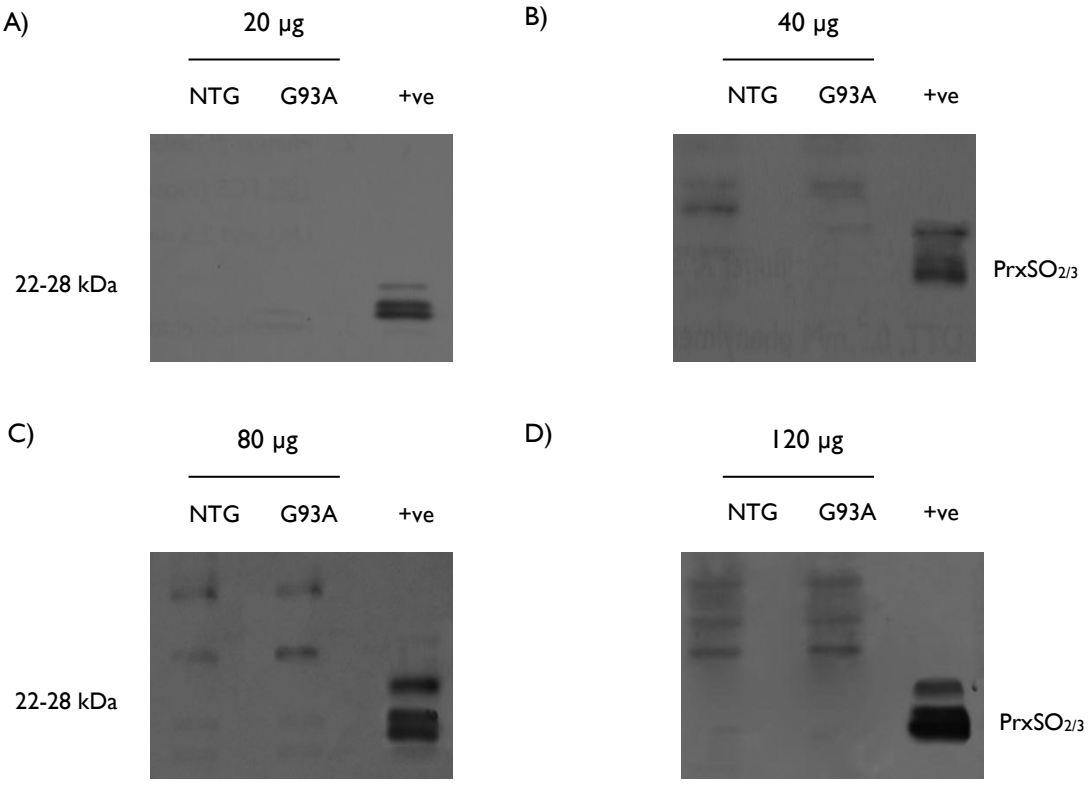

Figure 5.7: *Representative Western blots for $PrxSO_{2/3}$ in post-nuclear homogenates of whole spinal cord from one pair of 120 day-old G93A and littermate NTG transgenic mice. No $PrxSO_{2/3}$ bands were detected despite increasing protein loads.* ***A)*** *20 µg per lane* ***B)*** *40 µg per lane* ***C)*** *80 µg per lane and* ***D)*** *120 µg per lane. Whole cell lysate, 20 µg, from NTG NSC34 cells was used as a positive control (+ve) in each case. All blots were exposed for 15 min to improve the chances of detecting $PrxSO_{2/3}$ bands.*

E) Whole spinal cord

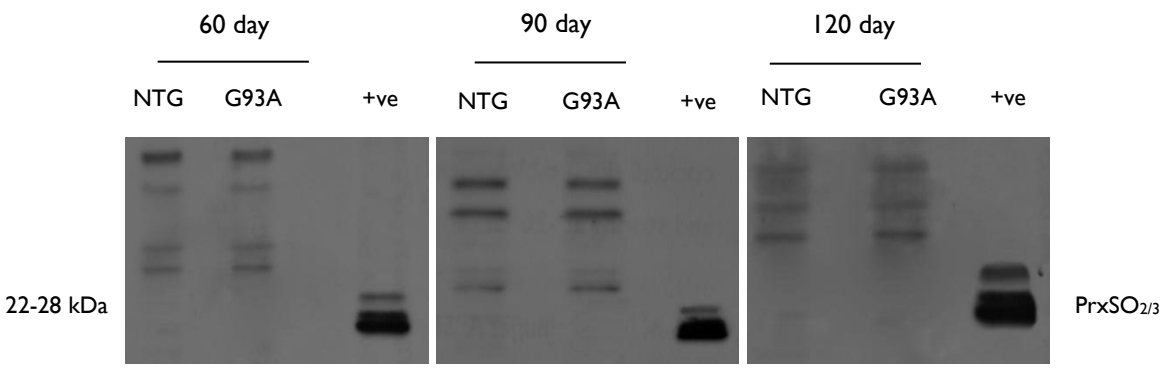

Figure 5.7: E) *Despite protein loads of 120 µg per lane, $PrxSO_{2/3}$ bands were not detected in post-nuclear homogenates of whole spinal cord tissue from G93A SOD1 transgenic mice or their NTG littermates at any of the three ages tested. Three independent littermate pairs of each age were blotted for $PrxSO_{2/3}$ in triplicate. +ve = whole cell lysate, 20 µg, from NTG NSC34 cells used as a positive control. Blots were exposed for 15 min to optimize the chances of detecting $PrxSO_{2/3}$ bands.*

$PrxSO_{2/3}$ bands were undetectable after Western blotting for $PrxSO_{2/3}$ in whole brain and spinal cord homogenates from three independent pairs of NTG and G93A littermate mice at 60, 90 and 120 days of age using the usual protein loads (20 - 40 µg). The protein loading was therefore increased up to 120 µg per lane and prolonged exposures of up to 15 min employed to optimize the chances of detecting what might be very small quantities of $PrxSO_{2/3}$. Despite these very high protein loads and long exposures, no overoxidized typical 2-cys Prx bands were detected in either G93A or NTG mouse CNS tissue, brain or cord, at any of the three disease stages tested. The ready detection of the usual triplet $PrxSO_{2/3}$ bands in the positive control (only 20 µg protein loaded per lane) made it unlikely that my failure to detect bands in the mouse CNS tissue was due to technical problems with the Western blotting. Furthermore, the results of Western blotting for total Prx 2 and Prx 3, had already confirmed the presence of plentiful typical 2-cys Prxs in the murine CNS homogenates making it impossible that an absence of 2-cys Prxs in the samples available to become overoxidized was responsible for the absence of $PrxSO_{2/3}$. Possible reasons why I was unable to detect $PrxSO_{2/3}$ in mouse CNS tissue, G93A or NTG, are discussed in Chapter 6, Section 6.10. In summary, however, it appeared that when CNS material was harvested from mice sacrificed with sucrose perfusion and care taken to minimize the time from last heart-beat to the snap-freezing of the tissue, no $PrxSO_{2/3}$ could be detected by Western blotting in these preparations. This in turn suggested that the $PrxSO_{2/3}$ observed in homogenates made from previously-banked murine CNS tissues (Fig. 5.2) might very well have been artifactual, most likely due to prolonged post-mortem delay and *in vitro* oxidation of the samples.

5.6 Levels of $PrxSO_{2/3}$ regenerators

I next wanted to know whether Srx 1 and Sesn 2, at the time both thought to be putative regenerators of $PrxSO_{2/3}$, could be detected in whole tissue brain or spinal cord homogenates of G93A transgenic mice and their NTG littermates and, if so, whether there was any detectable difference in the levels of either between the two. Western blotting for Srx 1 and Sesn 2 was carried out in triplicate in each of the three independent littermate pairs harvested at each of the three time points. At the time these experiments were carried out it was thought that overoxidized typical 2-cys Prxs could be returned to their reduced, active forms by the action of both sulfiredoxin 1 (Srx 1) and sestrin 2 (Sesn 2) (Budanov et al., 2004; Papadia et al., 2008; Woo et al., 2005). Since that time, however, evidence has arisen to suggest that whilst this is still true of sulfiredoxin, sestrin 2 is much less likely to play a role in the active reduction of $PrxSO_{2/3}$ (Woo et al., 2009).

5.6.1 Sulfiredoxin 1

Levels of Srx 1 were the first to be measured in whole brain and spinal cord homogenates (Fig. 5.8 A-D).

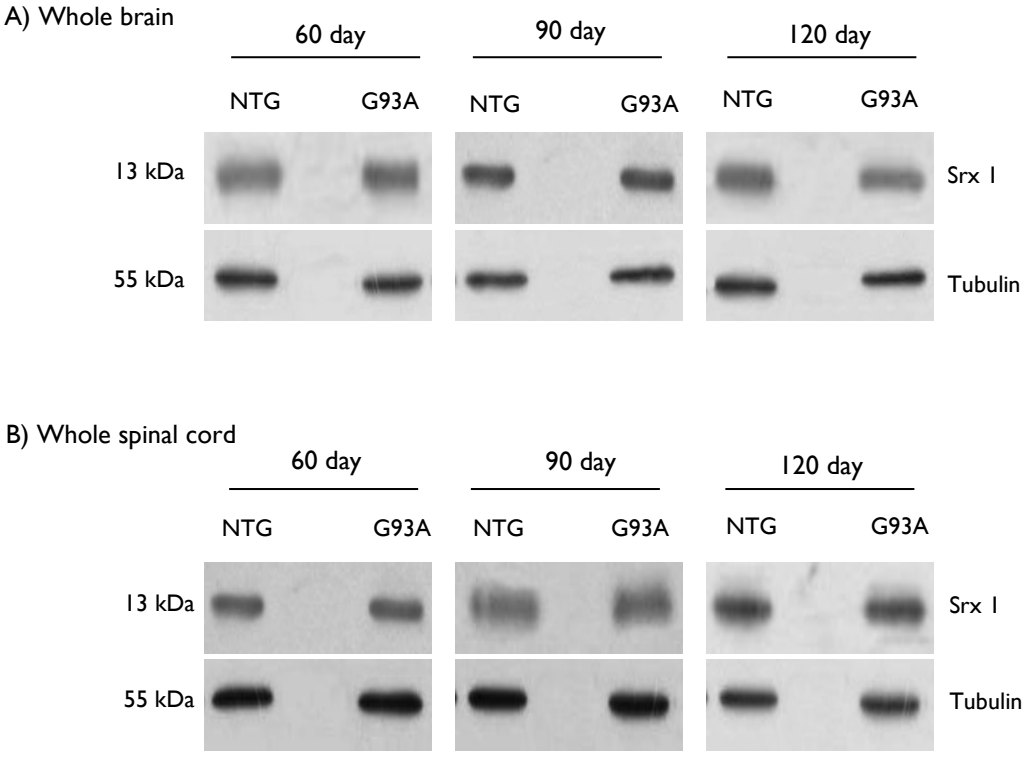

Figure 5.8: *Levels of Srx 1 were observed to be similar in **A)** whole brain and **B)** whole spinal cord post-nuclear homogenates from G93A transgenic mice and their NTG littermates of 60, 90 and 120 days of age. Representative Western blots for Srx 1 in one littermate pair sacrificed at each of 60, 90 and 120 days of age. Western blotting for Srx 1was performed in triplicate in each pair of mice. Lanes comprise: NTG = CNS homogenates from non-transgenic littermate mice and G93A = CNS homogenates from G93A SOD1 transgenic mice. Protein loads were 40 µg per lane. Srx 1 and tubulin blots were both exposed for 1.5 min.*

C)

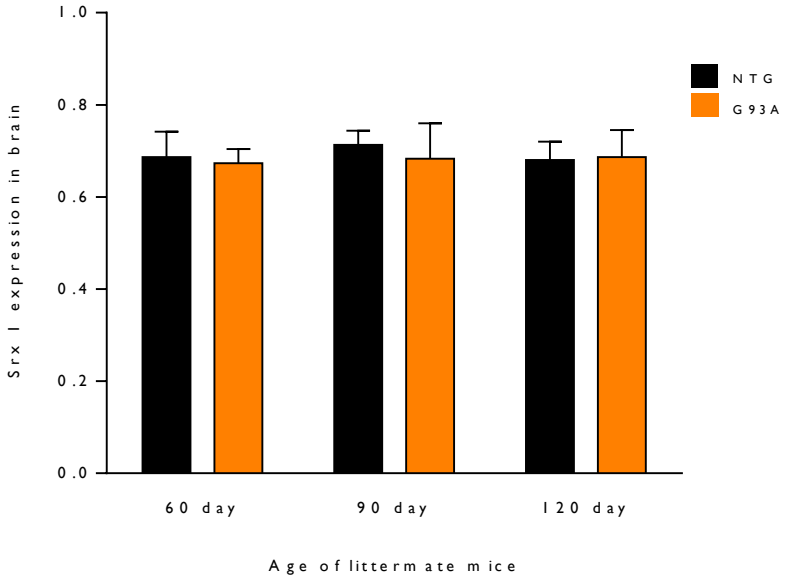

D)

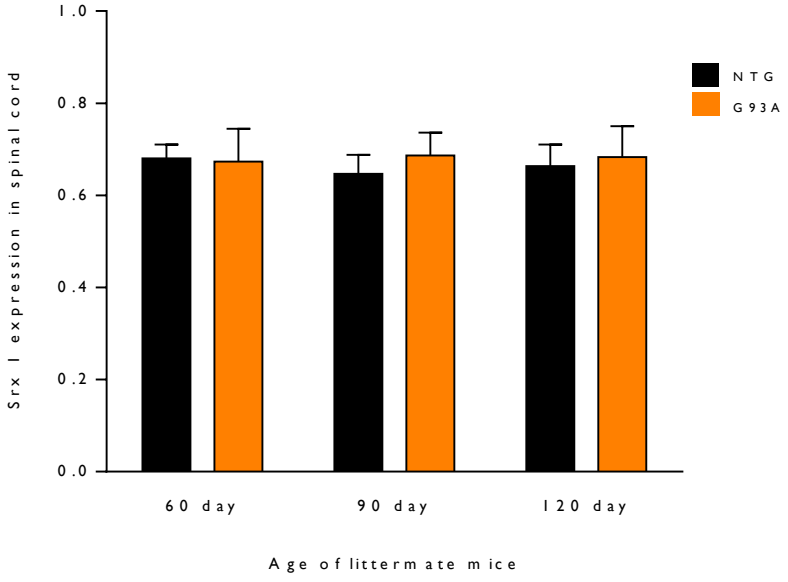

Figure 5.8: *Quantification of levels of Srx 1 in* ***C)*** *whole brain and* ***D)*** *whole spinal cord post-nuclear homogenates from G93A and NTG littermate mice at three different ages. Densitometry values of the Srx 1 bands were normalized to those of their respective tubulin bands to correct for protein loading. Data include triplicate blots for Srx 1 in each of three independent pairs of mice sacrificed at each of the three time points. Error bars represent standard error of the mean (SEM). A Student's t-test showed no statistically significant difference in Srx 1 levels in whole tissue homogenates of G93A and their NTG littermates in either brain homogenates: 60 day (p-value: 0.6994), 90 day (p-value: 0.6471) and 120 day (p-value: 0.7849) or in spinal cord homogenates: 60 day (p-value: 0.6812), 90 day (p-value: 0.7215) and 120 day (p-value: 0.7436).*

Sulfiredoxin 1 bands were readily detected by Western blotting of whole brain and spinal cord post-nuclear preparations of G93A mice and their NTG littermates sacrificed at 60, 90 and 120 days of age. Sulfiredoxin 1 levels in both whole brain and spinal cord homogenates were no different in G93A mice than in their NTG littermates. This was consistently the case in all three independent littermate pairs at all three ages tested and statistical analysis confirmed that there was no statistically significant difference in Srx 1 levels in CNS tissues from G93A and littermate NTG mice at any of the ages tested.

5.6.2 Sestrin 2

I next measured the levels of Sesn 2 in the same panel of CNS homogenates. Whole brain (Fig. 5.9 A-E) and whole spinal cord (Fig. 5.10 A-E) homogenates made from the three independent pairs of mice of each age were Western blotted in triplicate for Sesn 2 and actin to be used as a loading control (see Chapter 3, Section 3.1.1).

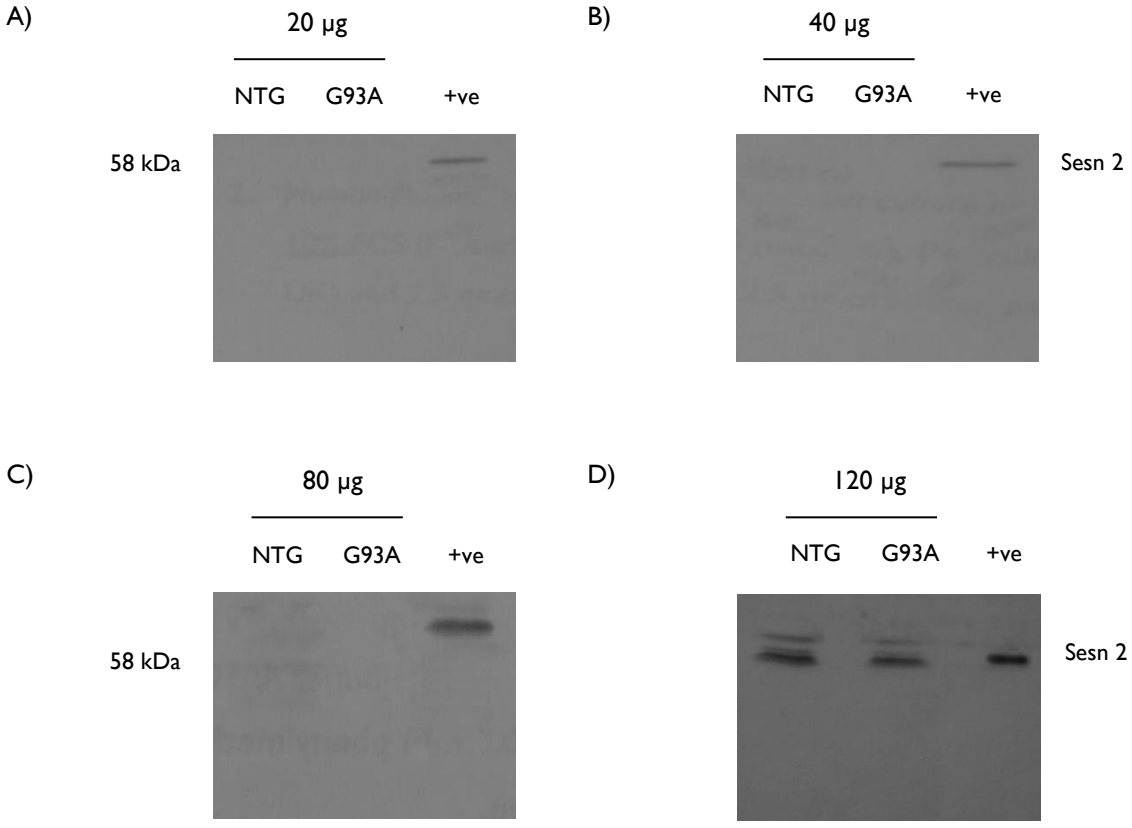

Figure 5.9: *Sestrin 2 bands were undetectable in whole brain homogenates made from 120 day-old G93A mice and their NTG littermates until the protein load was increased to 120 µg per lane when doublet bands appeared. Representative Western blots for Sesn 2 in whole brain homogenates from a pair of 120 day-old G93A and NTG littermate mice with protein loads of* ***A)*** *20 µg* ***B)*** *40 µg* ***C)*** *80 µg and* ***D)*** *120 µg per lane. +ve = Whole cell lysate, 20 µg, from NTG NSC34 cells used as a positive control. Blots were exposed for 15 min to optimize the chances of detecting sestrin 2 bands.*

E) Whole brain

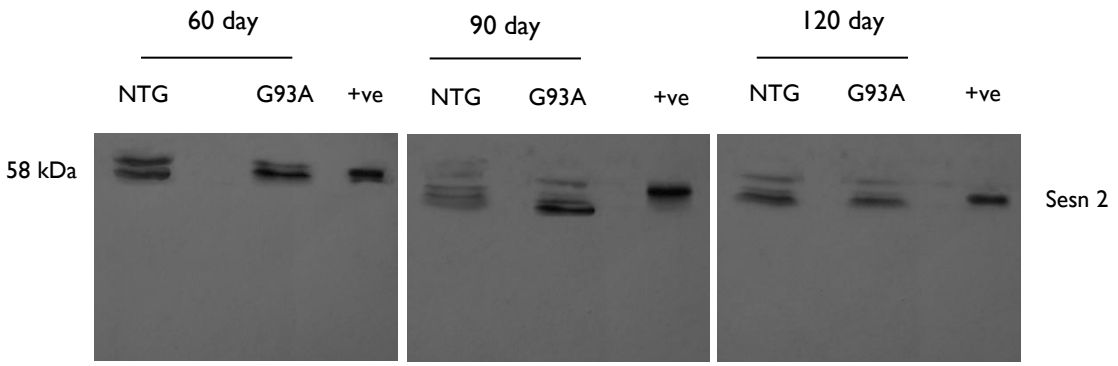

Figure 5.9: E) *Representative Western blots showing possible Sesn 2 bands in whole brain post-nuclear homogenates from G93A transgenic mice and their NTG littermates. Three independent littermate pairs each of 60, 90 and 120 days of age were investigated. Western blotting for Sesn 2 was done in triplicate for each pair. Lanes as before. +ve = whole cell lysate, 20 µg, from NTG NSC34 cells used as a positive control. Protein loads were 120 µg per lane. All blots were exposed for 15 min.*

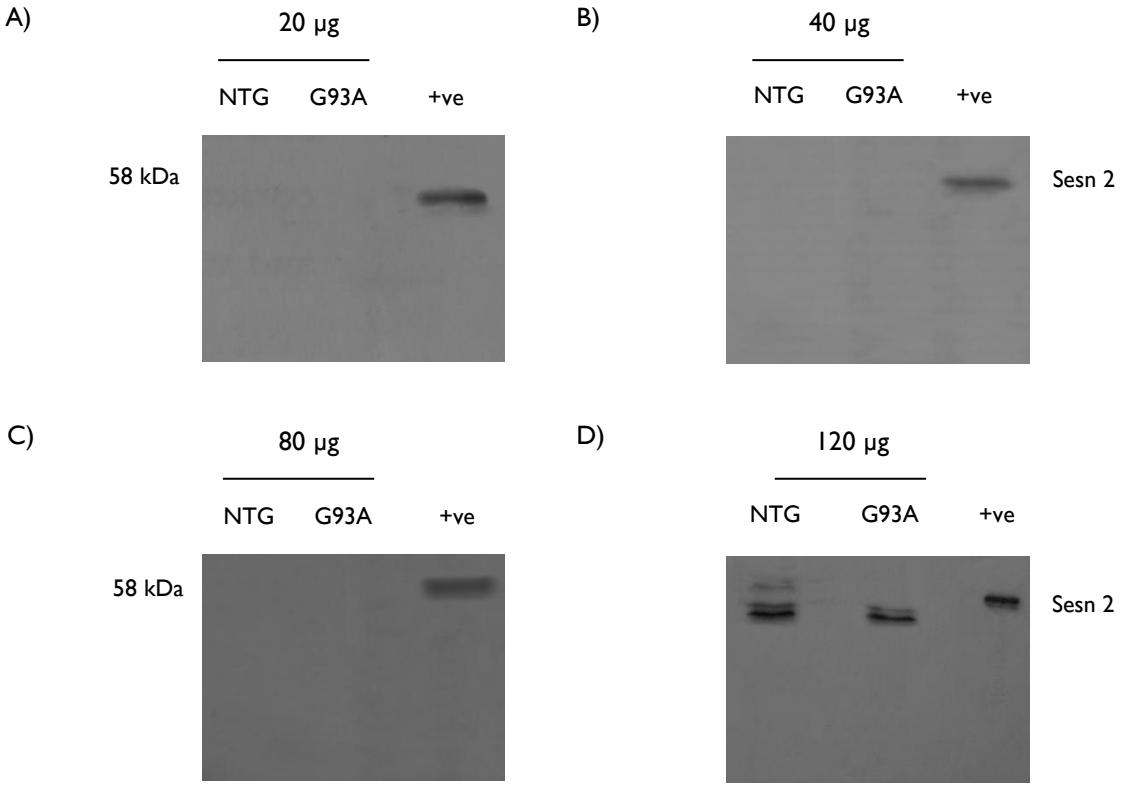

Figure 5.10: *Bands were not detected in 120 day-old G93A and NTG whole spinal cord post-nuclear homogenates blotted with an antibody to sestrin 2 until the protein load was increased to 120 µg per lane. Representative Western blot for Sesn 2 in a pair of 120 day-old G93A and NTG littermate mice with protein loads of **A)** 20 µg **B)** 40 µg **C)** 80 µg and **B)** 120 µg per lane. Lanes as previously. +ve = Whole cell lysate, 20 µg, from NTG NSC34 cells used as a positive control. All blots were exposed for 15 min.*

E) Whole spinal cord

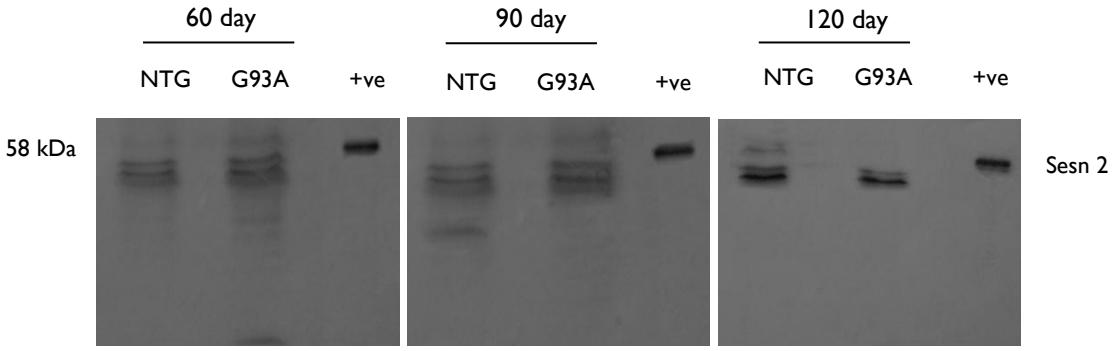

Figure 5.10: E) *Multiple bands were generated by NTG and G93A whole spinal cord homogenates from mice of 60, 90 and 120 days of age when Western blotted for Sesn 2 using protein loads of 120 µg per lane. Lanes as previously. +ve = Whole cell lysate, 20 µg, from NTG NSC34 cells used as a positive control. All blots were exposed for 15 min.*

Western blotting for sestrin 2 in whole brain and spinal cord homogenates prepared from G93A SOD1 transgenic mice and their NTG littermates sacrificed at 60, 90 and 120 days of age revealed no bands running at the expected molecular weight of 58 kDa at protein loads up to 80 µg per lane. When the protein load was increased to 120 µg per lane and blots were exposed for 15 min at least two bands, and on occasion more, including bands running at or close to the predicted MW of sestrin 2 (~58 kDa), were detected in both brain and spinal cord homogenates. The appearance of multiple bands at this relatively high protein load suggested that these bands might be the result of non-specific binding of the Sesn 2 antibody. It was difficult to ascertain which, if any, of the multiple bands visualized represented sestrin 2. In contrast, only 20 µg of the NTG NSC34 cell whole cell lysate used as a positive control was required to generate a clear, single band. Even had it been possible to clearly establish which of the multiple bands in the mouse CNS lanes represented sestrin 2, densitometry would have been impossible due to the proximity of so many other bands. Further analysis of the Sesn 2 blots of CNS homogenates was therefore not attempted, a decision reinforced by later emerging evidence that sestrin 2 likely does not, as had previously been claimed, act to reduce overoxidized typical 2-cys Prxs.

I originally hypothesized that there would be more overoxidized typical 2-cys Prxs in the disease state. Having failed to identify $PrxSO_{2/3}$ bands by Western blotting in whole brain and spinal cord homogenates from G93A SOD1 transgenic mice (or their non-transgenic littermates) even with very high protein loads and long exposures (Figs. 5.6 and 5.7) I wanted to know whether levels of physiologically oxidized typical 2-cys Prxs were greater in CNS tissues from G93A transgenic mice than their NTG littermates. As the typical 2-cys Prxs act as hydroperoxidases, reducing hydrogen peroxide to water, they become physiologically oxidized themselves with two Prx monomers becoming bound into a dimer by an intermolecular disulphide bond (Chapter 1, Fig. 1.3). This physiologically-oxidized dimer is then reduced back to a pair of active monomers by the action of thioredoxin or, in the presence of excess peroxide, may become further oxidized to $PrxSO_2$ then $PrxSO_3$. N-ethylmaleimide (NEM) is a thiol-blocking agent that blocks the further oxidation of free thiol groups of the typical 2-cys Prxs by covalently binding to free cysteine residues (Cox et al., 2009). If cells are treated with NEM prior to preparation of lysates, the typical 2-cys Prxs are "locked" into their existing oxidation state allowing levels of the physiologically oxidized dimer to be measured by Western blotting provided non-reducing conditions are utilized. Dimers remain as dimers and can become neither further oxidized nor reduced. Monomers cannot become physiologically oxidized to form dimers as their active cysteine has been blocked by the NEM adduct. Dimers run at double the expected molecular weight of their related monomers and thus can be identified as such on a non-reducing Western blot. For work in murine CNS tissue, free cysteine residues within 2-cys Prxs can be blocked by NEM in the same way if the animals are perfused with a modified sucrose perfusion buffer containing NEM at the time of sacrifice and prior to harvest of brain and spinal cord (Chapter 2, Section 2.17.6).

NEM- perfusion experiments were carried out to generate "locked" homogenates in which levels of physiologically-oxidized, dimerized typical 2-cys Prxs could be measured. Three pairs of G93A SOD1 mice and their NTG littermates (Pair 1 = 100 days of age, Pair 2 = 105 days, Pair 3 = 107 days) were used for these NEM-perfusion experiments. Brain and spinal cord were extracted from these NEM-treated pairs of mice and whole brain and spinal cord post-nuclear homogenates prepared in the same way as the non-NEM samples (but in a fume hood) according to the protocol described in Chapter 2, Section 2.17.6.

5.7 Confirmation of the transgenic status of the G93A and NTG murine samples

As in the previous SOD1 transgenic mice experiments, the genotype of the NTG and G93A samples to be blotted for 2-cys Prx dimers was first confirmed in the whole brain and spinal cord homogenates made from each pair of animals by Western blotting for SOD1 (Fig. 5.11 A & B overleaf).

A) Whole brain

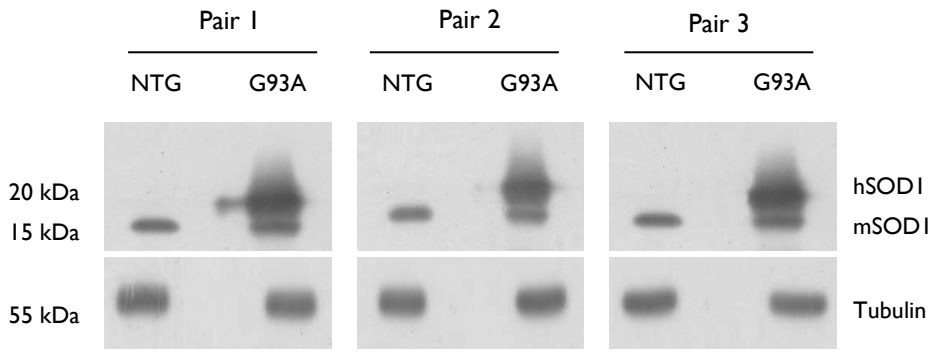

B) Whole spinal cord

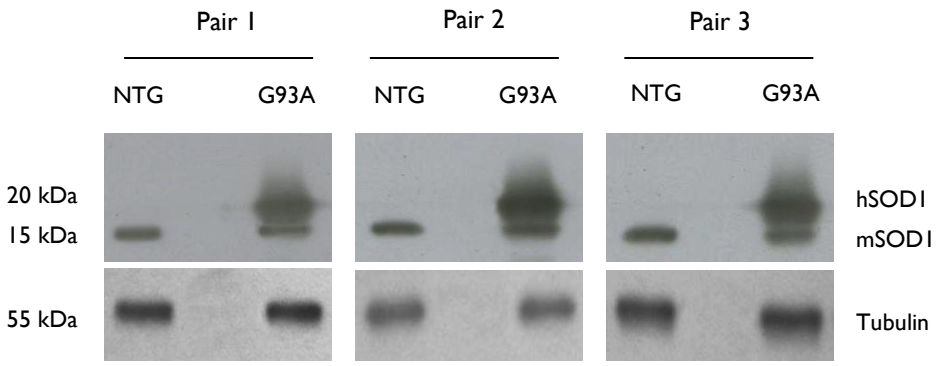

Figure 5.11: *Representative Western blots showing the levels of endogenous murine SOD1 (mSOD1) and overexpressed transgenic human SOD1 (hSOD1) in* ***A)*** *whole brain and in* ***B)*** *whole spinal cord homogenates from three independent pairs of G93A transgenic mice and their NTG littermates of approximately 100 days of age. Western blotting for SOD1 was performed in duplicate. The recorded genotypes of the mice were confirmed by the presence of two SOD1 bands, one the mSOD1 band running at ~15 kDa and the second hSOD1 band running at ~20 kDa in the G93A transgenic mice samples. Brain and spinal cord samples from the NTG mice displayed only one SOD1 band corresponding to mSOD1. Lanes comprise NTG = whole brain or spinal cord homogenate from non-transgenic littermate mice and G93A = whole brain or spinal cord homogenate from G93A SOD1 transgenic mice. Protein loads were 20 µg per lane. SOD1 and tubulin blots were both exposed for 1 min.*

Western blotting for SOD1 in the post-nuclear whole brain and spinal cord homogenates made from Pairs 1, 2 and 3 (100, 105 & 107 days of age respectively) of G93A mice and their NTG littermates confirmed the presence of endogenous murine SOD1 in all samples. As expected a second protein band corresponding to the overexpressed transgenic human SOD1 was only detected in those homogenates prepared from the G93A SOD1 transgenic mice.

5.8 Levels of monomeric and dimerized Prx 2 and Prx 3

Whole brain and spinal cord post-nuclear preparations were Western blotted for Prx 2 and Prx 3 in their monomeric and dimerized forms. The Abfrontier antibodies against Prx 2 and Prx 3 already used for Western blotting under reducing conditions were used here under non-reducing conditions. The NEM perfusion of the mice used for these experiments, together with the use of a non-reducing Western blotting protocol to maintain the dimerized protein in that state during processing (Chapter 2, Section 2.18) allowed for both monomeric and dimerized forms of each Prx to be recognized by their respective antibodies. Samples containing monomeric and dimerized forms of a particular 2-cys Prx were expected to display two protein bands, the first running at the expected MW of the Prx in question, the second at approximately double that MW. Western blotting for each of Prx 2 and Prx 3 was performed in triplicate in each of the three pairs of mice and levels quantified using the G-box (Fig. 5.12 A-J & Fig. 5.13 A-J).

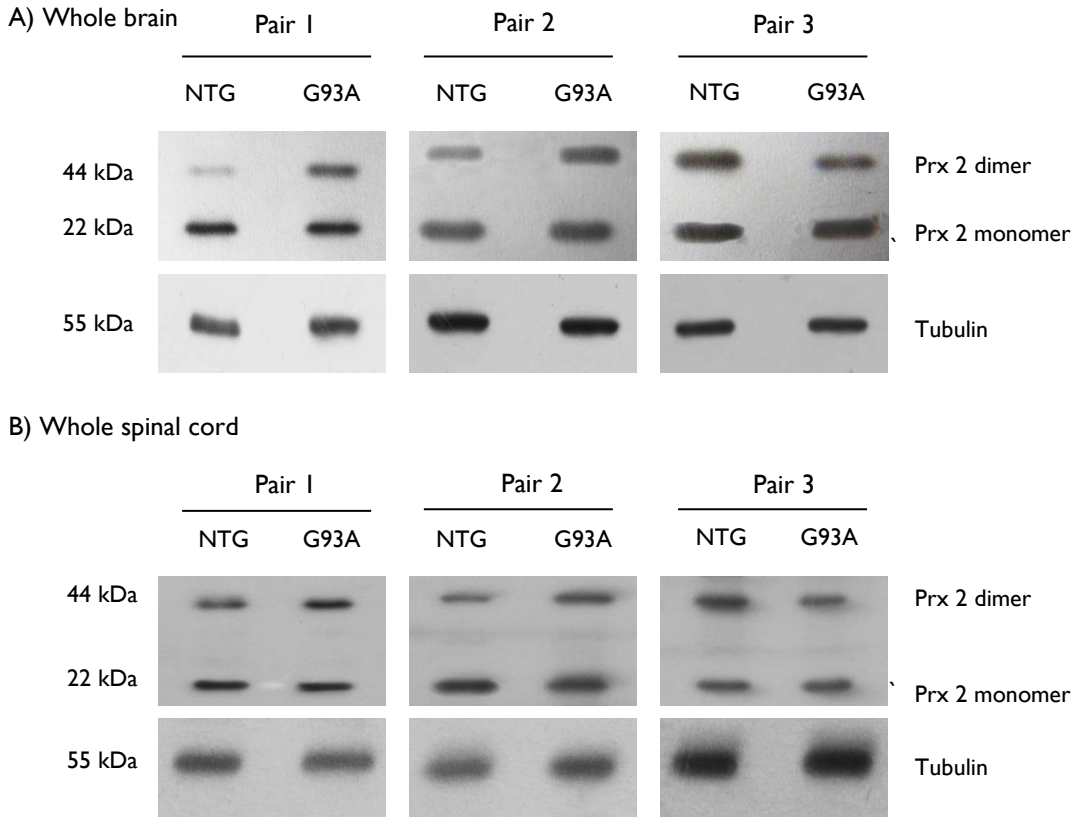

Figure 5.12: *Both monomeric and dimerized Prx 2 were detected in CNS homogenates from G93A and NTG mice of ~100 days of age. Levels of dimerized Prx 2 were increased in the G93A mice compared with their NTG littermates in Pair 1 (100 day) and Pair 2 (105 day) but apparently decreased in Pair 3 (107 day) in both* ***A)*** *whole brain and* ***B)*** *whole spinal cord homogenates. Three independent littermate pairs of approximately 100 days of age were investigated. Western blotting for monomeric and dimerized Prx 2 was performed in triplicate in whole brain and whole spinal cord homogenates made from each of the three littermate pairs of mice. Lanes comprise: G93A = G93A SOD1 transgenic mice, NTG = non-transgenic littermates. Protein loads were 20 µg per lane. Prx 2 and tubulin blots were both exposed for 1.5 min.*

C)

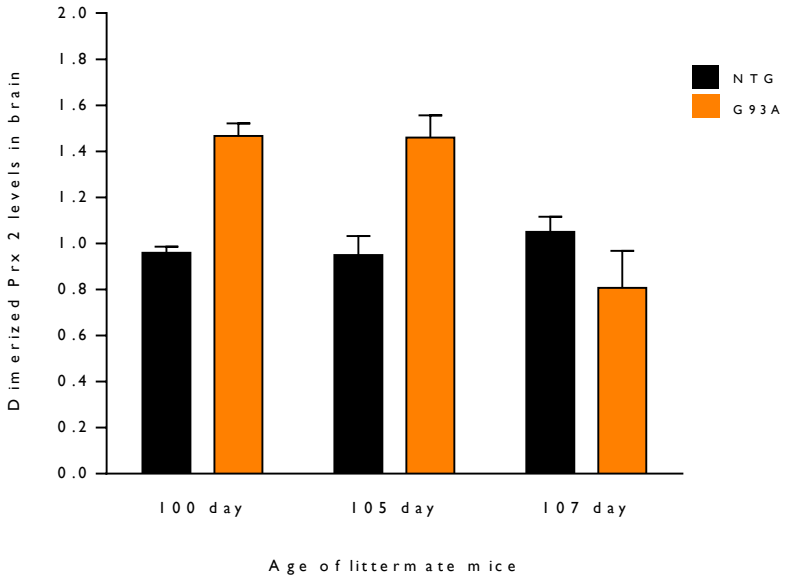

D)

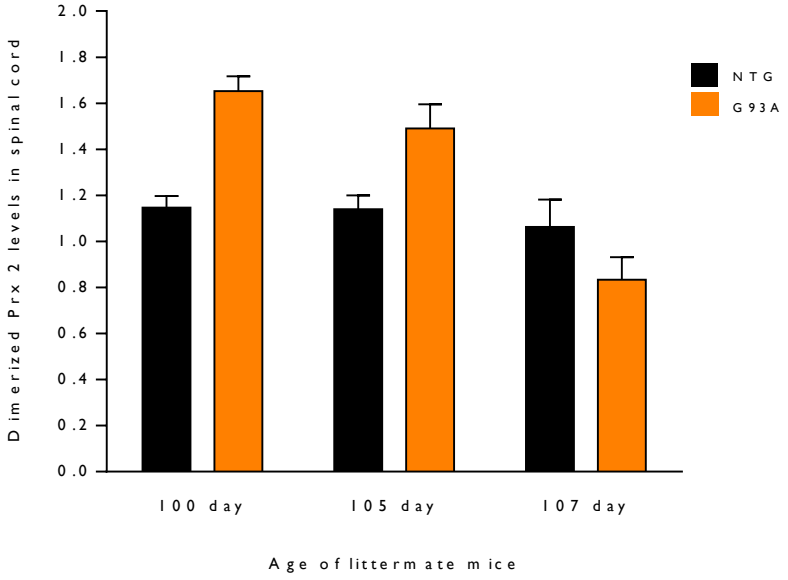

Figure 5.12: *Quantification of dimerized Prx 2 in* ***C)*** *whole brain and* ***D)*** *whole spinal cord homogenates of 3 pairs of NTG and G93A littermate mice of approximately 100 days of age. Graphs showing levels of dimerized Prx 2 normalized to tubulin from each individual pair of mice. Data include triplicate blots of dimerized Prx 2 in each of the three pairs of mice. In Pair 1 (100 day) and Pair 2 (105 day) levels of dimerized Prx 2 were apparently higher in both brain and spinal cord homogenates from G93A mice than in their NTG littermates. In Pair 3 (107 day) the opposite was the case. These findings were consistent in the triplicate blots of all three pairs Error bars represent standard error of the mean (SEM).*

E)

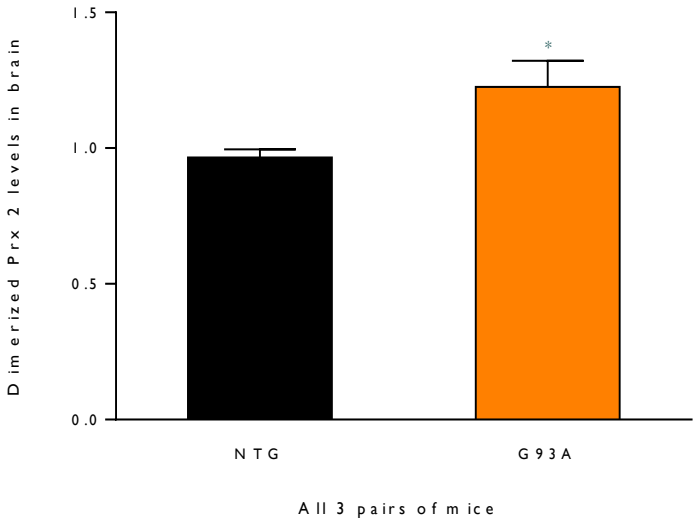

F)

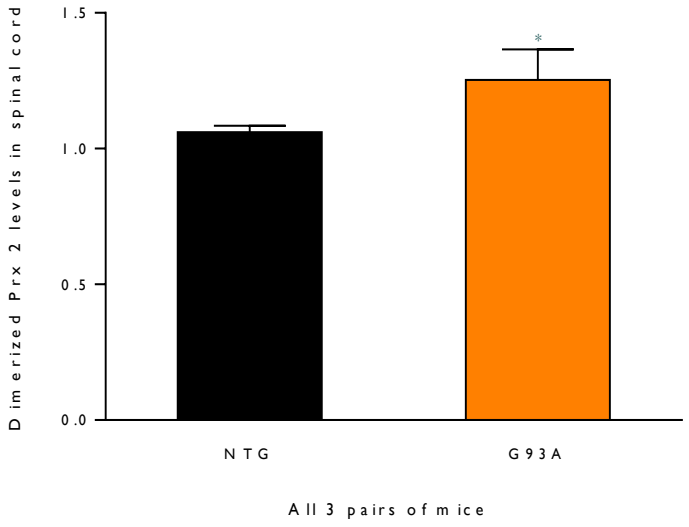

Figure 5.12: *Quantification of dimerized Prx 2 in* ***E)*** *whole brain and* ***F)*** *whole spinal cord homogenates from 3 pairs of G93A transgenic mice and their NTG littermates of approximately 100 days of age (one pair each at 100 days, 105 days and 107 days of age). Densitometry values for dimerized Prx 2 bands were normalized to those of their respective tubulin bands to correct for protein loading. Data include triplicate blots for dimerized Prx 2 in each of the three pairs of mice. Error bars represent standard error of the mean (SEM). A Student's t-test showed a statistically significant increase in the levels of dimerized Prx 2 in the G93A mice compared to their NTG littermates in both whole brain homogenates (p-value: 0. 0206) and whole spinal cord homogenates (p-value: 0.0324).*

G)

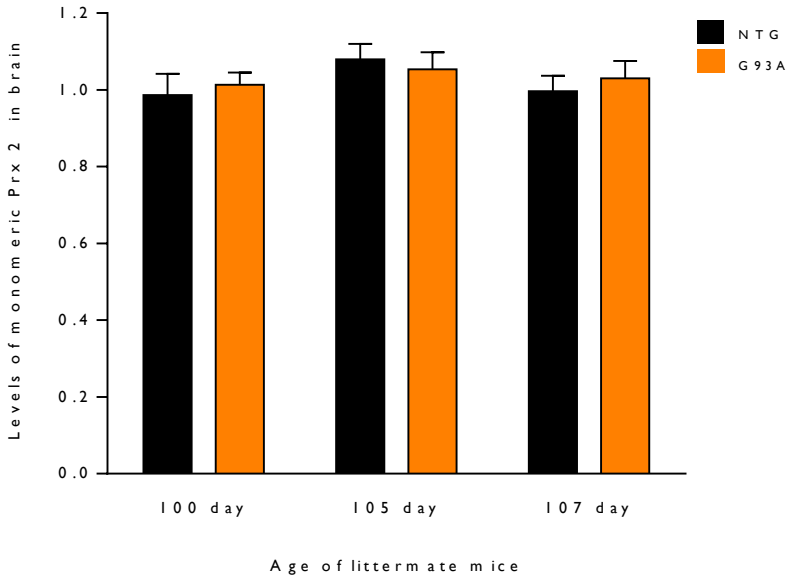

H)

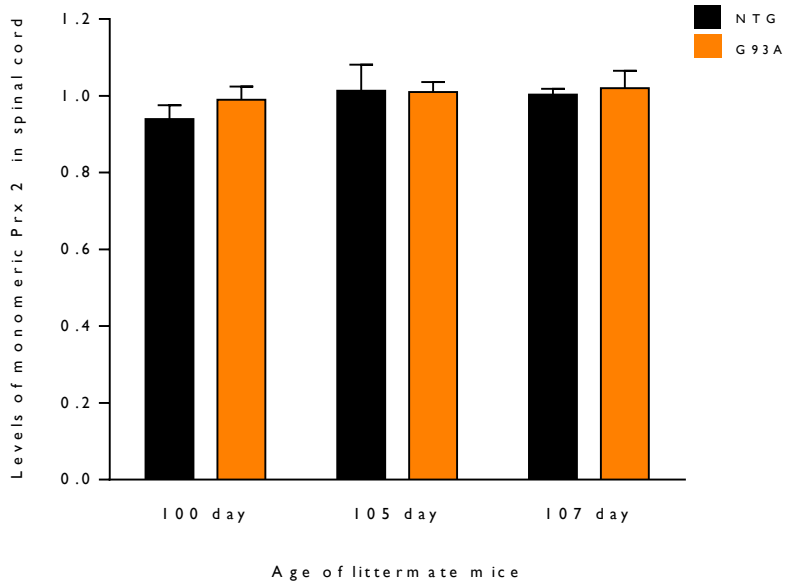

Figure 5.12: *Quantification of levels of monomeric Prx 2 in* ***G)*** *whole brain and* ***H)*** *whole spinal cord homogenates from 3 pairs of G93A transgenic mice and their NTG littermates of approximately 100 days of age. Levels of monomeric Prx 2 appeared to be broadly similar in all three G93A transgenic mice and their NTG littermates in both whole brain and whole spinal cord homogenates. Densitometry values for monomeric Prx 2 bands were normalized to those of their respective tubulin bands to correct for protein loading. Data include triplicate blots for monomeric Prx 2 in each of the three pairs of mice. Error bars represent standard error of the mean (SEM).*

I)

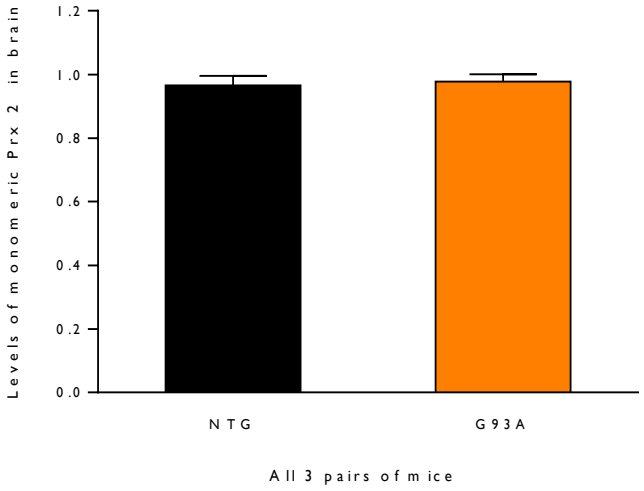

J)

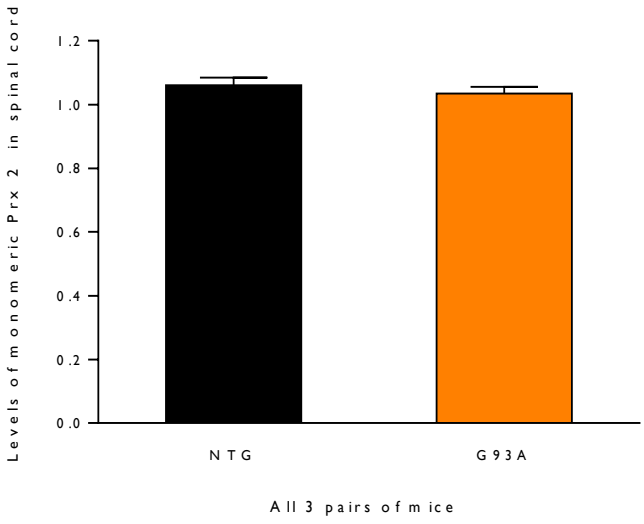

Figure 5.12: *Quantification of levels of Prx 2 monomer in* ***I)*** *whole brain and* ***J)*** *whole spinal cord homogenates from 3 pairs of G93A transgenic mice and their NTG littermates of approximately 100 days of age (one pair each at 100 days, 105 days and 107 days of age). Densitometry values for monomeric Prx 2 bands were normalized to those of their respective tubulin bands to correct for protein loading. Data include triplicate blots for monomeric Prx 2 in each of the three pairs of mice. Error bars represent standard error of the mean (SEM). A Student's t-test showed no statistically significant difference in the levels of monomeric Prx 2 between G93A and NTG mice in either whole brain homogenates (p-value: 0. 8742) or whole spinal cord homogenates (p-value: 0.9313).*

A) Whole brain

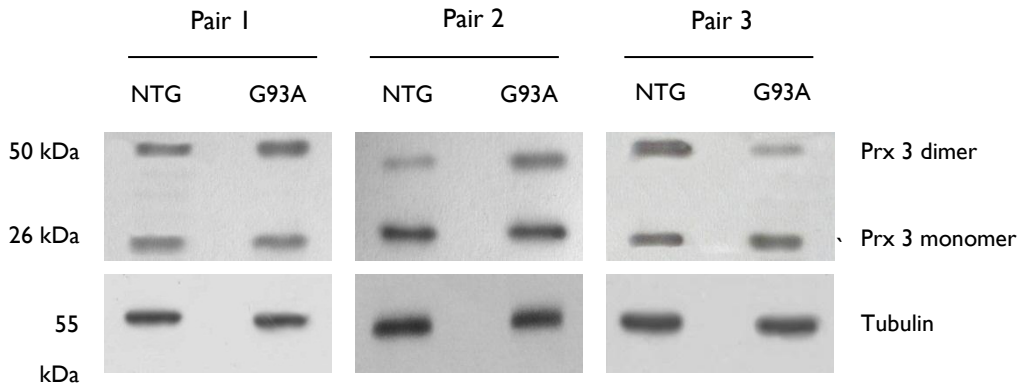

B) Whole spinal cord

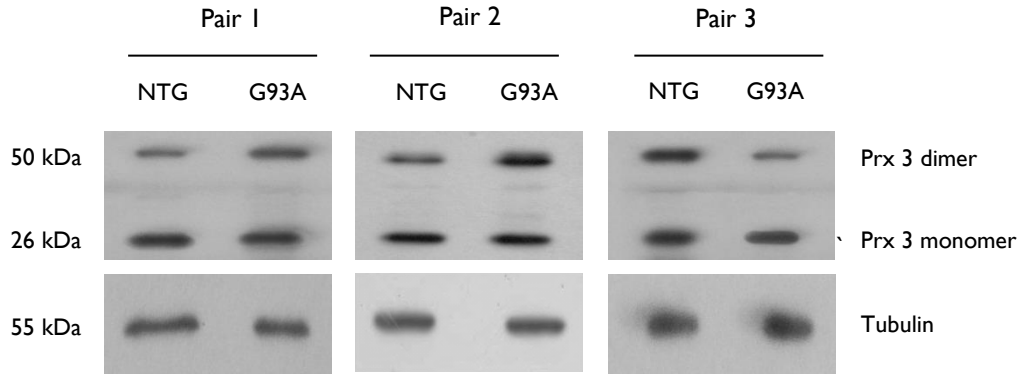

Figure 5.13: *Both monomeric and dimerized Prx 3 were detected in CNS homogenates from G93A and NTG mice of ~100 days of age. Levels of dimerized Prx 3 were increased in the G93A mice compared with their NTG littermates in Pair 1(100 day) and Pair 2 (105 day) but were apparently decreased in Pair 3 (107 day) in both* ***A)*** *whole brain and* ***B)*** *whole spinal cord homogenates. There was no apparent difference in the levels of Prx 3 monomer in whole spinal cord homogenates from any of the three pairs of mice examined. In whole brain homogenates prepared from Pair 1 (100day) and Pair 2 (105 day), there was also no apparent difference in levels of monomeric Prx 3. In whole brain homogenates from Pair 3 (107 days-old), however, there appeared to be slightly more Prx 3 monomer present in the G93A sample than in the NTG sample. This was the case in each of the triplicate Western blots performed in whole brain homogenates from this pair. Lanes comprise: G93A = G93A SOD1 transgenic mice, NTG = non-transgenic littermates. Protein loads were 20 µg per lane. Prx 3 and tubulin blots were both exposed for 1.5 min.*

C)

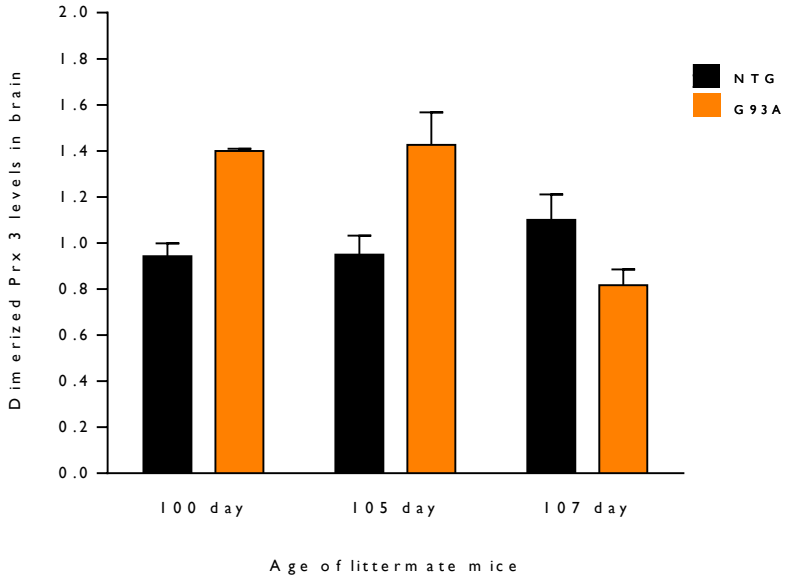

D)

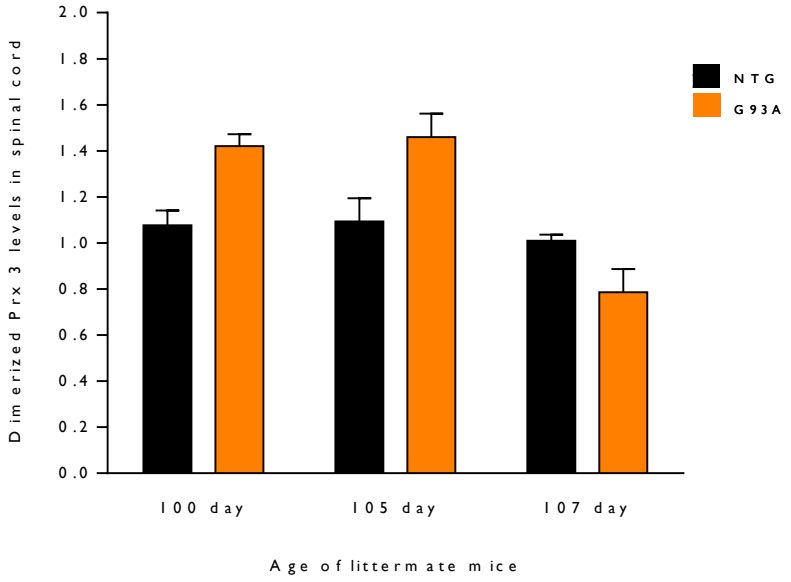

Figure 5.13: *Quantification of dimerized Prx 3 in* ***C)*** *whole brain and* ***D)*** *whole spinal cord homogenates from 3 pairs of G93A transgenic mice and their NTG littermates of approximately 100 days of age. In Pair 1 (100 day) and Pair 2 (105 day) there was more dimerized Prx 3 in the G93A animal (in both brain and spinal cord homogenates) compared to their NTG littermates whilst in Pair 3 (107 day) there was slightly less dimerized Prx 3 in the G93A mouse than in its littermate, again in both brain and spinal cord homogenates. Densitometry values for dimerized Prx 3 bands were normalized to those of their respective tubulin bands to correct for protein loading. Data include triplicate blots for dimerized Prx 3 in each of the three pairs of mice. Error bars represent standard error of the mean (SEM).*

E)

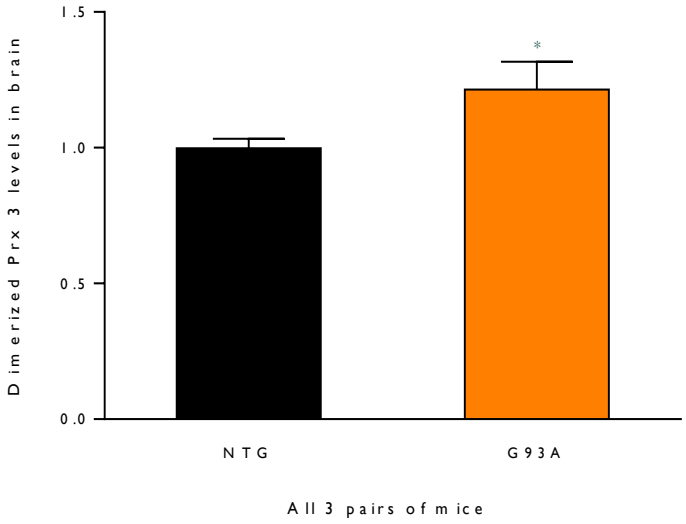

F)

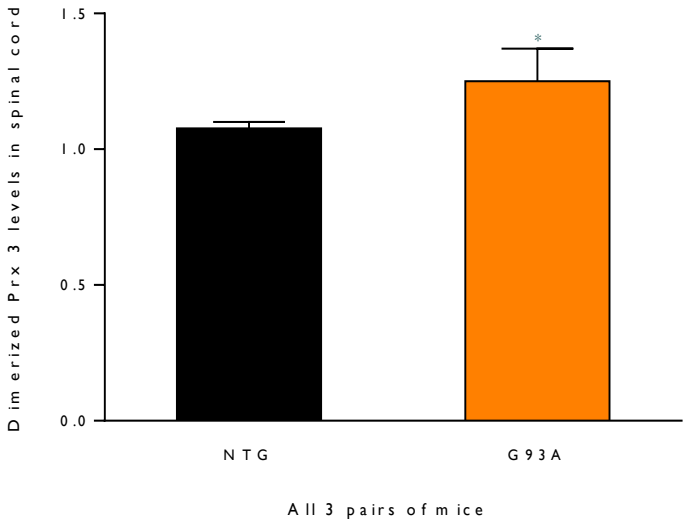

Figure 5.13: *Quantification of dimerized Prx 3 in* ***E)*** *whole brain and* ***F)*** *whole spinal cord homogenates from 3 pairs of G93A transgenic mice and their NTG littermates of approximately 100 days of age (one pair each at 100 days, 105 days and 107 days of age). Densitometry values for dimerized Prx 3 bands were normalized to those of their respective tubulin bands to correct for protein loading. Data include triplicate blots for dimerized Prx 3 in each of the 3 pairs of mice. Error bars represent standard error of the mean (SEM). A Student's t-test showed statistically significantly higher levels of dimerized Prx 3 in G93A mice compared to their NTG littermate mice in both whole brain homogenates (p-value: 0. 0413) and whole spinal cord homogenates (p-value: 0.0249).*

G)

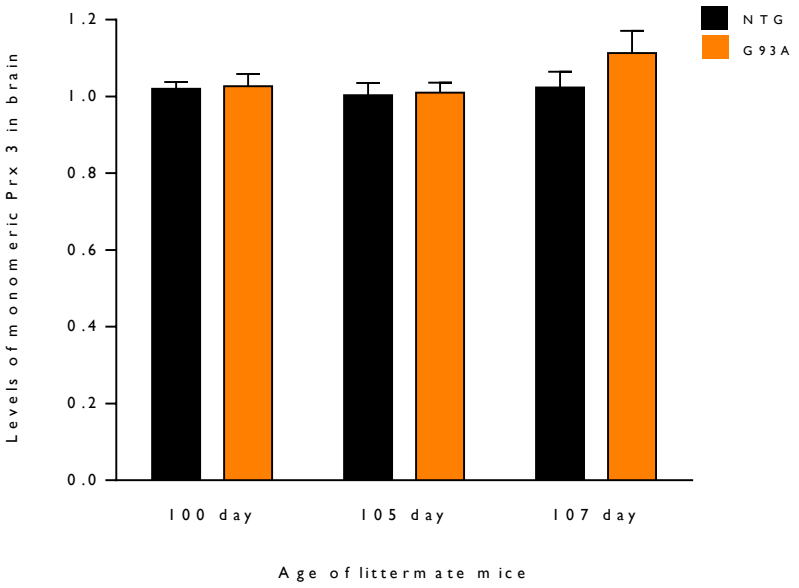

H)

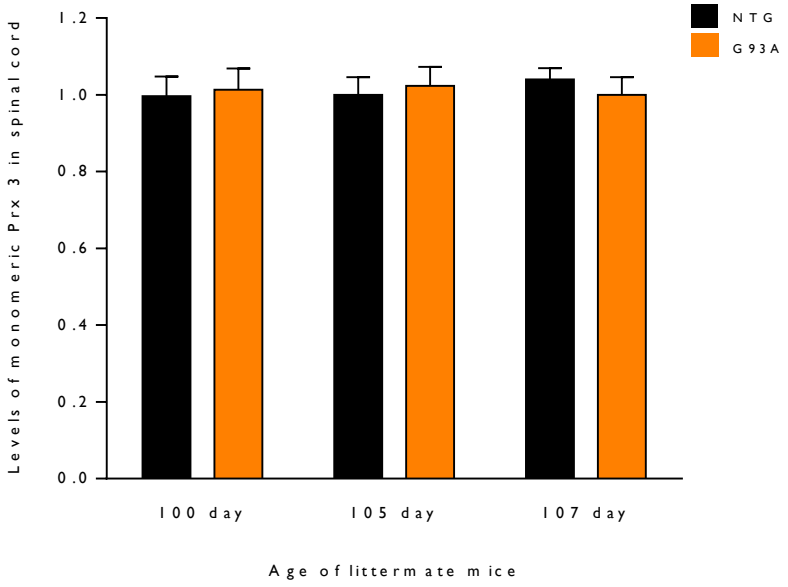

Figure 5.13: *Quantification of levels of Prx 3 monomer in* ***G)*** *whole brain and* ***H)*** *whole spinal cord homogenates from 3 pairs of G93A transgenic mice and their NTG littermates of approximately 100 days of age (one pair each at 100 days, 105 days and 107 days of age). Levels of monomeric Prx 3 in whole spinal cord homogenates from the G93A mice and their NTG littermates were very similar in all 3 pairs of mice. Levels of monomeric Prx 3 in whole brain homogenates from the G93A mice and their NTG littermates were also very similar to each other in Pairs 1 and 2. There appeared to be slightly more monomeric Prx 3 in the whole brain homogenate from the Pair 3 G93A mouse (107 days of age) than its NTG littermate, however. Densitometry values for monomeric Prx 3 bands were normalized to those of their respective tubulin bands to correct for protein loading. Data include triplicate blots for monomeric Prx 3 in each of the three pairs of mice. Error bars represent standard error of the mean (SEM).*

I)

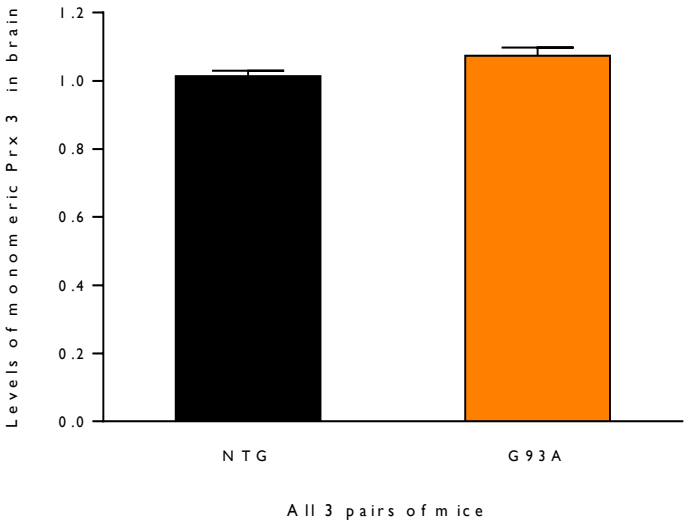

J)

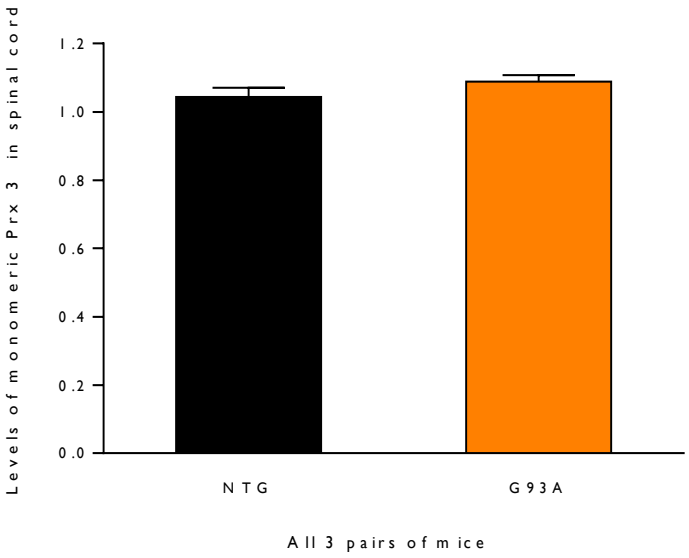

Figure 5.13: *Quantification of levels of Prx 3 monomer in* ***I)*** *whole brain and* ***J)*** *whole spinal cord homogenates from 3 pairs of NTG and G93A littermate mice of approximately 100 days of age (one pair each at 100 days, 105 days and 107 days of age). Densitometry values for monomeric Prx 3 bands were normalized to those of their respective tubulin bands to correct for protein loading. Data include triplicate blots for monomeric Prx 3 in each of the three pairs of mice. Error bars represent standard error of the mean (SEM). A Student's t-test showed no statistically significant difference in the levels of monomeric Prx 3 between G93A and NTG mice in either whole brain homogenates (p-value: 0. 7942) or whole spinal cord homogenates (p-value: 0.8695).*

Western blots for Prx 2 and Prx 3 of whole brain and spinal cord preparations made from three pairs of NEM-perfused G93A and NTG littermate mice of approximately 100 days of age (one pair each sacrificed at 100 days, 105 days and 107 days of age) showed increased levels of both dimerized Prx 2 and dimerized Prx 3 in the G93A mice compared to their NTG littermates. Whole tissue homogenates of both brain and spinal cord from two of the three pairs of G93A and NTG littermate mice (those sacrificed at 100 and 105 days), showed increased levels of both dimerized Prx 2 and dimerized Prx 3. However, levels of dimerized Prx 2 and dimerized Prx 3 in the CNS whole tissue homogenates from the G93A transgenic mouse of 107 days of age appeared to be somewhat lower than those in the homogenates made from its NTG littermate of the same age. This was the case in all three blots prepared from Pair 3. Despite this inconsistency, when combined, the overall data from all three pairs of mice showed a statistically significant increase in the levels of dimerized Prx 2 and dimerized Prx 3 in the G93A mice when compared to those in the NTG mice.

In contrast, Western blots for monomeric Prx 2 and Prx 3 in whole spinal cord homogenates and for monomeric Prx 2 in whole brain homogenates from all three pairs of mice showed no difference in the levels of the proteins between the G93A and NTG littermates. Western blots for monomeric Prx 3 of whole brain homogenates made from Pair 1 (100 days old) and Pair 2 (105 days old) also appeared to show very similar levels of monomeric Prx 2 and Prx 3 but levels in whole brain homogenates made from Pair 3 (107 days old) appeared to be slightly higher in the G93A animal than in its NTG littermate (Fig. 5.13 G). This apparent small increase in the level of Prx 3 monomer was seen in all three blots of the whole brain homogenates from this pair of animals, however, when the data from all three pairs of mice are combined, there is no statistically significant overall difference in levels of Prx 3 monomer between the G93A transgenic animals and their NTG littermates (Fig. 5.13 I).

Theoretically, the antibodies against Prx 2 and 3 used in these experiments should recognize all forms of the relevant monomer. This includes the physiologically reduced monomer that is able to act as a hydroperoxidase, as well as the monomeric overoxidized $PrxSO_2$ and $PrxSO_3$ forms of each protein. My earlier experiments (Section 5.5), however, indicated that there was minimal $PrxSO_{2/3}$ present in whole brain or whole spinal cord preparations from G93A and NTG littermate mice of 90 and 120 days of age. It seems most likely, therefore, that the monomeric bands detected in these NEM experiments overwhelmingly represent the active, reduced form of Prx 2 or Prx 3 monomer.

The implications of the increased levels of physiologically-dimerized Prx 2 and Prx 3 in whole brain and spinal cord homogenates measured in the three pairs of ~100 day old G93A transgenic mice when compared to their NTG littermates are discussed in Section 6.10. Given the inconsistency between results in Pairs 1 and 2 and Pair 3 it would have been desirable to carry out NEM-perfusion experiments in further pairs of mice of 100 days of age and also to carry out the same experiments in CNS homogenates from mice at just-symptomatic (60 days) and advanced stages (120 days) of disease. Unfortunately these animals were not available from the colony at the time.

REFERENCES

Budanov, A.V., Sablina, A.A., Feinstein, E., Koonin, E.V., and Chumakov, P.M. (2004). Regeneration of peroxiredoxins by p53-regulated sestrins, homologs of bacterial AhpD. Science *304*, 596-600.

Cox, A.G., Peskin, A.V., Paton, L.N., Winterbourn, C.C., and Hampton, M.B. (2009). Redox potential and peroxide reactivity of human peroxiredoxin 3. Biochemistry *48*, 6495-6501.

Goemaere, J., and Knoops, B. (2012). Peroxiredoxin distribution in the mouse brain with emphasis on neuronal populations affected in neurodegenerative disorders. The Journal of Comparative Neurology *520*, 258-280.

Jin, M.H., Lee, Y.H., Kim, J.M., Sun, H.N., Moon, E.Y., Shong, M.H., Kim, S.U., Lee, S.H., Lee, T.H., Yu, D.Y.*, et al.* (2005). Characterization of neural cell types expressing peroxiredoxins in mouse brain. Neurosci Lett *381*, 252-257.

Papadia, S., Soriano, F.X., Leveille, F., Martel, M.A., Dakin, K.A., Hansen, H.H., Kaindl, A., Sifringer, M., Fowler, J., Stefovska, V.*, et al.* (2008). Synaptic NMDA receptor activity boosts intrinsic antioxidant defenses. Nat Neurosci *11*, 476-487.

Woo, H.A., Bae, S.H., Park, S., and Rhee, S.G. (2009). Sestrin 2 is not a reductase for cysteine sulfinic acid of peroxiredoxins. Antioxid Redox Signal *11*, 739-745.

Woo, H.A., Jeong, W., Chang, T.S., Park, K.J., Park, S.J., Yang, J.S., and Rhee, S.G. (2005). Reduction of cysteine sulfinic acid by sulfiredoxin is specific to 2-cys peroxiredoxins. J Biol Chem *280*, 3125-3128.

6. DISCUSSION

BACKGROUND

Amyotrophic lateral sclerosis is a fatal neurodegenerative disorder for which there is still no really effective disease-modifying therapy. Despite extensive research and exciting recent discoveries of new genetic causes of the familial form of the disease, the mechanisms by which motor neurons die in ALS are still poorly understood. Typically, motor neuron degeneration progresses rapidly within the brain and spinal cord, and patients live only 3-5 years after diagnosis (Strong and Gordon, 2005). At present, Riluzole is the only drug that slows down the progression of the disease. On average patients on Riluzole gain only about 3 months additional survival (Bensimon et al., 1994; Lacomblez et al., 1996). There is therefore a pressing need to identify novel therapeutic targets.

In the current study, a possible role of the peroxiredoxins, a family of anti-oxidant proteins, is investigated in the pathogenesis of ALS. Previous studies have implicated some members of the Prx family to be involved in the disease (Chapter 1, Section 1.16.2). The levels of some typical 2-cys Prxs were altered at both mRNA and protein levels in motor neuronal NSC34 cells expressing mutant SOD1 (Wood-Allum et al., 2006), in G93A mice (Ferraiuolo et al., 2007) and in post-mortem material from SOD1 ALS patients (Fukada et al., 2004; Kato et al., 2004; Wood-Allum et al., 2006).

Peroxiredoxins are redox-sensitive anti-oxidant enzymes that serve to reduce hydrogen peroxide and other peroxides along with certain other potentially damaging free radicals (Rhee and Woo, 2011). Under conditions of oxidative stress when there are high levels of H_2O_2, typical 2-cys Prxs become overoxidized. Overoxidized 2-cys Prxs cannot function as hydroperoxidases but may form multimeric molecular chaperones (Wood et al., 2003). This redox-sensitive Prx switch enables the Prxs to function as either an anti-oxidant protein or a molecular chaperone depending upon the prevailing redox conditions. The abundance of the typical 2-cys Prxs and their widespread distribution across many subcellular organelles makes them important contributors to cellular anti-oxidant defence.

This work was prompted by earlier studies implicating the Prxs in ALS along with the dual anti-oxidant and protein chaperone functions of the 2-cys Prxs in the light of good evidence for oxidative stress, protein aggregation and mitochondrial dysfunction in the pathogenesis of ALS (Chapter 1, Section 1.7-1.12). I aimed to test the hypothesis that typical 2-cys Prxs exist in a more oxidized state in ALS than in health and that if proven this might contribute to disease progression.

SUMMARY

In this work I aimed to investigate the relevance of the oxidation state of a highly conserved family of anti-oxidants, the peroxiredoxins, in the disease pathogenesis and progression of amyotrophic lateral sclerosis. This work was designed to build on previous studies implicating certain of the typical 2-cys Prxs in ALS and was also prompted by what, in the light of current ideas regarding ALS pathogenesis, appeared to be very relevant Prx functions. These included the ability of the Prxs to reduce hydrogen peroxide and other peroxides to water by means of their hydroperoxidase activity, their reported ability to generate multimeric protein chaperones once in their overoxidized state and their abundance in particularly vulnerable compartments of the cell such as the mitochondrial matrix which lack other, more efficient hydroperoxidases.

I hypothesized that the typical 2-cys Prxs would exist in a higher oxidation state in ALS than in health and that this might be relevant to disease pathogenesis. In the knowledge of strong evidence for oxidative stress in the disease and evidence that mutant SOD1 could be a potent cause of oxidative stress, I first set out to investigate differences in the oxidation state of the typical 2-cys Prxs in models of SOD1 ALS. These included fibroblasts derived from I113T SOD1 patients and those derived from age- and sex-matched healthy controls. I also investigated motor neuronal NSC34 cells that stably express three forms of mutant SOD1 (H48Q, I113T and G93A) and wild-type SOD1 (WT) and G93A SOD1 transgenic mice and their non-transgenic littermates. Having identified interesting findings in the I113T SOD1 fibroblasts I then went on to examine three lines of fibroblasts derived from patients with mutant TDP43-related fALS.

Western blotting for overoxidized Prxs in mutant SOD1 and mutant TDP43-ALS fibroblasts demonstrated that under basal culture conditions, hardly any $PrxSO_{2/3}$ was present. Upon subjecting patient and control fibroblasts to oxidative stress by exposing them to H_2O_2, both generated similar amounts of $PrxSO_{2/3}$. This was true after both a saturating exposure to H_2O_2 (300 μM for 15 min) and a non-saturating exposure to H_2O_2 (30 μM for 15 min). When the I113T SOD1-ALS and matched control fibroblasts were allowed to recover for 24 hours post-H_2O_2 washout, however, an interesting difference in behaviour was noted. A statistically-significant delay in the disappearance of $PrxSO_{2/3}$ was observed in all three I113T SOD1 fibroblast lines and in one of the three mutant TDP43 patient (A321V) cell lines when compared to their respective matched healthy control fibroblasts. In the I113T SOD1 fibroblasts there was also a delayed and reduced induction of the $PrxSO_{2/3}$ regenerator sulfiredoxin 1 (Srx 1) when compared to that in control cells which is likely (but as association is not the same as causation not certain) to have been responsible for the delayed disappearance of $PrxSO_{2/3}$ from the patient cells. In turn the delayed and reduced Srx 1 induction in the I113T SOD1 patient fibroblasts may have been the result of the reduced activation of AP-1 (a Srx 1 transcription factor) in response to H_2O_2 exposure. This is summarized in Figure 6.1 overleaf.

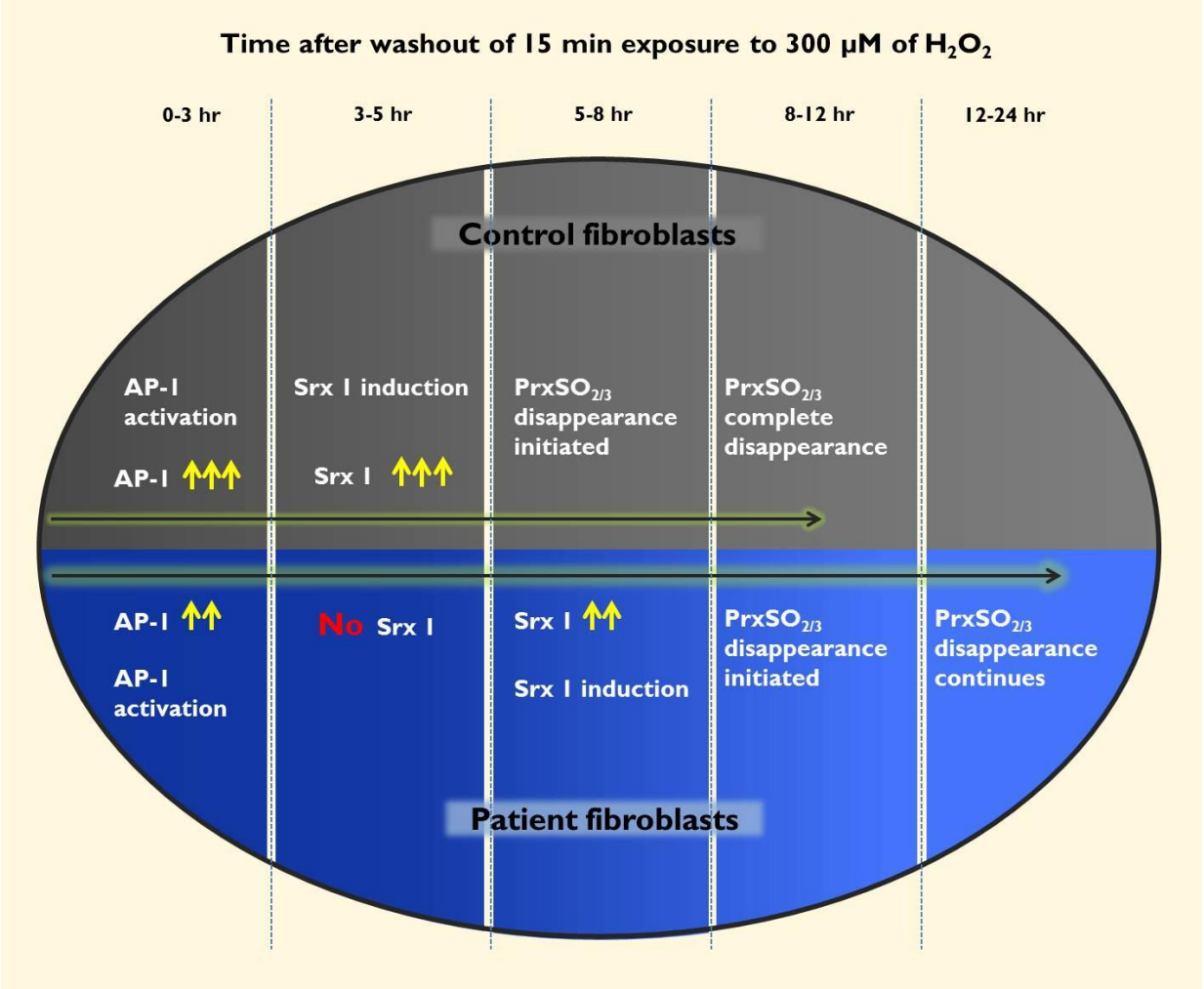

Figure 6.1: *A schematic representation of the results obtained in the I113T SOD1-ALS patient and control fibroblasts in the stress-recovery experiments.*

The results of the two-hit stress recovery experiments in I113T SOD1 fibroblasts suggest a cumulative effect of sequential exposures to non-saturating concentrations of H_2O_2. The disappearance of $PrxSO_{2/3}$ from both patient and control cells was prolonged after a second, identical exposure to a non-saturating concentration of H_2O_2. This prolongation was more pronounced in the I113T patient fibroblasts than in control cells. On the basis of these results it would be reasonable to assume that exposure of I113T SOD1 fibroblasts to multiple oxidative challenges might very well have a cumulative detrimental effect on the rate of recovery of $PrxSO_{2/3}$. It might also be suggested that fibroblasts expressing I113T SOD1 would deal less well with repetitive oxidative stress than would control fibroblasts, their overoxidized typical 2-cys Prxs taking progressively longer to recover with each oxidative insult leaving the cell more vulnerable to oxidative damage in the meantime. Were it possible to demonstrate similar behaviour in motor neurons in ALS there would be potential implications for pathogenesis. Such a mechanism might, for example, provide a plausible molecular substrate for the exercise hypothesis of ALS (Harwood et al., 2009).

In short, therefore, my original hypothesis was borne out in I113T SOD1 fibroblasts. After exposure to an oxidative stressor, typical 2-cys Prxs did become overoxidized. The increase in $PrxSO_{2/3}$ took hours longer to return to basal in cells expressing mutant SOD1, a delay further exacerbated by exposure to sequential oxidative challenge. Thus, whilst there was no difference in $PrxSO_{2/3}$ levels between fibroblasts expressing a fALS-causing mutation to SOD1 and control fibroblasts growing under basal culture conditions or immediately after oxidative challenge, recovery from oxidative challenge was defective in the patient cells. This deficit became more marked after sequential oxidative challenge. The I113T SOD1 mutation is the most prevalent SOD1 fALS mutation in the United Kingdom (Lopate et al., 2010). Patients with the I113T SOD1 mutation however present a range of clinical manifestations of the disease and show a range in the age of onset period and disease progression rates (Cudkowicz et al., 1997; Lopate et al., 2010). The consistency in the results obtained in the fibroblasts from three I113T ALS patients strongly indicates a dysfunction in the Prx redox pathway. In short, the defective recovery of $PrxSO_{2/3}$ after oxidative challenge in SOD1 fibroblasts provides support for my original hypothesis. In this ALS model at least the typical 2-cys Prxs do spend longer in an overoxidized form after oxidative challenge in fibroblasts derived from I113T SOD1-related ALS patients than in those derived from healthy controls.

Given these interesting findings in mutant SOD1-expressing fibroblasts I wanted to establish whether similar changes could be found in fibroblasts derived from patients suffering from fALS due to other genetic mutations. I had access to fibroblasts derived from three TDP43-fALS cases along with age and sex-matched controls. When the experiments described above were repeated in these cells, one patient/control fibroblast pair reiterated the reduced and delayed disappearance of $PrxSO_{2/3}$ after oxidative challenge, the other two did not. Further work will be required to clarify the situation in TDP43 derived fibroblasts and, ideally, fibroblasts derived from other inherited forms of ALS should also be examined. This is the subject of further discussion in the Future work section below.

The other main limitation of work in ALS fibroblasts is that there are many inherent qualities of skin cells that are not held in common with motor neurons. Whilst there is precedent for studies in other neurodegenerative diseases showing changes initially detected in fibroblasts being reiterated within the relevant neuronal cells, blind extrapolation of findings in fibroblasts to motor neurons is not appropriate. For this reason two neuronal ALS models were investigated, the motor neuronal NSC34 cell line and the G93A SOD1 transgenic mouse model of SOD1-related fALS.

The results of Western blotting for overoxidized Prxs in NSC34 cells were consistently inconsistent. Unlike the HEK293 cells used for experimental work up and the human fibroblasts in which negligible $PrxSO_{2/3}$ could be detected in cells grown under basal culture conditions NSC34 cells (both control and mutant SOD1-expressing) frequently demonstrated high levels of $PrxSO_{2/3}$. Control cells moreover frequently (but not always) had higher levels of $PrxSO_{2/3}$ than did NSC34 cells expressing

the various species of ALS-causing SOD1 mutations and there was relentless variability in levels of $PrxSO_{2/3}$ from preparation to preparation of the same cell line. After carrying out repeat experiments and careful troubleshooting without any improvement in inter-experiment consistency I reluctantly came to the conclusion that this model was unlikely to be informative for the Prx pathway. Possible reasons for this have been discussed below (Section 6.8). It seemed evident from the high levels of $PrxSO_{2/3}$ present in control NSC34 cells growing under basal culture conditions that these cells were stressed for no apparent reason. The inability to establish a consistent baseline for $PrxSO_{2/3}$ levels in any one NSC34 cell line made interpretation of oxidative stress experiments difficult and work was abandoned in this model.

Preliminary Western blotting of whole brain and whole spinal cord homogenates from three pairs of G93A SOD1 transgenic mice and their non-transgenic littermates of approximately 100 days of age showed that levels of physiologically oxidized neuronal typical 2-cys Prxs, dimerized Prx 2 and Prx 3, were higher in G93A mice in two of the three G93A/NTG littermate pairs examined, results that overall were statistically significant. Given it was only possible to carry out these experiments in three pairs of mice at one age, further experiments need to be repeated before firm conclusions can be drawn. This is discussed further in the Future work section below. In whole spinal cord and brain homogenates from 60 day, 90 day and 120 day old G93A/NTG littermate pairs, the neuronal typical 2-cys Prxs (Prx 2 and Prx 3), were readily detected by Western blotting but levels were no different between G93A and NTG littermate mice. It was not possible, however, to detect $PrxSO_{2/3}$ by Western blotting of the same preparations in either the G93A animals or their NTG littermates despite high protein loads, long exposures, the presence of abundant reduced Prxs and the presence of a 9-fold excess of the human G93A human SOD1 transgene in the transgenic animals. Potential reasons for this are considered in Section 6.10.

In conclusion my work identified defective recovery of the typical 2-cys Prxs in fibroblasts derived from I113T SOD1-related fALS and in doing so provided evidence from this model at least in support of my original hypothesis that the typical 2-cys Prxs might spend longer in an overoxidized form in the disease state than in health. At least some of these changes were reiterated in one of three pairs of fibroblasts derived from TDP43 related fALS but not in the other two. My efforts to find out whether the changes were reiterated in neuronal models of ALS were unsuccessful – possible reasons for this are discussed below along with a suggested approach to the future work my results indicate might be productive. Finally, I will discuss what defective recovery of the typical 2-cys Prxs after oxidative challenge might mean were it to be shown to be a feature of forms of the disease other than I113T SOD1-ALS and to manifest within motor neurons in the disease.

6.1 Protein levels under basal culture conditions

Basal levels of those typical 2-cys Prxs expressed in neurons (Prx 2 and Prx 3) were investigated in whole cell preparations from three pairs of I113T SOD1-ALS and control fibroblasts. Given evidence of alterations in the levels of Prx 2 and Prx 3 in the NSC34 motor neuronal cell model of mutant SOD1-related fALS (Kirby et al., 2005; Wood-Allum et al., 2006), I expected that levels of Prxs within I113T SOD1-ALS patient fibroblasts might differ in patient fibroblasts growing under basal culture conditions. Western blotting in patient and control fibroblast preparations however demonstrated similar levels of both Prx 2 and Prx 3 in all fibroblast pairs across all experimental repeats (Chapter 3, Fig. 3.8).

Given that the presence of mutant SOD1 is thought to generate oxidative stress (Barber and Shaw, 2010), levels of overoxidized Prxs were next measured in the fibroblasts. Western blotting for $PrxSO_{2/3}$ showed that hardly any $PrxSO_{2/3}$ was present in either patient or control fibroblasts growing under basal culture conditions. This absence of measurable $PrxSO_{2/3}$ in cells growing under basal conditions is consistent with the idea that overoxidized Prxs are a marker of oxidative stress (Low et al., 2007; Rhee and Woo, 2011). Although highly localized Prx overoxidation may occur transiently within cells to allow H_2O_2 signalling as suggested by Rhee et al., (Rhee et al., 2005), levels of $PrxSO_{2/3}$ in cells are generally noted to be undetectable in the absence of oxidative stress. It would appear that the expression of I113T mutant SOD1 was not, by itself, sufficient to bring about detectable overoxidation of the typical 2-cys Prxs.

I113T patient and healthy control fibroblasts were then Western blotted for two putative regenerators of the overoxidized Prxs, Srx 1 and Sesn 2. Levels of both these proteins were found to be the same in patient and control fibroblasts growing under basal culture conditions (Chapter 3, Fig. 3.10) suggesting that the presence of I113T mutant SOD1 in patient cells was not affecting the levels of Srx 1 or Sesn 2.

6.2 Levels of $PrxSO_{2/3}$ after exposure to H_2O_2

Overoxidation of the 2-cys Prxs can be brought about by exposing cells to H_2O_2 (Woo et al., 2003b). As minimal levels of $PrxSO_{2/3}$ were observed in both I113T patient and control fibroblasts growing under basal culture conditions, these cells were exposed to H_2O_2 in order to establish whether patient fibroblasts would show higher levels of $PrxSO_{2/3}$ than would control fibroblasts when subjected to an external oxidative stress. $PrxSO_{2/3}$ was readily detected in both patient and control cells after exposure to H_2O_2 as expected (Chapter 3, Fig. 3.11) but the levels of $PrxSO_{2/3}$ were the same in patient and control fibroblasts. The same samples were then Western blotted for total 2-cys Prxs. Levels of total typical 2-cys Prxs within patient and control cells were no different before and immediately after washout of H_2O_2 (Fig. 3.12). This indicated that the increase in $PrxSO_{2/3}$ was not

due to increase in levels of total Prxs but was rather due to the overoxidation of pre-existing typical 2-cys Prxs by the H_2O_2.

The lack of difference in $PrxSO_{2/3}$ levels in patient and control fibroblasts after exposure to 300 μM H_2O_2 suggested that there was no difference in the vulnerability to overoxidation of the typical 2-cys Prxs in patient and control cells. An alternative explanation, however, was that this concentration of H_2O_2 applied for 15 min was sufficient to overoxidize all typical 2-cys Prxs present within both patient and control cells to saturation. Given the absence of a difference in levels of total typical 2-cys Prxs, overoxidation to saturation by exposure to enough H_2O_2 might also generate the same results. In order to establish whether or not a 15 min exposure to 300 μM H_2O_2 did in fact constitute a saturating oxidative stress, a stress-titration experiment was conducted in one of the I113T patient fibroblast lines. This experiment indicated that overoxidation of the typical 2-cys Prxs present within the fibroblasts reached saturation when cells were subjected to a H_2O_2 concentration of 100 μM or higher for 15 minutes (Chapter 3, Fig. 3.13). This finding was compatible with previous studies performed by others which demonstrated that overoxidation of Prx 1 and Prx 2 to saturation by exposure to increasing H_2O_2 concentrations, occurs between 50 μM and 100 μM in cells including human umbilical vein endothelial cells, human erythrocytes and Jurkat cells (Low et al., 2007; Mitsumoto et al., 2001; Yang et al., 2002).

It was therefore likely that the lack of difference in levels of $PrxSO_{2/3}$ between patient and control fibroblasts when exposed to 300 μM H_2O_2 for 15 minutes was due to the H_2O_2 having overoxidized the typical 2-cys Prxs present in both cell types to saturation. The H_2O_2 dose response curve generated by the stress-titration experiment indicated that exposure to 30 μM H_2O_2 for 15 min would not overoxidize the 2-cys Prxs to saturation. The oxidative stress experiments were therefore repeated using this less severe oxidative stress. Despite the use of this significantly lower concentration of H_2O_2, there was still no difference in the resultant $PrxSO_{2/3}$ levels between patient and control fibroblasts. From this it was concluded that the typical 2-cys Prxs were no more likely to become overoxidized in response to an oxidative challenge due to H_2O_2 in patient than in control fibroblasts.

6.3 Recovery of overoxidized typical 2-cys Prxs after H_2O_2 exposure

As there were no identifiable differences in $PrxSO_{2/3}$ levels between I113T patient and control fibroblasts either grown under basal conditions or immediately after exposure to a saturating concentration of H_2O_2, the ability of I113T SOD1-ALS patient and control fibroblasts to clear the overoxidized 2-cys Prxs formed after H_2O_2 exposure was next investigated in a series of stress-recovery experiments. Reduction of overoxidized typical 2-cys Prxs has been shown to take between 6-12 hours in A549 human epithelial cells, HeLa cells and NIH3T3 mouse embryonic fibroblasts (Noh et al., 2009; Woo et al., 2009b). In the study by Noh et al., it was shown that $PrxSO_{2/3}$, generated by

exposing A549 and HeLa cells to 200 μM H_2O_2 for 10 min took 8-10 hours, after H_2O_2 washout, to decrease back to basal levels (Noh et al., 2009). Guided by this, the three pairs of I113T SOD1 patient and control fibroblasts were first subjected to a 15 min exposure to 300 μM H_2O_2 in order to induce overoxidation of the typical 2-cys Prxs to saturation. The H_2O_2 was then washed out and the cells were allowed to recover over a period of 26 hours with samples harvested at various time-points after H_2O_2-washout.

Interestingly, the rate of clearance of $PrxSO_{2/3}$ from patient and control fibroblasts was not the same. It was evident from Western blotting that patient fibroblasts consistently showed a delay in the disappearance of $PrxSO_{2/3}$ after H_2O_2 washout in comparison to the control cells (Chapter 3, Fig. 3.16 A). In control fibroblasts, $PrxSO_{2/3}$ had disappeared completely by 12 hours after the washout of H_2O_2. At the same experimental time point, however, there remained significant quantities of $PrxSO_{2/3}$ in patient fibroblasts. The delay in the disappearance of $PrxSO_{2/3}$ was statistically significant and consistent in all the three I113T SOD1-ALS patient fibroblast cell lines examined (Chapter 3, Fig 3.16 B). Overoxidized typical-2-cys Prxs lack hydroperoxidase activity. Given that the hydroperoxidase function of Prxs contributes to overall cellular anti-oxidant defence, it can be argued that if the typical 2-cys Prxs within patient fibroblasts remain overoxidized for some hours longer after an oxidative challenge than they do in control cells (and are thereby inactive as hydroperoxidases for hours longer) then patient cells might be expected to be more vulnerable to oxidative damage should further oxidative challenge occur before recovery is complete. Ultimately this might predispose patient cells to oxidative stress-mediated cell death (Barber and Shaw, 2010; Finkel, 1998). The presence of overoxidized typical 2-cys Prxs in patient cells for hours longer than is the case in control cells after oxidative challenge might also confer some protection if, as is theoretically possible, these overoxidized 2-cys Prxs coalesce to form multimeric protein chaperones. This might be a means by which an oxidative stress significant enough to bring about the overoxidation of enough 2-cys Prxs to form mulitmeric protein chaperones might better equip patient cells to deal with some of the consequences of subsequent oxidative stresses which might include aggregation of protein and formation of stress-granules (Bosco et al., 2010; Okado-Matsumoto and Fridovich, 2002).

Proteomic studies of the reduction of $PrxSO_{2/3}$ generated in HeLa cells treated with H_2O_2 exposure have shown that reduction of the various overoxidized typical 2-cys Prxs occurs at different rates (Chevallet et al., 2003; Woo et al., 2003a). Reduction of overoxidized Prx 1 and Prx 2 occurs much faster than reduction of Prx 3 and Prx 4. Recent evidence suggests that one potential reason for the delayed reduction of overoxidized Prx 3 is its localization within the mitochondrial matrix. Subtle structural features of Prx 3 have been shown to confer some additional resilience to overoxidation compared to Prxs 1, 2 and 4 but once Prx 3 is overoxidized, however, its reduction takes longer. This is most likely because the reduction of overoxidized Prx 3 is dependent upon the translocation of the active $PrxSO_{2/3}$ regenerator – sulfiredoxin 1 (Srx 1) from the cytosol through both outer and inner mitochondrial membranes into the mitochondrial matrix (Noh et al., 2009). Given that Prx 3 is

estimated to be responsible for the reduction of up to 90% of the H_2O_2 generated within mitochondria (Cox et al., 2010), a delay of hours in the reduction of inactive overoxidized Prx 3 back to its reduced, active form in ALS patient cells might be expected to lead to increased oxidative damage to mitochondrial macromolecules by unreduced H_2O_2 and might ultimately trigger mitochondrially-mediated apoptosis (Orrenius et al., 2003).

To verify that the gradual disappearance of $PrxSO_{2/3}$ from both patient and control cells in the 26 hours after exposure to H_2O_2 was not due to a decrease in the levels of total typical 2-cys Prxs, whole cell homogenates from the stress-recovery experiments were Western blotted for total 2-cys Prxs. There was no change in levels of total typical 2-cys Prxs in either patient or control fibroblasts in the first 8 hours after H_2O_2-washout. At 8 hours after washout levels of total typical 2-cys Prxs were found to be increased by 63 % in both patient and control cells (Chapter 3, Fig. 3.17) and this increase was maintained through to the endpoint of the experiment at t = 26 hr after H_2O_2-washout. There was no difference in the levels of total 2-cys Prxs between patient and control cells at any of the experimental time points during the recovery period. The increase in the levels of total 2-cys Prxs was likely a result of *de novo* protein synthesis designed to up-regulate cellular anti-oxidant defence after a significant oxidative challenge. In HeLa cells, *de novo* synthesis of typical 2-cys Prxs has been shown to occur around 12 hours after an externally-applied oxidative insult (Chevallet et al., 2003), a similar time course for the induction of 2-cys Prx transcription as observed in the fibroblasts after oxidative challenge.

6.4 Effect of H_2O_2 exposure on $PrxSO_{2/3}$ regenerators

Immediately after exposure to H_2O_2, levels of $PrxSO_{2/3}$ increased to a peak then gradually decreased back towards basal over the following 24 hours. This decrease was delayed in I113T fibroblasts compared to controls. Given that the induction of total 2-cys Prxs occurred at the same time and to the same extent in patient and control cells around 8 hours after oxidative challenge it was clear that the decrease in $PrxSO_{2/3}$ could not be attributed to a decrease in total 2-cys Prx levels but must either be due to removal of overoxidized 2-cys Prxs from the cells or else to their reduction. This regeneration of reduced, active 2-cys Prxs is mediated by sulfiredoxin 1 and possibly also sestrin 2 although more recent evidence suggests that the latter does not in fact serve this function (Woo et al., 2009a).

The work-up oxidative stress experiment carried out HEK293 cells (Chapter 3, Section 3.1.3) showed an increase in the levels of Sesn 2 about 7 hours after H_2O_2-washout (Chapter 3, Fig. 3.7). This induction was not observed in cells that were not subject to H_2O_2 stress, indicating that the induction was likely to be a response to the oxidative insult in the HEK293 cells. When samples from the stress-recovery experiments were Western blotted for Sesn 2, however, there were no alterations in the levels of Sesn 2 in either patient or control cells during the recovery period (Chapter 3, Fig. 3.19 A). The levels of Sesn 2 were similar, in both patient and control cells, before and after H_2O_2 exposure

implying that Sesn 2 may not in fact be involved in the reduction of $PrxSO_{2/3}$ in these cells (Chapter 3, Fig. 3.19 B). Although several earlier studies proposed that Sesn 2 was a regenerator of reduced Prxs from $PrxSO_{2/3}$ (Budanov et al., 2004; Papadia et al., 2008; Soriano et al., 2009b), the recent work by Woo et al., provides convincing evidence to the contrary (Woo et al., 2009a). His work in A549 mammalian cells and mouse embryonic fibroblasts derived from Sesn 2 knock-out mice showed that neither overexpression nor ablation of Sesn 2 affected the rate of reduction of overoxidized typical 2-cys Prxs whilst in contrast, alterations in the expression of Srx 1 have a profound effect (see Chapter 1, Section 1.14).

Western blotting for Srx 1 in samples from the stress-recovery experiments showed an induction of Srx 1 in both patient and control fibroblasts during the recovery period (Chapter 3, Fig. 3.18 A). Interestingly, this induction occurred just prior to the disappearance of $PrxSO_{2/3}$ in both patient and control fibroblasts, consistent with a role for Srx 1 in the reduction of $PrxSO_{2/3}$ as previously described (Biteau et al., 2003; Woo et al., 2005). Whilst the Srx 1 induction in control cells had begun by 3 hours after removal of H_2O_2, the Srx 1 induction within patient fibroblasts did not begin for a further 2 hours. This difference was statistically significant. In addition to delayed Srx 1 induction, levels of induced Srx 1 were significantly less in the patient cells than were they in the control cells (Chapter 3, Fig. 3.18 B).

Several studies have reported the effects of Srx 1 on the levels of $PrxSO_{2/3}$ (Jeong et al., 2006; Noh et al., 2009; Papadia et al., 2008; Rhee et al., 2007). Whilst overexpression of Srx 1 contributes to a faster reduction in levels of $PrxSO_{2/3}$, knock-out or silencing of Srx 1 abolishes $PrxSO_{2/3}$ reduction, as discussed in Chapter 1, Section 1.14.1 (Diet et al., 2007; Noh et al., 2009). Thus, the delayed and reduced induction of Srx 1 observed in my experiments in the I113T SOD1 ALS fibroblasts seems likely to be contributing to the delayed disappearance of $PrxSO_{2/3}$ also observed in the patient cell lines. It should be noted, however, that my experiments do not provide direct evidence for this. Srx 1 mediates the reduction of $PrxSO_2$. No evidence exists for the reduction of the still more oxidized $PrxSO_3$ forms of the proteins (Rhee et al., 2007; Woo et al., 2005) but further oxidation of $PrxSO_2$ to $PrxSO_3$ is now widely believed to initiate the oligomerization of Prxs to form multimeric protein chaperones, the dissociation of which, on the other hand, is not yet completely understood (Rhee and Woo, 2011; Wood et al., 2002). Reduction of $PrxSO_2$ has been postulated to take place through formation of a sulfinic phosphoryl ester intermediate that generates cysteine-sulfenic acid (-SOH), a physiologically-oxidized Prx form which is thereafter reduced by Trx/TrxR using electrons supplied by NADPH (Roussel et al., 2009). In a recent study of the mechanisms of action of plant Srx 1, formation of a Srx-Prx complex during the conversion of the phosphoryl ester Srx complex to cysteine-sulfenic acid (PrxSOH) was postulated (Iglesias-Baena et al., 2010; Jonsson et al., 2008). A schematic of this pathway is presented in Figure 6.2 overleaf.

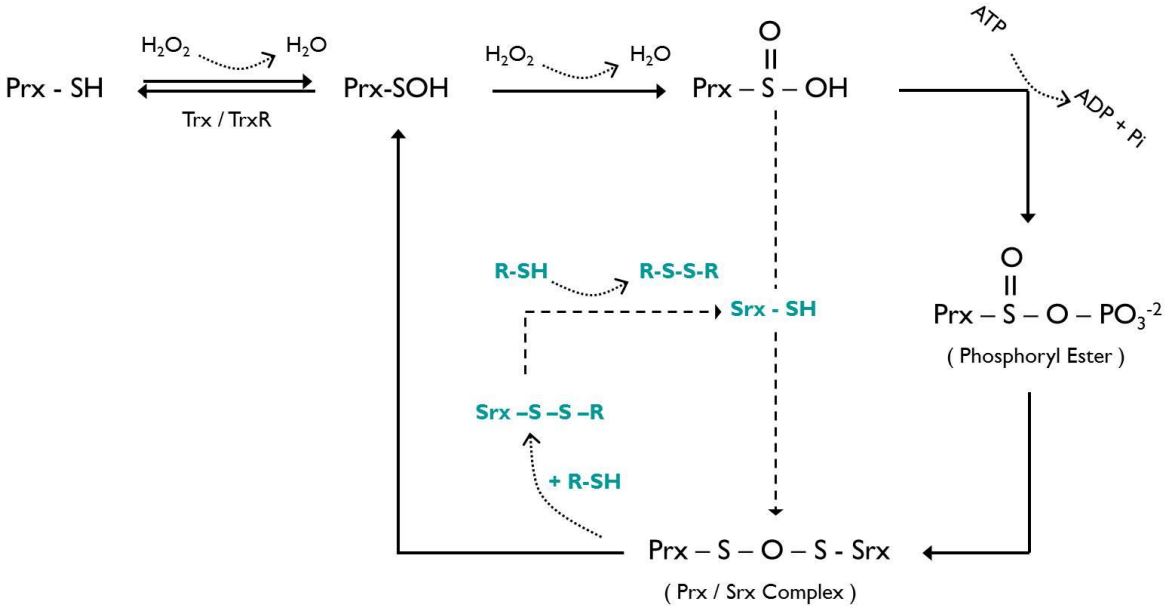

Figure 6.2: *Possible reduction mechanism of $PrxSO_{2/3}$ by Srx 1 as suggested by Iglesias Baena et al. (Iglesias-Baena et al., 2010). The cycle in blue represents potential reduction mechanism of oxidized Srx 1 by as yet unidentified thiol/s (R-SH).*

In rat cultured primary cortical neurons exposed to 200 µM H_2O_2, an induction of Srx 1 within 1 hour of H_2O_2-washout was observed using a luciferase-based reporter conjugated to the Srx 1 promoter (Papadia et al., 2008). In this work, levels of Srx 1 were shown to be regulated by two transcription factors, AP-1 and Nrf 2, the targeting sequences for both of which are present in the 3' UTR region of the sulfiredoxin 1 gene (Chapter 1, Section 1.14.1). The mechanisms by which AP-1 and Nrf 2 bring about the induction of Srx 1 has already been discussed in Section 1.14.1 (See Figure 1.6). The regulation of Srx 1 levels by the transcription factor AP-1 was first demonstrated by Glauser et. al., in pancreatic beta cells (Glauser et al., 2007). The transcriptional regulation of Srx 1 by AP-1 and Nrf 2 was confirmed in the studies that followed (Papadia et al., 2008; Soriano et al., 2009a; Soriano et al., 2008). In the light of these studies I sought to investigate levels of AP-1 in my stress-recovery experiments with the aim of identifying the cause of the delayed and reduced Srx 1 induction observed in the I113T SOD1-ALS patient fibroblasts.

The AP-1 transcription factor is a heterodimer comprising phosphorylated c-jun (activated c-jun) and c-fos proteins (see Fig. 1.6 in Chapter 1) (Angel and Karin, 1991). The levels of activated AP-1 can be measured indirectly using an antibody that recognizes activated c-jun as demonstrated by Lan et al., (Lan et al., 2012). Western blotting for AP-1 showed a biphasic increase in AP-1 levels in both patient and control fibroblasts after H_2O_2 exposure. The increases in AP-1 levels occurred immediately after H_2O_2-washout (t = 0 hours), prior to the induction of Srx 1 and again 1.5 hours after H_2O_2-washout (Chapter 3, Fig. 3.20 A). Although the timing of the two peaks in AP-1 were no different in patient and control cells the AP-1 induction in patient cells was reduced when compared to that in control cells. (Chapter 3, Fig. 3.20 B). The elevated levels of AP-1 measured in the stress-recovery experiments

immediately after H_2O_2-exposure suggest that the increase is a cellular response to the application of an external oxidative stress. The response of AP-1 to oxidative stress is now well characterized (Trachootham et al., 2008). AP-1 levels have been shown to be regulated by a phosphorylation cascade initiated by mitogen-activated protein kinases (MAPKases) and c-jun N-terminal kinases (JNK) (Shaulian and Karin, 2002). The induction of Srx 1 observed in both I113T patient and control cells after H_2O_2-exposure, therefore seems likely to have been at least partially due to the preceding increase in levels of AP-1. It is also plausible to hypothesize that the reduced levels of activated AP-1 observed within patient fibroblasts after H_2O_2-exposure may have been responsible for the delayed and reduced induction of Srx 1 seen in patient cells which in turn may have been responsible for the delayed clearance of $PrxSO_{2/3}$ from patient cells. Further experiments would be required to prove that these associated effects, all noted in response to an oxidative challenge, were causally linked, however.

6.5 New protein synthesis is required for the clearance of $PrxSO_{2/3}$

Evidence that new protein synthesis was required for the removal of $PrxSO_{2/3}$ during the recovery period after H_2O_2 exposure in patient and control fibroblasts was obtained by treatment of the cells with the translational blocking agent cycloheximide (CHX) prior to H_2O_2 exposure. Western blotting for $PrxSO_{2/3}$ in whole cell homogenates prepared from cells pre-treated with CHX showed an initial decrease of $PrxSO_{2/3}$ levels by about a third over the first 12 hours but no further decrease in $PrxSO_{2/3}$ was observed in either patient or control cells (Chapter 3, Fig. 3.21). After CHX pre-treatment it was observed that both patient and control fibroblasts showed similar levels of $PrxSO_{2/3}$ at each of the experimental time points. At the experimental end-point (t = 26 hr), both patient and control cells still contained $PrxSO_{2/3}$ at 72 % of the saturated $PrxSO_{2/3}$ levels at t = 0 hr after H_2O_2-washout. Consistent with the findings of the previous stress-recovery experiments, non-CHX pre-treated control fibroblasts showed a 91 % disappearance of $PrxSO_{2/3}$ 26 hours after H_2O_2-washout (t = 26 hr). As before, clearance of $PrxSO_{2/3}$ from non-CHX pre-treated patient cells was significantly delayed. Final amounts of $PrxSO_{2/3}$ in non-CHX pre-treated patient cells were ~26 % of those at t = 0 hr while those of controls were ~9 % of those at t = 0 hr as had been observed previously (Chapter 3, Fig. 3.16). Given that earlier Western blotting for sulfiredoxin 1, the main regenerator of $PrxSO_{2/3}$, in patient and control fibroblasts growing under basal culture conditions had shown detectable levels in both and no difference in Srx 1 levels between the two it seems most likely that the initial, limited clearance of $PrxSO_{2/3}$ seen in CHX pre-treated patient and control cells can be attributed to the action of pre-existing sulfiredoxin 1 in the cells.

Samples from the same CHX stress-recovery experiment were next Western blotted for Srx 1. As expected, pre-treatment of patient and control cells with CHX prior to the stress-recovery experiment completely abolished the induction of Srx 1 in both cell lines (Chapter 3, Fig. 3.22). After CHX pre-treatment, levels of Srx 1 decreased steeply to ~20 % of their initial levels by 8 hours after H_2O_2-washout in both patient and control cells. The half-life of Srx 1 in RAW 264.7 cells has been

estimated to be ~5.3 hr (Kim et al., 2010) which is consistent with my findings in the human fibroblasts.

When CHX was applied an hour prior to H_2O_2 exposure levels of $PrxSO_{2/3}$ fell by significantly less over the next 26 hours than did they in the absence of the translational blocker in both patient and control cells. By experiment's end at t = 26 hours $PrxSO_{2/3}$ levels remained at 72 % of those immediately after H_2O_2 washout in both patient and control cells. The Srx 1 induction that prefaced the gradual disappearance of $PrxSO_{2/3}$ in the absence of CHX pre-treatment was abolished when cells were pre-treated with CHX and indeed levels of Srx 1 fell off rapidly towards basal levels. Although these results do not prove that it is the induction of Srx 1 in response to H_2O_2-treatment that is responsible for the subsequent clearance of $PrxSO_{2/3}$ from both patient and control cells it seems reasonable to suggest that this might be the case.

To summarize, the reduction in Srx 1 levels and absence of the Srx 1 induction usually seen in response to H_2O_2 exposure in the absence of CHX pre-treatment taken together with the failure to clear $PrxSO_{2/3}$ from cells pre-treated with the translational blocking agent CHX prior to H_2O_2 exposure provide at least circumstantial evidence that the clearance of $PrxSO_{2/3}$ from the cells is brought about by Srx 1 which serves to reduce overoxidized typical 2-cys Prxs back to their active, reduced forms in a process that is dependent upon new protein synthesis. Reassuringly, the effects of CHX pre-treatment on the levels of $PrxSO_{2/3}$ and Srx 1 induction generated in response to H_2O_2 exposure were consistent with those reported in previous studies (Kim et al., 2010; Noh et al., 2009; Papadia et al., 2008). The biphasic induction of activator protein-1 (AP-1) seen in response to H_2O_2 exposure might account for the induction of Srx 1 as AP-1 is a known transcriptional regulator of Srx 1 although my experiments cannot prove causation, only association.

6.6 Two-hit stress-recovery experiments

The effect of multiple exposures to non-saturating oxidative stressors on I113T SOD1-ALS patient and healthy control fibroblasts was assessed using a two-hit stress-recovery experiment. I was interested to know whether sequential, milder oxidative challenges might exert a cumulative effect on the ability of cells to clear overoxidized 2-cys Prxs. In this experiment patient and control fibroblasts were first exposed to 30 μM H_2O_2 for 15 min, a non-saturating H_2O_2 concentration. After 16 hours when levels of $PrxSO_{2/3}$ had returned to basal levels, a second identical H_2O_2 exposure was applied and the cells were then allowed to recover once the H_2O_2 had been washed out. Western blotting for overoxidized Prxs showed that $PrxSO_{2/3}$ disappearance from patient cells after the first non-saturating H_2O_2 exposure was delayed when compared to the clearance of $PrxSO_{2/3}$ from control cells as had been observed in the one-hit stress-recovery experiments. Upon subjecting the cells to the second, identical oxidative challenge this delay was prolonged yet further in both patient and control cells but this prolongation was more marked in the patient cells. Clearly, subjecting patient and control fibroblasts to a repeated oxidative challenge caused the typical 2-cys Prxs within the ALS fibroblasts to

recover even more slowly than those within the control fibroblasts with the result that the 2-cys Prxs spent longer in their overoxidized state in the patient cells than did they in the control cells. This finding lends support to my original hypothesis.

Given the interesting findings in the one-hit stress-recovery experiments when levels of Srx 1 and AP-1 were measured as patient and control cells recovered from exposure to H_2O_2 it would have been interesting to measure these two protein species in the samples obtained from the two-hit stress-recovery experiments. Unfortunately shortage of time meant that this was not possible.

After the second, identical oxidative challenge, both I113T patient and control fibroblasts showed an increase in peak levels of $PrxSO_{2/3}$ measured immediately after H_2O_2 removal, reconfirming that the typical 2-cys Prxs were not overoxidized to saturation after the first oxidative challenge. Although the peak $PrxSO_{2/3}$ level reached immediately after washout of the second oxidative stress appeared to be higher in patient fibroblasts than in control fibroblasts this difference was not statistically significant. It would be interesting to subject patient and control cells to more consecutive non-saturating exposures to H_2O_2 to determine whether, eventually, a difference in the peak levels of $PrxSO_{2/3}$ generated might become greater in patient fibroblasts than in healthy control fibroblasts.

6.7 Work in mutant TDP43-ALS fibroblasts

To determine whether the defective clearance of $PrxSO_{2/3}$ observed in the I113T SOD1-ALS fibroblasts could also be identified in a fibroblast model of another form of fALS, stress-recovery experiments were carried out in three pairs of fibroblast cell lines derived from patients with TDP43-fALS and those derived from age- and sex-matched healthy controls. Minimal $PrxSO_{2/3}$ was detected in TDP-43 ALS fibroblasts growing under basal culture conditions (Chapter 3, Fig. 3.24), consistent with the findings in the three pairs of I113T SOD1-ALS and control fibroblasts (Chapter 3, Fig. 3.9). Stress-recovery experiments in the TDP43-ALS patient and control fibroblasts showed a delay in the disappearance of $PrxSO_{2/3}$ in patient cells compared to control cells in one of the three pairs of mutant TDP43 fibroblasts investigated (Fig. 3. 25). This delay was similar to the delay in the disappearance of $PrxSO_{2/3}$ observed in the I113T SOD1-ALS fibroblasts (Fig. 3.16). However, no delay in the disappearance of $PrxSO_{2/3}$ was observed in the remaining two mutant TDP43 patient fibroblasts (Chapter 3, Figs. 3.26 and 3.27).

Fibroblasts are derived from skin biopsies donated by individual patients and whilst the cells within such a cell line are relatively homogeneous some inherent variability between fibroblast cell lines is to be expected. The three TDP43 patients from whom the patient fibroblast lines used in my work were derived had ALS due to different mutations to the TDP43 protein. This might also account for some variability between cell lines. This said, it would be hoped that changes important to ALS pathogenesis would be a feature of all fibroblast cell lines obtained from patients with fALS due to mutations to the same protein. The fact that only one of three TDP43-ALS fibroblast cell lines reiterated the interesting

findings noted in all three I113T SOD1-ALS fibroblasts is therefore a concern. Examination of further TDP43-ALS fibroblasts would be needed before a definitive conclusion could be reached and at the time these experiments were carried out I did not have access to any other TDP43-ALS fibroblast cell lines.

WORK IN NSC34 CELLS

6.8 Immunoblotting in NSC34 cells grown under basal culture conditions

The NSC34 motor neuronal cell model used in my study comprised non-transgenic NSC34 cells (NTG) and NSC34 cells stably transfected with empty transfection vector only (pIRES), vector containing WT human SOD1 (WT) and vectors containing 3 forms of mutant human SOD1 (H48Q, I113T and G93A). Three mutant SOD1 lines were used in the current study to ensure that any changes detected could not be attributed solely to a clonal effect.

Three independent preparations of the cells growing under basal culture conditions were analyzed for levels of $PrxSO_{2/3}$ when cells were at less than passage 15. Western blotting of whole cell preparations of the NSC34 cells revealed abundant overoxidized Prxs across all six cell lines (Fig. 4.4). This was unexpected given that when grown under basal conditions, HEK293 cells and human fibroblasts contained barely any $PrxSO_{2/3}$. High levels of $PrxSO_{2/3}$ in the NTG and pIRES control NSC34 cell lines growing under basal conditions were particularly unexpected. In some preparations, the control NSC34 cell lines had higher levels of $PrxSO_{2/3}$ than did NSC34 cells expressing human WT or mutant SOD1. More perturbing still was the fact that variable levels of $PrxSO_{2/3}$ were observed within each NSC34 cell line from preparation to preparation. Extensive troubleshooting was carried out to try to address this inconsistency as has been described in Chapter 4, Section 4.4 but despite this it was impossible to obtain consistent results for basal levels of $PrxSO_{2/3}$ or Srx 1 in the NSC34 cells.

It appeared that my NSC34 cell lines were experiencing varied amounts of oxidative stress each time a harvest was performed. In the presence of this degree of variability, the extent to which the presence of mutant SOD1 might have contributed to the overoxidation of typical 2-cys Prxs in those cell lines expressing mutant SOD1 was impossible to judge. Although every effort was made to maintain consistency in the culture, passaging and harvesting of cells no improvement in consistency between preparations was achieved. It appeared that other less easy to control factors such as differential growth rates between different NSC34 cell lines which affected confluency at harvest were at play. It was observed that control cell lines had a tendency to grow faster than those expressing mutant SOD1. Control cells also adhered more strongly to the surface of the flask and as a result required more force to knock them off during harvesting. It may have been the case that variables such as cell confluency and the force required to harvest the cells from each flask may have affected the levels of

oxidative stress experienced by each cell line at the point of harvest, accounting for some of the variability in $PrxSO_{2/3}$ levels observed.

Western blotting of whole cell NSC34 preparations for other proteins involved in the redox cycle of the 2-cys peroxiredoxins was then carried out. Proteins assessed included both regenerators of $PrxSO_{2/3}$ - sestrin 2 (Sesn 2) (Budanov et al., 2004) and sulfiredoxin 1 (Srx 1) (Woo et al., 2005) and thioredoxin-interacting protein (Txnip), a protein that inhibits the function of thioredoxin (Trx) (Papadia et al., 2008). Given the variability in levels of $PrxSO_{2/3}$ between preparations we expected that levels of Srx 1, Sesn 2 and Txnip might also vary from preparation to preparation but that they might possibly have a consistent relationship with the level of $PrxSO_{2/3}$. This was not, however, the case. Across the three preparations made of the 6 NSC34 cell lines, Western blotting for Srx 1 and Txnip also displayed inconsistency of results within each individual cell line from preparation to preparation (Chapter 4, Fig. 4.7 and 4.9) and no consistent relationship with levels of $PrxSO_{2/3}$ could be identified. In contrast to the variable levels of Srx 1 and Txnip observed, levels of Sesn 2 in these preparations did not differ between the different NSC34 cell lines nor did it vary within cell lines preparation to preparation (Chapter 4, Fig. 4.8). Given this rather different behaviour to that of the other putative $PrxSO_{2/3}$ regenerator, Srx 1, it is interesting that sestrin 2 is no longer believed to be capable of reducing overoxidized 2-cys Prxs back to their active, reduced state.

Previously it has been shown that NSC34 cells expressing G93A mutant SOD1, have reduced Prx 3 both at mRNA level (Kirby et al., 2005) and at protein level (Wood-Allum et al., 2006) when compared to control NSC34 cells (WT and pIRES). Furthermore, levels of Prx 2 were observed to be increased at both an mRNA (Kirby et al., 2005) and at protein level (Wood-Allum et al., 2006). The current study, however, failed to replicate these findings. No differences in the expression levels of Prx 2 were observed between control cell lines (NTG, pIRES and WT) and cells expressing mutant SOD1 across three independent preparations of cells of passages less than 15 (Chapter 4, Fig. 4.2). Similarly, no change in Prx 3 levels were observed in I113T-expressing or G93A-expressing NSC34 cell compared to controls. Levels of Prx 3 in the H48Q-expressing cells consistently appeared to be reduced compared to WT-expressing cells across the three independent preparations (Chapter 4, Fig. 4.3 A) although this decrease was not statistically significant (Chapter 4, Fig. 4.3 B). It is important to note that the NSC34 cell lines used in my study had been remade *de novo* from NTG NSC34 cells between the earlier studies and the present one. The cells used in the present study used a different expression vector system to that used by the previous NSC34 cells. The NSC34 cell model, currently in use, employs the pIRES transfection vector (Clontech, California, USA) whereas the stable NSC34 cell lines used in previous studies in the laboratory made use of the pCEP4 transfection vector (Invitrogen, Paisley, UK). Apart the use of a different transfection vector, the relentless inconsistency within a single cell line between preparations in the current study suggests a more fundamental problem may have been be responsible for the difficulties experienced. It became clear that for

whatever reason, the NSC34 cell model of ALS was unlikely to be informative in the investigation of the oxidation state of the 2-cys Prxs.

6.9 Oxidative stress experiments

Four NSC34 cells (NTG, pIRES, WT and G93A) were exposed to H_2O_2 and levels of $PrxSO_{2/3}$ were measured by Western blotting. All four NSC34 cell lines showed increased levels of $PrxSO_{2/3}$ as would be expected. The extent to which $PrxSO_{2/3}$ levels increased after exposure to H_2O_2, however, were as variable preparation to preparation as were the basal $PrxSO_{2/3}$ levels (Chapter 4, Fig. 4.10). Given the variability of basal $PrxSO_{2/3}$ levels within each cell line under basal culture conditions, one reason for the variability of $PrxSO_{2/3}$ recorded post-H_2O_2 exposure may have been different levels of $PrxSO_{2/3}$ in the two flasks of the same cell line (one used as basal and the other treated with H_2O_2) at the start of the experiment. Despite the variability of the extent of the increase in $PrxSO_{2/3}$ levels after H_2O_2 exposure, there was a statistically significant increase in $PrxSO_{2/3}$ after H_2O_2 exposure in all the four cell lines (Chapter 4, Fig. 4.10 B). This increase, however, was similar in both G93A mutant SOD1-expressing cells and the WT SOD1-expressing control cells. The inconsistency in the levels of $PrxSO_{2/3}$ both pre-and post-oxidative stress made it very difficult to determine baseline $PrxSO_{2/3}$ levels against which any further experiments, for example stress-recovery experiments, could meaningfully be carried out. In the light of the difficulties experienced obtaining a consistent read-out from the NSC34 cellular model of ALS, attention was then turned to testing my basic hypothesis CNS tissues obtained from an *in vivo* ALS model – the G93A SOD1 transgenic mice.

WORK IN G93A SOD1 TRANSGENIC MICE

6.10 Immunoblotting in sucrose-perfused murine CNS tissues

Western blotting for reduced and overoxidized typical 2-cys peroxiredoxins and their regenerators was performed on post-nuclear whole tissue homogenates of brain and spinal cord from G93A SOD1 transgenic mice and their NTG littermates. Mice of 60 days, 90 days and 120 days of age were included in the study to allow the effects of disease progression on the levels of the 2-cys Prxs and their regenerators to be assessed. Given previous evidence of alterations in the levels of various of the 2-cys Prxs at both a protein and mRNA level in G93A murine CNS material (Ferraiuolo et al., 2007; Wood-Allum et al., 2006), I first aimed to confirm whether the presence of G93A mutant human SOD1 had any effect on the levels of total 2-cys Prxs in whole spinal cord and brain homogenates.

Western blotting for total Prx 2 and Prx 3, the principal motor neuronal typical 2-cys Prxs, demonstrated no difference in their levels in either whole brain or spinal cord preparations between G93A and NTG mice. Levels of Prx 2 and Prx 3 were the same in all homogenates prepared from mice at all three time points (Chapter 5, Figs. 5.4 and 5.5). In an earlier study, a decrease in Prx 3 was observed in mitochondrially-enriched preparations of whole spinal cord from G93A transgenic mice. In

this study the mitochondrial matrix protein prohibitin was used as a loading control (Wood-Allum et al., 2006). My experiments used the cytosolic protein tubulin as a loading control and the blotting was performed in whole spinal cord homogenates rather than in mitochondrially-enriched fractions of this tissue. These differences might themselves be sufficient to explain the differing results but it has recently also been shown in cardiac tissue that prohibitin levels may themselves increase in conditions of oxidative stress (Liu et al., 2009). The use of a cytosolic loading control rather than one expressed in the mitochondrial matrix also means that changes in overall mitochondrial mass within cells are not taken into account when corrections are made for protein loading.

Having established at a protein level in whole brain and spinal cord homogenates that there was no change in the levels of total Prx 2 or Prx 3, levels of $PrxSO_{2/3}$ were next measured in these preparations. Despite protein loads of up to 120 µg of protein per lane and prolonged exposures no $PrxSO_{2/3}$ bands could be identified in whole brain or whole spinal cord preparations at any of the 3 ages sampled (Chapter 5, Figs. 5.6 and 5.7).

Western blots for SOD1 had already demonstrated the presence of both endogenous murine SOD1 and human SOD1 in the G93A mice samples (Fig. 5.3) thereby confirming that the samples had not been inadvertently mixed up and that the absence of $PrxSO_{2/3}$ signal was not due to the presence of two NTG samples. Western blotting for Prx 2 and Prx 3 in the same samples had already shown that these typical 2-cys Prxs were present in abundance within the homogenates. An absence of typical 2-cys Prxs to become overoxidized could not, therefore, be the reason for the failure to detect $PrxSO_{2/3}$. Clearly one explanation for the failure to demonstrate any $PrxSO_{2/3}$ within either whole brain or whole spinal cord homogenates from G93A transgenic mice, as hypothesized, might be that typical 2-cys Prxs are not overoxidized in CNS tissue from G93A mice. Whole brain and cord homogenates, however, contain a relatively small number of motor neurons and a large volume of other types of neuron, glia, connective and vascular tissue. It remains a possibility that $PrxSO_{2/3}$ is present in a small subset of cells within the homogenates (motor neurons, for example) but the contribution made to the homogenate as a whole is so small as to render the $PrxSO_{2/3}$ undetectable by Western blotting. In short, if a subset of neurons containing $PrxSO_{2/3}$ are present in enough of a minority, the presence of $PrxSO_{2/3}$ might be undetectable by Western blotting as the signal they generated would be swamped out.

The murine CNS homogenates were also blotted for sulfiredoxin 1 and sestrin 2, both initially thought to be $PrxSO_{2/3}$ regenerators. Srx 1 was readily detected by Western blotting in both whole brain and spinal cord homogenates (Chapter 5, Fig. 5.8), although there was no difference in Srx 1 levels between G93A and NTG littermates. In contrast, Western blotting for Sesn 2 showed no protein bands with protein loads of up to 80 µg per lane and when 120 µg of protein was loaded per lane multiple bands appeared at the predicted molecular weight of sestrin 2 making it difficult to be sure which, if any, was the correct protein band (Chapter 5, Figs. 5.9 and 5.10). Given this, and subsequent

evidence to suggest that sestrin 2 does not in fact act as a regenerator of $PrxSO_{2/3}$ further analysis of the sestrin 2 blots was not carried out.

As it had proven impossible to detect overoxidized 2-cys Prxs in whole mouse brain or spinal cord homogenates from either G93A or NTG mice despite the presence of abundant reduced 2-cys Prxs, I went on to measure the levels of the physiologically-oxidized dimeric forms of the typical 2-cys Prxs. These represent a less oxidized species of the 2-cys Prxs than do $PrxSO_{2/3}$ and are formed as the 2-cys Prxs act as hydroperoxidases to reduce peroxides. Typical 2-cys Prxs form obligate homodimers during the reduction of H_2O_2 to H_2O (Chapter 1, Section 1.13.1). During the peroxide detoxification reaction, free thiol groups (-SH) are oxidized to cys-sulfenic acids (SOH). An *inter*-molecular disulphide bridge forms between two Prx monomers before thioredoxin reduces the dimer back to two monomers ready to begin the process again (Chapter 1, Fig. 1.3). Thiol blocking reagents such as N-ethylmaleimide (NEM) block oxidation of thiol groups by covalently binding free cysteine residues. By doing so, NEM can "lock" the 2-cys Prxs present within a cell line or animal tissue in the oxidation state they were in at the time NEM was applied. Western blotting of the resultant locked lysates for individual typical 2-cys Prxs under non-reducing conditions allows analysis of the relative abundance of the dimerized (physiologically oxidized) form of each 2-cys Prx in relation to the reduced monomeric form of the same 2-cys Prx (Kumar et al., 2009).

Using this technique I perfused 3 pairs of G93A transgenic mice of approximately 100 days of age and their NTG littermates with NEM prior to sacrifice. Whole brain and spinal cord homogenates were then prepared as previously and were blotted for Prx 2 and Prx 3 under non-reducing conditions to allow measurement of levels of the physiologically-oxidized dimeric form of both proteins present in the homogenates. My aim was to establish whether there were higher levels of dimerized Prx 2 or Prx 3 in CNS tissue from the G93A mice than their NTG littermates. In two of the three littermate pairs, levels of dimerized Prx 2 and Prx 3 were indeed higher in G93A mice in both brain and spinal cord homogenates in comparison to those from their NTG littermates (Figs. 5. 12 and 5.13). Overall levels of dimerized Prx 2 and Prx 3 were statistically-significantly higher in G93A homogenates than in NTG controls. Whilst these experiments on a very small number of mice of one age were encouraging, further experiments on more animals are needed to establish whether or not there really is an excess of physiologically-oxidized Prx 2 and 3 in the G93A mice. Unfortunately the necessary numbers of animals were not available from the colony at the time these experiments were carried out.

Given that SOD1 acts to convert the superoxide free radical to H_2O_2 and the 2-cys Prxs in turn reduce this H_2O_2 to water, high levels of physiologically-oxidized 2-cys Prxs in CNS tissue from the almost tenfold overexpressing G93A SOD1 transgenic mice were not unexpected. Without confirmatory work in more G93A/NTG littermate pairs of different ages and also examination of levels of dimeric Prx 2 and Prx 3 in WT human SOD1 transgenic mice it is unclear whether the increased

levels of dimerized 2-cys Prxs are a robust finding in the G93A mice and whether they are due to the presence of mutant SOD1 or simply to an excess of transgenic WT or G93A human SOD1. If increased dimerized Prx 2 and Prx 3 are confirmed by further experiments in more G93A/NTG littermate pairs and a similar increase in dimerized Prx 2 and 3 is absent in WT SOD1 overexpressing transgenic mice, these experiments would provide support for my original hypothesis – namely that the 2-cys Prxs exist in a more oxidized state in ALS than in health.

6.11 Immunoblotting of previously-banked samples of murine CNS tissue

Whilst awaiting mice to become available from our colony of G93A SOD1 transgenic mice for definitive experiments in sucrose-perfused CNS tissue, preliminary Western blotting experiments were carried out in previously-banked mouse CNS tissue. As discussed in Chapter 5, the method of CNS tissue extraction and the time taken from sacrifice of the animal to snap freezing of the tissue was unknown. Whole brain and spinal cord homogenates were prepared from three independent preparations of previously frozen CNS tissue from 120 day-old G93A transgenic mice and their NTG littermates along with the spinal cords of 135 day-old WT SOD1 overexpressing mice. These preparations were Western blotted for $PrxSO_{2/3}$. Whilst no $PrxSO_{2/3}$ could be detected by Western blotting in homogenates later prepared from sucrose-perfused animals despite very high protein loads and exposures, $PrxSO_{2/3}$ was readily detected in all the homogenates made from the pre-banked CNS material, including that from NTG animals (Fig. 5.2 A and B). Indeed, levels of $PrxSO_{2/3}$ were consistently less in CNS tissue from the G93A transgenic mice than in CNS tissue from their NTG littermates (Fig. 5.2 C and D).

Given the unknown post-mortem delay and method of extraction of CNS tissue of this material further analysis of these data was not felt to be appropriate. The presence of readily detectable $PrxSO_{2/3}$ in whole brain and spinal cord homogenates from pre-banked NTG mice was unexpected. This, and the absence of $PrxSO_{2/3}$ in CNS homogenates from optimally-harvested sucrose-perfused mice whether G93A or NTG, led me to consider the differences in the means by which the sucrose-perfused, snap-frozen mice samples and previously-banked mouse tissue (not sucrose-perfused and of unknown duration of post-mortem delay) had been obtained. Mice subjected to cerebral ischaemia have been shown to overoxidize typical 2-cys Prxs in their cortical neurons (Papadia et al., 2008). It is possible, therefore, that a sufficiently lengthy post-mortem delay may have led to the overoxidation of typical 2-cys Prxs prior to harvest of the CNS tissue in the previously-banked lab samples. Discussion of the results obtained in this material beyond acknowledgement of its limitations is therefore not warranted.

STUDY LIMITATIONS

In this study a deficit in the recovery of overoxidized typical 2-cys Prxs after oxidative challenge in a non-neuronal cellular model of I113T SOD1-related fALS was identified. Given that overoxidized 2-cys Prxs do not function as hydroperoxidases, this delay, measured in hours, might be expected to leave the cell vulnerable to oxidative damage to its cellular macromolecules should it experience further oxidative challenge before recovery of the typical 2-cys Prxs has occurred. Indeed, the results of the two-hit oxidative stress experiments suggested just such a cumulative vulnerability in response to sequential oxidative challenge that might, in theory, have a bearing on long-term cell viability and thereby on disease pathogenesis.

Due largely to the difficulties I experienced attempting to address my hypothesis in the NSC34 cell model of ALS (discussed above in Section 6.8 and 6.9) and the resultant time constraints I was unable to carry out experiments designed to establish whether what was an interesting finding in fibroblasts derived from patients with the I113T mutation of SOD1 was a feature more generally of ALS, whether the same defective clearance of $PrxSO_{2/3}$ was a feature of diseased motor neurons as well as of fibroblasts and what the functional consequences of this delayed $PrxSO_{2/3}$ recovery might be. These, and other, limitations to the work carried out are considered in more detail below.

The deficit in the recovery of $PrxSO_{2/3}$ was observed in a small subset of familial ALS cases that arise due to the I113T mutation in SOD1 and in one of three cases tested caused by the A321V TDP43 mutant. Shortage of time meant that I was unable to test further fibroblasts from TDP43 cases to clarify in what proportion of cases defective $PrxSO_{2/3}$ clearance was a feature nor was I able to test fibroblasts derived from cases expressing other ALS-causing SOD1 mutations, mutations to other proteins causing ALS such as C9Orf72, FUS/TLS and, most importantly of all, fibroblasts derived from patients with sporadic ALS (which accounts for up to 95% of all ALS cases).

The delayed recovery of $PrxSO_{2/3}$ was identified in fibroblasts derived from fALS patients. As mentioned in Chapter 2, Section 2.3, fibroblasts are self-replicating skin cells and as such have limitations as a model for motor neurons. Given significant differences in the morphology and function of fibroblasts and motor neurons, extrapolation of the current findings in fibroblasts to motor neurons cannot be assumed. For this reason it was important to establish whether the deficit identified in the I113T SOD1-ALS fibroblasts was also present in ALS motor neurons. My attempts to address this question by testing the hypothesis in the NSC34 motor neuronal cell model of SOD1-ALS and in whole CNS homogenates from the G93A SOD1 transgenic mouse were unsuccessful. The reasons for this have already been considered. Approaches that might be helpful in addressing this question in future work are discussed below.

The oxidative insult utilized in my experiments (exposure to 300 μM H_2O_2 for 15 minutes) likely represents a more severe oxidative stress than any physiological oxidative stressor cells are likely to encounter. Given sufficient time it would have been ideal to determine whether defective recovery of $PrxSO_{2/3}$ is observed when fibroblasts are challenged with less severe direct/indirect oxidative insults. This is considered further in the Future work section below.

The levels of activated AP-1 measured in the stress recovery experiments in I113T SOD1-ALS fibroblasts were measured in post-nuclear whole cell homogenates. As AP-1 forms in the cytosol in response to an oxidative stress then translocates into the nucleus these measurements provide only part of the picture as AP-1 already within the nucleus will not have been measured. To obtain an overall picture of AP-1 within the cell it would have been helpful to determine the levels of AP-1 in both cytosol and nucleus.

Due to a lack of G93A and NTG littermate mice of the correct age from our colony only preliminary NEM-perfusion experiments could not be carried out in murine CNS tissue. Whole spinal cord and brain homogenates from a total of 3 littermate pairs of G93A and NTG mice of approximately 100 days of age were examined for levels of physiologically-oxidized (dimerized) Prx 2 and Prx 3. These preliminary results were interesting with more dimerized Prx 2 and Prx 3 present in both spinal cord and brain in two of the three pairs. Clearly further animals would need to be examined for firm conclusions to be reached. This is discussed below in the Future work section.

FUTURE WORK

In the time available to complete the work described here it was not possible to fully explore all the avenues opened up by what were relatively late positive findings in the I113T SOD1 human fibroblasts. Some of the limitations discussed in the section above are to be the focus of immediate future work and are discussed below along with other lines of enquiry suggested by my findings.

The first aim of any future work would be to establish to what extent the defective recovery of overoxidized typical 2-cys Prxs observed in I113T SOD1-ALS fibroblasts is reiterated in fibroblast models of other forms of ALS. Similar stress-recovery experiments to those described in this work would need to be carried out in these cells. Clearly, were defective $PrxSO_{2/3}$ recovery found to be a feature of other fibroblast models of ALS the significance of the finding in I113T SOD1-ALS fibroblasts would be increased. In the first instance, fibroblasts derived from SOD1-related fALS patients caused by other mutations of SOD1 should be investigated. Ideally this work would include representative mutations from the so-called wild-type (WT) SOD1 group, which have a normal or near normal dismutase capability, and the metal binding-region (MBR) group which do not. Next, fibroblasts derived

from patients with disease attributable to other non-SOD1 forms of familial ALS such as C9Orf 72, TDP43 and FUS should be examined. Although the recent focus of work in the field has been on the recently discovered new genes for familial ALS, the fact remains that the majority of patients with the disease have no family history and do not transmit the disease to their children. It would therefore be important to establish whether or not defective clearance of $PrxSO_{2/3}$ is a feature of fibroblasts derived from patients with sporadic ALS.

Next, verification that there is defective recovery of $PrxSO_{2/3}$ in ALS motor neuronal models would need to be attempted. My experience suggests that the neuroblastoma-based NSC34 cell line frequently used to serve this end will not be fit for purpose for the investigation of this particular pathway and other neuronal models would need to be considered. Options might include the use of an alternative immortalized cell line such as the N2a murine neuroblastoma cell line (Vance et al., 2009) or the SH-SY5Y metastatic neuroblastoma cell line (Carri et al., 1997), both of which have previously been transfected with mutant genes known to be responsible for ALS and used as neuronal ALS models (Vance et al., 2009). Another option would be the use of primary embryonic motor neurons explanted from murine models of SOD1 and other forms of fALS and grown up in culture. The volume of material that can be obtained for these studies is much smaller than that available from immortalized cell lines and would impose limits on the experiments that can be performed at a protein level. Whilst these cells are destined to become adult motor neurons, at the time they are explanted they are embryonic. They may not, therefore, respond in the same way as the adult cells they were destined to become. Quantitative-PCR to identify the induction of sulfiredoxin 1 could readily be performed in the volume of material obtainable from primary motor neuronal cultures. Quantification of post-translational modifications such as overoxidation of the typical 2-cys Prxs in primary motor neurons would be more difficult, but not impossible.

It was disappointing not to have been able to identify overoxidized 2-cys Prxs by Western blotting in either whole brain or spinal cord tissue from G93A SOD1 transgenic mice at any of the disease stages tested. Possible reasons for this have already been discussed above including whether the relatively small contribution made by motor neurons to whole spinal cord and even more so whole brain homogenates might have made detection of $PrxSO_{2/3}$ in motor neurons by Western blotting in these samples impossible. Immunohistochemistry for $PrxSO_{2/3}$ in sections of spinal cord and cortex from the G93A SOD1 transgenic mice, their non-transgenic littermates and WT-SOD1 transgenic mice at various ages would allow identification of $PrxSO_{2/3}$ present in only a small subset of cells within the tissue, for example motor neurons, and dual labelling with cell-type specific markers might enable identification of those cell types in which there was $PrxSO_{2/3}$ staining. The same antibody raised against overoxidized forms of all the typical 2-cys Prxs used in my Western blotting experiments could be used. Whilst immunohistochemistry is not a truly quantitative technique it might nevertheless provide some idea as to whether there is an excess of overoxidized 2-cys Prxs within motor neurons in the disease state compared with controls. The same technique could equally be applied to sections of

spinal cord and motor cortex obtained from donated post-mortem CNS tissue from patients with ALS. Given the strikingly different results obtained with Western blotting for $PrxSO_{2/3}$ in optimally harvested CNS murine tissue and in pre-banked tissue (with an assumed longer post-mortem delay), however, interpretation of the results of experiments in donated human CNS tissue might be difficult given the often prolonged period from death to CNS tissue harvest.

Of course, another reason why no $PrxSO_{2/3}$ was identified in whole CNS homogenates from the G93A mice might be because there is none there to be identified. It was for this reason that I attempted to establish whether there was any difference in the levels of physiologically-oxidized (dimerized) neuronally-expressed typical 2-cys Prxs between G93A mice and their NTG littermates. The NEM-perfusion experiments in G93A and NTG mice served to "lock" the oxidation state of the 2-cys Prxs at the time the animals were sacrificed, preventing any subsequent post-mortem oxidation during processing of the tissue. A non-reducing Western blotting protocol was then used to preserve the physiologically-oxidized dimers which could then be quantified. Unfortunately, a shortage of animals of the correct ages at the time these experiments were carried out prevented me from clarifying what, if confirmed in adequate numbers of animals, could be interesting results. In two of the three pairs of G93A/NTG littermates investigated at approximately 100 days of age there were higher levels of physiologically-oxidized Prx 2 and Prx 3 dimers in the G93A animals in both whole spinal cord and brain homogenates. The third pair of animals showed the opposite change for both Prx 2 and Prx 3. In the first instance, non-reducing Western blotting of G93A and NTG littermate mice whole spinal cord and brain homogenates obtained at various disease stages (initially 60, 90, and 120 days of age), for dimerized Prx 2 and Prx 3 could be carried out. If a statistically-significant increase in the levels of dimerized Prx 2 and 3 is confirmed in the G93A animals compared with their NTG littermates, similar experiments in WT SOD1 transgenic mice would then needed to be done to confirm whether the changes observed were due to the overexpression of human SOD1 regardless of type (e.g., G93A or WT), or else was a mutant SOD1-specific change.

It would be interesting to know whether the delayed disappearance of $PrxSO_{2/3}$ from I113T SOD1-expressing human fibroblasts after exposure to H_2O_2 is also seen after different oxidative challenges. The recovery of $PrxSO_{2/3}$ is delayed after both saturating and non-saturating exposures to H_2O_2, however, it might still be argued that H_2O_2 treatment *per se* is not particularly physiological and identification of a similar defective $PrxSO_{2/3}$ clearance after alternative oxidative challenge would be reassuring. Such alternative oxidative stresses might include serum withdrawal or treatment with arsenic or menadione (Criddle et al., 2006; Flora, 2011). Furthermore, the exacerbated delay in recovery of $PrxSO_{2/3}$ seen after two consecutive non-saturating exposures to H_2O_2 suggests that further study of the effects of repeated, milder oxidative stresses on 2-cys Prx overoxidation and recovery might provide more physiologically relevant information about how post-mitotic motor neurons with a lifespan measured in decades handle a lifetime of oxidative challenge.

There was inadequate time for me to investigate the functional consequences of the delayed clearance of overoxidized 2-cys Prxs from the I113T SOD1 fibroblasts. As was discussed in Chapter 1, Section 1.14, overoxidized 2-cys Prxs are unable to function as hydroperoxidases but formation of multimers with a protein chaperone function from overoxidized 2-cys Prxs has been demonstrated in numerous studies (Moon et al., 2005; Rhee and Woo, 2011). It is possible to measure both the protein chaperone activity of the 2-cys Prxs (Kim et al., 2011) and their hydroperoxidase activity, the latter using a Trx-NADPH based, Prx hydroperoxidase assay (Kim et al., 2005). An obvious next step would be to measure both hydroperoxidase and protein chaperone activities of the typical 2-cys Prxs as ALS and control fibroblasts recover from an oxidative stress. This would provide some information about whether the slow clearance of $PrxSO_{2/3}$ from fibroblasts carrying an ALS-causing SOD1 mutation does in fact confer the functional consequences that might be inferred from the switch in function brought about by 2-cys Prx overoxidation.

This work was hypothesis-based and as such focused on the response of one group of proteins involved in the response of the cell to oxidative challenge. The typical 2-cys Prxs and their regenerators, however, do not provide the sole cellular response to oxidative challenge but rather operate alongside several other redox pathways, some of which are controlled by the same master transcription factors, most notably Nrf 2. Investigation of the effects of H_2O_2 exposure on other cellular anti-oxidant proteins and related transcriptional responses would clearly contribute to the knowledge developed from this study. The therapeutic potential of Nrf 2 has been widely investigated in ALS, given its function to transcribe a number of anti-oxidant proteins under conditions of oxidative stress (Petri et al., 2012). As the activation of Nrf 2 is a principal response to oxidative stress (Nguyen et al., 2009) and levels of Srx 1 are transcriptionally regulated by Nrf 2 (Papadia et al., 2008; Soriano et al., 2009a; Soriano et al., 2008), it will be particularly important in future work to delineate the role of Nrf 2 in the recovery of ALS fibroblasts after oxidative challenge.

If the findings identified in I113T SOD1-ALS fibroblasts are reiterated in fibroblast models of other forms of the disease and consistent differences in the performance of the typical 2-cys Prxs after oxidative challenge are observed between disease and control states in neuronal models of ALS it would then be appropriate to go on to investigate what the consequences for cell survival of these deficits are. If it could be demonstrated that a delay in recovery of the hydroperoxidase function of the 2-cys Prxs within motor neurons rendered them more vulnerable to further oxidative challenge and subsequent cell death then interventions designed to ameliorate this vulnerability would become of interest. These experiments might include manipulations to increase the expression of neuronally-expressed typical 2-cys Prxs; those to increase the expression of sulfiredoxin 1, the main $PrxSO_{2/3}$ regenerator, or those to decrease the expression of Txnip within models of ALS. The effects of these manipulations on the cell's ability to withstand oxidative stress could then be tested and the likely therapeutic usefulness of the manipulation assessed.

REFERENCES

Angel, P., and Karin, M. (1991). The role of Jun, Fos and the AP-1 complex in cell-proliferation and transformation. Biochim Biophys Acta *1072*, 129-157.

Barber, S.C., and Shaw, P.J. (2010). Oxidative stress in ALS: key role in motor neuron injury and therapeutic target. Free Radical Biology & Medicine *48*, 629-641.

Bensimon, G., Lacomblez, L., and Meininger, V. (1994). A controlled trial of riluzole in amyotrophic lateral sclerosis. ALS/Riluzole Study Group. N Engl J Med *330*, 585-591.

Biteau, B., Labarre, J., and Toledano, M.B. (2003). ATP-dependent reduction of cysteine-sulphinic acid by S. cerevisiae sulphiredoxin. Nature *425*, 980-984.

Bosco, D.A., Lemay, N., Ko, H.K., Zhou, H., Burke, C., Kwiatkowski, T.J., Jr., Sapp, P., McKenna-Yasek, D., Brown, R.H., Jr., and Hayward, L.J. (2010). Mutant FUS proteins that cause amyotrophic lateral sclerosis incorporate into stress granules. Hum Mol Genet *19*, 4160-4175.

Budanov, A.V., Sablina, A.A., Feinstein, E., Koonin, E.V., and Chumakov, P.M. (2004). Regeneration of peroxiredoxins by p53-regulated sestrins, homologs of bacterial AhpD. Science *304*, 596-600.

Carri, M.T., Ferri, A., Battistoni, A., Famhy, L., Gabbianelli, R., Poccia, F., and Rotilio, G. (1997). Expression of a Cu,Zn superoxide dismutase typical of familial amyotrophic lateral sclerosis induces mitochondrial alteration and increase of cytosolic Ca2+ concentration in transfected neuroblastoma SH-SY5Y cells. FEBS Lett *414*, 365-368.

Chevallet, M., Wagner, E., Luche, S., van Dorsselaer, A., Leize-Wagner, E., and Rabilloud, T. (2003). Regeneration of peroxiredoxins during recovery after oxidative stress: only some overoxidized peroxiredoxins can be reduced during recovery after oxidative stress. J Biol Chem *278*, 37146-37153.

Cox, A.G., Winterbourn, C.C., and Hampton, M.B. (2010). Mitochondrial peroxiredoxin involvement in antioxidant defence and redox signalling. Biochem J *425*, 313-325.

Criddle, D.N., Gillies, S., Baumgartner-Wilson, H.K., Jaffar, M., Chinje, E.C., Passmore, S., Chvanov, M., Barrow, S., Gerasimenko, O.V., Tepikin, A.V.*, et al.* (2006). Menadione-induced reactive oxygen species generation via redox cycling promotes apoptosis of murine pancreatic acinar cells. J Biol Chem *281*, 40485-40492.

Cudkowicz, M.E., McKenna-Yasek, D., Sapp, P.E., Chin, W., Geller, B., Hayden, D.L., Schoenfeld, D.A., Hosler, B.A., Horvitz, H.R., and Brown, R.H. (1997). Epidemiology of mutations in superoxide dismutase in amyotrophic lateral sclerosis. Ann Neurol *41*, 210-221.

Diet, A., Abbas, K., Bouton, C., Guillon, B., Tomasello, F., Fourquet, S., Toledano, M.B., and Drapier, J.C. (2007). Regulation of peroxiredoxins by nitric oxide in immunostimulated macrophages. The Journal of Biological Chemistry *282*, 36199-36205.

Ferraiuolo, L., Heath, P.R., Holden, H., Kasher, P., Kirby, J., and Shaw, P.J. (2007). Microarray analysis of the cellular pathways involved in the adaptation to and progression of motor neuron injury in the SOD1 G93A mouse model of familial ALS. J Neurosci *27*, 9201-9219.

Finkel, T. (1998). Oxygen radicals and signaling. Curr Opin Cell Biol *10*, 248-253.

Flora, S.J. (2011). Arsenic-induced oxidative stress and its reversibility. Free Radic Biol Med *51*, 257-281.

Fukada, K., Zhang, F., Vien, A., Cashman, N.R., and Zhu, H. (2004). Mitochondrial proteomic analysis of a cell line model of familial amyotrophic lateral sclerosis. Mol Cell Proteomics *3*, 1211-1223.

Glauser, D.A., Brun, T., Gauthier, B.R., and Schlegel, W. (2007). Transcriptional response of pancreatic beta cells to metabolic stimulation: large scale identification of immediate-early and secondary response genes. BMC Molecular Biology *8*, 54.

Harwood, C.A., McDermott, C.J., and Shaw, P.J. (2009). Physical activity as an exogenous risk factor in motor neuron disease (MND): a review of the evidence. Amyotroph Lateral Scler *10*, 191-204.

Iglesias-Baena, I., Barranco-Medina, S., Lazaro-Payo, A., Lopez-Jaramillo, F.J., Sevilla, F., and Lazaro, J.J. (2010). Characterization of plant sulfiredoxin and role of sulphinic form of 2-Cys peroxiredoxin. Journal of Experimental Botany *61*, 1509-1521.

Jeong, W., Park, S.J., Chang, T.S., Lee, D.Y., and Rhee, S.G. (2006). Molecular mechanism of the reduction of cysteine sulfinic acid of peroxiredoxin to cysteine by mammalian sulfiredoxin. The Journal of Biological Chemistry *281*, 14400-14407.

Jonsson, T.J., Johnson, L.C., and Lowther, W.T. (2008). Structure of the sulphiredoxin-peroxiredoxin complex reveals an essential repair embrace. Nature *451*, 98-101.

Kato, S., Saeki, Y., Aoki, M., Nagai, M., Ishigaki, A., Itoyama, Y., Kato, M., Asayama, K., Awaya, A., Hirano, A., *et al.* (2004). Histological evidence of redox system breakdown caused by superoxide dismutase 1 (SOD1) aggregation is common to SOD1-mutated motor neurons in humans and animal models. Acta Neuropathology (Berlin) *107*, 149-158.

Kim, H., Jung, Y., Shin, B.S., Song, H., Bae, S.H., Rhee, S.G., and Jeong, W. (2010). Redox regulation of lipopolysaccharide-mediated sulfiredoxin induction, which depends on both AP-1 and Nrf2. The Journal of Biological Chemistry *285*, 34419-34428.

Kim, J.A., Park, S., Kim, K., Rhee, S.G., and Kang, S.W. (2005). Activity assay of mammalian 2-cys peroxiredoxins using yeast thioredoxin reductase system. Anal Biochem *338*, 216-223.

Kim, S.Y., Paeng, S.K., Nawkar, G.M., Maibam, P., Lee, E.S., Kim, K.S., Lee, D.H., Park, D.J., Kang, S.B., Kim, M.R., *et al.* (2011). The 1-Cys peroxiredoxin, a regulator of seed dormancy, functions as a molecular chaperone under oxidative stress conditions. Plant Science : an international Journal of Experimental Plant Biology *181*, 119-124.

Kirby, J., Halligan, E., Baptista, M.J., Allen, S., Heath, P.R., Holden, H., Barber, S.C., Loynes, C.A., Wood-Allum, C.A., Lunec, J., *et al.* (2005). Mutant SOD1 alters the motor neuronal transcriptome: implications for familial ALS. Brain *128*, 1686-1706.

Kumar, V., Kitaeff, N., Hampton, M.B., Cannell, M.B., and Winterbourn, C.C. (2009). Reversible oxidation of mitochondrial peroxiredoxin 3 in mouse heart subjected to ischemia and reperfusion. FEBS Lett *583*, 997-1000.

Lacomblez, L., Bensimon, G., Leigh, P.N., Guillet, P., and Meininger, V. (1996). Dose-ranging study of riluzole in amyotrophic lateral sclerosis. Amyotrophic Lateral Sclerosis/Riluzole Study Group II. Lancet *347*, 1425-1431.

Lan, R., Geng, H., Polichnowski, A.J., Singha, P.K., Saikumar, P., McEwen, D.G., Griffin, K.A., Koesters, R., Weinberg, J.M., Bidani, A.K., *et al.* (2012). PTEN loss defines a TGF-beta-induced tubule phenotype of failed differentiation and JNK signaling during renal fibrosis. American Journal of Physiology Renal Physiology *302*, F1210-1223.

Liu, X., Ren, Z., Zhan, R., Wang, X., Zhang, Z., Leng, X., Yang, Z., and Qian, L. (2009). Prohibitin protects against oxidative stress-induced cell injury in cultured neonatal cardiomyocyte. Cell Stress & Chaperones *14*, 311-319.

Lopate, G., Baloh, R.H., Al-Lozi, M.T., Miller, T.M., Fernandes Filho, J.A., Ni, O., Leston, A., Florence, J., Schierbecker, J., and Allred, P. (2010). Familial ALS with extreme phenotypic variability due to the I113T SOD1 mutation. Amyotroph Lateral Scler *11*, 232-236.

Low, F.M., Hampton, M.B., Peskin, A.V., and Winterbourn, C.C. (2007). Peroxiredoxin 2 functions as a noncatalytic scavenger of low-level hydrogen peroxide in the erythrocyte. Blood *109*, 2611-2617.

Mitsumoto, A., Takanezawa, Y., Okawa, K., Iwamatsu, A., and Nakagawa, Y. (2001). Variants of peroxiredoxins expression in response to hydroperoxide stress. Free Radic Biol Med *30*, 625-635.

Moon, J.C., Hah, Y.S., Kim, W.Y., Jung, B.G., Jang, H.H., Lee, J.R., Kim, S.Y., Lee, Y.M., Jeon, M.G., Kim, C.W., *et al.* (2005). Oxidative stress-dependent structural and functional switching of a human 2-Cys peroxiredoxin isotype II that enhances HeLa cell resistance to H2O2-induced cell death. J Biol Chem *280*, 28775-28784.

Nguyen, T., Nioi, P., and Pickett, C.B. (2009). The Nrf2-antioxidant response element signaling pathway and its activation by oxidative stress. J Biol Chem *284*, 13291-13295.

Noh, Y.H., Baek, J.Y., Jeong, W., Rhee, S.G., and Chang, T.S. (2009). Sulfiredoxin Translocation into Mitochondria Plays a Crucial Role in Reducing Hyperoxidized Peroxiredoxin III. J Biol Chem *284*, 8470-8477.

Okado-Matsumoto, A., and Fridovich, I. (2002). Amyotrophic lateral sclerosis: a proposed mechanism. Proc Natl Acad Sci U S A *99*, 9010-9014.

Orrenius, S., Zhivotovsky, B., and Nicotera, P. (2003). Regulation of cell death: the calcium-apoptosis link. Nat Rev Mol Cell Biol *4*, 552-565.

Papadia, S., Soriano, F.X., Leveille, F., Martel, M.A., Dakin, K.A., Hansen, H.H., Kaindl, A., Sifringer, M., Fowler, J., Stefovska, V.*, et al.* (2008). Synaptic NMDA receptor activity boosts intrinsic antioxidant defenses. Nat Neurosci *11*, 476-487.

Petri, S., Korner, S., and Kiaei, M. (2012). Nrf2/ARE Signaling Pathway: Key Mediator in Oxidative Stress and Potential Therapeutic Target in ALS. Neurology Research International *2012*, 878030.

Rhee, S.G., Jeong, W., Chang, T.S., and Woo, H.A. (2007). Sulfiredoxin, the cysteine sulfinic acid reductase specific to 2-Cys peroxiredoxin: its discovery, mechanism of action, and biological significance. Kidney Int Suppl, S3-8.

Rhee, S.G., Kang, S.W., Jeong, W., Chang, T.S., Yang, K.S., and Woo, H.A. (2005). Intracellular messenger function of hydrogen peroxide and its regulation by peroxiredoxins. Curr Opin Cell Biol *17*, 183-189.

Rhee, S.G., and Woo, H.A. (2011). Multiple functions of peroxiredoxins: peroxidases, sensors and regulators of the intracellular messenger HO, and protein chaperones. Antioxid Redox Signal *15*, 781-794.

Roussel, X., Kriznik, A., Richard, C., Rahuel-Clermont, S., and Branlant, G. (2009). Catalytic mechanism of Sulfiredoxin from Saccharomyces cerevisiae passes through an oxidized disulfide sulfiredoxin intermediate that is reduced by thioredoxin. J Biol Chem *284*, 33048-33055.

Shaulian, E., and Karin, M. (2002). AP-1 as a regulator of cell life and death. Nat Cell Biol *4*, E131-136.

Soriano, F.X., Baxter, P., Murray, L.M., Sporn, M.B., Gillingwater, T.H., and Hardingham, G.E. (2009a). Transcriptional regulation of the AP-1 and Nrf2 target gene sulfiredoxin. Mol Cells *27*, 279-282.

Soriano, F.X., Leveille, F., Papadia, S., Higgins, L.G., Varley, J., Baxter, P., Hayes, J.D., and Hardingham, G.E. (2008). Induction of sulfiredoxin expression and reduction of peroxiredoxin hyperoxidation by the neuroprotective Nrf2 activator 3H-1,2-dithiole-3-thione. J Neurochem *107*, 533-543.

Soriano, F.X., Papadia, S., Bell, K.F., and Hardingham, G.E. (2009b). Role of histone acetylation in the activity-dependent regulation of sulfiredoxin and sestrin 2. Epigenetics *4*, 152-158.

Strong, M.J., and Gordon, P.H. (2005). Primary lateral sclerosis, hereditary spastic paraplegia and amyotrophic lateral sclerosis: discrete entities or spectrum? Amyotroph Lateral Scler Other Motor Neuron Disord *6*, 8-16.

Trachootham, D., Lu, W., Ogasawara, M.A., Nilsa, R.D., and Huang, P. (2008). Redox regulation of cell survival. Antioxid Redox Signal *10*, 1343-1374.

Vance, C., Rogelj, B., Hortobagyi, T., De Vos, K.J., Nishimura, A.L., Sreedharan, J., Hu, X., Smith, B., Ruddy, D., Wright, P.*, et al.* (2009). Mutations in FUS, an RNA processing protein, cause familial amyotrophic lateral sclerosis type 6. Science *323*, 1208-1211.

Woo, H.A., Bae, S.H., Park, S., and Rhee, S.G. (2009a). Sestrin 2 is not a reductase for cysteine sulfinic acid of peroxiredoxins. Antioxid Redox Signal *11*, 739-745.

Woo, H.A., Bae, S.H., Park, S., and Rhee, S.G. (2009b). Sestrin 2 is not a reductase for cysteine sulfinic acid of peroxiredoxins. Antioxidants & Redox Signaling *11*, 739-745.

Woo, H.A., Chae, H.Z., Hwang, S.C., Yang, K.S., Kang, S.W., Kim, K., and Rhee, S.G. (2003a). Reversing the inactivation of peroxiredoxins caused by cysteine sulfinic acid formation. Science *300*, 653-656.

Woo, H.A., Jeong, W., Chang, T.S., Park, K.J., Park, S.J., Yang, J.S., and Rhee, S.G. (2005). Reduction of cysteine sulfinic acid by sulfiredoxin is specific to 2-cys peroxiredoxins. J Biol Chem *280*, 3125-3128.

Woo, H.A., Kang, S.W., Kim, H.K., Yang, K.S., Chae, H.Z., and Rhee, S.G. (2003b). Reversible oxidation of the active site cysteine of peroxiredoxins to cysteine sulfinic acid. Immunoblot detection with antibodies specific for the hyperoxidized cysteine-containing sequence. J Biol Chem *278*, 47361-47364.

Wood-Allum, C.A., Barber, S.C., Kirby, J., Heath, P., Holden, H., Mead, R., Higginbottom, A., Allen, S., Beaujeux, T., Alexson, S.E., *et al.* (2006). Impairment of mitochondrial anti-oxidant defence in SOD1-related motor neuron injury and amelioration by ebselen. Brain *129*, 1693-1709.

Wood, Z.A., Poole, L.B., Hantgan, R.R., and Karplus, P.A. (2002). Dimers to doughnuts: redox-sensitive oligomerization of 2-cysteine peroxiredoxins. Biochemistry *41*, 5493-5504.

Wood, Z.A., Schroder, E., Robin Harris, J., and Poole, L.B. (2003). Structure, mechanism and regulation of peroxiredoxins. Trends Biochem Sci *28*, 32-40.

Yang, K.S., Kang, S.W., Woo, H.A., Hwang, S.C., Chae, H.Z., Kim, K., and Rhee, S.G. (2002). Inactivation of human peroxiredoxin I during catalysis as the result of the oxidation of the catalytic site cysteine to cysteine-sulfinic acid. J Biol Chem *277*, 38029-38036.